NOISE REMOVAL IN TREE RADAR B-SCAN IMAGES
BASED ON SHEARLET

Jian Wen, Zhaoxi Li, Jiang Xiao
School of Technology, Beijing Forestry University
Beijing, P.R. China

ABSTRACT

There are often many scars and hollows in ancient and famous trees. As a convenient and effective non-destructive testing tool, ground-penetrating (GPR) has a technical advantage in detecting abnormality in trees. But the tree radar images always inherit some extent of noise in them. Thus, denoising is very important to extract useful information from a tree radar image. Shearlet is a directional multi-scale framework, which has been shown effective to identify sparse anisotropic edges even in the presence of a large quantity of noise. This article presents an efficient denoising method based on shearlet applied on the tree radar images. Experimental results on forward modeling and standing trees radar data substantiate that the proposed method has the best denoising performance, especially in preserving the edge information as compared with the other methods which are based on wavelet, curvelet and contourlet.

KEYWORDS: Tree radar image, denoising, the shearlet transform.

INTRODUCTION

The characterization of the structure and the evaluation of the property are essential for managing and protecting ancient and famous trees. In the last decade a considerable amount of non-destructive testing methods has been devoted to the trees. Such as, ultrasonic tomography (Bucur 2005), electrical blocking imaging (Bao and Wang 2013), infrared imaging (Catena 2003), X-ray tomography (Liang et al. 2008) and stress wave (Zhang et al. 2010, Khaled et al. 2012). Even though these methods enable to acquire relatively accurate results, they are expensive, time-consuming and vulnerable to external interference.

Ground-penetrating radar (GPR), as a non-destructive, sufficient detection, simple operation, rapids ampling, high-resolution geophysical tool, has raised a substantial interest in non-destructive testing workers. This tool has been considered reliable for evaluation of geological disaster survey (Tang et al. 2011), concrete bridge decks (Sun et al. 2018), road investigations (Poikajärvi et al. 2012), dielectric structures testing (Ivashov et al. 2018) and

underground structure detection (Lai et al. 2018). Meanwhile, it has been gradually applied to the non destructive testing (NDT) of trees. (Martínez-Sala et al. 2013, Li, W. et al. 2018).

While capturing the tree radar images, noise is automatically introduced. Due to the noise, the interpretability of the tree radar image is been degraded and the extraction of the valuable information is difficult. Thus, the denoising of a tree radar image is one of the most important and basic steps in tree radar image processing.

Large numbers of noise filtering algorithms are present in the literature. Non-liner filters such as median (MED) filters are popular techniques for denoising because of their simplicity and low computational cost. The main shortcoming of MED is that it tends to blur image edges that may be especially significant at higher noise levels. Wavelet have been used in a wide variety of image denoising (Goyal and Tiwari 2013, Ghiyamat et al. 2015).The wavelet shows great effect when dealing with 1-D signal with point singularity features as well as good at dealing isolating discontinuities across horizontal or vertical edges for the 2-D image. However, the isotropic nature of the 2DWT atom renders it inefficient for the description of curvilinear singularities, namely the edge-like details in 2-D image. While for the 2-Dimage, the main characteristics were characterized by the edges.

For 2-D signals there is a large class of representations with a further sensitivity to directional information, useful to deal with the problem of the wavelet transform. Here is worth mentioning curvelet, contourlet and shearlet. Tzanis (2015) used the discrete Curvelet transform to remove noise in the 2-D GPR data to recover features associated with spatial scales and geometry. Terrasse et al. (2015) also used the curvelet for pipe detection. A medical image denoising algorithm using contourlet transform was proposed by Satheesh and Prasad (2011), the results showed that the contourlet transform has higher peak signal-to-noise ratio than the wavelet transform. However, the curvelet and contourlet transform subdivides the image into several layers in the frequency domain, which affects the expression of the sparsity of the image to a certain extent. The shearlet representation has many similarities to the curvelet, but with the additional advantage of a simplified mathematical structure.

The shearlet is a new multiple-scale and multiple-direction geometric analysis technique, which provides optimal approximation properties for images with edges and optimally efficient in representing functions with point wise singularities. This method has been successfully applied in many fields. Gao et al. (2015) proposed a new two-stage method by introducing shearlet transform method to the filtering stage for the removal of impulse noise. Since traditional CT reconstruction algorithms result in instability to noise, and may give inaccurate results for small ROI. Bubba et al. (2017) proposed a non smooth convex optimization model based on shearlet regularization to handle this difficulty. Huang et al. (2018) and Cheng et al. (2018) discussed the infrared and visible image fusion based on non-subsampled shearlet transform (NSST) which is used to deal with the lack of detail in the fusion image because of the artifacts. A cascaded framework that presents a fusion approach for multimodal medical information in non-subsampled shearlet (NSST) domain was proposed by Liu et al. (2017) and Singh et al. (2018). Li, L. et al. (2018) developed a novel microscopy mineral image enhancement approach based on NSST according to the multi-scale and multi-direction analysis characteristics of NSST.

The aim of this paper is to present an algorithm which can remove noise and preserve edge information effectively on the tree radar wave image. The shearlet transform is applied on the denoising of forward modeling radar data and standing trees radar data, and compared with the other three algorithms respectively on wavelet, curvelet, contourlet. Although the shearlet is widely used in image processing, it is of great significance for tree radar wave image processing.

MATERIALS AND METHODS

The continuous shearlet transform

A shearlet frame is an affine-like system of function based on the theory of composite wavelets which is generated by the dilation, shearling and translation of a function $\psi \in L^2(R^2)$. The system is defined in Eq. 1.

$$A_{AS}(\psi) = \left\{ \psi_{j,l,k}(x) = |det A|^{\frac{j}{2}} \psi(S^l A^j x - k) : j, l \in Z, k \in Z^2 \right\} \tag{1}$$

where: j, l and k are scale, direction, and shift parameters, respectively. A - dilation matrix, controls the scale of the shearlets. The shear matrix S is associated to a directional transformation. The matrix A and S defined respectively by Eq. 2:

$$A = \begin{pmatrix} a & 0 \\ 0 & \sqrt{a} \end{pmatrix}, S = \begin{pmatrix} 1 & s \\ 0 & 1 \end{pmatrix} \tag{2}$$

shearlets provide a decomposition of any $L^2(R^2)$ function into its frequency components according to the tiling of frequency domain by such trapezoids. In order to ensure the effect of decomposition in different directions, the frequency plane is partitioned into four cones C_1-C_4 and a centered rectangle R according to the direction. They are defined as Eqs. 3-7:

$$C_1 = \{(\xi_1, \xi_2) \in R^2 : \xi_1 \geq 1, |\xi_2/\xi_1| \leq 1\} \tag{3}$$

$$C_2 = \{(\xi_1, \xi_2) \in R^2 : \xi_2 \geq 1, |\xi_1/\xi_2| \leq 1\} \tag{4}$$

$$C_3 = \{(\xi_1, \xi_2) \in R^2 : \xi_1 \leq -1, |\xi_2/\xi_1| \leq 1\} \tag{5}$$

$$C_4 = \{(\xi_1, \xi_2) \in R^2 : \xi_2 \geq -1, |\xi_1/\xi_2| \leq 1\} \tag{6}$$

$$R = \{(\xi_1, \xi_2) \in R^2; \|(\xi_1, \xi_2)\|_\infty < 1\} \tag{7}$$
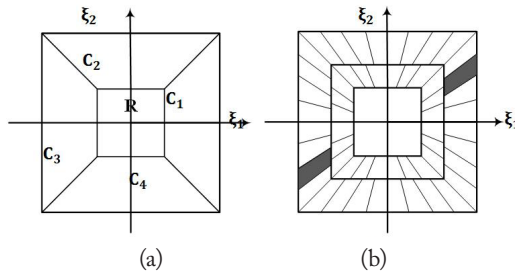

(a)   (b)

Fig. 1: Shearlet frequency domain subdivision.

As showed in Fig. 1a, the ξ_1, ξ_2 represent the horizontal and vertical coordinates respectively, the low frequency content of a signal is expressed by the rectangle R, C1 and C3 represent the horizontal region and C2 and C4 represent the horizontal vertical region. The gray trapezoid in Fig. 1b represents a pair of shearlet bases in the cones C1 and C3 which were planed.

Since the interest points of an image are associated with high frequencies, the contribution of low-frequency was not considered here.

The shearlet transform SH(f)of a signal $f \in L^2(R^2)$ is defined by Eq. 8.

$$SH(f)(a,s,t) = \langle f, \psi_{a,s,t} \rangle \tag{8}$$

where: $\langle f, \psi_{a,s,t} \rangle$ is the scalar product in $L^2(R^2)$, which is composed by the scaling fuction $\Phi \in L^2(R^2)$ and the shearing function $\Psi, \Psi \in L^2(R^2)$. Hence, the shearlet transform can also be given by Eqs. 9-11.

$$SH(\varphi, \phi, \bar{\phi}) = \Phi(\varphi)\Psi(\phi)\bar{\Psi}(\bar{\phi}) \tag{9}$$

$$\Phi(\varphi) = \{\varphi_t = \varphi(-t) : t \in R^2\} \tag{10}$$

$$\Psi(\phi) = \left\{\phi_{a,s,t} = a^{-\frac{3}{4}}\phi(A_a^{-1}S_s^{-1}(-t)) : a \in (0,1], s \in [-(1+\sqrt{a}), 1+\sqrt{a}], t \in R^2\right\} \tag{11}$$

where: a <0being the scale parameter, s ∈ Rbeing the shear parameter, and t ∈ R^2 being the translation parameter. When s<|1|, this produces the cone adapted continuous shearlet transform.

setting:

$$S_{come} = \left\{(a,s,t) : a \in (0,1], s \in [-(1+\sqrt{a}), 1+\sqrt{a}], t \in R^2\right\} \tag{12}$$

When $SH_{\varphi,\phi,\bar{\phi}}f : R^2 \times S_{come}^2 \to C^3$, we obtain the continuous system in Eqs. 13:

$$SH_{\varphi,\phi,\bar{\phi}}f\left(t', (a,s,t), (\bar{a}, \bar{s}, \bar{t})\right) = (\langle f, \varphi_{t'} \rangle, \langle f, \phi_{a,s,t} \rangle, \langle f, \phi_{\bar{a},\bar{s},\bar{t}} \rangle) \tag{13}$$

The discrete shearlet transform

Digital shearlet systems are defined by sampling continuous shearlet systems on a discrete subset of the space of parameters $R_+ \times R^3$ and by sampling the signal on a grid.

For the horizontal cones C1 and C3, S$^D_{come}$ is discretized as Eqs. 14.

$$S_{come}^D = \left\{(2^{-j}, k2^{-j/2}), S_{2^{-j/2}k}A_{2^{-j}}M_c m : j \geq 0, k \in \{-[2^{j/2}], \cdots, [2^{j/2}]\}, m \in Z^2\right\} \tag{14}$$

where: c = (c$_1$, c$_2$) ∈ (R$^+$)^2 denoted the sampling parameter, M denoted sampling matrix.

For vertical areas, a similar processing method can be used for discretization processing. Hence, the discrete shearlet transform was considered as the following formulations:

$$SH^D(c; \varphi, \phi, \bar{\phi}) = \Phi(c_1, \varphi)\Psi(c, \phi)\bar{\Psi}(c, \bar{\phi} \tag{15}$$

$$\Phi(c_1, \varphi) = \{\varphi_m = \varphi(-c_1 m) : m \in Z^2\} \tag{16}$$

$$\Psi(c, \phi) = \left\{\phi_{j,k,m} = 2^{-3j/4}\phi(S_{-k}A_{2^j} - M_c m) : j \geq 0, |k| \leq [2^{j/2}], m \in Z^2\right\} \tag{17}$$

setting:
$$\Lambda_{come} = \left\{(j, k, m) : j \geq 0, |k| \leq 2^{j/2}, m \in Z^2\right\} \tag{18}$$

When $SH^D_{\varphi,\phi,\bar{\phi}}f : Z^2 \times \Lambda^2_{come} \to C^3$, we obtain the discrete system in Eqs. 19.

$$SH^D_{\varphi,\phi,\bar{\phi}}f\left(m',(j,k,m),(\bar{j},\bar{k},\bar{m})\right) = (\langle f, \varphi_{m'}\rangle, \langle f, \phi_{j,k,m}\rangle, \langle f, \phi_{\bar{j},\bar{k},\bar{m}}\rangle) \tag{19}$$

where: $f \in L^2(R^2)$.

Denoising with the shearlet transform

In this section, the process of denoising with the shearlet transform was introduced. Given the tree radar images M=G+N, where G represents the GPR signals, N represents noise. The M is transformed into low frequency and high frequency coefficients at each scale using DST. The high frequency coefficients then distribute in different scales and directions.

Since the energy of the tree radar image signal is stronger than the energy of random noise, the shearlet coefficients of the tree radar image signal is bigger than which of noise. Then making the shearlet coefficients which are smaller than the threshold value become zero. In this way, random noise can be removed. Thus, we choose the soft threshold function, which is defined by Eq. 20:

$$T_{soft}(w_{j,k}) = \begin{cases} 0 & |w_{j,k}| < \lambda \\ sgn(w_{j,k}) * (|w_{j,k}| - \lambda) & |w_{j,k}| \geq \lambda \end{cases} \tag{20}$$

where: *sgn* denotes symbolic function, T_{soft} denotes the decomposition coefficient after the soft threshold operation. The threshold values λ is calculated by The Visu Shrink threshold which is defined as Eq. 21:

$$\lambda = \sigma_n \sqrt{2 \ln N} \tag{21}$$

where: σ_n is the standard deviation of Gaussian white noise with a mean of zero. N is the length of the signal.

After threshold processing, reconstructing and adding high frequency coefficient at different scales to obtain high frequency coefficients, as below:

$$\hat{G} = S^{-1}T_{soft}(w_{j,k}) \tag{22}$$

Finally, combine the decomposed low frequency coefficients with the reconstructed high frequency coefficients; we can obtain an image after noise removal which is given as Eq. 23

$$\hat{M} = \hat{G} + N \tag{23}$$

RESULTS AND DISCUSSION

Performance measure

In order to evaluate the efficiency of the shearlet-based denoising method on tree radar image. The performance of the proposed method was extensively compared qualitatively and quantitatively with some existing methods, including wavelet, curvelet and contourlet.

To judge the quantitative performance, three standard measures such as signal-to-noise ratio (SNR), i.e. the ratio of image information and noise contained in the image, the peak signal-to-noise ratio (PSNR) and the edge preservation index (EPI) were used.

These can be considered as indicators of the performance of the filtering method well-denoised by identifying the parameters which results in the highest SNR and PSNR and the value of EPI should be close to 1. The measures are defined in Eqs. 24-27 respectively.

$$\text{SNR} = 20 \times \log_{10} \left\{ \sum_{i=1}^{i=N} \sum_{j=1}^{j=M} \frac{rawrata^2(i,j)}{prodata^2(i,j) - rawdata^2(i,j)} \right\} \; (\text{dB}) \qquad (24)$$

$$\text{PSNR} = 20 \times \log_{10} \left\{ \frac{\max (rawdata^2(i,j))}{\sqrt{MSE}} \right\} \; (\text{dB}) \qquad (25)$$

$$\text{MSE} = \frac{\sum_{i=1}^{i=N} \sum_{j=1}^{j=M} (prodata^2(i,j) - rawdata^2(i,j))}{M \times N} \; (P^2) \qquad (26)$$

$$\text{EPI} = \sum_i \sum_j \frac{|I_{pro}(i,j+1) - I_{pro}(i,j)|}{|I_{raw}(i,i+1) - I_{raw}(i,j)|} \qquad (27)$$

where, raw data represents the original image and prodata represents the denoised image. M×N describes the size of GPR data.

Though PSNR can measure the intensity difference between the images, the visual analysis of the image quality is extremely important for subjective evaluation. For quantitative performance measure, these methods were applied on the forward modeling radar data and standing trees radar data. In the experiment, all the methods are implemented in MATLAB2016.

Experiment on forward data
The experiment was performed on the forward data firstly. The tree radar image was simulated by finite-difference tine-domain (FDTD) method, and GprMax software which is an open source software that simulates electromagnetic wave propagation was employed.
The model design of tree trunk B-san image is as follows. The geological background is wood, and the hollow is air. The radius of the tree model is 60 cm. The electrical conductivity of bark is 5 S·m⁻¹, the electrical conductivity of sapwood is 11 S·m⁻¹, the electrical conductivity of heartwood is 13 S·m⁻¹. To better mimic the appearance of the real tree trunk image, there are two defects designed in the tree trunk, one is a scar A on sapwood whose electrical conductivity is 6 S·m⁻¹, the other one is a hollow B on heartwood whose electrical conductivity is 16 S·m⁻¹. The tree radar B-scan image model produced by GprMax is showed in Fig. 2. It can be noted that different defects represent different curve characteristics.
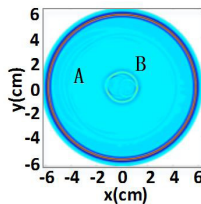

Fig. 2: Forward tree radar B-scan image model.

The forward tree radar B-scan image was noise-free while the image actually acquired was disturbed by various factors and contained noise. The most simplifying assumption while solving image noise problems has been contaminated with Additive White Gaussian Noise. Sothe Additive white Gaussian Noise is taken as the model noise in this work.
The noisy tree radar B-scan image is showed in Fig. 3a. As shown in Fig. 3a, the

characteristics of defect inside the tree trunk was covered by noise, especially the characteristics of scar A which was almost blur.
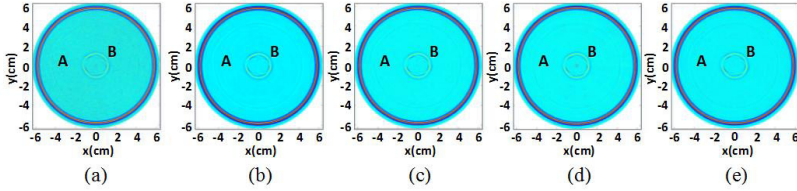

(a)   (b)   (c)   (d)   (e)

Fig. 3: Denoising results for the forward tree radar B–scan image (a) Noisy image (b) Results using Wavelet (c) Results using Curvelet (d) Results using Contourlet (e) Results using Shearlet.

Fig. 3 shows the comparison with the other three methods; we found that all of the denoising methods can effectively enhance visual quality of the defect characteristics from noise. However, the shearlet-based method significantly reduce the noise with remaining the edge features of defects, compared to the wavelet-based method, whose edge features with more saw tooth sensation. Whereas with the results of curvelet and contourlet, the differences of the visual effects at a glance are little, and our evaluations are sometimes inferior.

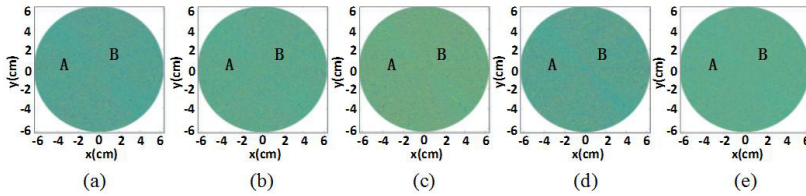(a)   (b)   (c)   (d)   (e)

Fig. 4: Difference between noisy image and denoised image (a) Original noise (b) Difference of Wavelet (c) Difference of Curvelet (d) Difference of Contourlet (e) Difference of Shearlet.

The other evaluation value comes from the difference between noisy image and denoised image as shown in Fig. 4. The difference images of shearlet-based method are not over-smoothed unlike the other' difference and have significantly closer similarity to the original noisy image than the other method. Particularly for the curvelet and contourlet-based methods, the difference images are over-smoothed, this indicates that of which the noise removal is not enough. It shows that the shearlet-based denoising performs best ability to reduce noise while preserving the edge features of defects for the noisy tree radar forward image.

The contents of SNR, PSNR and EPI in the forward tree radar data of different denoising methods are listed in Tab. 1. Quantitatively, our proposed method gives highest PSNR and SNR results than those of the other compared methods. Moreover, the EPI of shearlet-based was closest to 1. Thus, it confirms that the proposed method not only has best denoising performance, it also keeps the images more faithful to the noise-free images after denoising.

Tab. 1: The digital results of 4 denoising methods in forward tree radar B-scan image.

Parameter	Wavelet	Curvelet	Contourlet	Shearlet
PSNR	65.1270	67.0891	66.3956	68.4431
SNR	31.2289	36.2057	34.7803	53.6284
EPI	0.0520	0.2601	0.3073	0.3186

Experiment on standing trees radar data

The tree radar used in this paper is the TRU tree radar detection system produced by TreeWin Company of the United States. The tree radar detection system mainly includes two parts: a radar wave medium coupling antenna and a data collector. The medium-coupled antenna internally includes a set of transmit-receive antenna pairs and radar wave generating circuits for transmitting and receiving radar waves. The data collector is used to set the mode of the radar wave detection system. Such as the root detection or trunk detection, this paper mainly uses the TRU detection system to detect the defects inside the trunk. The data collector is also used to set the scan diameter of the probe since selecting the appropriate measurement diameter can make the test results more accurate. The data collector stores the echo signals received in a binary data format in a file with a suffix of *.dzt for subsequent data reading and processing.

Fig. 5 shows hundreds of years old tree at south of Jiehu Bridge in Summer Palace. In this paper, radar wave scanning was performed on the cross sections of the trunks at 0.6 m, 0.9 m, 1.5 m and 1.8 m from the ground. The red vertical line was the starting position of scanning. The perimeters of cross sections were 5.21 m, 4.67 m, 4.91 m, 5.08 m separately. Therefore, the value of the scanning diameter 130 cm was used in this experiment.

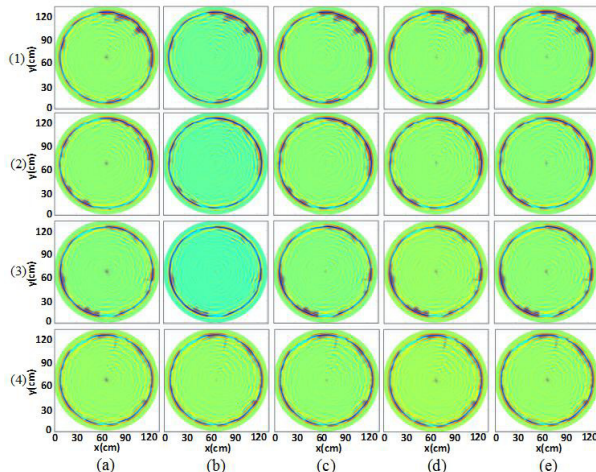*Fig. 5: The old willow at south of Jiehu Bridge in Summer Palace.*

Fig. 6: Denoising results for the standing tree radar B-scan image: (a) Scanning image of 0.6 m, 0.9 m, 1.5 m, 1.8 m (b) Results using Wavelet (c) Results using Curvelet (d) Results using Contourlet (e) Results using Shearlet.

The scanning results of 0.6 m, 0.9 m, 1.5 m and 1.8 m are shown in the first column of Fig. 6 (1)-(4) from top to bottom. It shows that the ancient tree has suffered from a large area of hollows, scars and other defects. Four denoising methods were performed for the tree radar images of four scanning heights respectively, which were showed in Fig. 6b-e. Furthermore, the quantitative performances are listed in Tab. 2.

Tab. 2: The digital results in tree radar images of four cross sectional heights by fourdenoising methods for standing tree.

Height	0.6m			0.9m			1.5m			1.8m		
Parameter	PSNR	SNR	EPI	PSNR	SNR	EPI	PSNR	SNR	EPI	PSNR	SNR	EPI
Wavelet	65.037	19.933	0.251	65.024	18.935	0.251	64.928	17.470	0.205	64.928	18.170	0.211
Curvelet	65.908	22.679	0.304	66.271	21.655	0.304	66.748	21.502	0.419	66.854	22.374	0.359
Contourlet	66.297	21.829	0.350	65.978	21.014	0.350	66.086	20.078	0.362	66.037	20.343	0.387
Shearlet	68.717	27.535	0.428	68.697	26.538	0.429	68.742	25.462	0.436	68.716	26.045	0.428

As indicated by the results, the contourlet and shearlet-based methods perform better in denoising. In addition, the shearlet-based method outperforms the other three methods both in noisy removal quality index and edge preservation index. Thus, it confirms the validity of the proposed method in both appearance and numerical evaluation in comparison with the other three methods.

The multi-scale analysis is widely used in image processing by other author, such as in reinforced concrete, underground pipeline, medical image and so on. But the application of multi-scale analysis in standing trees in this article is of great significance. Comparison of four common filtering methods is presented in this article. Through appearance and numerical evaluation, the conclusion is concluded that the shearlet transform is the most suitable noise removal algorithm in non-destructive testing of standing trees.

CONCLUSIONS

In this paper, the shearlet-based denoising method was proposed for the tree radar image. The continuous shearlet transform and a discrete setting were presented, then the denoising with shearlet transform was discussed on image.

Two experiments were performed on noise images, the first one was forward modeling tree radar data affected by the Additive white Gaussian Noise. On one hand the numerical evaluation results achieved by the proposed method surpasses the other three methods by a large margin, on the other hand the edges and details preserved by the proposed method are obviously better than the other methods and most faithful to the noise free image. The second one was tree radar B-scan images acquired by the standing trees where the images included noise effects. The proposed method shows significantly better performance over the other three methods by achieving satisfactory results in both numerical and visual evaluation.

Future areas of further development of our research include the expansion of our method to the denoising of the tree radar images and such work is currently underway.

ACKNOWLEDGEMENT

REFERENCES

1. Bao, Z., Wang, H., 2013: Application of electrical resistance testing method in detection of decay in standing trees. College of Engineering and Technology 29 (6): 47-51.
2. Bubba, T.A., Porta, F., Zanghirati, G., Bonettini, S., 2017: A nonsmooth regularization approach based on shearlets for Poisson noise removal in ROI tomography. Applied Mathematics & Computation 318: 131- 152.
3. Bucur, V., 2005: Ultrasonic techniques for nondestructive testing of standing trees. Ultrasonics 43(3): 237-239.
4. Catena, A., 2003: Thermography reveals hidden tree decay. Arboricultural Association Journal 27 (1): 27-42.
5. Cheng, B., Jin, L., Li, G., 2018: Adaptive fusion framework of infrared and visual image using saliency detection and improved dual-channel PCNN in the LNSST domain. Infrared Physics & Technology 92: 30-43.
6. Gao, G., Liu, Y., Labate, D., 2015: A two-stage shearlet-based approach for the removal of random-valued impulse noise in images. Journal of Visual Communication and Image Representation 32: 83-94.
7. Ghiyamat, A., Shafri, H.Z.M., Mahdiraji, G.A., Ashurov, R., Mansour, S., 2015: Airborne hyperspectral discrimination of tree species with different ages using discrete wavelet transform. International Journal of Remote Sensing 36 (1): 318-342.
8. Goyal, P., Tiwari, V.M., 2013: Application of the continuous wavelet transform of gravity and magnetic data to estimate sub-basalt sediment thickness. Geophysical Prospecting 62 (1): 148-157.
9. Huang, Y., Bi, D., Wu, D., 2018: Infrared and visible image fusion based on different constraints in the non-subsampled shearlet transform domain. Sensors 18 (4): 1169.
10. Ivashov, S.I., Bugaev, A.S. , Zhuravlev, A.V. , Razevig, V.V., Chizh, M.A., Ivashov, A.I., 2018: Holographic subsurface radar technique for nondestructive testing of dielectric structures. Technical Physics 63 (2): 260-267.
11. Horáček, P., Tippner, J., Hassan, K.T., 2012: Nondestructive evaluation of static bending properties of scots pine wood using stress wave technique. Wood Research 57(3): 359-366.
12. Poikajärvi, J., Peisa, K., Herronen, T., Aursand, P.O., Maijala, P., Narbro, A., 2012: GPR in road investigations – equipment tests and quality assurance of new asphalt pavement. Nondestructive Testing Communications 27 (3): 293-303.
13. Lai, W., Chang, R.K.W., Sham, J.F.C., 2018: A blind test of nondestructive underground void detection by ground penetrating radar (GPR). Journal of Applied Geophysics 149: 10-17.
14. Liang, S., Wang, X., Cai, Z., Ross, R.J., Bruce, R., Fu, A., 2008: Elastic wave tomography in standing tree decay detection. Research Institute of Wood Industry: 44 (5): 109-114.
15. Li, L., Si, Y., Jia, Z., 2018: Microscopy mineral image enhancement based on improved adaptive threshold in nonsubsampled shearlet transform domain. AIP Advances 8(3): 035002.

16. Li, W., Wen, J., Xiao, Z., Xu, S.X., 2018: Application of ground-penetrating radar for detecting internal anomalies in tree trunks with irregular contours. Sensors 18(2): 649.

17. Liu, X., Mei, W., Du, H., 2017: Structure tensor and nonsubsampled shearlet transform based algorithm for CT and MRI image fusion. Neurocomputing 235: 131-139.

18. Martínez-Sala, R., Rodríguez-Abad, I., Barra, R.D., Capuz-Lladró, R., 2013: Assessment of the dielectric anisotropy in timber using the nondestructive GPR technique. Construction & Building Materials 38: 903-911.

19. Satheesh, S., Prasad, K., 2011: Medical image denoising using adaptive threshold based on contourlet transform. Advanced Computing an International Journal 2 (2): 52-58.

20. Singh, S., Anand, R.S., Gupta, D., 2018: CT and MR image information fusion scheme using a cascaded framework in ripplet and NSST domain. IET Image Processing 12(5): 696-707.

21. Sun, H., Pashoutani, S., Zhu, J., 2018: Nondestructive evaluation of concrete bridge decks with automated acoustic scanning system and ground penetrating radar. Sensors 18(6): 1955.

22. Tang, X., Sun, T., Tang, Z., Zhou, Z., Wei, B., 2011: Geological disaster survey based on curvelet transform with borehole ground penetrating radar in Tonglushan old mine site. Journal of Environmental Sciences 23 (Supplement): S78 - S83.

23. Tzanis, A., 2015: The curvelet transform in the analysis of 2-D GPR data: Signal enhancement and extraction of orientation-and-scale-dependent information. Journal of Applied Geophysics 115: 145-170.

24. Terrasse, G., Nicolas, J.M., Trouve, E., Drouet, E., 2015: Application of the curvelet transform for pipe detection in GPR images, Geoscience and Remote Sensing Symposium. IEEE 2015: 4308- 4311.

25. Zhang, H., Wang, C., Su, J., Robert, J.R, 2010: Investigation of stress wave propagation mechanism in American red pine trees. Journal of Beijing Forestry University 32(2): 145-148.

Jian Wen, Zhaoxi Li, Jiang Xiao*
School of Technology
Beijing Forestry University
Beijing 100083, P.R. China
*Corresponding author: XIAOJIANG56@126.COM

SITE INFLUENCE ON ANATOMICAL STRUCTURE OF BALD CYPRESS

Dušan Jokanović, Dragica Vilotić, Vesna Nikolić Jokanović, Sara Lukić
Belgrade University, Faculty of Forestry
Belgrade, Republic of Serbia

Tatjana Ćirković-Mitrović
Institute of Forestry
Belgrade, Republic of Serbia

ABSTRACT

The paper deals with length of tracheids of bald cypress at two alluvial sites in Serbia. Scope of the paper was to establish site influence (climate, soil, etc.) on mentioned anatomical feature and to quantify it, as well. Axial tracheid changes have been observed depending on three factors: cambial age, zone inside growth ring and stem height where sampling was performed. The paper established gradually increasing of axial tracheid length with cambial age and that did not depend on zone inside growth ring and stem height. There was also significant influence of the zone inside growth ring to axial tracheid length, while stem height where sampling was performed does not have significant influence. There was found relation between factors that determine site such as physical and chemical soil properties and climate from one and axial tracheid length from another side.

INTRODUCTION

Bald cypress (*Taxodium distichum* (L.) Rich.) wood is valuable, especially in its natural habitat – North America. Some important characteristics of bald cypress such as fast radial and height increment, decorative and technical value confirm its forestry significance. Bald cypress was introduced in Europe in 1640 and at first planted as ornamental species, but later it was also used for forest plantations establishing (Vidaković 1982). In Serbia, bald cypress can be considered as introduced species characterized by relatively fast growth. As for Serbia, there is a group of bald cypress stems in Banja Koviljača park (Tucović and Ocokoljić 2005) and it is also present in some parts of Belgrade (Veliko ratno ostrvo and Bačka Palanka), as well as in Novi Sad, Vršac Vrnjačka banja and Kraljevo.

There are a lot of papers such as Vilotić and Knežević (1994), Vilotić (1992, 1992a), Vilotic et al. (2015), Jacobsen et al. (2007), Günthardt-Goerg et al. (2013), Luostarinen et al. (2017) etc. that confirmed influence of ecological factors (soil and climate) on wood anatomical structure.

The scope of the paper was to explain how tracheid length changes depending on zone inside growth ring, stem height that was sampled and cambial age. Bearing on mind that tracheids play both mechanical and conductive role by conifers, the goal was to investigate site factors influence on these elements.

MATERIAL AND METHODS

Material selected for this research originates from two locations – Veliko ratno ostrvo and Bačka Palanka – Republic of Serbia. Veliko ratno ostrvo is protected natural area situated between 1,169 km and 1,172 km of the Danube river flow close to Belgrade. On the other side, Bačka Palanka is located in the northern part of Serbia (Vojvodina) and there is the only seed stand of bald cypress in the whole Republic.

Climate
Based on data obtained from meteorological stations Belgrade and Bački Petrovac, two climate factors were analyzed – an average monthly air temperature and medium monthly rainfall quantity. As for Bačka Palanka, an average monthly air temperature during a year was 11.2°C, while an average monthly air temperature during vegetation season was 18.0°C. Overall annual rainfall quantity at this locality was 618 mm, while during vegetation season it was 350 mm, which means that about 57% from the whole rainfall quantity occurs during vegetation season. At Veliko ratno ostrvo, an average monthly air temperature during a year was 12.2°C, and during vegetation season it was 18.9°C. Overall annual rainfall quantity at this locality was 693 mm, while during vegetation season it was 395 mm, which means that about 57% from the whole rainfall quantity occurs during vegetation season. Based on obtained data related to observed climate factors, we can deduce there are very suitable conditions for growth and development of bald cypress at both localities.

Soil
Physical and chemical soil features at researched sites were established according to pedological analysis. As for texture composition of soil, more suitable conditions were found at Veliko ratno ostrvo. Texture classes such as sandy loam and loam, recorded at Veliko ratno ostrvo, have much greater useful water capacity than texture classes recorded in Bačka Palanka (sand and loamy sand), so there is much more available water for plants at Veliko ratno ostrvo (Popović 2014, Jokanović 2016). As for chemical structure, there was also present more nutrients at Veliko ratno ostrvo (Jokanović 2016). Ivanišević (1993) and Pekeč (2010) concluded there are significant differences between some texture classes related to optimal hydrological conditions for plants growth.

Samples preparing
Overall six trees of bald cypress (*Taxodium distichum* (L.) Rich.) from both localities were harvested. Each test tree was marked on the side facing north because of further investigations on anatomical properties. Disks, approximately 5 cm thick, were cut at the base (0.3 m) and on breast height (1.3 m) from each tree. Radial segments (north-south orientation) were cut from each disc and annual growth rings were marked along one radius. All growth rings from the pith to the bark were included.

As for laboratory work, mentioned discs were transported into Laboratory for wood anatomy at Faculty of Forestry in Belgrade. Maceration had to be performed in order to measure tracheid length. Maceration was performed according to Franklin's method (Franklin 1945).

Wood tissue maceration of *Taxodium distichum* (L.) Rich. samples was carried out using Franklin's reagent (mixture of 30% of hydrogen peroxide and glacial acetic acid in 1:1 proportion) in the Laboratory for wood anatomy, Faculty of Forestry, Belgrade. The prepared reagent was dosed onto chopped wooden samples in glass test tubes, closed with glass plugs, and left in a dryer for 24 hours, exposed to a temperature of 65°C. The sampled material was transformed into pulp, which was later rinsed with distilled water. Macerated material was stained using safranin, then placed on microscope (Trinocular Microscope model IS.1153-EPL, Euromex, Holland) slides and mounted in glycerin gelatin (Figs. 2 and 4). In order to perform tracheid length measurements, overall four zones were established: (1) close to the core that includes a few initial growth rings, (2) situated in juvenile wood zone, (3) in the central part, and finally (4) close to the bark (Jokanović 2016).

Statistical analysis of results was carried out using Statistica 7. Repeated measures analysis of variance (ANOVA) was used to test significance of differences in radial distribution of selected tracheid characteristics, as well as their variations within and between two bald cypress populations.

RESULTS AND DISCUSSION

As for Bačka Palanka stems on the base (0.3 m), an average tracheid length in earlywood was 1.68 mm, while minimal and maximal values were 0.3 mm and 2.9 mm, respectively. Standard deviation was 0.5184. As for latewood tracheids at the same locality and on the same height, its average value was 1.69 mm, while extreme values were 0.2 mm and 2.9 mm, respectively. Standard deviation was 0.6153. Based on Tab. 1, it can be established there is no statistically significant difference in tracheid length between earlywood and latewood. Based on Tab. 1, it can be established there is no statistically significant difference between early- and latewood tracheid length.

Tab. 1: Medium tracheid length in early- and latewood (Bačka Palanka).

Tukey HSD test		
Homogenous groups, alpha = 0.05000		
	Early-late wood, 0.3 m	**Early-late wood, 1.3 m**
Early wood	1.685152[a]	1.682348[a]
Late wood	1.694621[a]	1.806212[b]
	Error: Between MS = 0.32372, df = 2638.0	Error: Between MS = 0.31646, df = 2638.0

Average values in the same column with different letter (a, b) are statistically different for p < 0.05 (Post hoc Tukey's HSD test)

On the Fig. 1a is displayed changing of an average tracheid length at the base depending on cambial age. Earlywood tracheids are the shortest at the beginning, in juvenile zone. As for earlywood tracheids, close to the pith (1-4 growth rings) was established the lowest value of medium tracheid length, 0.99 mm. With cambial age, earlywood tracheids gradually become longer and culmination was reached between 35th and 44th growth ring, 2.11 mm. After that going to the bark an average earlywood tracheid length decreases.

15

As for latewood tracheids at the same height (0.3 m) in the same locality (Bačka Palanka), the same tendency as in the early wood close to the pith was established – there are the shortest tracheids long about 0.80 mm. After that its length gradually increases until 54th growth ring, but maximal medium tracheid value was established between 45th and 54th growth ring, 2.28 mm. Next phase was characterized by reducing of latewood tracheid value.

As for Bačka Palanka on the breast height (1.3 m), an average earlywood tracheid length was 1.81 mm, while extreme values were 0.5 mm and 2.9 mm, respectively (Tab. 1). Standard deviation was 0.4804.
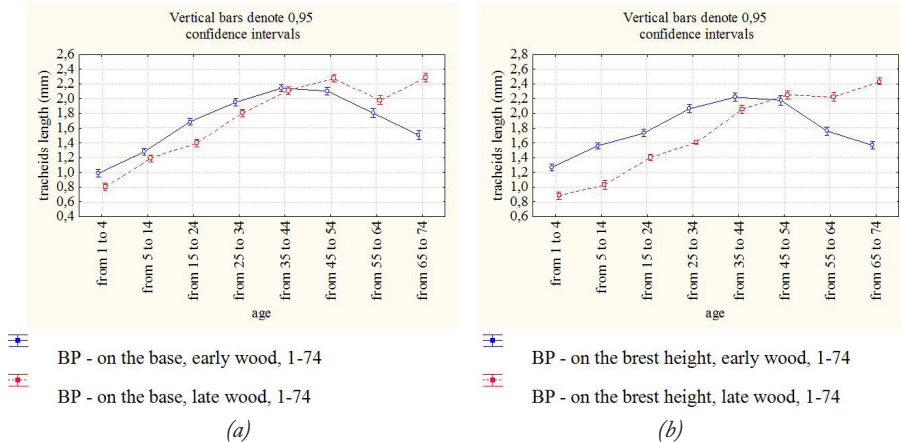

(a)   (b)

Fig. 1: Changes of an average tracheid length in early– and latewood at the base (0.3 m) and on the breast height (1.3 m) depending on cambial age (Bačka Palanka).

As for latewood tracheids, an average length was 1.68 mm, while minimum and maximum were 0.3 mm and 2.9 mm, respectively (Tab. 1). Standard deviation was 0.6341.

Earlywood tracheids on the breast height (1.3 m) in Bačka Palanka are the shortest close to the pith – 1.27 mm. After that, they become longer with cambial age and the greatest values were recorded between 35th and 44th growth ring – 2.22 mm. Next phase was characterized by its length reducing with the lowest values in final growth rings – 1.57 mm (Fig. 1b).

Latewood tracheids are also the shortest close to the pith (0.88 mm), and after that was established constant rising of tracheid length with maximal values close to the bark – 2.43 mm (Fig. 1b).
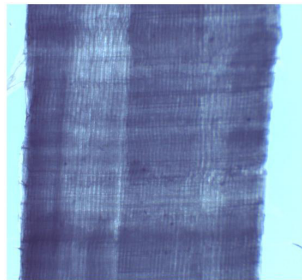

Fig. 2: Strings of macerated early– and latewood tracheids (x 40).

An average early- and latewood tracheid length comparing between each other in Bačka Palanka at the base (0.3 m) shows existing of statistically significant differences up to 35-44 interval, because between these growth rings earlywood tracheids are much longer than latewood. During 35-44 intervals, there was no significant difference, and after it up to the final growth rings, there was established gradual increasing of latewood tracheid length and decreasing of earlywood tracheid length. There is no statistically significant difference in interval 45-54. Before mentioned interval, earlywood tracheids are much longer, unlike after this interval.

As for Veliko ratno ostrvo, at the base (0.3 m), an average earlywood tracheid length is 2.49 mm (Tab. 2). Extreme values are 0.4 mm and 4.6 mm, respectively, while standard deviation was 1.0608. Medium latewood tracheid length was 1.03 mm (Tab. 2), minimal 0.3 mm and maximal 2.3 mm with standard deviation of 0.4311.

Tab. 2: Medium tracheid length in early- and latewood (Veliko ratno ostrvo).

Tukey HSD test		
Homogenous groups, alpha = 0.05000		
	Early-late wood, 0.3 m	Early–late wood, 1.3 m
Early wood	2.490625a	2.810625a
Late wood	1.028125b	0.953750b
	Error: Between MS = 0.85956, df = 958.00	Error: Between MS = 0.59385, df = 958.00

Average values in the same column with different letter (a, b) are statistically different for p < 0.05 (Post hoc Tukey's HSD test).

On the base (0.3 m), with cambial age, an average earlywood tracheid length constantly increases with maximal value in the final growth rings – 4.02 mm (Fig. 3a).

As for latewood tracheids on the same height and in the same locality (Veliko ratno ostrvo), there are no significant changes of its length close to the pith and in juvenile wood zone. After that comes to its significant increasing to maximal 1.55 mm and that was followed with reducing of its value to minimum – 0.71 mm (Fig. 3a). The same tendency was recorded for both early- and latewood tracheid length on the breast height (1.3 m) on Veliko ratno ostrvo (Fig. 3b).
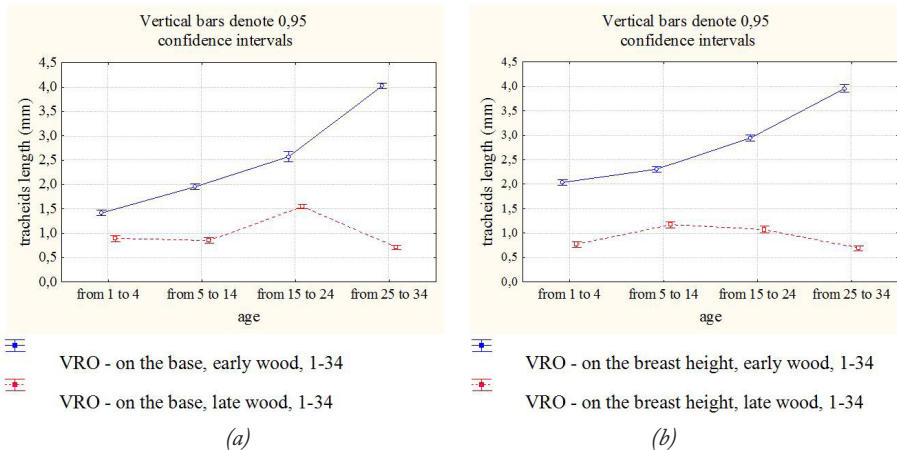

Fig. 3: Changes of an average tracheid length in early- and latewood at the base (0.3 m) and on the breast height (1.3 m) depending on cambial age (Veliko ratno ostrvo).

Fig. 4: Macerated tracheids (x 400).

Based on obtained results, significant difference was established, not only in values, but also in growth tendencies of tracheid length with cambial age depending on locality.

In Bačka Palanka, earlywood tracheids are the shortest in juvenile zone, then become longer with culmination between 35th and 44th growth ring, and then its length decreases going to the bark. As for latewood tracheids, they are also the shortest close to the pith, and then become longer with maximal value close to the bark. The same tendencies were recorded both at the base and on the breast height in Bačka Palanka.

As for Veliko ratno ostrvo, unlike earlywood tracheids with remarkable length increasing from the pith to the bark, there is decreasing of latewood tracheid length apart from interval 15-24 when culmination was reached. On the breast height was also recorded that earlywood tracheids are much longer than these situated in latewood. Like on the base, on another height (1.3 m) was recorded the same tendency –by latewood tracheids, apart from interval 5-14, reducing of tracheids length was obvious with minimum reached in the final growth rings.

Comparative analysis of an average tracheid length in radial direction at breast height from both localities has been shown on the Fig. 5. As for the value of this element, it gradually rises from the pith to the bark going to the mutual age of 34.
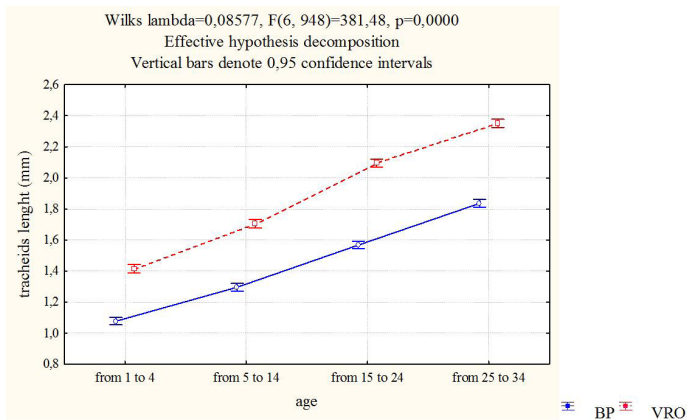

Fig. 5: Distribution of an average tracheid length in radial direction at both localities.

The influence of different sites and tracheid distance from the pith to the bark to its length has been shown in the Tab. 3.

Tab. 3: Results of variance analysis of tracheid length properties from two localities in radial direction, from the pith to the bark.

Effect	Sum of Squares	Degree of freedom	Mean Square	F-Ratio	P-Value
Univariate tests of significance for tracheid length Sigma-restricted parameterization Effective hypothesis decomposition					
Site	24.0457	1	24.0457	1224.08	0.0000
Age (annual rings 1-34)	49.7512	3	16.5837	844.22	0.0000
Site * age (annual rings 1-34)	0.732752	3	0.244251	12.43	0.0000
Error	9.27187	472	0.0196438		

*All F-ratios are based on the residual mean square error.

The values of p-test show statistical significance each of factors. Because obtained values are less than 0.05, both factors have a statistically significant influence on tracheid length at the significance level of 95%. According to soil type and impact of climate characteristics, Veliko ratno ostrvo should be considered as more suitable for bald cypress growth and development than Bačka Palanka. Vasiljević and Hafić (1959) observed relation between tracheid width and length by fir. They concluded that this relation is changeable going from one to another tracheid. As for mentioned relation, they also found there is no significant difference between early and late wood zone. By fast-growing species, tracheids are longer in the first a few growth rings, and then they gradually become shorter (Stairs et al. 1966). This is not compatible with obtained results for bald cypress.

Some research (Seth 1981, Shiokura and Sudo 1984) established that tracheids are very short close to the core, and after that they become much longer, from the juvenile zone up to the bark. This is compatible with obtained results for tracheid length by bald cypress on both locations. By Serbian spruce (Matijević 1988), tracheids are a little bit longer – in the early wood about 4.36 mm, and in the late wood on average 4.70 mm. The longest tracheids are within Sequoia genus – even 10 mm (Vilotić 2000).

Sirvio and Karenlampi (2001) followed relation between maturation and growth rate from one side and spruce tracheids features from another side. They concluded that tracheid length rises from the pith to the bark, then that aging process contributes to tracheid localization in some part of the meristem, and finally that tracheid shape depends the most on growth rate. By bald cypress, tracheid length increases with ages, and their shape depends a lot on growth rate – in narrower growth rings, tracheids have irregular shape, while in wider growth rings, they are much more regular.

Frimpong-Mensah (1987) found that tracheids are longer by species with a low growth rate compared to these with a high growth rate, even though there are some different results.

Axial tracheids distribution by bald cypress is usually in radial strings, that is similar to tracheids distribution by fir from Veliki Jastrebac mountain (Vilotić 1992a).

Lim and Soh (1997) established by pines that tracheids reduction occurs as a result of, not only decreased length of initial cells, but also because of decreased rate of stem growth.

Measured tracheid length by spruce (Bergqvist et al. 1997), showed that length of undamaged tracheids varies between 2.77 and 3.00 mm. In this research by bald cypress, an average tracheid length goes up to 4 mm, while minimal values are much lower compared to spruce.

Research conducted on five Canadian woody species (Fujiwara and Yang, 2000), that was related to correlation between tracheid length and growth rings width, established that wider growth rings caused longer axial tracheids. Variation of tracheid dimensions can indicate short term intensity variation of some ecological factors (Vysotskaya and Vaganov1989), while water availability plays a very important role in tracheid length increasing (Abe and Nakai 1999). This coincides with results obtained for bald cypress – much longer tracheids of early wood are present in Veliko ratno ostrvo, whose soil texture is very suitable for useful water capacity increasing (Jokanović 2016).

There was established that latewood tracheids by bald cypress are a bit longer in Bačka Palanka, that can be related to narrower growth rings that affect greater latewood proportion. Ištok et al. (2017) established increasing of wood fibres length by white poplar going from the pith to the bark. All mentioned results completely coincide with tracheid length behaviour depending on cambial age by bald cypress. Jokanović et al. (2017) concluded that latewood proportion is related to site conditions less suitable for bald cypress growth that finally affects narrower growth rings forming. It was also found that radial increment depends a lot on physical and chemical soil features and on quantity of available water (Jokanović et al. 2018).

CONCLUSIONS

Based on obtained results for tracheid length by bald cypress on two alluvial sites in Serbia, we can deduce that medium tracheid length is greater by early- than by latewood tracheids.

It should be emphasized the difference was not so obvious in Bačka Palanka. In Bačka Palanka, at 0.3 m an average values of tracheid length were the same (1.69 mm), while at 1.3 m latewood tracheids were a bit longer (1.80 mm), than in earlywood (1.68 mm). As for Veliko ratno ostrvo earlywood tracheids were much longer at both heights (2.49 mm at 0.3 m and 2.81 mm at 1.3 m), than latewood tracheids (1.02 mm at 0.3 m and 0.95 mm at 1.3 m).

An average tracheid length in early wood was characterized by gradual increasing with stem height at both localities. As for Veliko ratno ostrvo, at both heights, there was established gradual increasing of earlywood tracheid length going from the pith to the bark. The same relation was also found in latewood zone apart from a few final growth rings with reducing of tracheid length not depending on stem height. In Bačka Palanka, in earlywood at both heights, tracheids gradually become longer with cambial age with a weak reducing of these values in the final growth rings.

As for latewood zone in the same locality, the longest tracheids are situated in the final growth rings. Tracheid length depends the most on zone where sampling was performed – in earlywood tracheids are much longer in Veliko ratno ostrvo, unlike Bačka Palanka with a small advantage of latewood tracheids. Site conditions are much more suitable in Veliko ratno ostrvo that finally affects faster radial increment and forming of longer tracheids.

Based on all above mentioned, we can conclude that much more attention has to be paid to bald cypress in Serbia because of its, not only decorative, but also forestry importance. Bearing on mind its tracheid length that is greater than by many autochtonous conifers, bald cypress should be much more used for wood utilization purposes.

REFERENCES

1. Abe, H., Nakai, T., 1999: Effect of the water status within a tree on tracheidmorphogenesis in *Cryptomeria japonica*. Trees 14: 124-129.

2. Bergqvist, G., Bergsten, U., Ahlqvist, B., 1997: Effects of radial increment core diameter on tracheid length measurement in Norway spruce. Wood Science and Technology 31(4): 241-250.

3. Franklin, G. L., 1945: Preparation of thin-wood sections of synthetic resins and wood-resin composites, and a new macerating method for wood. Nature 155: 51.

4. Frimpong-Mensah, K., 1987. Fibre length and basic density variation in the wood of Norway spruce (*Picea abies* L Karst) from northern Norway. Communications of the Norwegian Forest Research Institute 40 (1): 1-25.

5. Fujiwara, S., Yang, K.C., 2000: The relationship between cell length and ring width and circumferential growth rate in five Canadian species. IAWA Journal 21(3): 335-345.

6. Günthardt-Goerg, M. S., Kuster, T. M., Arend, M., Vollenweider, P., 2013: Foliage response of young central European oaks to air warming, drought and soil type. Plant Biology 15: 185-197.

7. Ištok, I., Šefc, B., Hasan, M., Popović, G., Sedlar, T., 2017: Fiber characteristics of white poplar (*Populus alba* L.) juvenile wood along the Drava river. Drvna Industrija 68(3): 241-247.

8. Ivanišević, P., 1993: Uticaj svojstava zemljišta na rast ožiljenica: *Populus euramericana* Guinier (Dode) cl. I-214 i *Populus deltoides* Bartr. cl. I 69/55. Doktorska disertacija Šumarski fakultet, Univerzitet u Beogradu, (In English: Influence of soil properties on growth of cuttings: *Populus euramericana* Guinier (Dode) cl. I-214 and *Populus deltoides* Bartr. cl. I 69/55), Pp 1-206.

9. Jacobsen A.L., Agenbag L., Esler K.J., Pratt R.B., Ewers F.W., Davis S.D., 2007: Xylem density, biomechanics and anatomical traits correlate with water stress in 17 evergreen shrub species of the Mediterranean-type climate region of South Africa. Journal of Ecology 95: 171-183.

10. Jokanović, D. 2016: Anatomical characteristics of *Taxodium distichum* (L.) Rich. on alluvial sites in Serbia. Doctoral dissertation, Faculty of Forestry – Belgrade University, Pp 1-203.

11. Jokanović, D., Vilotić, D., Nikolić, V., Nonić, M., Devetaković, J., Stanković, D., 2017: Latewood proportion inside growth rings by bald cypress stems in Serbia. Fresenius Environmental Bulletin. 26 (12 A): 7925-7930.

12. Jokanović, D., Vilotić, D., Nikolić, V., Šijačić-Nikolić, M., Lakušić, B., Jović, Đ., 2018: Growth rings width of bald cypress stems from two alluvial sites in Serbia. Fresenius Environmental Bulletin 27 (1): 306-312.

13. Lim, D.O. and Soh, W.Y., 1997: Cambial development and tracheid length of dwarf pines (*Pinus densiflora* and *P.thunbergii*). IAWA Journal 18 (3): 301-310.

14. Luostarinen,K., Hakkarainen, K., Kaksonen, H., 2017: Connection of growth and wood density with wood anatomy in downy birch grown in two different soil types, Scandinavian Journal of Forest Research 32 (8): 789-797.

15. Matijević, B., 1988: Anatomska građa drveta *Picea omorika* (Pančić) Purkyne sa lokaliteta Crvene stene – Tara. In: Monography „Flora of the National Park Tara". Bajina Bašta, (In English: Anatomy structure of *Picea omorika* (Pančić) Purkyne timber from Crvene stene locality – Tara), pp. 557-561.

16. Pekeč, S., 2010: Pedološke i hidrografske karakteristike zaštićenog dela aluvijalne ravni aluvijuma u Srednjem Podunavlju. Doktorska disertacija, Poljoprivredni fakultet, Univerzitet u Novom Sadu, Novi Sad, (In English: Pedological and hydrographic characteristics of the protected part of the alluvial site of alluvium in the Central Danube region), Pp 1-212.

17. Popović, V., 2014: Procena genetskog potencijala taksodijuma (*Taxodium distichum* (L.) Rich.) u semenskoj sastojini kod Bačke Palanke. Doktorska disertacija, Faculty of Forestry – Belgrade University, (In English: Assessment of bald cypress (*Taxodium distichum* (L.) Rich.) genetic potential in seed stand near Backa Palanka), Pp 1-205.

18. Seth, M. K., 1981: Variation in tracheid length in blue pine (*Pinus wallichiana* A.B. Jackson). Part 2: Radial pattern of variation in tracheid length in the first-formed earlywood from pith to bark. Wood Science and Technology 15: 275-286.

19. Shiokura, T., Sudo, S., 1984: The classification of juvenile wood and its perimeter in coniferous trees. Proceedings, Pacific Regional Wood Anatomy Conference, October 1-7, Tsukuba, Ibaraki, Japan, Pp 76-78.

20. Sirvio, J., Karenlampi, P., 2001: The effects of maturity and growth rate on the properties of spruce wood tracheids. Wood Science and Technology 35 (6): 541-554.

21. Stairs, G.R., Marton, R., Brown, A.F., Rizzio, M., Petrik, A., 1966: Anatomical and pulping properties of fast-and-slow-grown Norway spruce. Tappi Journal 49 (7): 296-300.

22. Tucović, A., Ocokoljić, M., 2005: *Taxodium ascendens* Brongn. – alohtona vrsta četinara u Srbiji. (In English: *Taxodium ascendens* Brongn. – Allochthonous conifer species in Serbia). Glasnik Šumarskog fakulteta 92: 159-166.

23. Vasiljević, S., Hafić, V., 1959: Istraživanje radijalne širine traheida kod *Picea excelsa* L. i *Abies pectinata* DC. Glasnik Šumarskog fakulteta, (In English: Examination of radial width of tracheids in *Picea excelsa* L. and *Abies pectinata* DC.), Pp 363-379.

24. Vidaković, M., 1982: Četinjače, Familija Taxodiaceae, JAZU, Zagreb, pp. 604-608.

25. Vilotić, D., 1992: Anatomical structure of trees Virginia Live Oak (*Quercus virgiliana* Ten./Ten.) at different sites of the Deliblato sand. PhD, University of Belgrade, Faculty of Forestry, Belgrade, Serbia, Pp 1-117.

26. Vilotić, D., 1992a: Anatomska građa debla jele (*Abies alba* Mill.), In: Monografija „Flora severnog dela Velikog Jastrepca". Kruševac, (In English: Anatomical structure of fir trunks (*Abies alba* Mill.) In: Monography "Flora of northern part of Veliki Jastrebac"), Pp 350-351.

27. Vilotić, D., 2000: Uporedna anatomija drveta, Šumarski fakultet – Univerzitet u Beogradu, (In English: Comparative wood anatomy), Pp 1-176.

28. Vilotić, D., Knežević, M., 1994: Study of Virginia Live Oak (*Quercus virgiliana* /Ten./ Ten.) width of vessel elements at different sites of the Deliblato sand. The Deliblato sands – Proceedings VI (2): 299-306, Belgrade.

29. Vilotić, D., Popović, J., Mitrović, S., Šijačić-Nikolić, M., Ocokoljić, M., Novović, J., Veselinović, M., 2015: Dimensions of mechanical fibres in *Paulownia elongata* S.Y. Hu Wood from different habitats. Drvna Industrija 66 (3): 229-234.

30. Vysotskaya, L.G., Vaganov, E.A., 1989: Components of the variability of radial cell size in tree rings of conifers, IAWA Bulletin10 (4): 417-426.

Dušan Jokanović*, Dragica Vilotić, Vesna Nikolić Jokanović, Sara Lukić
Belgrade University
Faculty of Forestry
Kneza Višeslava 1
11030 Belgrade
Republic of Serbia
*Corresponding author: dusan.jokanovic@sfb.bg.ac.rs

Tatjana Ćirković-Mitrović
Institute of Forestry
Kneza Višeslava 3
11030 Belgrade
Republic of Serbia

PAPER SUBSTRATES FOR INKJET PRINTING OF UHF RFID ANTENNAS

Juraj Gigac, Mária Fišerová, Maroš Kováč, Monika Stankovská
Pulp and Paper Research Institute Bratislava
Slovak Republic

ABSTRACT

Conventional papers are not suitable for printed electronics because they have a rougher surface than the plastic film commonly used for electronics printing. The paper surfaces were modified by coating and calendering processes to reduce surface roughness and electrical resistance of inkjet-printed UHF RFID antennas. The composition of coatings, the main component which included aluminum oxide pigment, had an influence on the surface roughness, the surface pore content and the electrical resistance of the inkjet-printed UHF RFID antennas on coated papers. Papers coated with a mixture containing 25% polyvinyl alcohol binder in combination with the cationic polymer PDADMAC without glyoxal crosslinker had the lowest surface roughnesses and the lowest electrical resistances of the inkjet-printed antennas. As the coating basis weight increased, the electrical resistance of the antennas increased. Reduction of the electrical resistance of the antennas was achieved after calendering coated paper. The design of the antennas had a significant effect on their electrical resistance, which increased with the length of the antenna.

KEYWORDS: Paper, coating, calendering, surface roughness, inkjet printing, RFID antenna, electrical resistance.

INTRODUCTION

The popularity of radio frequency identification (RFID) has lately increased significantly, particularly in relation to printing of antennas on paper substrates. Low-cost and recyclable paper substrates are being considered for various printed applications. RFID technology is dedicated to contactless identification of various objects. It is applied in the industry, trade, security and in almost all other socioeconomic areas. The applied RFID components have to meet various technological, environmental and, above all, low-cost requirements, because they must be integrated with various objects that are characterized by different physical properties.

RFID is an automated identification technology that consists of a reader, a reader antenna

and a tag which consists of a tag antenna and a chip. The antenna is relatively large compared to the chip size. RFID technology uses radio waves to transfer the information between the reader and the tag at distances of 2 cm up to 20 m. The RFID tag, depending on the type, may operate at different frequencies: low (LF: 125 kHz or 134 kHz), high (HF: 13.56 MHz) or ultrahigh radio frequency ranges (UHF: 860–960 MHz).

Conventional production of RFID antennas was realized by etching of metallized plastic, which is costly and environmentally unfriendly, so there is an effort to produce printed RFID antennas. Different printing technologies are used: flexography, gravure printing, inkjet printing, screen and thermal transfer printing. Different printing technologies enable different accuracy, resolution and conductive layer thickness.

Printed antennas are usually applied to different plastic films (Chin et al. 2008, Janeczek 2010, Arazna et al. 2017) or paper substrates (Melampi et al. 2007, Rida et al. 2009, Lakafosis et al. 2010, Xi et al. 2011, Zichner and Bauman 2011, Öhlund and Andersson 2012, Bollström and Toivakka 2013, Kavčič et al. 2014, He et al. 2016). There are many aspects of paper that make it an excellent candidate for a low-cost and environmentally-friendly substrate for printed electronics. The different types of paper have various density, coating, thickness, texture and dielectric properties.

Modifications of paper substrates and printing processes are required in order to obtain working electronic devices. The paper substrate for printed electronic must be compatible with all phases of the tag manufacturing process such as good printability and resistance of the sintering process and no shrinkage without cracking. Another important factors are the electrical properties of the printed paper substrate over a wide range of frequencies, temperature and humidity.

Paper has a rougher surface compared to the plastic film. Irregular surfaces and structural properties of conventional papers require higher ink consumption, allowing them to be used only for electronic components with lower resolution or print quality requirements. In order to improve printability, research of label and packaging paper production technology is aimed at improving surface smoothness and absorption properties.

Coating and calendering processes can be used to modify the paper surface. The paper surface is usually smoothed with a dispersion coating consisting of mineral pigments and organic binders. The smoothness of the paper surface depends on composition of coatings, the amount and layers of the coating and the final surface finish. Depending on the composition of the coatings, properties such as smoothness, porosity, permeability and surface energy as well as optical properties (brightness and opacity) can be varied. The surface properties of papers can be adjusted at the same time to achieve the desired functional properties, such as water, oil and grease resistance, low vapor and gas permeability, and flame retardation.

Nanoscale coating techniques including layer-by-layer and liquid flame spray coating have been studied that allow surface functionalization with significantly reduced coating amounts. Controlling the surface properties of nanoparticles is essential to achieve good performance in electronic applications (Perelaer et al. 2010).

Knowledge of the interactions between functional materials formulated and applied on paper as inks makes possible to create a paper-based substrate that can be used for printed electronics. The surface pore volume and pore size can be optimized for a given printing process and ink through a choice of pigment type and coating layer thickness. The printing of functional inks on paper offers the possibility of light weight, thin film electronic devices that increase the value of the product and reduce the overall cost of implementation. One application for such technology is the printing of RFID antennas directly to packaging materials.

Pigment shape, size and size distribution have a significant impact on coating coverage. The pigment structure and particle shape are the key parameters that control the coverage, porosity and ink absorption of the coated substrate. The binder is an important part of the coating formulation because it not only imparts strength to the coating layer, but it also impacts the porosity, ink absorption, and optical properties of the coating (Lehtinen 2000).

Colour gamut area, black ink optical density, print sharpness, porosity, surface wetting by water and inkjet ink, base fibrous matrix and surface roughness were used for evaluation of inkjet print quality. Inkjet ink contact angle is a suitable parameter for prediction of colour gamut area of inkjet paper (Gigac et al. 2015). Coating base papers with silica-based coating resulted in the best colour gamut area, print sharpness and fastness to water because of good water and cyan ink wettability of surface. Papers coated with calcium carbonate did not achieve such colour gamut area and sharpness as silica coated paper. Paper coated with coating colour of film-forming polyvinyl alcohol as binder had better colour gamut area compared to cationic starch (Gigac et al. 2016 a, b).

Inkjet printing is a digital and non-contact technique that is almost free of chemical waste and doesn't require special facilities for its use. Furthermore, the possibility of using well known substrates like paper or polymer film enables flexible, cheap and disposable device. It is ideal for fast prototyping and promises high throughput, low cost and improved environment-friendliness (Albrecht et al. 2016). The printed ink layer is thin and the particles in the ink must be very small and uniformly spread.

The inks used for electronic printing are typically made of copper and/or silver nanoparticles due to their high electrical conductivity in some kind of organic solvent and polymer coating (Dearden et al. 2004, Perelaer et al. 2006, Park et al. 2007). The polymer coating of the metal nanoparticles serves as a stabilizer the dispersed particles in the ink to prevent them from coalescing, merging into larger aggregates, and clogging the print head nozzles in the inkjet printer. Polyelectrolytes combining both electrostatic and steric stabilization effect are in general very effective stabilizers. Examples of stabilizers of Ag nanoparticles are poly(N-vinyl-2-pyrrolidone), carboxylmethylcellulose sodium salt, polynaphthene sulfonate formaldehyde condensate, Daxad 19, Disperbyk, which is a high molecular weight block copolymer with acidic affinic groups and poly(acrylic acid) salts (Kamyshny et al. 2011).

The printing of the conductive elements with metallic nanoparticle inks must be followed by an additional sintering step, usually achieved by heating to elevated temperatures. Without sintering the printed trace of the metallic particles, nano-silver ink acts as an insulator in the dried state. Sintering is the material atomic diffusion process driven by the reduction of interfacial energy between the metal particles. Densification only occurs when the distance between the centers of the particles change. Sintering not only renders the printed ink tracks conductive, but also affects the physical and electrical properties of the metal nanoparticle tracks. One major property that is linked to sintering is electrical resistance. With lower sintering temperatures, the electrical resistivity of the printed metal nanoparticle tracks can be up to 2 to 3 times lower than its theoretical bulk resistivity (Greer and Street 2007).

The silver nanoparticle-based ink for printing of electronics has been developed, having a built-in sintering mechanism, which is triggered during drying of the printed pattern (Grouchko et al. 2011). This ink is mainly a dispersion of electrosterically stabilized silver nanoparticles, together with a low concentration of destabilizer, which acts as a sintering agent and comes into action only upon drying of dispersion. The sintering agent, which can be a simple electrolyte such as sodium chloride, destabilizes the silver nanoparticles and leads to their close contact. The chloride ions replace and detach the anchoring groups of the polymeric stabilizer

from the nanoparticles surface and thus enable their coalescence and sintering. Fig. 1 illustrates the sintering process of silver nanoparticles triggered by changing the chloride ions concentration.
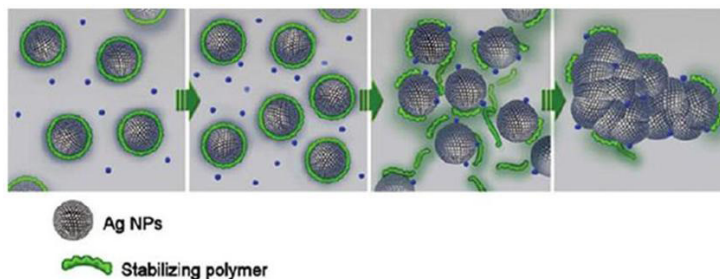
Source: Grouchko et al. 2011.

Fig. 1: Schematic illustration of stabilizer detachment, which leads to the nanoparticle sintering (the green represent the polymeric stabilizer, the blue sphere represents the sintering agent).

In this study, the effect of coating compositions on surface roughness, surface pore content and electrical resistance of inkjet-printed UHF RFID antennas on experimentally coated and calendered papers were investigated. The electrical resistance of the antennas on the paper substrates was compared to the electrical resistance of the antennas on the PET film.

MATERIAL AND METHODS

Materials
Base papers for coating experiments were commercial calendered double-sided coated offset papers (A and B).

Polyethylene terephthalate (PET) film NOVELE from NovaCentrix was used as a reference substrate for printing UHF RFID antennas.

Inkjet ink METALON JS-B25P containing Ag nanoparticles from NovaCentrix.

Antennas design for inkjet printing:

UHF RFID antenna 1 – Type DogBone, from the Smartrac division of the company Avery Dennison, compatible with chip NXP UCODE G2iL/iM or Impinj Monza 5.

UHF RFID antenna 2 – Type undefined,

UHF RFID antenna 3 – Type AD-227m5 from the company Avery Dennison, compatible with chip Impinj Monza 5.

Coatings compositions: Aerodisp W 630 (Al2O3), Mowiol 6-88 (polyvinyl alcohol – PVOH), Cartabond TSI (glyoxal), polydiallyldimethylammonium chloride (PDADMAC), Despumol (defoamer), KCl – sintering agent, glucose and ascorbic acid – reducing agents.

Methods
Coating of base papers A and B with aluminum oxide aquous dispersions was performed using bar with a wound wire of different thickness (T1 to T5).

Calendering of papers was performed by two passes in a laboratory calender Kleinewefers at a pressure of 260 kPa and a metal roller temperature of 80°C.

Wettability was determined as contact angle of water on surface of base and coated papers by

"Sessile drop" method using the tensiometer OCA 35 (Dataphysics Instruments).

Surface rougness of paper substrates was determined as optical variability of surface (OVS) using photoclinometry. Surface roughness OVS_{CLINO} was calculated as arithmetic mean of grey levels variation coefficients from machine direction $(OVS_{CLINO})_{MD}$ and cross direction $(OVS_{CLINO})_{CD}$ histograms. The surface of paper substrates was displayed by Nikon Coolpix E4500 CCD camera in macro mode. Specification of scanned images: 10° inclined illumination in machine direction (MD) and cross direction (CD), magnification X4, image size 2272 x 1704 pixels. These images can be transformed into a surface map with different heigh levels. From these images, the optical variability of surface was determined, which is defined by the light and dark (shadowed) image areas. ImageJ software was used for image analysis of paper substrate surface. It expresses the surface roughness in a similar way as the roughness parameter Rq (average surface root means squared roughness), described in ISO 4287 standard (Gigac et al. 2013).

Surface pore content of coated paper surface was determined by high magnification scanning electron microscopy (SEM). The coated paper surfaces were covered with gold in the BALZER SCD 040 sputtering device in 0.15 bar vacuum for a period of 40 s with 50 mA electric current. JEOL 760F scanning electron microscope equipped with Schottky thermo emission cathode (thermal FEG – W platting by ZrO_2) and with energy and wavelength dispersive spectrometer (Oxford Instruments) was used. Specification of scanned images: magnification X10000, accelerating voltage 2 kV, work distance 7.9 mm, image size 2530 x 1890 pixels, image resolution 0.005 μm/pixel. The software of harmonic and fractal analysis (HarFA 5.3) by couting method for image analysis was used (Gigac et al. 2013).

Antennas printing was performed with a EPSON STYLUS C88+ piezoelectric inkjet printer.

Sintering (curing) of inkjet-printed antennas was caried out at downforce of 75 kPa of the metal plate heated to 130°C for 15 seconds.

Electrical resistance of the printed antennas was measured using a multimeter UNIT-T, Model UT70B.

Viscosity of the aqueous coating composition was determined by the standard test method ASTM D 1200 – 10 (2018) by Ford Viscosity Cup.

RESULTS AND DISCUSSION

The aim of base paper coating and calendering was to improve their surface smoothness and the quality of the inkjet-printed UHF RFID antennas in order to achieve the highest electrical conductivity, respective, the lowest electrical resistance. With lower antenna resistance, a higher reading range is achieved. The overall coating result is determined by the composition and properties of the coating dispersions. The proper representation of binders and other excipients is required, a perfect dispersion of filler particles in which each particle is separated and wetted by the binder. Concentration, viscosity and rheological properties of the coating dispersions are also important.

Base papers A and B were experimentally coated with top coatings, whose basic component was an aqueous dispersion of hydrophilic micronized pigment Al_2O_3 with polyvinyl alcohol (PVOH) as a binder, glyoxal as a crosslinking agent, and a defoamer. In addition to these components, polydiallyldimethylammonium chloride (PDADMAC) was added as a high charge density cationic polymer, KCl as a sintering agent, glucose and ascorbic acid as reducing agents.

The top coating compositions used in experiments E1 to E7 for coating base papers A and B are presented in Tab. 1. Viscosity of the aqueous coating dispersions measured with the Ford 4 Cup was around 14 s, the solids content of dispersions ranged from 10 to 11% and the pH was

around 4.5. The coating basis weight on the paper varied depending on the thickness of the wound wire on the used bar (T1 to T5) when coating.

Tab. 1: Composition of top coatings in experiments 1 to 7.

Coating composition	Experiment no.						
	E1	E2	E3	E4	E5	E6	E7
Al_2O_3 – Aerodisp 630 (%)	100	100	100	100	100	100	100
PVOH – Mowiol 6-88 (%)	25	25	15	15	15	15	15
Glyoxal – Cartabond TSI (%)	2	0	2	2	3	3	3
PDADMAC - cationic polymer (%)	5	5	0	0	0	0	0
Despumol – defoamer (%)	0.01	0.01	0.01	0.01	0.01	0.01	0.01
KCl – sintering agent (%)					0.2	0.3	0.3
Glucose – reducing agent (%)				0.3			0.3
Ascorbic acid – reducing agent (%)					0.3	0.4	

Influence of coating compositions on surface roughness and surface pore content

The purpose of coating hydrophobic base papers with a contact angle of more than 90° was to increase the wettability and smoothness of the paper surfaces and improve inkjet printing quality using ink with silver nanoparticles. The formulation of coating compositions was based on the results of our previous work (Gigac et al. 2014, Gigac et al. 2015). Optimal inkjet printing quality is achieved if the paper surface is capable of rapidly absorbing solvent (water) from the ink and Ag nanoparticles remain anchored to the surface. This was achieved with coating pigments based on aluminum oxide, silica and precipitated calcium carbonate. The presence of large pores allowed rapid absorption of the ink solvent. The large surface area of pigment with the fine pores in combination with the cationic polymer PDADMAC allowed the fixation of Ag nanoparticles on the surface. In addition, the smoothed surface of the coated paper allowed the inkjet ink to spread evenly.

The surface roughnesses and surface pore contents of uncoated and coated papers A and B with top coatings are listened in Tab. 2. The influence of the coating basis weight and the calendering process on the surface roughness is presented as well. The compositions of top coatings are in Tab. 1. The surface roughness of paper was determined as the optical variability of the surface using the photoclinometric method and the surface pore content was determined by SEM microscopy. The surface roughness of base paper B was lower (6.5%) than base paper A (7.8%). The surface roughnesses of coated papers A were reduced to values of 5.3 to 6.1%, which represents a reduction of 22-32%. The surface roughnesses of coated papers B reduced to of 5.5 to 6.2%, this represents a reduction of 5-15%. The surface roughnesses decreased more after coating of base paper A than base paper B. The surface roughness was reduced more after coating of base paper with higher surface roughness.

Increased coating basis weight on both types of coated papers increased the surface roughness or reduced the surface smoothness, respectively. The surface roughness of coated paper A-E6-T2 with the coating basis weight of 2.4 $g \cdot m^{-2}$ was higher (6.1%) than the surface roughness of coated paper A-E6-T1 with half coating basis weight (5.6%). Similarly, the surface roughness of coated paper B-E7-T4 with a coating basis weight of 4.8 $g \cdot m^{-2}$ was higher (6.0%) than the surface roughness of coated paper B-E7-T2 with half coating basis weight (5.7%).

After calendering, the surface roughness of both coated paper types was reduced. The surface roughness of coated paper A-E7-T4 decreased from 5.7 to 5.1% CAL-A-E7-T4. Similarly, the surface roughness of coated paper B-E7-T4 decreased from 6.0 to 5.4% CAL-B-E7-T4.

The effect of base papers A and B coating as well as the calendering of coated papers on the surface pore content is presented in Tab. 2. The surface pore content of base paper B (19.4%) was higher than that of base paper A (15.4%). After coating, the surface pore content increased for both types of base papers. The surface pore contents of coated papers A were in the range of 20.9% to 23.9%, which represents an increase of 36 - 55% after coating. The coated papers B had surface pore contents in the range of 22.6% to 25.0%, which represents an increase of 16 - 29.0% after coating.

Tab. 2: Effect of base papers A and B, coating compositions and calendering of coated papers on surface roughness and surface pore content.

Coating experiments	Base paper A		Base paper B	
	Surface roughness (%)	Surface pore content (%)	Surface roughness (%)	Surface pore content (%)
Base paper	7.8	15.4	6.5	19.4
E1-T1	5.7	22.3	6.0	23.0
E2-T1	5.4	20.9	5.5	22.6
E3-T5	5.4	22.4	5.7	23.6
E4-T5	5.3	21.1	5.6	24.5
E5-T4	6.0	23.5	6.2	24.9
E6-T1	5.6	23.4	5.7	25.0
E6-T2	6.1	23.0	6.2	24.2
E7-T2	5.4	23.9	5.7	24.5
E7-T4	5.7	22.9	6.0	23.5
CAL-E7-T4	5.1	22.4	5.4	22.9

The quality of coating depends on the base paper, the coating composition and the coating basis weight. An inappropriate combination of base paper and coating composition causes cracking of surface already also even at lower coating basis weights.

The surface roughness of the base paper had an effect on the surface roughness of the coated papers. After coating a base paper with a higher surface roughness, the surface roughness decreased more compared to a base paper with a lower surface roughness. After coating of base papers with the same coating compositions, the surface roughnesses of the coated papers A were lower than that of coated papers B.

Similarly as the surface roughness also the surface pore content of the base paper had an influence on the surface porosity of the coated papers. After coating a base paper with a lower surface pore content, the surface pore content increased more compared to a base paper B with a higher surface pore content. After coating base papers with the same coating compositions, the surface pore contents of the coated papers A were lower than the coated papers B.

Influence of coating compositions on electrical resistance of UHF RFID antennas

UHF RFID antennas were inkjet-printed on base papers A and B, coated papers and PET film. The designs of antennas are presented in Fig. 2. The electrical resistance of inkjet-printed antennas was measured after drying and sintering as the antennas must be conductive.
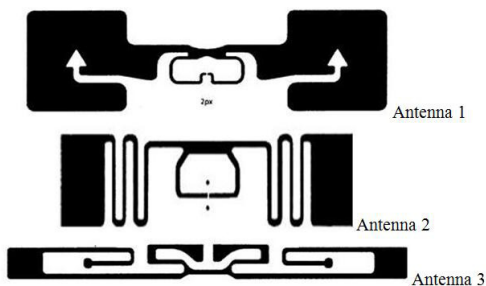
Fig. 2: UHF RFID antennas designs.

Figs. 3 and 4 compare the electrical resistances of UHF RFID inkjet-printed antennas on base and coated papers with antennas printed on commercial PET film, which is a suitable substrate for printing UHF RFID antennas. The top coating compositions used in experiments (E1 to E7) are shown in Tab. 1. Antenna 1 printed on PET film had an electrical resistance of 2.5 Ω, antenna 2 of 20 Ω, and antenna 3 of 8.5 Ω. The antennas printed on base papers A and B had significantly higher electrical resistances compared with antennas printed on PET film, what is related to the hydrophobic and rough surface of the paper. The antennas printed on base paper A had lower electrical resistances (Fig. 3) than the antennas on base paper B (Fig. 4).
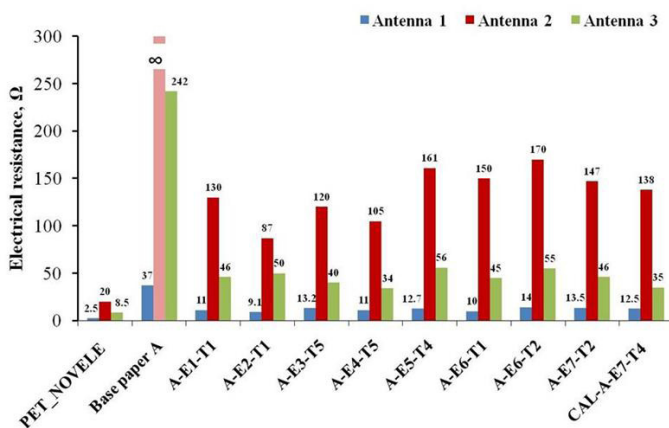

Fig. 3: Comparison of electrical resistances of inkjet-printed UHF RFID antennas on base paper A and coated papers with antennas printed on PET film.

After coating of base papers A and B, the electrical resistance of the antennas decreased significantly (Figs. 3 and 4) but did not reach the level of the antennas on the PET film. Reducing the electrical resistance of the antennas allowed a hydrophilic and less rough surface of the coated papers compared to base paper. A comparison of the electrical resistances of the antennas shows that in this case, the electrical resistances of the antennas printed on coated papers A were also lower than the electrical resistances of the antennas printed on coated papers B.

Antennas printed on A-E2-T1 and B-E2-T1 papers coated with the composition containing 25% binder PVOH in combination with a cationic polymer PDADMAC without of glyoxal crosslinking agent had the lowest electrical resistance. The beneficial effect of the cationic

polymer PDADMAC on the electrical resistance of antennas printed with Ag nanoparticle ink has also been confirmed in the work (Magdassi et al. 2010).

The electrical resistances of antennas printed on papers A-E1-T1 and B-E1-T1 coated with the composition containing 2% glyoxal were higher than electrical resistances antennas printed on papers A-E2-T1 and B-E2-T1 coated with the composition without glyoxal (Figs. 3 and 4).
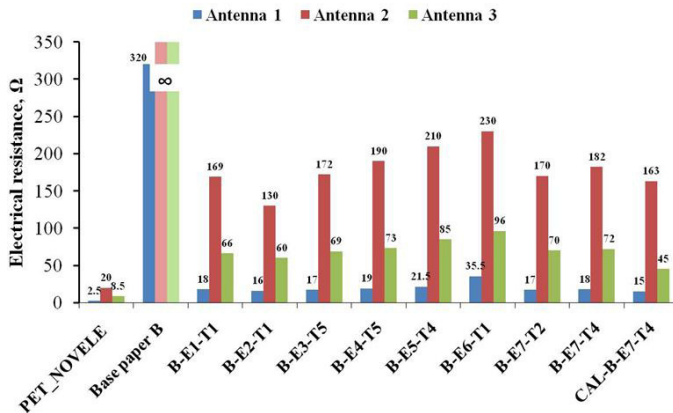

Fig. 4: Comparison of electrical resistances of inkjet–printed UHF RFID antennas on base paper B and coated papers with antennas printed on PET film.

The addition of sintering agent KCl and reducing agents glucose or ascorbic acid to the coating compositions (Tab. 1, E3 to E7) had no significant effect on the electrical resistances of the antennas printed on coated papers (Figs. 3 and 4).

The results show that antenna design has a significant effect on their electrical resistance. Antenna 1 had the lowest electrical resistance, then antenna 3, while the electrical resistance of the meander antenna 2 was considerably higher related to the longest antenna length. In Fig. 5 is an illustration of the measuring points on the antenna 2.

Fig. 5: Measurement of electrical resistance of UHF RFID antennas with UNIT-T multimeter, model UT70B.

The effect of the coating basis weight on the electrical resistances of the inkjet-printed antennas was determined based on the electrical resistances of the antennas printed on coated papers A-E6-T1 and A-E6-T2 (Fig. 3). Antennas printed on coated paper A-E6-T1 with the coating basis weight of 1.4 $g \cdot m^{-2}$ had lower electrical resistances than antennas printed on paper

A-E6-T2, which had twice higher coating basis weight. Analogous results were obtained for coated papers B-E7-T2 and B-E7-T4 (Fig. 4). The electrical resistances of the antennas printed on coated paper B-E7-T2 with the coating basis weight of 2.8 $g \cdot m^{-2}$ were lower than the electrical resistances of the antennas printed on coated paper B-E7-T4 with a coating basis weight of 5.6 $g \cdot m^{-2}$.

The calendering process of coated papers had a positive effect on the electrical resistance of inkjet-printed antennas. Antennas printed on calendered coated paper CAL-A-E7-T4 had lower electrical resistances than antennas printed only on coated paper A-E7-T4 (Fig. 3). Similar results were obtained for antennas printed on calendered coated paper CAL-B-E7-T4, these ones had lower electrical resistances than antennas printed only on coated paper B-E7-T4 (Fig. 4).

CONCLUSIONS

Paper substrates are more advantageous for printing of UHF RFID antennas than plastic films as they are recyclable and several times cheaper. However, the surface of conventional papers is not suitable for printed electronics, as they have a rougher surface compared to plastic film, but their advantage is higher rigidity and low expansion. Reducing the surface roughness and hence the electrical resistance of the inkjet-printed antennas on papers was achieved by coating and subsequent calendering processes.

The properties of the base paper and the composition of the coatings, the main component of which was the aluminum oxide pigment, had an influence on the surface roughness, the surface pore content and the electrical resistance of the inkjet-printed antennas on the coated papers. Antennas printed on coated paper with the composition, which contained 25% PVOH binder in combination with the cationic polymer PDADMAC without glyoxal crosslinker, they had the least electrical resistance. The addition of sintering agent KCl and reducing agents glucose or ascorbic acid to the coating compositions had no significant effect on the electrical resistances of inkjet-printed UHF RFID antennas. Electrical resistance of the antennas was higher for antennas printed on paper with a higher coating basis weight.

Electrical resistances of inkjet printed UHF RFID antennas decreased after calendering of coated papers, however, as the coating basis weight on paper increased, electrical resistance of the antennas increased.

The design of inkjet-printed UHF RFID antennas on paper substrates had a significant effect on their electrical resistance, which depends on the length of the antenna and is strongly influenced by the geometric dimensions of its narrowest part.

ACKNOWLEDGMENT

REFERENCES

1. Albrecht, A., Rivadeneyra, A., Salmerón, J., Abdellah, A., Lugli, P., 2016: Inkjet printing and photonic sintering of silver and copper oxide nanoparticles for ultra-low-cost conductive patterns. Journal of Materials Chemistry C (4): 3546–3554.

2. Arazna, A., Janeczek, K., Futera, K., 2017: Mechanical and thermal reliability of conductive circuits inkjet printed on flexible substrates. Circuit World 43(1): 9-12.

3. Bollström, R., Toivakka, M., 2013: Paper substrate for preinted functionality. 15th Fundamental Research Symposium. Cambridge, September 2013, Pp 945-966.

4. Dearden, A., Smith, P., Shin, D.Y., Reis, N., Derby, B., Paul O'Brien, P., 2004: A low curing temperature silver ink for use in ink-jet printing and subsequent production of conductive tracks. Macromolecular Rapid Communications 26(4): 315-318.

5. Gigac, J., Kasajová, M., Maholányiová, M., Stankovská, M., Letko, M., 2013: Prediction of surface structure of coated paper and of ink setting time by infrared spectroscopy. Nordic Pulp & Paper Research Journal 28(2): 274-281.

6. Gigac, J., Stankovská, M., Letko, M., Opálená, E., 2014: The effect of base paper properties on inkjet print quality. Wood Research 59(5): 717-730.

7. Gigac, J., Stankovská, M., Fišerová, M., Opálená, E., 2015: Improvement of inkjet print quality via hydrophylic polymers and base paper. Wood Research 60(5): 739-746.

8. Gigac, J., Stankovská, M., Opálená, E., Pažitný, A., 2016a: The effect of pigments and binders on inkjet print quality. Wood Research 61(2): 215-226.

9. Gigac, J., Stankovská, M., Pažitný, A., 2016b: Influence of the coating formulations and base papers on inkjet printability. Wood Research 61(6): 915-926.

10. Greer, J.R., Street, R.A., 2007: Thermal Cure effects on electrical performance of nanoparticle silver inks. Acta Materialia 55 (18): 6345-6349.

11. Grouchko, M. Kamyshny, A., Mihailescu, C.F., Anghel, D.F., Magdassi, S., 2011: Conductive inks with a „built-in" mechanism that enables sintering at room temperature. ACS Nano 5(4): 3354-3359.

12. He, H., Sydänheimo, L., Virkki, J., Ukkonen, L., 2016: Experimental study on inkjet-printed passive UHF RFID tags on versatile paper-based substrates. International Journal of Antennas and Propagation, Article ID 9265159, 8 pp.

13. Chin, K.C., Tsai, C.H., Chang, L.C., Wei, C.L., Chen, W.T., Chen, C.S., Lai, S.J., 2008: Design of flexible RFID tag and rectifier circuit using low cost screen printing process. IPC - IPC Printed Circuits Expo, APEX and the Designers Summit 2008.

14. Janeczek, K., 2010: Performance of RFID tag antennas printed on flexible substrates. XII International PhD Workshop, Wisla, Poland.

15. Kamyshny, A., Steinke, J., Magdassi, S., 2011: Metal-based inkjet ink for printed electronics. The Open Applied Physics Journal (4): 19-36.

16. Kavčič, U., Pivar, M., Dokič, M., Svetec, D.G., Pavlovič, L., Muck, T., 2014: UHF RFID tags with printed antennas on recycled papers and cardboards. Materials and Technology 48(2): 261-267.

17. Lakafosis, V, Rida, A., Vyas, R., Li, Y., Nikolaou, S., Tentzeris, M.M., 2010: Progress towards the first wireless sensor networks consisting of inkjet-printed, paper-based RFID-enabled sensor tags, Proceedings of the IEEE 98 (9): 1601-1609.

18. Lehtinen, E., 2000: Pigments coating and surface sizing of paper. Papermaking Science and Technology, Vol. 11, TAPPI Press, 2000.

19. Merilampi, S., Ukkonen, L., Sydanheimo, L., Ruuskanen, P., Kivikoski, M., 2007: Analysis of silver ink bow-tie RFID tag antennas printed on paper substrates. International Journal of Antennas and Propagation, Article ID 90762, 9 pp.

20. Öhlund, T., Andersson, M., 2012: Effect of paper on electrical conductivity and pattern definition for silver nanoparticle inkjet ink. Proceedings LOPE-C, January 2012, Pp. 115-119.

21. Park, B.K., Dongjo Kim, D., Sunho, J., Moon, J., Jang Sub Kim, J.S., 2007: Direct writing of copper conductive patterns by ink-jet printing. Thin Solid Films 515 (2007): 7706-7711.

22. Perelaer, J., de Gans, B.J., Ultrich S. Schubert, U.S., 2006: Ink-jet printing and microwave sintering of conductive silver tracks. Advanced Materials 18(16): 2101-2104.

23. Rida, A., Li, Y., Vyas, R., Tentzeris, M.M., 2009: Conductive inkjet-printed antennas on flexible low-cost paper-based substrates for RFID and WSN applications. Antennas and Propagation Magazine, IEEE 51 (3): 13-23.

24. Xi, J., Zhu, H., Ye, T.T., 2011: Exploration of printing-friendly RFID antenna designs on paper substrates. 2011 IEEE International Conference on RFID, Pp 38-44.

25. Zichner, R., Baumann, R.R., 2011: Communication Quality of Printed UHF RFID transponder antennas. LOPE-C, Messe Frankfurt, Germany, Pp 361-363.

Juraj Gigac*, Mária Fišerová, Maroš Kováč, Monika Stankovská
Pulp and Paper Research Institute
Dúbravská Cesta 14
841 04 Bratislava
Slovak Republic
*Corresponding author: gigac@vupc.sk

HYGROTHERMAL EFFECT ON AXIAL COMPRESSIVE PROPERTIES OF BIONIC BAMBOO ELEMENT

Wei Yan[1,2], Wansi Fu[2], Bin Zhang[2], Jianbo Zhou[3,2]

[1]Hengshui College of Vocational Technology, Hengshui, China
[2]Beijing Forestry Machinery Research Institute of The State Forestry and Grassland Administration, Beijing, China
[3]Research Institute of Forestry New Technology, Chinese Academy of Forestry Beijing, China

ABSTRACT

Bionic bamboo element is innovative form inspired by honeycomb, and its axial compressive strength and node's contribution to strength under different environment were studied to explore the mechanical properties. Crack morphology and stress distribution were analyzed. The results indicated that, the strength of bionic bamboo element was 50.72 MPa, while the strength declined by 39.74%, 43.85% and 36.05% after being immersed in water for 30 days and hygrothermal pretreatment for 30 days and 15 days. Node had negative influence on strength due to fiber hydroscopic swelling and loose compared with the control samples, and lower humidity condition was beneficial to enhance the compressive strength, e.g. the strength of samples in humidity 20% condition for 30 days improved by 56.70% compared with the control group. Crack showed hierarchical damage with fibers' tear in length and fracture in lateral, stress distribution exhibited symmetry, and the maximum stress focused on the end of bionic bamboo element, and its thin wall was susceptible damaged. Bionic bamboo element retained the mechanical superiority of bamboo culm and promoted its recombination utilization.

KEYWORDS: Bionic bamboo element, hygrothermal environment, compressive strength, crack morphology, finite element method (FEM).

INTRODUCTION

Bamboo resource is abundant in China and its utilization has been alleviating wood shortage. Bamboo endows natural structures with excellent mechanical properties and is environment-friendly material (Zheng et al. 2014, van der Lugt et al. 2006), especially that bamboo utilization in original status not only improve sits utilization ratio but also embodies the natural structure of bamboo sufficiently (Zhou et al. 2015, Zhou et al. 2016, Yan et al. 2017a b).

Natural selection has perfected the structure and form of organisms, such as bamboo, to adapt the various environments (Yuan et al. 2017). More and more attention has been focused on mechanical research of bamboo in original status, and the utilization follows and respects the natural laws at the maximum level.

A fresh idea "bamboo recombining in original status (BROS)" has been proposed firstly by Professor Wansi Fu in 2006 (Fu and Zhou 2010a, b). The idea means that bamboo elements for recombination are processed based on a principle: natural structure of bamboo is reserved at maximum degree. The idea of BROS enriches the utilization type of bamboo and respects to nature compared with traditional bamboo products which are made of bamboo strands, bamboo strip, bamboo skin, bamboo filament and bamboo veneer.

It is a fact that honeycomb structure is typically lightweight and strength composite (Yuan et al. 2017). As one type of the BROS, bionic recombining technology of bamboo in original status which is also called multi-side bamboo recombining in original status (M-BROS) is innovative and belongs to bionic structure inspired by honeycomb (Fig. 1a).
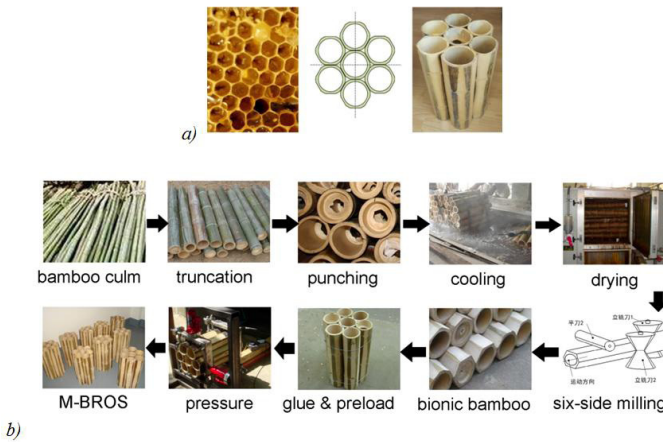
Fig. 1: Basic idea (a) and process (b) of bionic bamboo recombination.

Hexagon degree has been identified due to bamboo original features and the processing characteristic, which is a ratio of the side length (L_1) of bionic bamboo element to that (L_0) of standard hexagon with the same diameter, that is d= L_1 / L_0, and the schematic diagram is indicated in Fig. 2. Hexagon degree with 0.6 ~ 0.8 is appropriate for recombining based on previous test reports (Fu and Zhou 2010a).

Fig. 2: Schematic diagram of hexagon degree.

It is undoubted that bionic bamboo element is the most important constituent of the composite and has significantly impact on the whole mechanical property (Zhang et al. 2017a, b). Besides that, bamboo is biomaterial and its properties depend on environment temperature and humidity strongly. However, as a creative utilization type of bamboo in original status, mech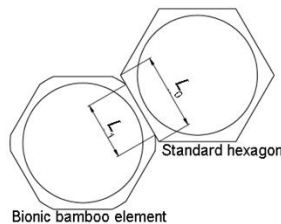anical characteristics of bionic bamboo element especially the characteristics under different temperature and humidity conditions are rarely conducted and reported. Mechanical test results of bionic bamboo element differ from that of traditional bamboo element, therefore, the purpose of this study was to explore the undiscovered mechanical property and its change regular of the bionic bamboo element under various environments, and this research will supply basic support for practical application of the late-model bamboo recombining material.

MATERIALS AND METHODS

Bamboo culm of Moso bamboo (*Phyllostachys pubescens*) which is widespread utilization was optimum to manufacture bionic bamboo element for its larger diameter class and abundant resource. Moso bamboo of 4 years age in this study was adopted from Yiyang, Hunan Province, China. The outer diameter of bamboo culm was (101.87 ± 2.32) mm which is appropriate to product bionic bamboo element (Fan et al. 2012, Liu et al. 2012, 2013), and the inner diameter was (86.07 ± 1.84) mm.

ISO 22157-1 "Bamboo-Determination of physical and mechanical properties. Part 1 Requirements." was referred for no relevant standard about hexagon bamboo element. The test specimens with length of 100 mm were taken from the similar bamboo for reducing individual differences within bamboo culms. Bamboo specimens with and without node were selected to research their axial compressive properties under different conditions.

Four test conditions with different temperature, humidity and pretreated time were set based on practical nature environment in China to conduct hygrothermal pretreatment. Specimens were divided into five groups (every group had two types of samples), and marked as A, B, C, D and E, and the number of every type in every group was no less than 10. The details are shown in Tab.1. Test specimens of group A were immerged in water for 30 days at room temperature, test specimens of group B were placed in test box environment (40°C, 90%) for 30 days, test specimens of group C were placed in test box environment (40°C, 90%) for 15 days, while the pretreatment condition of group D was temperature 40°C and humidity 20 % for 30 days. Group E was control.

Tab. 1: Pretreatment conditions of test specimens.

Group	Pretreatment condition	Temperature (°C)	Humidity (%)	Time (days)
A	Immerged in water	29 ± 1.2	-	30
B	Hygrothermal environment	40	90	30
C	Hygrothermal environment	40	90	15
D	Hygrothermal environment	40	20	30
E	Control (room environment)	22 ± 2.1	52 ± 2.3	-

Mechanical test and crack observation

Inner diameter, outer diameter and length of every test sample were measured and recorded before and after the pretreatment to calculate the deformation ratio following Eq. 1:

$$\alpha = \frac{l_2 - l_1}{l_1} \times 100 \tag{1}$$

Where: α means deformation ratio of bionic bamboo element (%); l_2 means dimension of sample after pretreatment (mm); l_1 means dimension of sample before pretreatment (mm).

Axial compressive test was conducted with the help of YH 229WG universal testing machine (Shanghai Yihuan Instrument Technology Co., Ltd., China) with a 200 kN load cell capacity. Samples were put into hermetic bag after pretreatment in order to reduce the moisture content (MC) change, and the mechanical test was accomplished within 5 min.

Compressive strength in axial was calculated referring to Eqs. 2 and 3 which were based on standard hexagon model.

$$\sigma = \frac{F}{S} \tag{2}$$

$$S = \frac{3\sqrt{3}R^2}{2} - \pi r^2 \tag{3}$$

Where, σ is compressive strength (MPa); F means the peak load (N); S means cross-section area of standard hexagon model (mm^2); R means the outer radius (mm); r means the inner radius (mm).

Correction factor of the bionic bamboo element comparing to standard hexagon element is 0.85 (Han et al. 2014), and the value has been achieved in previous study of own team.

After mechanical test, samples with typical crack were selected to be processed appropriate size within 5 x 5 x 5 mm, then the crack morphology was observed with the help of scan elastic microscope (SEM, Hitachi S-4800) after the little specimens' drying and spray-gold.

Finite element method

Axial compression of the control bionic bamboo element was emulated by ANSYS 14.0. Solid 182 was selected to establish hexagonal bamboo model which was assumed as orthogonal isotropic material (Triboulot et al. 1984, Shao 2012, Fu et al. 2013, Zhao et al. 2013, 2015).

The inner diameter, outer diameter, length and hexagon degree of the model were 90 mm, 110 mm, 100 mm and 0.76 respectively. And the mechanical parameters in the three directions (E_L, E_R, E_Z, P_{RT}, P_{TL}, P_{RL}, G_{TL}, G_{RL}) of Moso bamboo are shown in Tab. 2.

Tab. 2: Mechanical parameters of Moso bamboo.

	Elasticity modulus (GPa)			Poisson's ratio (-)			Shear Modulus (GPa)		
	E_L	E_R	E_Z	P_{RT}	P_{TL}	P_{RL}	G_{RT}	G_{TL}	G_{RL}
Bamboo (Bai et al. 1999)	10.35	0.50	0.69	0.308	0.023	0.019	0.29	0.90	0.83

Subsequently, the model was meshed by free triangle, then the press strength 50.71 MPa obtained by practical experiment was set on one end of the bionic bamboo model, while the other end was set displacement constraint. X and Y directions were radial direction of bionic bamboo element, and Z direction was the grain orientation, details of the model are shown in Fig. 3. Finally, results of stress and strain were achieved after solution operation and indicated by nephogram.
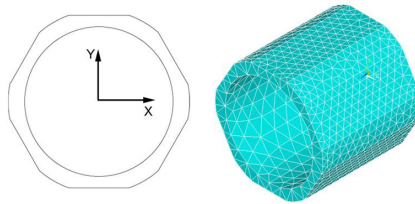
Fig. 3: Modeling of bionic bamboo element with Finite Element Method.

RESULTS AND DISCUSSION

Deformation analysis

Dry shrinkage and wet expansion characteristics are the intrinsic characteristics of bamboo for the existence of hydroxyl (-OH) in cellulose, hemicellulose and lignin, so deformation occurs when bamboo is put in different temperature and humidity environments. Change ratio of specimen's deformation was analyzed and compared, as shown in Fig. 4.

It was found that the change ratio of outer diameter of bionic bamboo element of every pretreatment group was the maximum, followed by inner diameter, and the deformation of length was the minimum. Samples' deformation of group A was the most evident, the average change ratio of their outer diameter, inner diameter and length were 3.35%, 1.92% and 0.57% respectively.

The dimension turned larger when samples were put in high humidity environment, while the shrinkage occurred when samples were set in lower humidity, e.g. deformation of bionic bamboo elements in group D. It was observed that higher humidity or lower humidity means more obvious dimension deformation at the same temperature.
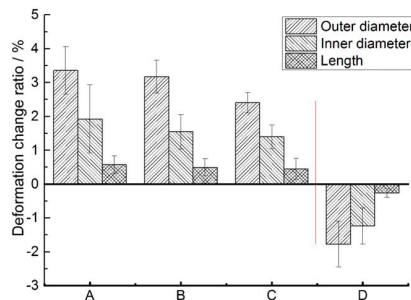
Fig. 4: Deformation change ratio of bionic bamboo element under different conditions.

Node impact on compressive strength

Node has important influence on bamboo growth and its mechanical properties (Liese 1998). It is a fact that node enhances axial compressive property of bamboo culm which is not pretreated, while no significant difference exists in bamboo culm specimens with and without node (Shao et al. 2008, Oka et al. 2014). However, it was observed that bionic bamboo element with and without node showed different characteristics after various pretreatment, and the strength comparison is indicated in Fig. 5. Compressive strength of bionic bamboo elements in control one (group E) was consistent with the predication (Shao et al. 2008, Oka et al. 2014).

In group E, axial compressive strength of samples with node was larger than that of samples without node, and difference of compressive strength between the two types was not significant (sig. > 0.05), as shown in Tab. 3. While compressive strength of samples with and without node in group C and D showed the same regularity with the control group.
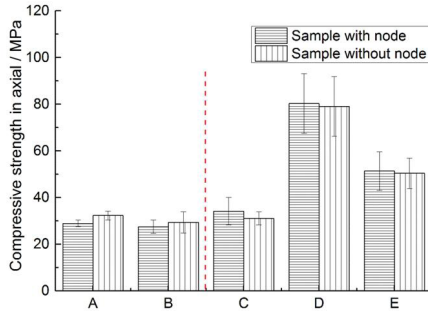

Fig. 5: Compressive strength of bionic bamboo element with and without node.

However, the mechanical property of bionic bamboo element in group A and B displayed opposite law, superior compressive property was showed by bionic bamboo element without node.

Tab. 3: Independent-sample t test of five groups.

		Levene's test for quality of variances				T-test for equality of means				
		F	Sig.	t	df	Sig. (2-tailed)	Mean difference	Stand errors	95% Confid. interval	
									Lower	Upper
A	Equal variances assumed	0.584	0.467	-3.204	8	0.013	-4.02342	1.25560	-6.91883	-1.12800
	Equal variances not assumed			-3.204	7.458	0.014	-4.02342	1.25560	-6.95591	-1.09093
B	Equal variances assumed	0.434	0.527	-0.810	9	0.439	-2.21936	2.73880	-8.41498	3.97624
	Equal variances not assumed			-0.847	8.462	0.420	-2.21936	2.62068	-8.20566	3.76694
C	Equal variances assumed	3.419	0.097	1.161	9	0.275	3.64552	3.13973	-3.45703	10.74808
	Equal variances not assumed			1.087	5.425	0.323	3.64552	3.35300	-4.77427	12.06531
D	Equal variances assumed	0.041	0.847	0.133	6	0.898	1.46958	11.02873	-25.51675	28.45591
	Equal variances not assumed			0.133	4.356	0.900	1.46958	11.01486	-28.15246	31.09162
E	Equal variances assumed	3.210	0.111	0.164	8	0.974	1.78939	10.93284	-23.42178	27.00055
	Equal variances not assumed			0.200	5.740	0.848	1.78939	8.93931	-20.32694	23.90572

Particularly, the compressive strength of samples with and without node in group A were 37.97 MPa and 33.94 MPa, and significant difference was indicated (sig. < 0.05). While compressive strength difference of samples with and without node in group B was not significant (sig. > 0.05). It could be deduced that pretreatment time will obviously change the mechanical property difference of bamboo with and without node by comparing pretreatment conditions of group A and B, and this will provide important guidance for bamboo utilization in nature environment.

The mechanical difference between groups may be induced by the fact that fibers in vascular bundles and ground tissues in bamboo wall turned swelled and loose for absorbing water molecule in a long time (30 days). The swelling of bionic bamboo element resulted in weaker binding force between fibers, and further led to the compressive strength decline. It is a fact that vascular bundles within bamboo node are short and twisty (Liese 1998), so as to fibers' binding force of the node part dropped more easily than that of the internode.

Different conditions impact on axial compression

As biomaterial, bamboo is sensitive to environmental temperature and humidity, these results in its strength change with various environments. Compressive strength in axial of bionic bamboo element and the compressive deformation ratio after mechanical damage were calculated and analyzed, the results are displayed in Fig. 6. It was clear that the strength of groups A, B and C were lower than that of control samples of group E, while the strength of group D was more excellent than that of the control one. The strength of group E was 50.72 MPa, and the strength of group A, B, C were 30.56 MPa, 28.48 MPa and 32.43 MPa respectively and strength loss ratio were 39.74%, 43.85% and 36.05% successively, while the strength of group D was improved by 56.70% compared with the control group.
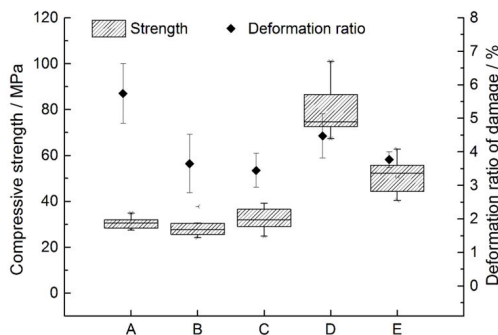

Fig. 6: Axial compressive strength of bionic bamboo element under different conditions.

It was also found that all the strength of pretreated groups taken place significant difference (sig. < 0.05) compared with the control one, as shown in Tab. 4. While the difference within groups A, B and C was not significant (sig. > 0.05).

Tab. 4: Significant difference analysis of compressive strength in axial of every sample.

(I) Group	(J) Group	Mean difference (I-J)	Stand errors	Significant	95% Confidence interval	
					Lower	Upper
A	B	2.08237	3.59770	0.566	-5.1638	9.3285
	C	-1.87112	3.59770	0.606	-9.1173	5.3750
	D	-48.91358*	3.90574	0.000	-56.7801	-41.0470
	E	-14.74908*	3.68237	0.000	-22.1657	-7.3324
B	A	-2.08237	3.59770	0.566	-9.3285	5.1638
	C	-3.95349	3.51100	0.266	-11.0250	3.1180
	D	-50.99595*	3.82602	0.000	-58.7019	-43.2899
	E	-16.83145*	3.59770	0.000	-24.0776	-9.5853
C	A	1.87112	3.59770	0.606	-5.3750	9.1173
	B	3.95349	3.51100	0.266	-3.1180	11.0250
	D	-47.04246*	3.82602	0.000	-54.7485	-39.3365
	E	-12.87796*	3.59770	0.001	-20.1241	-5.6318
D	A	48.91358*	3.90574	0.000	41.0470	56.7801
	B	50.99595*	3.82602	0.000	43.2899	58.7019
	C	47.04246*	3.82602	0.000	39.3365	54.7485
	E	34.16450*	3.90574	0.000	26.2979	42.0311
E	A	14.74908*	3.68237	0.000	7.3324	22.1657
	B	16.83145*	3.59770	0.000	9.5853	24.0776
	C	12.87796*	3.59770	0.001	5.6318	20.1241
	D	-34.16450*	3.90574	0.000	-42.0311	-26.2979

Note: * difference was significant at level 0.05.

Besides that, deformation ratio of bionic bamboo element after test had been discussed. The average ratio of group E was 3.77%, and the value of group A and group D were larger than that of the control one, this means more toughness of the two group samples. However, the damage deformation ratio of group B and group C were smaller than that of group E, which means the lower strength and weak deformability, this may be induced by high moisture content (MC) and mould of bamboo. It was concluded that conditions play important roles in mechanical capacity of bionic bamboo element.

Crack morphology

As we known, crack is always companied with mechanical test. It was observed that two kinds of crack were occurred in bionic bamboo element, the microscopic images are exhibited in Fig. 7. Crack was propagated along the fiber length, seriously, the fiber was fractured, as marked by arrows in Fig. 7a. While the crack in lateral was different with that, ground tissue of bamboo was fractured with flat edge, conversely, the vascular bundle damage was up faulted only with few destroyed fibers, as indicated in Fig. 7b.

Fracture of bamboo is failure process of intricate interplay of multiple damage modes (Shao et al. 2012), it was concluded that hierarchical structure of bamboo was beneficial to enhance its mechanical properties.
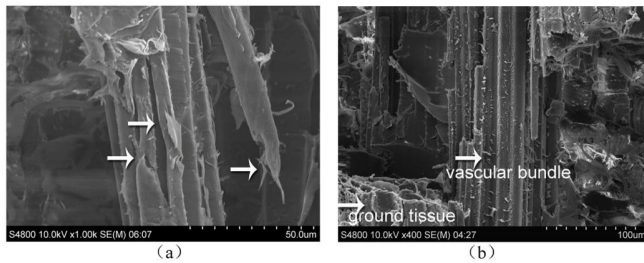
Fig. 7: Morphology of crack in grain orientation (a) and lateral direction (b).

Finite element method (FEM) modelling

Results of FEM on axial compression of bionic bamboo element are indicated by stress and strain nephogram in Fig. 8. Stress component in six directions (X, Y, Z, YZ, XZ and XY) were symmetrical distribution, and shear stress was consisted of tensile stress (positive value in nephogram) and compressive stress (negative value nephogram). Larger stress was appeared on the end of bionic bamboo element, and stretched to the middle part. The maximum stress in X, Y and Z directions were 1.6 MPa, 1.9 MPa and 55.8 MPa respectively. Stress difference in radial and grain direction was the manifestation of bamboo anisotropy.

It was found that strain distribution was according with stress nehpogram, and exhibited symmetry. As shown in Fig. 8b, tensile and compressive strain in six directions was not uniform, and the minimum strain occurred on the thicker part of bamboo wall.

Besides that, Von Mises stress and Von Mises strain were also analyzed in this study, as shown in Fig. 9 and Fig. 10.

The Von Mises stress nephogram of bionic bamboo element in Fig. 9a indicated that the maximum stress was 53.9 MPa which was in the end part. While bamboo culm was introduced, as shown in Fig. 9b, to compare the stress distribution with that of bionic bamboo element. Similarly, the maximum stress of bamboo culm taken place on the end part, and the value was 53.0 MPa. This indicated that no obvious difference of axial compressive strength existed between bionic bamboo element and bamboo culm, and the finding was consistent with the practical experimental results (Han et al. 2014).
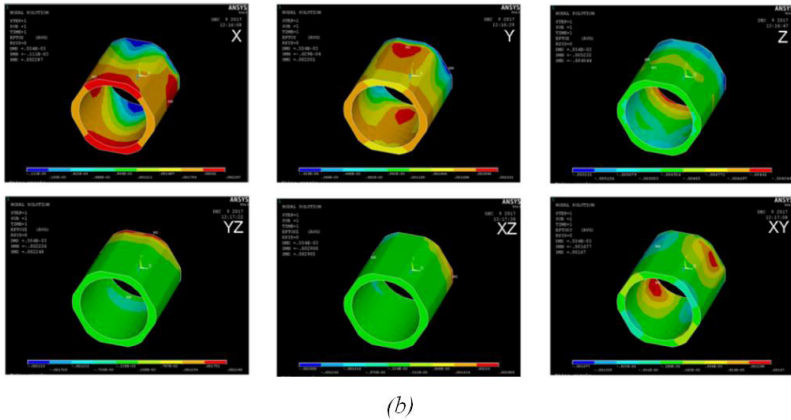

(a)

(b)
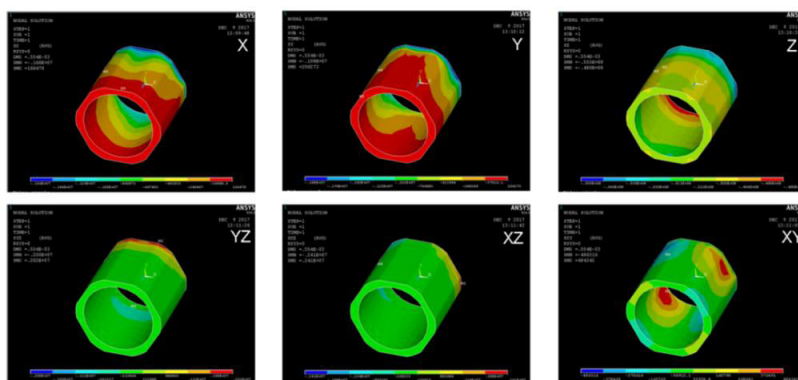
Fig. 8: Stress distribution (a) and strain distribution (b) of bionic bamboo element under axial compression.
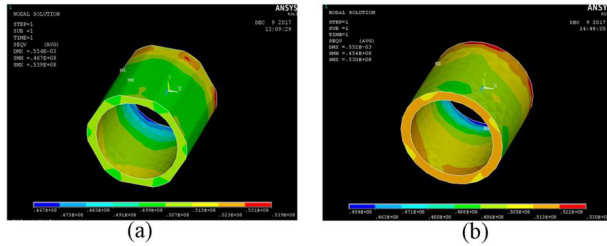
Fig. 9: Von Mises stress of bionic bamboo element (a) and bamboo culm (b).

Deformation of bionic bamboo element is shown in Fig. 10a, it was clear that length of the model was shortened and the circumferential size was expanded. The Von Mises strain comparison of bionic bamboo element (Fig. 10b) and bamboo culm (Fig. 10c) indicated that the strain in the thin wall of bionic bamboo was spread along the length direction, this phenomenon was consistent with practical compressive damage of bionic bamboo element.
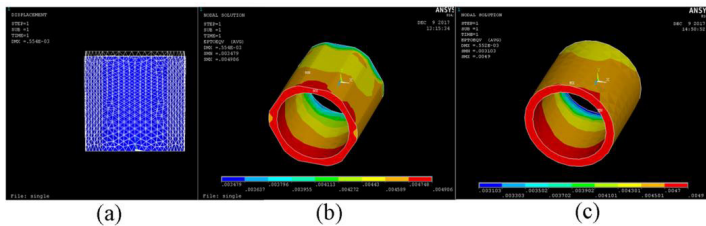
Fig. 10: Deformation and Von Mises strain of bionic bamboo element (a, b), bamboo culm (c).

The stress and strain difference of bionic bamboo element and bamboo culm showed that hexagonal bamboo technology was reasonable and meaningful. The technology is innovative and significant, and retains the mechanical superiority of bamboo culm and promoted its recombination utilization at the same time.

DISCUSSION

Bamboo is composed of many vascular bundles embedded in ground tissue, and the arrangement of vascular bundles in internode is parallel to axis, while the arrangement is horizontal and twisty in node and its vascular bundles is smallish (Liese 1998). It could be deduced that the structure difference of internode and node is crucial reason for that bamboo specimens with node or without node show contrastive properties under high humidity conditions. It should be noted that contribution of node to compressive strength will change when its serving in different environment especially the humidity varied. This property is critical to guidance practical utilization of bamboo and ensures the security and stability of load-carrying bamboo artifacts.

It is a fact that plentiful hydroxyl (-OH) of cellulose, hemicellulose are the main absorption points of moisture, which will lead to bamboo deformation and even fiber soften, and further reduce the resistance to compression. The founding that axial compressive strength of bionic bamboo element was declined after high humidity pretreatment is consistent with Xu's report (Xu et al. 2014). Higher moisture content of bamboo leads to greater toughness, and the strength of bamboo showed transition from rigidity to toughness by comparing the damage deformation ratio of bionic bamboo element after undergoing different pretreatment conditions. As we known, many starch granules exist in the cell lumen of bamboo (Liese 1998), and the nutriment easily leads to mildew, this may also contribute to more strength decrease under higher humidity environment. All these suggest that bamboo protection is indispensable in practical application to avoid strength decline at the most extent.

The unique structure of bamboo culm is evolved for million years natural selection and ensures the excellent mechanical properties, hierarchical structure and inherent density gradient of bamboo (Amada and Untao 2001), and it is gratifying that bionic bamboo element and its composite reserve the rare and commendable characteristics sufficiently. Strength of bionic bamboo element was almost equal to that of bamboo culm, this suggests that process technology of hexagon bamboo is successful and practical. The novel application of bamboo in original status improves the utilization ratio and processing efficiency of raw materials compared process technology of bamboo strand, bamboo strip or bamboo veneer (Fu and Zhou 2010a). So it is not exaggerated that the bionic bamboo composite is green, economical, and energy-efficient material.

CONCLUSIONS

Compressive properties in axial of bionic bamboo element under different temperature and humidity environment were researched, and the stress and strain distribution characteristics were analyzed by Finite Element Method, the conclusions as follows:

(1) Temperature and humidity have impressive influence on the axial compressive property of bionic bamboo element, especially the strength of bionic bamboo element decrease significantly after being immersed in water and pretreated with 40°C and 90% for 15 days and 30 days.

(2) Node's contribution to strength varies under different conditions, strength of bionic bamboo element with node under water or high humidity environment for long time weaken obviously for the fiber loose within node. Crack mainly occurs on the thin wall with fibers' tear in length direction and fracture in horizontal direction, and shows hierarchical damage.

(3) Stress and strain distributions of bionic bamboo element are symmetrical, and the maximum value is on the end part, this is similar with that of bamboo culm. While strain in the thin wall of bionic bamboo element is propagated along the grain direction.

(4) The hexagon pattern promotes recombination utilization of bamboo culm without destroying its natural structure, and bionic bamboo element possesses rationalization and is innovative utilization of bamboo.

ACKNOWLEDGEMENTS

REFERENCES

1. Amada, S., Untao, S., 2001: Fracture properties of bamboo. Composites: Part B (32): 451-459.
2. Bai, X., Lee, A.W.C., Thompson, L.L., Rosowsky, D.V., 1999: Finite element analysis of Moso bamboo-reinforced Southern pine OSB composite beams. Wood and Fiber Science 31(4): 403-415.
3. Fan, L., Fu, W., Zhou, J., 2012: Research of hexagon processing technology on bamboo original multiparty recombination. Wood Processing Machinery (04): 10 and 50-52.
4. Fu, W., Zhou, J., 2010a: Preliminary study of original state polygonal recombined bamboo. China Forest Products Industry 37(3): 45-48.
5. Fu, W., Zhou, J., 2010b: Study on industrial manufacturing technology of natural arc-bamboo laminated lumber. Wood Processing Machinery (06):7-11 and 15.
6. Fu, W., Zhao, Z., Han, W., Zhou, J., 2013: Research on Finite Element Model for Parallel to Bamboo Culms Axial Shear. Applied Mechanics and Materials Vol. 477-478: 986-989.
7. Han, W., Fu, W., Zhou, J., 2014: Study on mechanical properties of original state polygonal recombination bamboo unit. Wood Processing Machinery 25(03): 33-36.
8. Liese, W., 1998: The anatomy of bamboo culms. Technical Report. Int. network for bamboo and rattan. Beijing, Eindhoven, New Delhi, Pp 79, 92-94.
9. Liu, X., Fu, W., Zhao, Z., Zhou, J., 2012: The current research status and development trend of finger-jointed technology in China. Wood Processing Machinery (05): 62-67.
10. Liu, X., Fu, W., Zhao, Z., Zhou, J., Han, W., 2013: Research on the unit finger technology and mechanical properties of original state polygonal recombinant material of bamboo. Wood Processing Machinery (02): 17-20.
11. Oka, G.M., Triwiyono, A., Awaludin, A., Siswosukarto, S., 2014: Effects of node, internode and height position on the mechanical properties of *Gigantochloa atroviolacea* bamboo. Procedia Engineering 95: 31-37.
12. Shao, Z., 2012: Fracture mechanics of plant materials (wood, bamboo). Science Press, Beijing, Pp 4-6.
13. Shao, Z., Huang, S., Wu, F., Zhou, L., Clement, A., 2008: A study on the difference of structure and strength between internodes and nodes of Moso bamboo. Journal of Bamboo Research 27(2): 48-52.

14. Shao, Z., Wu, Y., Wang, F., 2012: The physical model and energy absorbing mechanism of bamboo transverse fracture: the cracking of parenchyma tissue and layering of interface. Scientia Silvae Sinicae 48(7): 108-113.

15. Triboulot, P., Jodin, P., Pluvinage, G., 1984: Validity of fracture mechanics concepts applied to wood by finite element calculation. Wood Science and Technology 18(1): 51-58.

16. van der Lugt, P., van den Dobbelsteen, A.A.J.F., Janssen, J.J.A., 2006: An environmental, economic and practical assessment of bamboo as a building material for supporting structures. Construction and Building Materials 20: 648-656.

17. Xu, Q., Harries, K., Li, X., Liu, Q., Gottron, J., 2014: Mechanical properties of structural bamboo following immersion in water. Engineering Structures 81: 230-239.

18. Yan, W., Zhou, J., Zhang, B., Fu, W., Chen, Z., 2017a: Development design and mechanical properties of arc bamboo. Wood Research 62(3): 365-372.

19. Yan, W., Zhang, B., Fu, W., Zhou, J., 2017b: Strain characterization and mechanism study on annular shrinkage of bamboo culm (*Phyllostachys pubescens*) China Forest Products Industry 44(10): 16-20 and 26.

20. Yuan, Y., Yu, X., Yang, X., Xiao, Y., Xiang, B., Wang, Y., 2017: Bionic building energy efficiency and bionic green architecture: A review. Renewable and Sustainable Energy Reviews 74: 771-787.

21. Zhang, B., Fu, W., Zhou, J., Yan, W., 2017a: Axial compressive properties of glue-pressed engineered honeycomb bamboo(GPEHB). Wood Processing Machinery 28(2): 27-31.

22. Zhang, B., Fu, W., Zhou, J., Yan, W., Ma, C., 2017b: Effect of finger-joint position on compressive properties of glue pressed engineered honeycomb bamboo (GPEHB). Wood Processing Machinery 28(4): 29-32 and 38.

23. Zhao, Z., Fu, W., Han, W., Zhou, J., 2013: Study on bamboo culm used for structure axial compression performance numerical simulation. Advanced Materials Research 842: 13-17.

24. Zhao, Z., Yang, G., Fu, W., Chen, Z., Zhang, B., 2015: Study on bamboo culm cracking performancenumerical simulation. Wood Processing Machinery: 26 (6): 4-6.

25. Zheng, Y., Jiang, Z., Sun, Z., Ren, H., 2014: Effect of microwave-assisted curing on bamboo glue strength: Bonded by thermosetting phenolic resin. Construction and Building Materials 68: 320-325.

26. Zhou, J., Chen, L., Fu, W., Chen, Z., Zhao, Z., Cheng, W., Zhang, Z., 2016: Preparation and performance evaluation of bamboo lumber prepared by assembly and glue-curing of naturally arc-shaped segments with finger joints. Bioresources 11(1): 267-280.

27. Zhou, J., Fu, W., Qing, Y., Han, W., Zhao, Z., Zhang, B., 2015: Fabrication and performance of a glue-pressed engineered honeycomb bamboo (GPEHB) structure with finger-jointed ends as a potential substitute for wood lumber. Bioresources 10 (2): 3302-3313.

Wei Yan
[1]Hengshui College of Vocational Technology
Hengshui, Hebei Province, 053000, China
[2]Beijing Forestry Machinery Research Institute of The State Forestry and Grassland Administration
Beijing, 100029
China

Wansi Fu, Bin Zhang, Jianbo Zhou*
2Beijing Forestry Machinery Research Institute of The State Forestry and
Grassland Administration
Beijing, 100029
China

Jianbo Zhou*
3Research Institute of Forestry New Technology, Chinese Academy of Forestry
Beijing, 100091
China
*Corresponding author: zhoujianbol@126.com

SUSTAINABLE BIO-BASED ADHESIVES FOR
ECO-FRIENDLY WOOD COMPOSITES. A REVIEW

Petar Antov, Viktor Savov, Nikolay Neykov
University of Forestry
Sofia, Bulgaria

ABSTRACT

The aim of the present review is to summarize the current state of research in the field of sustainable bio-based adhesives used for production of eco-friendly wood composite materials. The article is focused mainly on the use of lignin, starch and tannins as raw materials and alternatives to the existing conventional adhesives. It is expected that increased amounts of bio-based adhesives will be used in the production of wood composites in order to meet the current needs for development of sustainable and innovative materials which will make the wood-based panel industry more sustainable and lower its dependence on fossil fuels. However, there are still substantial challenges for the complete replacement of petroleum-based wood adhesives with bio-based adhesives, mainly because of their relatively poor water resistance, low bonding strength and large natural variations due to different growing conditions. In this respect, fundamental research is still need in order to determine the factors for formulating bio-based adhesives with optimal properties and broaden their application in wood-based panel industry.

KEYWORDS: Bio-based adhesives; lignin, tannins, starch, wood-based composites.

INTRODUCTION

The bioeconomy strategy, launched by the European Commission, and the transition to a stronger, circular and low-carbon economy have posed new actions and requirements towards a greater and more sustainable use of natural resources by sustainably increasing the primary production and conversion of waste into value-added products, enhanced production and resource efficiency. The extended use of bio-based products, defined as "products, wholly or partly derived from materials of biological origin, excluding materials embedded in geological formations and/or fossilized" can make the economy more sustainable and lower its dependence on fossil fuels (European Biomass Industry Association 2019). As they are derived from renewable raw materials such as plants, bio-based products can help reduce CO_2 and have other advantages such as lower toxicity or innovative product characteristics. For this reason, the European Union has

declared the bio-based products sector to be a priority area with high potential for future growth, reindustrialization, and addressing societal challenges (European Commission 2018).

The conventional adhesives for production of wood composites are made mainly from fossil-derived polymers, based on phenol, urea, melamine, formaldehyde, isocyanate, etc. (Youngquist 1999, Frihart 2012, Ferdosian et al. 2017). These fossil-derived adhesives are cost-effective and perform very well regarding bonding performance, mechanical properties, thermal stability and water resistance (Jin et al. 2010, Zhang et al. 2013, Jivkov et al. 2013a, Jivkov et al. 2013b, Yang et al. 2015). Most of the industrially used wood adhesives comprise formaldehyde which is a highly reactive compound, making it well suited for its intended use. However, formaldehyde has been identified as a hazardous and toxic compound and in 2004 was re-classified from "probable human carcinogen" to "known human carcinogen" by the International Agency for Research on Cancer (IARC 2004, EPA 2017). There is sufficient evidence that long-term formaldehyde exposure can cause cancer of the nasopharynx and leukaemia. Also, a positive association has been observed between exposure to formaldehyde and sinonasal cancer (IARC 2006). Thus, the concern about free formaldehyde emissions from wood composites, especially in indoor applications, along with the increased environmental consciousness related to the sustainability of raw materials and final products, as well as the new stricter environmental legislation, are the main driving factors for shifting the scientific and industrial interest from the traditional formaldehyde-based synthetic resins to the new bio-based adhesives for production of eco-friendly wood composites (Dunky 2004, Frihart 2005, Kües 2007, Pizzi 2006, Navarrete et al. 2013, Valyova et al. 2017). It should be noted that nowadays there are only a few bio-based adhesives for production of wood composites and they are not economically feasible to mainstream the production of wood composites. For these adhesives and for the ones still in development, a synthetic cross-linker is usually required to reach the required properties at reasonable cost (Hemmilä et al. 2017).

Different biomass resources such as lignin (Klasnja and Kopitovic 1992, Pizzi 2006, Kunaver et al. 2010, Li et al. 2018, Gadhave et al. 2019), starch (Wang et al. 2015, Li et al. 2015), tannins (Trosa and Pizzi 2001, Santos et al. 2017, Ndiwe et al. 2019), etc. have been used as renewable raw materials for production of bio-based adhesives. The aim of the present review is to summarize the current state of research in the field of natural, bio-based adhesives used for production of eco-friendly wood composite materials. The article is focused mainly on the use of lignin, starch and tannins as raw materials.

Wood-based composite production in Europe

Following the European economic recovery, European wood-based composite production increased by 2.8% in 2016, to 74.7 million m^3, despite lower production of wet process hardboard and stagnant particleboard production (European Panel Federation 2017, UNECE/FAO 2017). Particleboard comprised more than half of total wood-based composite production in Europe in 2016, fibreboard accounted for 30% and OSB for almost 9% of the total production. The particleboard production increased by 0.5% in 2016, to 37.8 million m^3, still far below the peak of 44.4 million m^3 in 2007. The production of fibreboard increased by 739 000 m^3 (+3.2%) in Europe in 2016, to 23.7 million m^3. The top five producing countries were, in descending order, Germany, Turkey, Poland, Spain and France, together accounting for about 75% of production in the subregion. MDF production in European Panel Federation member countries increased by 2% in 2016, to 12 million m^3. Turkey contributed a substantial 5.1 million m^3 to total production in the European subregion and had the largest growth in volume (292 000 m^3 + 6.1%). Despite four years of growth, Europe's MDF production is still significantly lower than the achieved peak of 21.6 million m^3 in 2007. OSB production increased in Europe by 9.6% in 2016, to 6.7 million m^3, as Romania and Germany are the two largest OSB producers in Europe. Poland became the

third-largest following an expansion in 2015 (European Panel Federation 2017). European plywood production increased by 5.3% in 2016, to just less than 4.9 million m^3. Finland is the most important producer in the subregion, accounting for more than 23% of total production. The rest four top producers - Slovakia, Poland, Romania and Spain (in descending order, by volume) reported positive trends in production, with an average growth of 5.4% (European Panel Federation 2017).

Bio-based adhesives
Lignin

After cellulose, lignin is the second most important component of plant biomass with an estimated 300 billion total tons in the biosphere and an annually resynthesis of about 20 billion tons (Glasser and Kelly 1987). It is present in lignocellulosics including wood, grass, agricultural residues, and other plants (Fu et al. 2010). Worldwide, more than 50 million tons of lignin accumulate annually as by-product of pulp production (lignosulfonate from sulfite pulping processes and kraft lignin from sulfate pulping processes) (Kües et al. 2007). About 10% of the technical lignins are exploited industrially whilst the rest is combusted or not utilized at all (Kharazipour et al. 1991, Gargulak and Lebo 2000, Chakar and Ragauskas 2004, Gosselink et al. 2004). The possibilities for use of lignin in adhesive applications have been extensively studied by many authors (Hemmilä et al. 2017, Ferdosian et al. 2017, Ghaffar et al. 2014, Pizzi, 2010, 2016). The main interest in lignin is due to its phenolic structure with several favourable properties for formulation of wood adhesives such as high hydrophobicity and low polydispersity. However, the chemical structure of lignin lowers the reactivity of the resin, which is a disadvantage in applications where fast curing times are needed.

Lignin-based adhesives can be classified into two groups - lignin-based phenol-formaldehyde adhesives, where lignin is used as a partial replacement of phenol, and formaldehyde-free lignin-based adhesives. In different studies lignin is often combined with synthetic resins such as phenol-formaldehyde (Cetin et al. 2002, 2003, Ghaffar and Fan 2014, Olivares et al. 1995, Guo et al. 2015, Pizzi 2016) or urea-formaldehyde resins (Podschun et al. 2016) to decrease the cost (Shimatani et al. 1994) or free formaldehyde emissions (Yang et al. 2015). Certain interest in this field represent the laboratory studies for manufacturing MDF by adding lignin as a binder (Zouh et al. 2011, Nasir et al. 2014) which allow the production of ecological low-toxic panels. Another studies in the MDF field considered adding laccase enzyme-activated lignin to the fibres or activating the lignin in the fibres by enzyme treatment (Kharazipour et al. 1991, 1998) but this needed the addition of 1% isocyanate to the panel to press at acceptably short press times or significantly extending the pressing time (Felby et al. 1997). There are also a number of successful attempts to produce MDF in laboratory conditions on the basis of lignosulfonates (Yotov et al. 2017, Savov and Mihajlova 2017a, Savov and Mihajlova 2017b, Savov et al. 2019, Antov et al. 2019).

Akhtar et al. (2011) used lignosulfonate as a replacement of phenol in the synthesis of phenol-formaldehyde resin at a relatively high replacement level (up to 50 wt %). Phenol-formaldehyde resin composed of 50% lignosulfonate had better strength properties in comparison with the commercial adhesives with a great economic effect. The highest values of shear strength in both wet and dry conditions were achieved at twenty percent substitution of phenol by lignosulfonate.

Another study was focused on the application of Kraft lignin-based phenol-formaldehyde resin (50 wt % Kraft lignin) as an adhesive for production of oriented strand board panels (Donmez Cavdar et al. 2008). In hardboards, addition of 3 - 8% kraft lignin made a post-heat-treatment unnecessary for reduction of swelling, regardless of when lignin was added - prior

or after fibre production (Westin et al. 2001). In another study, water stability (swelling in thickness and water absorption), internal bond strength, and mechanical properties were reported to be improved in panels made from fibres of softwood residues defibrated in presence of extra lignin (Anglès et al. 2001).

Application of enzymatic hydrolysis lignin in the production of phenol-formaldehyde resin has also been studied (Jin et al. 2010, Qiao et al. 2014).

The number of studies on the synthesis of formaldehyde-free lignin-based adhesives is relatively low. Geng and Li (2006) prepared a formaldehyde-free wood adhesive using Kraft lignin and polyethylenimine for production of plywood. Yuan et al. studied the physical and mechanical properties of a modified ammonium lignosulfonate/ polyethylenimine mixture as a green adhesive for MDF production (Yuan et al. 2014). El Mansouri et al. (2007) developed a novel process to substitute formaldehyde in wood adhesive for particleboard production. The prepared formulation met the requirement of the international standard EN 312 for exterior-grade panels and demonstrated comparable reactivity to formaldehyde-based adhesives. Navarrete et al. (2010) prepared a novel bio-based adhesive derived from a low molecular mass lignin and tannin without incorporating any synthetic resin. The obtained adhesive classified as an effective zero formaldehyde emission based on the desiccator method. A novel bio-adhesive for wood using kenaf core lignin and glyoxal was developed and tested (Hazwan et al. 2019).

Starch

Starch is a natural polymer and has attracted much attention in applications including food, papermaking, additives and adhesives, mainly because of its renewability, abundance, good adhesion and low price (Imam et al. 1999, Qiao et al. 2016, Norström et al. 2018, Zhao et al. 2018, Gu et al. 2019). Starch is the admixture of two distinct polysaccharide fractions: amylose and amylopectin; both are composed of glucose with different sizes and shapes (Tester et al. 2004). The proportion of amylose to amylopectin varies in accordance with the botanical origin of the starch and affects the properties of the wood adhesive (Norström et al. 2018).

Starch-based adhesives rely on hydrogen bonding forces, which are much weaker than chemical bonds. They also easily form hydrogen bonds with water molecules, leading to poor water resistance. Therefore, it is necessary to modify starch in order to increase its performance for adhesive applications. Higher bonding strength and better water resistance can be achieved by combining starch with another component, for example polyvinyl alcohol, formaldehyde, isocyanates, and tannins (Qiao et al. 2016). There are several studies about starch-based adhesives prepared by grafting vinyl acetate onto starch using ammonium persulfate as the initiator (Wang et al. 2011, Wang et al. 2012). It was demonstrated that the graft efficiency was important and had a large effect on the bonding performance of the starch adhesive (Wang et al. 2015). A typical chemical modification of starch by converting hydroxyl groups into esters in order to improve the hydrophobic properties of starch is esterification. Qiao et al. (2016) obtained esterified corn starch by reacting with maleic anhydride and then crosslinking with a polyisocyanate pre-polymer. The optimal amount of pre-polymer was determined to be 10 wt %, resulting in the dry and wet shear strengths of 12 and 4 MPa, respectively. Other researches (Tan et al. 2011) modified a starch-based adhesive by addition of blocked isocyanate and auxiliary agent. Gu et al. (2019) synthesized an environmentally friendly starch-based adhesive for wood-based panels by grafting polymerization of vinyl acetate monomer onto corn starch and crosslinking polymerization with N-methylol acrylamide. The water resistance of the obtained adhesive was significantly improved to more than 1 MPa. The authors found that the improved performance is due to increased crosslinking density and formation of complex network structure.

Another universal synthetic adhesive that can be used as a crosslinker of starch and other bio-based adhesives is epoxy resin. Epoxy resins have been tested mainly for veneer gluing, e.g. in combination with polyvinyl acetate grafted starch adhesives. Epoxy groups form three-dimensional networks that provide good shear strength in both dry and humid conditions (Nie et al. 2013).

Protein-starch composite (Anderson et al. 2011, Gadhave et al. 2017) and tannin-starch composite (Moubrik et al. 2010) can also be used for wood and wood composites adhesives which is eco-friendly system with zero formaldehyde emissions. Moubarik et al. (2009) reported a partial substitution of phenol-formaldehyde with corn starch-quebarcho tannin-based resin in the production of plywood. The optimal replacement value was determined to be 20% (15% cornstarch and 5% quebracho tannin). The addition of this resin improved the water resistant properties and reduced the formaldehyde emissions. The same authors developed a non-volatile and non-toxic cornstarch-tannin adhesive for interior plywood (Moubarik et al. 2010). The mechanical properties of the produced plywood were greater in comparison with the conventional phenol-formaldehyde resin. The addition of tannin made the starch-based wood adhesive less toxic and more environmentally-friendly; it also shortened the reaction time.

In some other studied urea-formaldehyde resin was reactively blended with various concentration of starch (Dimas et al. 2013), esterified starch (Liu 2013, Zhu 2014) and oxidized starch (Ni 2014, Sun et al. 2016) as wood and wood composite adhesive. It was found that new system with urea starch blending has lower brittleness and formaldehyde emission. Oxidized starch blended urea-formaldehyde resin adhesive has good chemical stability, insulating properties, temperature resistance, aging resistance, and oil resistance and can be applied to wood adhesion (Dunkey 1997, Bloembergen et al. 2005).

Another strategy to improve the performance of starch-based adhesives is to incorporate fillers or additives into the formulated adhesives. Wang et al. (Wang et al. 2011) demonstrated that the bonding strength, water resistance as well as thermal stability of the starch-based adhesive were improved significantly by silica nanoparticles. An addition of 10% silica led to the shear strength values of 5.12 MPa and 2.98 MPa in dry and wet condition, respectively.

Tannins

Tannins are natural polyphenols divided into two classes of chemical compounds of mainly phenolic nature: hydrolysable tannins and condensed tannins (Kües et al. 2007). Tannins occur naturally in bark, wood, leaves and fruits of different plant species but only a few plants have high enough concentration to make their extractions worthwhile. Tannins can be extracted from pine, oak, chestnut, wattle, eucalyptus, myrtle, maple, birch, willow, etc. Different extraction methods exist and they have a significant impact on the adhesive properties of tannin extracts. Extraction of the plant material and subsequent purification of the isolates, followed by spray drying, yield powdered tannins (Pizzi 2003). Other components of the extraction include sugars, pectins and other polymeric carbohydrates, amino acids, as well as other substances (Dunky 2003).

Hydrolysable tannins have been successfully used as partial substitutes (up to 50%) of phenol in the manufacture of phenol-formaldehyde resins (Kulvik 1976, 1977). However, the naturally low macromolecular structure, the low level of phenol substitution they allow, limited worldwide production, and relative high price makes them less interesting compared to the condensed tannins (Pizzi 2003, 2006). Condensed tannins with a yearly production of 200 000 tons make up more than 90% of the world´s commercial production (Pizzi 2003, 2006).

The application of tannins as adhesives for wood-based panels depends mainly on the content of reactive polyphenols and the reactivity of these components towards formaldehyde. Tannins

can be used as adhesives alone (with a formaldehyde component as crosslinker) or in combination with aminoplastic or phenolic resins. MDF produced with tannins replacing parts of phenol in phenol-ureaformaldehyde resins or even with 100% tannin resin can meet interior grade requirements but usually not exterior grade specifications (Roffael et al. 2000, López-Suevos and Riedl 2003). Different tannin sources and time of tannin addition in the process chain of MDF production (e.g. before or after defibration of wood chips) have been shown to influence of the characteristics of resulting boards (Dix and Schneider 2006). Adhesive formulations for wood applications, prepared using different hardeners and tannin powder from Turkish red pine bark, have been developed and tested by Gonultas (2018) and Uçar et al. (2013). A thermosetting tannin-based wood adhesive system from formaldehyde reaction with both condensed and hydrolysable tannin has been studied by Özacar et al. 2006.

Some studies focused on developing resins totally free of formaldehyde by combining tannins with other bio-based material, e.g. protein (Li et al. 2004). Santos et al. 2017 have studied the possibility of completely removing formaldehyde from adhesive formulations by developing particleboard adhesive based on tannins, extracted from rom industrial lignocellulosic wastes, namely chestnut shell, chestnut bur and eucalyptus bark. Nath et al. (2018) have studied the properties and possibilities for production of particleboard with tannin-based adhesive from mangrove species. Cui et al. (2015) added cellulose nanofibers into tannin-based adhesives for particleboard production and reported significant increase of the mechanical properties of the produced panels.

Tannins have been used as adhesives for production of wood-based panels in South Africa, Australia, Zimbabwe, Chile, Argentina, Brazil, and New Zealand (Li and Maplesden 1998, Dunky and Pizzi 2002). The application in Europe is rather limited, only for special products with specific properties.

CONCLUSIONS

Bio-based adhesives provide an eco-friendly and sustainable alternative to the conventional adhesive systems used in wood-based panel industry. All natural adhesive raw materials, presented above, can significantly reduce the negative environmental impact of harmful formaldehyde and volatile organic compound emissions from wood-based panels. At the same time, bio-based adhesives can enhance the transition to circular economy by meeting the current needs for development of sustainable and innovative materials which will make the wood-based panel industry more sustainable and lower its dependence on fossil fuels.

However, there are still substantial challenges for the complete replacement of petroleum-based wood adhesives with bio-based adhesives, mainly because of their relatively poor water resistance, low bonding strength and large natural variations due to different growing conditions. There are successful solutions how to overcome these drawbacks, but most of them have been tested in laboratory conditions and not in large-scale industrial production. In this respect, fundamental research is still need in order to determine the factors for formulating bio-based adhesives with optimal properties and broaden their application in wood-based panel industry.

ACKNOWLEDGEMENTS

REFERENCES

1. Akhtar, T., Lutfullah, G., Ullah, Z., 2011: Ligonsulfonate-phenolformaldehyde adhesive: A potential binder for wood panel industries. Journal of the Chemical Society of Pakistan 33: 535–538.

2. Anderson, K.R., Porter, M.A., Satyavolu, J.V., 2011: Protein and starch compositions, methods for making and uses thereof. EP 2307494 A1, 13 April 2011.

3. Anglès, M.N., Ferrando, F., Farriol, X., Salvadó, J., 2001: Suitability of steam exploded residual softwood for the production of binderless panels. Effect of the pre-treatment severity and lignin addition. Biomass & Bioenergy 21: 211-224.

4. Antov, P., Valchev, I., Savov, V., 2019: Experimental and statistical modeling of the exploitation properties of eco-friendly MDF through variation of lignosulfonate concentration and hot pressing temperature, Proceedings of the 2nd International Congress of Biorefinery of Lignocellulosic Materials (IWBLCM 2019), Pp 104-109.

5. Bloembergen, S., Kappen, F., Beelen, B., 2005: Environmentally friendly bio-polymer adhesives and applications based thereon. Patent US 6921430 B2.

6. Cetin, Nihat, Özmen, N., 2002: Use of organosolv lignin in phenol-formaldehyde resins for particleboard production: II. Particleboard production and properties. International Journal of Adhesion and Adhesives 22(6): 481-486.

7. Cetin, Nihat, Özmen, N., 2003: Studies on lignin-based adhesives for particleboard panels. Turkish Journal of Agriculture and Forestry 27: 183-189.

8. Chakar, F.S., Ragauskas, A.J., 2004: Review of current and future softwood kraft lignin process chemistry. Industrial Crops and Products 20: 131-141.

9. Cui, J., Lu, X., Zhou, X., Chrusciel, L., Deng, Y., Zhou, H., Zhu, S., Brosse, N., 2015: Enhancement of mechanical strength of particleboard using environmentally friendly pine (*Pinus pinaster* L.) tannin adhesives with cellulose nanofibers. Annals of forest science 72: 27-32.

10. Dimas, B.J., Osemeahon, S.A., Maitera, O.N., Hotton, A.J., 2013: Influence of starch addition on properties of urea formaldehyde/starch copolymer blends for application as a binder in the coating industry. Journal of Environmental Chemistry and Ecotoxicology 5: 181-189.

11. Donmez Cavdar, A., Kalaycioglu, H., Hiziroglu, S., 2008: Some of the properties of oriented strandboard manufactured using kraft lignin phenolic resin. Journal of Materials Processing Technology 202: 559-563.

12. Dunkey, M., 1997: Urea-formaldehyde (UF) adhesive resins for wood. International Journal of Adhesion and Adhesives 18: 95-107.

13. Dunky, M., Pizzi, A., 2002: Wood adhesives. In: Chaudhury, M. and Pocius, A.V. (Eds.), Adhesive Science and Engineering - 2: Surfaces, Chemistry and Applications. Elsevier, Amsterdam, chap. 23, Pp 1039-1103.

14. Dunky, M., 2003: Adhesives in the wood industry. Handbook of Adhesive Technology, Third Edition, chap. 47: 872-941.

15. Dunky, M., 2004: Adhesives based on formaldehyde condensation resins. Macromolecular Symposia 217: 417-429.

16. El Mansouri, N.E., Pizzi, A., Salvado, J., 2007: Lignin-based wood panel adhesives without formaldehyde. Holz als Roh- und Werkstoff 65: 65-70.

17. Felby, C., Pedersen, L.S., Nielsen, B.R., 1997: Enhanced auto adhesion of wood fibers using phenol oxidases. Holzforschung 51: 281-286

18. Ferdosian, F., Pan, Z., Gao, G., Zhao, B., 2017: Bio-based adhesives and evaluation for wood composites application. Polymers 9(2): 70/1-/294.

19. Frihart, C.R., 2005: Wood adhesion and adhesives. In: Rowell, R.M. (Ed.) Handbook of wood chemistry and wood composites. CRC Press, Boca Raton, FL, Pp 215-278.

20. Frihart, C., 2012: 9 Wood Adhesion and Adhesives. In: Rowell, R.M. (Ed.) Handbook of Wood Chemistry and Wood Composites. 10.1201/b124 87-13

21. Fu D., Mazza G, Tamaki Y., 2010: Lignin extraction from straw by ionic liquids and enzymatic hydrolysis of the cellulosic residues. Journal of Agricultural and Food Chemistry; 58(5): 2915-2922

22. Gadhave, R.V., Mahanwar, P.A. and Gadekar, P.T., 2017: Starch-based adhesives for wood/wood composite bonding: Review. Open Journal of Polymer Chemistry 7: 19-32.

23. Gadhave, R.V., Srivastava, S., Mahanwar, P.A. and Gadekar, P.T., 2019: Lignin: Renewable Raw Material for Adhesive. Open Journal of Polymer Chemistry 9: 27-38.

24. Gargulak, J.D., Lebo, S.E., 2000: Commercial use of lignin-based materials. In: Glasser, W.G., Northey, R.A. & Schultz, T.P. (Eds.) Lignin: historical, biological, and material perspectives. American Chemical Society, Washington, DC, Pp 304-320.

25. Geng, X., Li, K., 2006: Investigation of wood adhesives from kraft lignin and polyethylenimine. Journal of Adhesion Science and Technology 20: 847–858.

26. Ghaffar, S.H., Fan, M., 2014: Lignin in straw and its applications as an adhesive. International Journal of Adhesion and Adhesives 48: 92-101.

27. Glasser, W.G., Kelly, S.S., 1987: Lignin. In: Mark, H.F., Bikales, N., Overberger, C.G., Menges, G., Kroschwitz, J.I. (Eds.) Encyclopedia of polymer science and engineering. Volume 8, 2nd edition. Wiley, New York, NY, Pp 795-852.

28. Gonultas, O., 2018: Properties of Pine Bark Tannin-based Adhesive Produced with Various Hardeners. Bioresources 13: 9066-9078.

29. Gosselink, R.J.A., de Jong, E., Guran, B., Abacherli, A., 2004: Co-ordination network for lignin - standardisation, production and applications adapted to market requirements (EUROLIGNIN). Industrial Crops and Products 20: 121-129.

30. Gu, Y., Cheng, L., Gu, Z., Hong, Y., Li, Z., Li, C., 2019: Preparation, characterization and properties of starch-based adhesive for wood-based panels. International journal of biological macromolecules 134: 247-254.

31. Guo, Z.; Liu, Z.; Ye, L.; Ge, K.; Zhao, T., 2015: The production of lignin-phenol-formaldehyde resin derived carbon fibers stabilized by BN preceramic polymer. Materials Letters 142: 49–51.

32. Hazwan Hussin, M., Aziz, A. Abdul, Iqbal, A., Ibrahim, M. Nasir Mohamad, Latif, N. Hanis Abd., 2019: Development and characterization novel bio-adhesive for wood using kenaf core (*Hibiscus cannabinus*) lignin and glyoxal. International journal of biological macromolecules 122: 713-722.

33. Hemmilä, V., Adamopoulos, S., Karlsson, O., Kumar, A., 2017: Development of sustainable bio-adhesives for engineered wood panels – A Review. RSC Advances 7(61): 38604–38630.

34. IARC 2006: Formaldehyde, 2-butoxyethanol and 1-tertbutoxypropan-2-ol. IARC Monographs on the Evaluation of Carcinogenic Risks to Humans 88: 1–478.

35. Imam S.H., Mao, L., Chen, L., Greene R.V., 1999: Wood adhesive from crosslinked poly (vinyl alcohol) and partially gelatinized starch: preparation and properties, Starch – Stärke 51(6): 225–229.

36. Jin, Y., Cheng, X., Zheng, Z., 2010: Preparation and characterization of phenol-formaldehyde adhesives modified with enzymatic hydrolysis lignin. Bioresource Technology 101: 2046–2048.

37. Jivkov, V., Simeonova, R., Marinova, A., 2013b: Influence of the veneer quality and load direction on the strength properties of beech plywood as structural material for furniture. Innovations in Woodworking Industry and Engineering Design. Vol. 02, pp. 86-92.

38. Jivkov, V., Simeonova, R., Marinova, A., Gradeva, G., 2013a: Study on the gluing abilities of solid surface composites with different wood based materials and foamed PVC. In: Proceedings of the 24th International Scientific Conference Wood is Good – User Oriented Material, Technology and Design, ISBN: 978-953-292-031-4.

39. Kharazipour, A., Haars, A., Shekholeslami, M., Hüttermann, A., 1991: Enzymgebundene Holzwerkstoffe auf der Basis von Lignin und Phenoloxidasen. Adhäsion 35: 30–36.

40. Kharazipour A., Mai C., Hüttermann A., 1998: Polyphenols for compounded materials. Polymer Degradation and Stability 59: 237–243.

41. Kharazipour, A., Haars, A., Shekholeslami, M., Hüttermann, A., 1991: Enzymgebundene Holzwerkstoffe auf der Basis von Lignin und Phenoloxidasen. Adhäsion 5: 30-36.

42. Klasnja, B., Kopitovic, S., 1992: Lignin-phenol-formaldehyde resins as adhesive in the production of plywood. Holz als Roh- und Werkstoff 50: 282–285.

43. Kües, U., 2007: Wood production, wood technology, and biotechnological impacts, Universitätsverlag Göttingen, 635 pp.

44. Kulvik, E., 1976: Chestnut wood tannin extract in plywood adhesives. Adhesives Age 20: 19-21.

45. Kulvik, E., 1977: Tannin extract as cure accelerator for phenol-formaldehyde wood adhesives. Adhesives Age 19: 33-34.

46. Kunaver, M., Medved, S., Čuk, N., Jasiukaityte, E., Poljanšek, I., Strnad, T., 2010: Application of liquefied wood as a new particle board adhesive system. Bioresource Technology 101: 1361–1368.

47. Li, B.E., Maplesden, F., 1998: Commercial production of tannins from Radiata pine bark for wood adhesives. IPENZ Transactions 25: 46-52.

48. Li, K., Geng, X., Simonsen, J., Karchesy, J., 2004: Novel wood adhesives from condensed tannins and polyethylenimine. International Journal of Adhesion and Adhesives 24: 327-333.

49. Li, R. J., Gutierrez, J., Chung, Y., Frank, C. W., Billington, S. L., Sattely, E. S., 2018: A lignin-epoxy resin derived from biomass as an alternative to formaldehyde-based wood adhesives. Green chemistry 20: 1459-1466.

50. Li, Z. Wang, J., Li, C., Gu, Z., Cheng, L., Hong, Y., 2015: Effects of montmorillonite addition on the performance of starch-based wood adhesive. Carbohydrate Polymers 115: 394-400.

51. Liu, R., 2013: Modified urea-formaldehyde resin. CN 103360559 A 13.

52. López-Suevos, F., Riedl, B., 2003: Effects of *Pinus pinaster* bark extracts on the cure properties of tannin modified adhesives and on bonding of exterior grade MDF. Journal of Adhesion Science and Technology 17: 1507-1522.

53. Marra, G.G., 1972: The future of wood as an engineered material. Forest Products Journal 22: 43-51.

54. Moubarik, A., Allal, A., Pizzi, A., Charrier, F., Charrier, B., 2010: Characterization of a formaldehyde-free cornstarch-tannin wood adhesive for interior plywood. European Journal of Wood and Wood Products 68. 427–433.

55. Moubarik, A., Pizzi, A., Allal, A., Charrier, F., Charrier, B., 2010: Cornstarch and tannin in phenol-formaldehyde resins for plywood production. Industrial Crops and Products 30: 188-193.

56. Moubarik, A., Allal, A., Pizzi, A., Charrier, F., Charrier, B., 2010: Preparation and mechanical characterization of particleboard made from Maritime pine and glued with bio-adhesives based on cornstarch and tannins. Maderas. Ciencia y Tecnología 12: 189-197.

57. Nasir, M., Gupta, A., Beg, M., Chua, GK., Kumar, A., 2014: Physical and mechanical properties of medium density fiberboard using soy-lignin adhesives. Journal of tropical forest science (1): 41-49.

58. Nath, S., Islam, M. Nazrul, Rahman, K., Rana, M. Nasim., 2018: Tannin-based adhesive from *Ceriops decandra* (Griff.) bark for the production of particleboard. Journal of the Indian Academy of Wood Science 15: 21-27.

59. Navarrete, P., Mansouri, H.R., Pizzi, A., Tapin-Lingua, S., Benjelloun-Mlayah, B., Pasch, H., 2010: Wood panel adhesives from low molecular mass lignin and tannin without synthetic resins. Journal of Adhesion Science and Technology 24: 1597-1610.

60. Navarrete, P., Kebbi, Z., Michenot, F., Lemonon, J., Rogaume, C., Masson, E., Rogaume,Y., Pizzi, A., 2013: Formaldehyde and VOCs emissions from bio-particleboards, Journal of Adhesion Science and Technology 27 (7): 748-762.

61. Ndiwe, B., Pizzi, A., Tibi, B., Danwe, R., Konai, N., Amirou, S., 2019: African tree bark exudate extracts as biohardeners of fully biosourced thermoset tannin adhesives for wood panels. Industrial crops and products 132: 253-268.

62. Ni, K., 2014: Oxidized starch modified urea-formaldehyde resin adhesive. CN 103911103 A. 15.

63. Nie, Y., Tian, X., Liu, Y., Wu, K., Wang, J., 2013: Research on starch-g-poly-vinyl acetate and epoxy resin-modified corn starch adhesive. Polymer Composites 34: 77-87.

64. Norström, E., Demircan, D., Fogelström, L., Khabbaz, F., Malmström, E., 2018: Green binders for wood adhesives. In Applied adhesive bonding in science and technology, Pp 49-71.

65. Olivares, M., Aceituno, H., Neiman, G., Rivera, E., Sellers, T.J., 1995: Lignin-modified phenolic adhesives for bonding radiata pine plywood. Forest Products Journal 45: 63–67.

66. Özacar, M., Soykan, C. and Şengil, I. A., 2006: Studies on synthesis, characterization, and metal adsorption of mimosa and valonia tannin resins. Journal of Applied Polymer Science 102: 786-797.

67. Pizzi, A., 2006: Recent developments in eco-efficient bio-based adhesives for wood bonding: opportunities and issues, Journal of Adhesion Science and Technology 20(8): 829-846.

68. Pizzi, A., 2003: Natural phenolic adhesives I: Tannin. In: Pizzi, A. and Mittal, K.L. (Eds,) Handbook of Adhesive Technology (2nd ed.), Marcel Dekker, New York, Chap. 27: 573-587.

69. Pizzi, A., 2006: Recent developments in eco-efficient bio-based adhesives for wood bonding: opportunities and issues. Journal of Adhesion Science and Technology 20: 829-846.

70. Pizzi, A., 2016: Wood products and green chemistry, Annals of Forest Science 73: 185–203.

71. Podschun J., Stücker A., Buchholz R.I., Heitmann M., Schreiber A., Saake B., 2016: Phenolated lignins as reactive precursors in wood veneer and particleboard adhesion. Industrial and Engineering Chemistry Research 55(18): 5231-5237.

72. Qiao, W.,Li, S., Guo, G., Han, S., Ren, S., Ma, Y., 2014: Synthesis and characterization of phenol-formaldehyde resin using enzymatic hydrolysis lignin. Journal of Industrial and Engineering Chemistry 21: 1417–1422.

73. Qiao, Z., Gu, J., Lv, S., Cao, J., Tan, H., Zhang, Y., 2016: Preparation and properties of normal temperature cured starch-based wood adhesive. BioResources 11: 4839-4849.

74. Roffael, E., Dix, B., Okum, J., 2000: Use of spruce tannin as a binder in particleboards and medium density fibreboards (MDF). Holz als Roh- und Werkstoff 58: 301-305.

75. Santos, J., Antorrena, G., Freire, M. Sonia, Pizzi, A., González-Álvarez, J., 2017: Environmentally friendly wood adhesives based on chestnut (*Castanea sativa*) shell tannins. European journal of wood and wood products 75: 89-10.

76. Savov, V., Valchev, I., Antov, P., 2019: Processing factors affecting the exploitation properties of environmentally friendly medium density fibreboards based on lignosulfonate Adhesives, Proceedings of the 2nd International Congress of Biorefinery of Lignocellulosic Materials (IWBLCM2019), Pp 165-169.

77. Savov, V., Mihajlova, J., 2017a: Influence of the content of lignosulfonate on physical properties of medium density fiberboard. International Conference "Wood Science and Engineering in the Third Millennium" – ICWSE. Pp 348-352.

78. Savov, V., Mihajlova, J., 2017b: Influence of the content of lignosulfonate on mechanical properties of medium density fiberboard. Proceedings of International Conference "Wood Science and Engineering in the Third Millennium" – ICWSE. Pp 353-357.

79. Shimatani K., Sano Y., Sasaya T., 1994: Preparation of moderate-temperature setting adhesives from softwood Kraft lignin. Part 2. Effect of some factors on strength properties and characteristics of lignin-based adhesives. Holzforschung 48(4): 337-342.

80. Sun. J, Li L., Cheng. H., Huang, W., 2016: Preparation, characterization and properties of an organic siloxane-modified cassava starch-based wood adhesive. The Journal of Adhesion 94(4): 278-293.

81. Tan, H., Zhang, Y., Weng, X., 2011: Preparation of the plywood using starch-based adhesives modified with blocked isocyanates. Procedia Engineering 15: 1171–1175.

82. Tester, R.F., Karkalas, J., Qi, X., 2004: Starch - Composition, fine structure and architecture. Journal of Cereal Science 39: 151–165.

83. Trosa, A., Pizzi, A., 2001: A no-aldehyde emission hardener for tannin-based wood adhesives. Holz als Roh- und Werkstoff 59: 266–271.

84. Uçar, M. B., Uçar, G., Pizzi, A., Gonultas, O., 2013: Characterization of *Pinus brutia* bark tannin by MALDI-TOF MS and 13C NMR, Industrial crops and products49: 697-704.

85. Valyova, M., Ivanova, Y., Koynov, D., 2017: Investigation of free formaldehyde quantity in production of plywood with modified urea - formaldehyde resin. International Journal Wood, Design and Technology 6(1): 72-76.

86. Vnučec, D., Kutnar, A., Goršek, A., 2017: Soy-based adhesives for wood-bonding – a review, Journal of Adhesion Science and Technology 31(8): 910-931.

87. Wang, P., Cheng, L., Gu, Z, Li, Z., Hong, Y., 2015: Assessment of starch-based wood adhesive quality by confocal Raman microscopic detection of reaction homogeneity. Carbohydrate Polymers 131: 75-79.

88. Wang, Z., Gu, Z., Hong, Y., Cheng, L., Li, Z., 2011: Bonding strength and water resistance of starch-based wood adhesive improved by silica nanoparticles. Carbohydrate Polymers 86: 72-76.

89. Wang, Z., Li, Z., Gu, Z., Hong, Y., Cheng, L., 2012: Preparation, characterization and properties of starch-based wood adhesive. Carbohydrate Polymers 88: 699-706.

90. Wang, P., Cheng, L., Gu, Z., Li, Z., Hong, Y., 2015: Assessment of starch-based wood adhesive, quality by confocal Raman microscopic detection of reaction homogeneity. Carbohydrate Polymers 2015: 131, 75–79.

91. Wang, Z., Gu, Z., Hong, Y., Cheng, L., Li, Z., 2011: Bonding strength and water resistance of starch-based wood adhesive improved by silica nanoparticles. Carbohydrate Polymers 86: 72–76.

92. Westin, M., Simonson, R., Östman, B., 2001: Kraft lignin wood fiberboards – the effect of kraft lignin addition to wood chips or board pulp prior to fiberboard production. Holz als Roh- und Werkstoff 58: 393-400.

93. Yang, S., Zhang, Y., Yuan, T.Q., Sun, R.C., 2015: Lignin–phenol–formaldehyde resin adhesives prepared with biorefinery technical lignins. Journal of Applied Polymer Science 132: 42493.

94. Yotov, N., Valchev, I., Petrin, St., Savov, V., 2017: Lignosulphonate and waste technical hydrolysis lignin as adhesives for eco-friendly fiberboard. Bulgarian Chemical Communications, Vol. 49/2017, Special Issue L, Pp 92-97.

95. Youngquist, J.A., 1999: Wood-base composites and panel products. In Wood Handbook: Wood as an engineering material; USDA Forest Service, Forest Products Laboratory, Madison, WI, USA, Pp 1-31.

96. Yuan, Y., Guo, M., Liu, F., 2014: Preparation and evaluation of green composites using modified ammonium lignosulfonate and polyethylenimine as a binder. BioResources 9: 836-848.

97. Zhang, W., Ma, Y., Wang, C., Li, S., Zhang, M., Chu, F., 2013: Preparation and properties of lignin-phenol-formaldehyde resins based on different biorefinery residues of agricultural biomass. Industrial Crops and Products 43: 326-333.

98. Zhao, L., Liu, Y., Xu, Z. Y., Zhang, Y., Zhao, F., Zhan, S., 2011: State of research and trends in development of wood adhesives 13(4): 321-326.

99. Zhao, X., Peng, L., Wang, H., Wang, Y., Zhang, H., 2018: Environment-friendly urea-oxidized starch adhesive with zero formaldehyde-emission. Carbohydrate polymers 181: 1112-1118.

100. Zhu, L., 2014: Preparation method for high-strength water-resistant starch adhesive for corrugated paperboards. CN 104119816 A 14.

101. Zouh, X., Tan, L., Zhang, W., Chenlong, Lv., Zheng, F., Zhang, R., Du, G., Tang., B., Liu, Xu., 2011: Enzymatic hydrolysis lignin derived from corn stoves as an instant binder from bio-composites: effect of fiber moisture content and pressing temperature on board's properties. Bio-resources 6(1): 253-264.

Petar Antov*, Viktor Savov
University of Forestry
Faculty of Forest Industry
Department of Mechanical Wood Technology
10 Kliment Ohridski Blvd
1791 Sofia
Bulgaria
*Corresponding author: p.antov@ltu.bg

Nikolay Neykov
University of Forestry
Faculty of Business Management
10 Kliment Ohridski Blvd
1797 Sofia
Bulgaria

CALCULATION OF SOUND INSULATION OF SOFTWOOD SAMPLES AT NORMAL INCIDENCE AND COMPARISON WITH EXPERIMENTAL DATA

Zehui Ju, Qian He, Tianyi Zhan, Haiyang Zhang, Lu Hong, Xiaoning Lu
Nanjing Forestry University
Nanjing, PR China

ABSTRACT

The acoustic simulations were carried out for softwood and composites in order to evaluate their sound properties. Theoretical value of sound insulation was predicted by regarding the substances in the wood cell wall as equivalence to specific medium based on Biot model, and the wood microscopic characteristics, such as the length and diameter of tracheid, diameter of pit, and porosity, were taken into account for determining the equivalent density and bulk modulus of wood. By comparing the tested and predicted values of sound insulation, the conclusions were drawn as follows: the predicted values of sound insulation were significantly correlated with the tested values for wood and wood composites. As for Masson pine, the adjacent of earlywood and latewood was considered as sandwich structure for the calculation of sound insulation. The transfer function involved in sound insulation simulation provided an effective method to characterize the sound insulation volume of wood and wood composite in construction and decoration areas.

KEYWORDS: Sound insulation simulation, equivalent medium, transfer function, wood microscopic characteristics, earlywood, latewood.

INTRODUCTION

Wood is one of the most environmental renewable building materials, which has been widely utilized in construction, transportation and decoration industry (Smardzewski 2009, Klašnja et al. 2008). Sound insulation has been investigated for a long time as one of the most crucial and interesting issue among the building environments (Beranek 1960, 1971). The traditional building insulation materials consisted of dense and homogeneous material. The sound insulation of single material increased with the increase of density, which conformed to the law of mass action (Shuku and Ishihara 1973). The gas mainly permeated through the tracheid pore in softwood,

of which the percentage was over 90% (Bao and Hou 2001, Watanabe and Norimoto 2000). The gas permeability in softwood was closely related with its flowing characteristics and rules in tracheids (Zhan 2014, Liu et al. 2012). In hence, it was significance to investigate the sound insulation of wood defined as the porous structure material. In the 1970s, the sound insulation performance of porous acoustic materials has been widely studied, mainly focusing on the sound insulation theory and materials (Whole and Elmallawany 1969). From the aspect of the sound insulation theory, António proposed a new ring structure material, established acoustic model by the traditional acoustic theory, and compared the theoretical value with the test sound insulation of plate material as the same time (António et al. 2004). Tadeu considered fully the coupling effect between the air and medium of the acoustic material by ignoring the thickness of material, and established the analysis model of plate material (Tadeu et al. 2004). Lee established a new method to evaluate the sound transmission loss of multilayer composite material by modifying the transfer matrix (Lee and Xu 2009). From the perspective of kinds of sound insulation material, the multi-layer gypsum board insulation materials were studied by Matsumoto et al. (2006). The results showed that sound insulation performance of multilayer composite significantly improved as that of layer increased from 2-lay to 4-lay by the different characteristics of different layers of the composite. From the aspect of theory of wood sound insulation, the microscopic characteristics of wood played a significance role in the sound insulation theory. However, it has been rarely investigated by researchers as a porous material especially involved in the model of the wood sound insulation.

According to the microscopic characteristics of wood materials, the length and diameter of tracheids, the diameter of pits and porosity were considered as the influencing factors of wood sound insulation model. The special flow resistance of wood material was used to modify the model, and the theory was applied to the simulation of softwood sound insulation. The sound insulation of Chinese fir and Masson pine was measured by experimental method under wide frequency and compared with the predicted value of the model.

Sound insulation simulation

The material was assumed to be transversely infinite and the sound wave was perpendicular to the surface of the plate in air medium. The pi represented the incident wave, the pr represented the reflected wave, and the pt represented the transmitted wave. The wood frame was assumed as a rigid body. The sound propagation in wood can be considered as a fluid motion, which can be equivalent to the calculation of fluid model. The sound propagation theory of Biot elastic porous medium was applied in the model. Besides, the effect of viscosity between air and pore wall and the effect of heat exchange were also considered, which were described in the Zwikker model and Kosten model respectively (Zwikker and Kosten 1949, Biot 1956, Allard 1993, Wilson 1993). The ρ represented equivalent density (kg·m^{-3}) and the K represented equivalent bulk modulus (MPa). Allard proposed that the function of $G_J (B^2\omega)$ could be replaced by the $F (B^2\omega)$ in the Stin-son model (Allard 1993), so the $F (B^2\omega)$ can be obtained in the Johnson model. Meanwhile, the feature size Λ (m) was included and the expression of $G_J (\varpi)$ was easier than that of $G_J (\omega)$ to calculate. So the equivalent density ρ in Johnson model and equivalent bulk modulus K can be calculated with the following Eqs.:

$$\rho = \rho_0 \alpha_\infty (1 + \frac{\sigma\phi}{j\alpha_\infty \rho_0 \omega} G_J(\varpi)) \quad \text{(kg·m}^{-3}) \tag{1}$$

$$K = \frac{\gamma P_0}{\gamma - (\gamma-1)[1 + \frac{\sigma\phi}{jB^2\omega\rho_0\alpha_\infty} G_J'(B^2\omega)]^{-1}} \quad \text{(MPa)} \tag{2}$$

The ρ_0 was the density of air (kg·m⁻³) and P_0 was the air pressure (MPa). The γ was the ratio of the specific heats of air at constant pressure and constant volume and B^2 was the Prandtl constant. The σ, ϕ and ω represented the flow resistance of porous material (Pa·s·m⁻²), the porosity and the angular velocity (rad·s⁻¹) respectively. The α_∞ was tortuosity.

$$G'_J(B^2\omega) = \left(1 + \frac{4j\alpha_\infty^2\eta\rho_0\omega B^2}{\sigma^2\Lambda'^2\phi^2}\right)^{\frac{1}{2}} \tag{3}$$

$$G_J(\varpi) = (1 + \frac{4j\alpha_\infty^2\eta\rho_0\omega}{\sigma^2\Lambda^2\phi^2})^{\frac{1}{2}} \tag{4}$$

$$\Lambda = \frac{1}{c}(\frac{8\eta\alpha_\infty}{\sigma\phi})^{\frac{1}{2}} \quad \text{(m)} \tag{5}$$

$$k_0 = \omega/c_0 \tag{6}$$

In this study, the standard state (at 18°C, 103.3 kPa, air parameter η = 1.84×10-5 kg·m⁻¹s⁻¹, γ =1.4, B2= 0.71) was used in the simulation. The c was sound wave velocity (ms⁻¹) and k_0 was the wave number inside wood. The ρ_0, c_0 and k_0 were the corresponding amount in the condition of air respectively. The d represented the thickness of wood (m) and k was the number of wood (Song and Bolton 2000, Zhang et al. 2010, Varivodina et al. 2010, Buksnowitz et al. 2010). The η was the shear viscosity of air (Pa.s) and the r was radius of the pore (m). For circular pores, c =1. The flow resistance of porous material can be characterized by the degree of difficulty of acoustic wave entering the material. The greater the flow resistance is, the more difficult the wave enters the material. However, there were still huge differences from the aspect of micro-characteristics in wood. The flow resistance of wood should be introduced to better predict the wood sound insulation (Bao and Hou 2002):

$$\sigma = \frac{n * n_{pt} * (1-b) * \pi * r^4 * L * (1-\alpha)}{D_e^2 * 8 * \eta * L_{pm}} * 1.013 * 10^6 \quad \text{(Pa·s·m⁻²)} \tag{7}$$

$A=D^2_e$, The D_e was the tracheid diameter (m), A was the cross-sectional area of tracheids (m²), npt was the number of pits, n was the average number of micro pit membrane in each pit, b was the occlusion rate of pits, r was average radius of micro pit membrane (m) and L was average length of tracheid (m). The layer i material was considered as the object of study, the transfer relationship between sound pressure p (MPa) and velocity v (m·s⁻¹) at the point M_i and M_{i+1} were expressed as:

$$\begin{bmatrix} p_{M_i} \\ v_{M_i} \end{bmatrix} = T_i \begin{bmatrix} p_{M_{i+1}} \\ v_{M_{i+1}} \end{bmatrix} \tag{8}$$

$$T_i = \begin{bmatrix} \cos(k_i d_i) & j\sin(k_i d_i)Z_c \\ j\sin(k_i d_i)/Z_c & \cos(k_i d_i) \end{bmatrix} \tag{9}$$

$$k_i = \omega(\frac{\rho_i}{K_i})^{\frac{1}{2}} \tag{10}$$

The d_i was the thickness of the material layer (m), and k_i was the wave number of the material, Z_c was the characteristic impedance of air. The relationship the interfaces of the material can be established as follows:

$$\begin{bmatrix} p_i + p_r \\ (p_i - p_r)\dfrac{k_0}{\omega\rho_0} \end{bmatrix} = \prod_{i=1}^{n} T_i \begin{bmatrix} p_t \\ p_t\dfrac{k_0}{\omega\rho_0} \end{bmatrix} \tag{11}$$

The k_0 and ρ_0 were the wave number and density of air medium. The total transfer matrix of the composite plate were obtained:

$$\begin{bmatrix} p_i + p_r \\ (p_i - p_r)\dfrac{k_0}{\omega\rho_0} \end{bmatrix} = \begin{bmatrix} T_{1,1} & T_{1,2} \\ T_{2,1} & T_{2,2} \end{bmatrix} \begin{bmatrix} p_t \\ p_t\dfrac{k_0}{\omega\rho_0} \end{bmatrix} \tag{12}$$

The transmission coefficients of multilayer materials can be obtained as follows:

$$t_p = \frac{2}{T_{1,2} + T_{2,2} + T_{1,2}\dfrac{k_0}{\omega\rho_0} + T_{2,1}\dfrac{\omega\rho_0}{k_0}} \tag{13}$$

The sound insulation (R) of the multilayer material was expressed as:

$$R = 20\lg\left|\frac{1}{t_p}\right| \quad \text{(dB)} \tag{14}$$

MATERIAL AND METHODS

Materials

The Chinese fir (*Cunninghamia lanceolata* Lamb.) was collected from Xunyi County of Shanxi province of China with 0.22 m diameter and 4 m length. The average air-dried density was 320 kg·m^{-3}. The Masson pine (*Pinus massoniana* Lamb.) was collected from Guangdong Province of China with 0.24 m diameter and 4 m length. Its average air-dried density was 460 kg·m^{-3}. The Chinese fir block and the Masson pine block were T-R surfaces.

Material 1 represented single ply testing sample of fir. Material 2 represented single ply testing sample of Masson Pine. Material 3 represented two-ply Chinese fir. The PF adhesive was self-made in the laboratory and utilized in the fabrication of wood composites. Material 4 represented two-ply sample of fir and Masson, the incident surface of sound wave was Chinese fir in the test. The PF adhesive was also used in Material 4. Material 5 was the same structure of Material 4, but the incident surface of sound wave was Masson pine. Material 6 represented by three-ply sample of Chinese fir.

Methods

Scanning electron microscope (SEM)

The sample of 5 × 5 × 5 mm was cut from disc. The samples of the three sections were cut flat by a blade. The samples were stored at room temperature until processing for SEM (TM-1000, Japan) observation. The samples were coated with osmiun tetroxide (O_SO_4) in a Plasma Coater (HPC-1SW, Vacuum Device Inc) before imaging.

Mercury intrusion porosimetry (MIP)

A disc (15 mm diameter, 10 mm thickness) was cut from the middle of each material. The samples were dried in an oven at 103 ± 2°C for 24 hours. The MIP characterizing process

employed an Autopore TM IV 9500 Automated Mercury Porosimeter (Micromeritics Instrument Corp., US). The pore distribution was determined with the Washburn equation (Suleiman et al. 1999).

Test instrument of sound insulation

The sound absorption test was carried out according to Chinese Standard GB/T18696.1-2004. The test system was Beijing prestige R-Cabin test system.

RESULTS AND DISCUSSION

Wood microscopic characteristics by SEM

It was found that the gas permeability of softwood was closely related to its flow characteristics and regularities in the tracheid. The SEM of wood microscopic characteristics was described in the Fig. 1. The arrangement of tracheids in softwood was uniform, which fited the requirement of theoretical simulation. So the microscopic characteristics of wood should be introduced into the theory to modify the model. The characteristic of tracheids and pits were described in the Tab. 1.
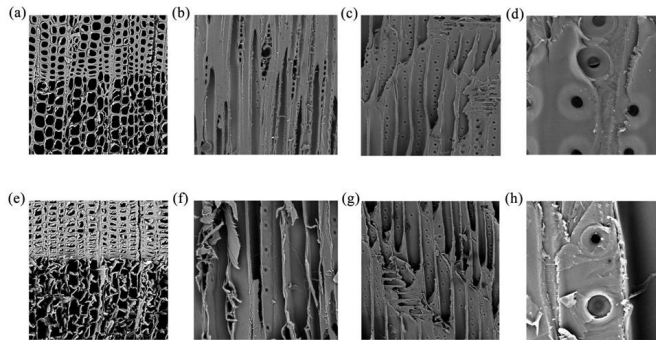

Fig. 1: Chinese fir: (a) transverse section (×300), (b) tangential section (×300), (c) radial section (×300),(d) pit and aspirated pit (×2000). Masson Pine: (e) transverse section (×300), (f) tangential section (×300), (g) radial section (×300),(h) pit and aspirated pit (×2000).

Tab. 1: Weighted average of some structural parameters of tracheids from sampling measurement.

		L_{pm} (µm)	D_{e1} (µm)	D_{e2} (µm)		α (%)	b (%)	D_1 (µm)	D_2 (µm)	D_3 (µm)	D_4 (µm)	n_{pt} (number)	n (number)
Material 1	Chinese fir	4210.70		D_e		2.13	40.20	2.00	5.00	15.00	0.10	25	163
				37.43									
Material 2	Masson Pine	4502.90	45.23	44.83		2.40	56.80	5.00	9.00	20.00	0.20	20	155
Material 3	Chinese fir	4211.44	36.97			2.13	40.20	2.00	5.00	15.00	0.10	25	159
	Chinese fir	4210.55	37.44			2.13	40.20	2.00	5.00	15.00	0.10	25	160
Material 4	Chinese fir	4255.40	37.56			2.13	40.20	2.00	5.00	15.00	0.10	25	155
	Masson Pine	4512.43	45.43	44.83		2.37	55.67	5.00	9.00	20.00	0.20	20	154
Material 5	Masson Pine	4512.43	45.43	44.83		2.37	55.67	5.00	9.00	20.00	0.20	20	154
	Chinese fir	4255.40	37.56			2.13	40.20	2.00	5.00	15.00	0.10	25	155
Material 6	Chinese fir	4215.77	37.00			2.13	40.20	2.00	5.00	15.00	0.10	25	167
	Chinese fir	4216.50	37.50			2.13	40.20	2.00	5.00	15.00	0.10	25	165
	Chinese fir	4250.7	37.46			2.13	40.20	2.00	5.00	15.00	0.10	25	163

L_{pm} - tracheid length; D_e - tracheid diameter; D_{e1} - early wood tracheid diameter; D_{e2} - latewood tracheíd diameter; α - percentage of tracheid overlap; b - percentage of aspirated pit; D_1 - diameter of pitaperture; D_2 - torus diameter; D_3 - diameter of pit membrane; D_4 - diameter of pore on pit membrane; n_{pt} - number of pits on the over-lap face of tracheid; n - number of pit membrane openings of a tracheíd.

Determination of porosity and pore size by MIP

The results of the MIP measurement were shown in Tab. 2. The test results were used to calculate the theoretical simulation of sound insulation.

Tab. 2: The MIP test results.

Number		Median pore diameter (μm)	Porosity (%)	Density (g·cm⁻³)
Material 1	Chinese fir	37.5	77.424	0.32
Material 2	Masson Pine	45.2	65.54	0.45
Material 3	Chinese fir	37.1	76.4	0.32
	Chinese fir	37.6	77.2	0.32
Material 4	Chinese fir	37.2	76.4	0.32
	Masson Pine	45.1	67.2	0.46
Material 5	Masson Pine	45.1	67.2	0.46
	Chinese fir	37.2	76.4	0.32
Material 6	Chinese fir	37.5	76.4	0.32
	Chinese fir	37.1	77.1	0.32
	Chinese fir	38.0	76.9	0.32

Sound insulation simulation of single layer Chinese fir

The test values obtained from the three tests were compared with the theoretical simulation values. The analog 1 curve was obtained by the theoretical model based on classical flow resistance, the analog 2 curve was calculated by the theoretical model of flow resistance based on wood characteristics, and the curves were corrected simultaneously. As can be seen, the analog 2 was better to reflect the sound insulation of Chinese fir than the analog 1 (Fig. 2).
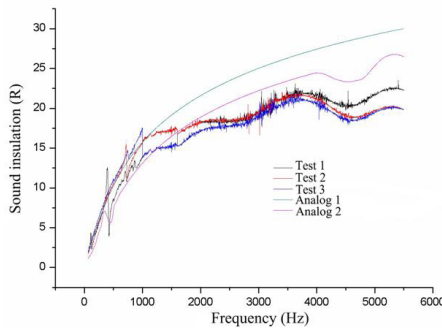
Fig. 2: Simulated sound insulation and measured value of Chinese fir.

As shown in Fig. 2, the sound insulation increased with the increase of frequency. The material was mainly controlled by the stiffness of the material at low frequency, so it was easy to reduce the sound insulation of the material by the resonance effect at low frequency. With the increase of frequency, the material was mainly affected by the law of mass. When the frequency of

sound wave reached the critical frequency, there will be a coincidence effect, resulting in the low sound insulation at the high frequency. There were two main reasons that the sound insulation of materials at low frequency was lower than that at high frequency. (1) The characteristic pore size of wood was far smaller than the wavelength at low frequency. The sound wave was reflected when it propagated on the material surface. The wavelength of the high frequency was relatively smaller than that of the low frequency, so it was easy for sound wave to enter the interior of wood at high frequency. (2) The sound insulation process can be divided into two stages according to the frequency, i.e. isothermal process and adiabatic process. The isothermal process mainly occurred at the low frequency. The part of the sound energy was converted into heat energy under the action of friction resistance by the adhesion between the air and the internal pores. However, the process carried out heat exchange with the outside world by the long time, so that the material can maintain the isothermal process. For the high-frequency, it was mainly the adiabatic process. The action time of this process was relatively short, and the energy conversion was relatively fast, so the material cannot exchange energy with the outside world in the process. Therefore, the sound wave in the high-frequency can be considered as the adiabatic process.

With the increase of the frequency, the sound insulation decreased obviously at high frequency. The main reason was that the part of the sound wave was reflected back in the process of propagation. When the incident wave and the reflected wave were superposed, the coincidence effect was produced, and the sound insulation decreased.

The errors between the analog 1 and the analog 2 were mainly due to the fact that wood flow resistance can more accurately reflect the permeability of the gas in the wood. Analog 2 was more accurate than Analog 1. The reason was that the theoretical model based on wood flow resistance can more accurately reflect the propagation characteristics of sound wave in wood. There were some errors between the three test values in Fig. 2. The main reasons were that there was a certain gap between the sample and the test instrument in the experiment. At the same time, the flatness of the wood surface cannot be guaranteed, which led to errors in the low frequency range, but it can still reflect the sound insulation of wood. Analog 2 was related to three groups of test results. The error between the test and simulation value was large in the low frequency part, especially in the case of less than 315 Hz. The main reason was that wood belonged to porous material, and the loss of sound transmission was small, which led to a large error of sound insulation. In addition, the resonance phenomenon of wood at low frequency led to the reduction of sound insulation, which also engendered the error between test and simulation value.

The error between the theoretical sound insulation and the test value was very small between 315 - 4000 Hz. However, there was still error at frequency of more than 4000 Hz. The main reasons were that there was a critical frequency of wood in this frequency range, and the material had a coincidence effect, which led to the reduction of sound insulation. In addition, the theoretical model only considered the radial flow resistance of wood, ignored the transverse and tangential flow resistance of wood. The critical frequency of Chinese fir was generated at 4520 Hz. The coincidence effect was occurred at the interval of 4000 - 5000 Hz, and the simulated values can be revised at this interval by repeating tests. Throughout the analog 2 curve, the simulation value still had errors by ignoring all the test errors. Research showed that the difference of earlywood and latewood of Chinese fir was small, and the classification was difficult, which was the main reason of the error of simulation value.

Sound insulation simulation of single layer Masson pine

As shown in Fig. 3, the test data obtained from the three tests were compared with the theoretical simulation values. The analog 1 curve was obtained by the theoretical model based on classical flow resistance. The analog 2 curve was calculated by the theoretical model of flow

resistance based on wood characteristics. The earlywood and latewood of Masson pine were divided into two layers. The flow resistance characteristics of earlywood and latewood were introduced, and the theoretical model was modified to obtain the analog 3 curve. The analog 3 curve was correlated with the three test results respectively. The error was similar to that of Chinese fir. The error between the test and simulation value was large in the low frequency part (especially < 315 Hz). The main reasons were that Masson belonged to porous material, and the loss of sound transmission was small, which led to a large error of sound insulation. In addition, the resonance phenomenon of wood at low frequency led to the reduction of sound insulation, which also produced the error between test and simulation value. The error between theoretical sound insulation property and the test value was very small in the range of 315 - 4000 Hz. But there were still errors at frequencies of more than 4000 Hz. The main reasons were that the critical frequency at high frequency of Masson pine led to the coincidence effect. Meanwhile, the theoretical model only considered the radial flow resistance of wood and the transverse and tangential flow resistance of wood was ignored. The critical frequency of Masson pine was generated at 4375 Hz. The coincidence effect was occurred at the interval of 3500 - 5000 Hz, and the simulated values can be revised at this interval by repeating tests.
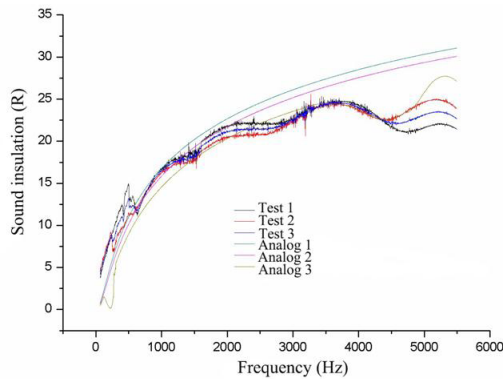

Fig. 3: Simulated sound insulation and measured value of Masson pine.

It was found that the sound insulation formula can be used to predict the sound insulation by the study of single board.

Sound insulation simulation of two-ply of fir

The comparison between the simulated and measured sound insulation of material 3 was shown in the Fig. 4. The analog 1 curve was obtained by the theoretical model based on classical flow resistance. The analog 2 curve was calculated by microscopic characteristics of wood and the correction of high-frequency error of material 3. The analog 2 curve perfectly reflected the sound insulation of fir double layer composite board. The main reason for the error between analog 1 and analog 2 was that the flow resistance based on the microscopic characteristics of wood can more accurately reflect the propagation characteristics of sound waves in wood.
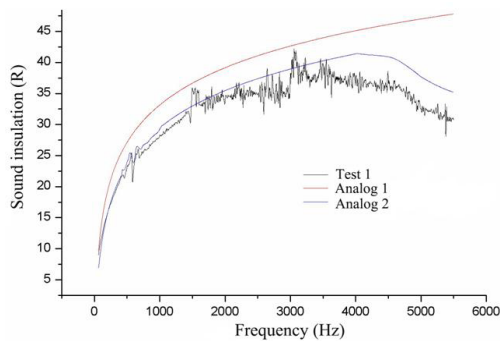
Fig. 4: Simulated sound insulation and measured value of two-ply of fir.

It was proved that the theoretical formula can better predict the sound insulation performance of fir double layer composite board. In the next composite plate experiment, the classical formula will not be used to predict the sound insulation performance of materials because the improved formula can better simulate the sound insulation of composite plate. In the case of ignoring the test error, the theoretical error still existed in the whole frequency range, which may be that the influence of the adhesive layer was not considered.

Sound insulation simulation of two-ply of fir and Masson pine

The simulation and test values of Material 4 and Material 5 were showed in Fig. 5. The test 1 curve was test value of Material 4. The test 2 curve is test value of Material 5. The microscopic characteristics of wood and the flow resistance characteristics of earlywood and latewood were introduced, the theoretical model was modified, and the analog 1 curve of Material 4 and the analog 2 curve of Material 4 were obtained.
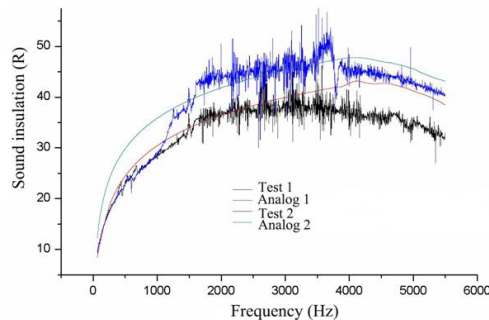
Fig. 5: Simulated sound insulation and measured value of two-ply of fir and Masson pine.

When the average density and modulus of Material 4 were the same as that of Material 5, the sound insulation varied with the surface density of the sample. The higher the surface density is, the better the sound insulation performance of the composite is. The increasing the surface density of the material had a positive significance to the sound insulation performance of the material. At the same time, it showed that the increase of the material surface density can effectively inhibit the anastomotic effect by the shallowness of the anastomotic valley. The main reason was related to the resonance frequency and critical frequency of the material. The high frequency of

71

the sound wave was mainly absorbed by the interior of the material. For low-frequency, this part was absorbed by the surface of the material. With the increase of surface density, the attenuation of internal material increased and the attenuation of surface decreased. The results showed that using high-density material as the face-plate can effectively improve the sound insulation, but it did not work at low frequency. Therefore, the sound insulation performance could be affected by different surface panels.

Single and double layer and the three layer of Chinese fir composite plate sound insulation simulation

The simulation and test values of Material 1, 3 and 6 were displayed in the Fig. 6. The test 1 curve was the test value of Material 6. The analog 1 curve was the simulation value of material 6 by the theoretical model of flow resistance based on wood characteristics. The test 2 curve was the test value of Material 3 and the analog 2 curve was the simulation value of Material 3. The test 3 curve was the test value of material 1 and the analog 3 was the simulation value of material 1.
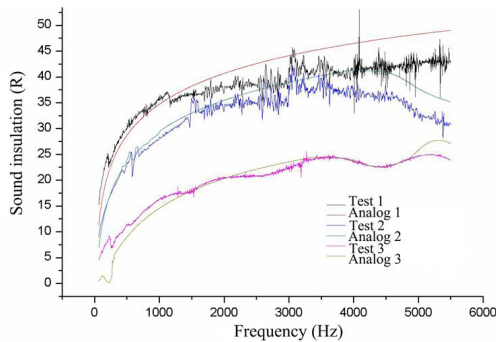

Fig. 6: Simulated sound insulation and measured value of Single and double layer and the three layer of Chinese fir composite plate.

It was found that the sound insulation increased significantly with the increase of the number of Chinese fir layers. The trend of the increase of sound insulation was more obvious in the middle and high frequency band (> 500Hz). The main reasons for this phenomenon were that the smaller the number of wood layers, the lower the flow resistance of the composite material, the easier the sound wave propagation, and the more able to penetrate the interior of the material. The flow resistance of the material increased with the increase of the number of wood layers. The force between the sound wave and the internal pores of the material increased with the increase of the flow resistance of the sound wave passing through the material. As a result, the sound energy loss increased when the sound wave propagated to the material. At the same time, it can be found that the critical frequency of the material shifted to the high frequency with the increase of the number of layers. The main reason was that the elastic modulus of the materials increased with the increase of the number of layers.

The more layers of composite materials, the greater the sound insulation. However, it was found that the increment of sound insulation decreased with the increase of composite layers by compared with three groups of data. In hence, increasing the thickness of material was not the effective method to improve the sound insulation performance, which was due to the coincidence effect shifting to the high frequency. At the same time, the increase of the number of layers cannot effectively suppress the resonance phenomenon.

CONCLUSIONS

The simulation model of wood sound insulation was established by the classical theoretical model and the microscopic characteristics of wood. Theoretical value of sound insulation was predicted by regarding the substances in wood cell wall as equivalence to specific medium based on Biot model, and the wood microscopic characteristics were taken into account for determining the equivalent density and bulk modulus of wood. The adjacent of earlywood and latewood was considered as sandwich structure in the sound insulation calculation of Masson pine. The transfer matrix and theoretical calculation formula of sound insulation provided a valuable method for investigating the high performance wood composite insulating board. For the composite materials, the sound insulation could be effectively improved by using the high density material as surface panel, but it did not work at low frequency. Increasing the thickness of material was not an effective method to improve the sound insulation performance.

ACKNOWLEDGEMENTS

REFERENCES

1. António, J., Godinho, L., Tadeu, A., 2004: Acoustic insulation provided by circular and infinite plane walls. Journal of Sound and Vibration 273(3): 681-691.
2. Allard, J.F., 1993: Propagation of sound in porous media: Modeling sound absorbing materials. Chapman & Hall. London, 284pp.
3. Biot, M.A., 1956: Theory of propagation of elastic waves in a fluid-saturated porous solid-I: low-frequency range. Journal of the Acoustical Society of America 28: 168-178.
4. Bao, F.C., Hou, Z.Q., 2001: Gas flow resistance and permeability coefficient of conifer wood. Scientia Silvae Sinicae 37(4): 80-87.
5. Bao, F.C., Hou, Z.Q., 2002: Three dimensional flow resistance network of longitudinal gas permeation in coniferous wood. Scientia Silvae Sinicae 38 (4): 111-116.
6. Buksnowitz, C., Teischinger, A., Grabner, M., Müller, U., 2010: Tracheid length in Norway spruce (*Picea abies* (L.) Karst.) analysis of three databases regarding tree age, cambial age, tree height, inter-annual variation, radial distance to pith and log qualities. Wood Research 55(4): 1-13.
7. Beranek, L.L., 1960: Noise reduction. McGraw-Hill. New York, 752 pp.
8. Beranek, L.L., 1971: Noise and Vibration Control. McGraw-Hill. New York, 804 pp.
9. Lee, C.-R., Xu, Y., 2009: A modied transfer matrix method for prediction of transmission loss of multilayer acoustic materials. Journal of Sound and Vibration 326(1): 290-301.
10. Klašnja, B., Orlovič, S., Galić, Z., Drekić, M., 2008: Poplar biomass of high density short rotation plantations as raw material for energy production. Wood Research 53(2): 27-38.
11. Liu, X.-J., Liu, J.L., Xu, B.-J., Gao, W.-D., 2012: Acoustic analysis for a sound absorbing structure with multi-layered porous material. Journal of Vibration and Shock 31(5): 106-117.

12. Matsumoto, T., Uchida, M., Sugaya, H., Tachibana, H., 2006: Development of multiple dry wall with high sound insulation performance. Applied Acoustics 67(6): 595-608.
13. Rowell, R.M., 1984: Penetration and reactivity of cell wall components. In: The chemistry of solid wood (ed. Rowell RM). American Chemical Society, Washington, Pp. 175-210.
14. Suleiman, B.M., Larfeldt, J., Leckner, B., Gustavsson, M., 1999: Thermal conductivity and diffusivity of wood. Wood Science and Technology 33(6): 465-473.
15. Shuku, T., Ishihara, K., 1973: The analysis of the acoustic field in irregularly shaped rooms by the finite element method. Journal of Sound and Vibration 29(1): 67-76.
16. Smardzewski, J., 2009: The reliability of joints and cabinet furniture. Wood Research 54(1): 67-76.
17. Song, B.H., Bolton, J.S., 2000: A transfer-matrix approach for estimating the characteristic impedance and wave numbers of limp and rigid porous materials. Journal of the Acoustical Society of America 107(3): 1131-1152.
18. Tadeu, A., António, J., Diogo, M., 2004: Sound insulation provided by single anddouble panel walls: a comparison of analytical solutions versus experimental results. Applied Acoustics 65(1): 15-29.
19. Varivodina, I., Kosichenko, N., Varivodin, V., Sedliačik, J., 2010: Interconnections among the rate of growth, porosity and wood water absorption. Wood Research 55(1): 59-66.
20. Whole, W., Elmallawany, A., 1969: Generalized model of application of statistical energy analysis for the sound propagation in a complicated structure. Journal of Sound and Vibration 40(2): 233-241.
21. Watanabe, U., Norimoto, M., 2000: Three dimensional analysis of elastic constants of the wood cell wall. Wood Research 87: 1-7.
22. Wilson, D.K., 1993: Relaxation-matched modeling of propagation through porous media, including fractal pore structure. Journal of the Acoustical Society of America 94: 1136-1145.
23. Zhang, Z.G., Zhang, X.L., Zhang, N., 2010: Study on sound insulation properties of materials by transfer matrix standing wave tube method. Materials Review 5: 118-121.
24. Zhan, P., 2014: Study on sound insulation properties of composite structures with air and porous materials. Applied Acoustics 33(5): 426-432.
25. Zwikker, B.C., Kosten, C.W., 1949: Sound absorbing materials. Elsevier publishing company. New York, 173 pp.

Zehui Ju, Qian He, Tianyi Zhan, Haiyang Zhang, Lu Hong, Xiaoning Lu*
Nanjing Forestry University
College of Materials Science and Engineering
Nanjing 210037
P.R. China
*Corresponding author: luxiaoning@njfu.edu.cn

VARIATIONS OF WOOD PROPERTIES OF BIRCH (*BETULA PENDULA* ROTH) FROM A 23-YEAR OLD SEED ORCHARD

Marcin Jakubowski, Arkadiusz Tomczak, Tomasz Jelonek
Witold Grzywiński
Poznan University of Life Sciences
Poznań, Poland

ABSTRACT

This work presents the results of selected wood properties in birch trees grown on a provenance experiment plot established as a seed orchard. The study concerned: basic density, oven-dry density and compression strength along the grain at a moisture content of 0% and at moisture content above fiber saturation point. Analyses were performed on 971 wood samples collected from 28 trees at the level of breast height. It was found high variability for diameter of breast height (22%) and relatively low for basic density (9%) and oven-dry density (11%). Average basic density was 446.5 kg·m^{-3} and average oven-dry density was 537.9 kg·m^{-3}. The compression strength at 0% moisture content was four times higher (65 MPa) than the strength at moisture content above the fiber saturation point (16.6 MPa). Most of clones had similar properties within the limits of statistical errors, but a few clones exhibited statistically significant low value.

KEYWORDS: Forest plantations, seed orchard, compression strength, wood density, wood quality, wood moisture content.

INTRODUCTION

Wood consumption has increased consistently in recent years in close relation to the popularity of wood as an environmentally friendly material. Wood from stands has better technical parameters than that from plantations, however wood resources in forests are limited, which results in the development of plantations as a natural alternative. In 2001 over 50 million ha of plantations worldwide produced approximately 20% of harvested timber. In some countries (China, Russia, the United States, Brazil, Indonesia, Sudan, Chile) plantations have become important sources of timber (West 2006, Zwoliński 2008). Wood from plantations has slightly different properties and stem characteristics, limiting its applications considerably. Plantations

in Europe are generally oriented towards biomass and energy production and contain the tree species belonging mainly to the genera Salix and Populus (Klašnja et al. 2008, Šefc et al. 2015, Mola-Yudego et al. 2017). This is mainly due to plantations being managed as monocultures, however attempts are being made to introduce mixed cultures (Gartner 2005, Kelty 2006). Despite the development of plantations, a decrease in forested area may be observed as a result of timber harvesting (Stibig et al. 2014, Margono et al. 2014). In Poland plantations of fast-growing trees have not been of great importance due to the predominance of the traditional model of forest economy, although the potential use of plantation culture is being considered, particularly for wood as an energy source (Bijak et al. 2013, Szczukowski and Stolarski 2013, Bronisz et al. 2016, Mola-Yudego et al. 2017). The wood industry still requires raw material of a high technological standard. In the case of plantations it is essential to select appropriate genotypes that ensure adequate wood quality. Plantations are typically established using specially prepared seedlings. Seed orchards serve a completely different function, ensuring continuous seed production by specimens with valuable genotypes, although even in this form of plantations the genotype is narrowed down (Przybylski 2015). Seed orchards are established by grafting fragments of maternal trees onto rootstock of the same species. Many experimental plantations in Poland established in previous decades have already reached an age which allows the wood to be examined in depth. Individual specimens have a similar appearance to the maternal trees. By definition the purpose is seed production; however in view of the rapid individual growth and preservation of traits of the maternal tree, it appears appropriate to considering production by vegetative propagation of selected clones. Stems of trees on existing plantations have already reached dimensions sufficient for testing (Jakubowski et al. 2013, Szaban et al. 2014).

Provenance experiments have taken on great importance in recent years, and birch is seen as an important source of good quality wood. Consequently research in this field is being conducted in various European countries, including the United Kingdom (Lee et al. 2015), Finland (Maja et. al. 2015, Haapala et al. 2017), Island (Riege and Sigurgeirsson 2018), Poland (Lachowicz et al. 2019) and others (Cameron 1996, Baliuckienė, and Baliuckas 2006, Henynen et al. 2010), as well as in countries outside Europe such as China (Wang et al. 2015, 2018).

In this work it is assumed that the wood density and compression strength will be different for the tested clones, and this will help in the selection of the most promising specimens. The samples from the seed orchard are unique because of restricted conditions of cuttings. These studies were conducted on wood collected from the last schematic cuttings. The plantation reached the final spacing in 2007. The material from these cuttings is particularly valuable, because further samples may come from incidental cuttings only. All tests were carried out in 2008 and the results were stored in our archives. Due to the growing interest in birch wood, we decided to analyze the collected data. The aim of this study was to compare wood density and compressive strength along the grain in birch wood of various provenances.

MATERIAL AND METHODS

Plantation Birch II was established in the years 1984-1985 in the Susz Forest Division in north-eastern Poland and was intended for the production of seeds. All plantations in Poland are registered and are under the control of the Forest Research Institute (Register of seed orchards). The plantation was set up in a block design with replications typical of provenance studies. Analyses were performed on 28 clones represented by 28 trees. Diameter at breast height was measured in two directions: north-south and east-west. The measurements were averaged and

the selected trees were felled. Because all of the trees are of the same age and have the same number of annual rings we omitted the measurement of rings. The experimental material for crash tests consisted of small wood samples with dimensions of 20 x 20 x 30 mm along the grain (x, y, z). Samples were collected from the stem cross-section at two levels according to the diagram (Fig. 1). Radial rows of samples were oriented in the east-west direction.
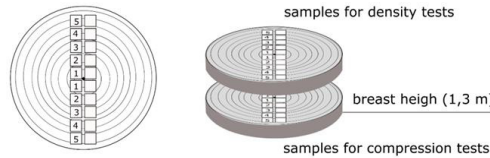

Fig. 1: Scheme for wood sample collection from the stem cross–section.

Mechanical tests were conducted in two ways: first (for row 1) - at a sample moisture content above the fiber saturation point (> 30%) and second (for row 2) at a moisture content of 0%. Standard mechanical tests are carried out at 12% of moisture content and we consider this a good point for comparison with other research. Oven-dry wood is rarely used for tests: we do it in order to observe compression strength after drying. Differences between results for wood with moisture content above the fiber saturation point and oven-dry wood may demonstrate certain changes in the wood structure after drying. For the first method, samples were immersed in water for 72 hours. For the second, samples were dried in an electric drier at 105°C until they reached constant mass. The mass of samples was measured with laboratory scales to an accuracy of 0.001 g. Dimensions of samples were measured immediately before the crash test with using an electronic caliper. The volume of samples was calculated from the dimensions (x, y, z). Wood strength was determined using a TiraTest 2300 testing machine controlled by Matest Service software. Compression strength along the grain was determined using the following Eq.:

$$CS_{0\%} = \frac{F}{A} \qquad \text{(MPa)} \qquad (1)$$

where: $CS_{0\%}$ - compression strength along the grain for oven-dry samples,
F - the applied load (N),
A - specimen area (mm^2),

$$CS_{30\%} = \frac{F}{A} \qquad \text{(MPa)} \qquad (2)$$

where: $CS_{>30\%}$ - compression strength along the grain for wet samples (moisture content above fiber saturation point),
F – the applied load (N),
A - specimen area (mm^2).
Oven-dry density was determined using the following Eq.:

$$OD = \frac{M_{0\%}}{V_{0\%}} \qquad \text{(kg·m}^{-3}) \qquad (3)$$

where: OD = oven-dry density,
M0% = mass of sample at 0% moisture content,
V0% = volume of sample at 0% moisture content.

Basic density (green density) was determined using the following Eq.:

$$BD = \frac{M_{0\%}}{V_{max}} \qquad (\text{kg·m}^{-3}) \qquad (4)$$

where: BD - basic density,
M_{0\%} - mass of sample at 0% moisture content,
V_{max} - volume of sample at maximum swelling.

The collected measurements were analyzed using descriptive statistics and analysis of variance (low significance differences test and Tukey test). Statistical calculations were performed in Statistica software and for visualization we used the R language.

RESULTS AND DISCUSSION

The trees on the plantation showed large variation in stem thickness. The average diameter at breast height equaled 25.78 cm, with values for individual specimens ranging from 15.2 to 38.5 cm (Tab. 1). Wood properties show a deeper look into whole population, a total of 971 samples from 28 trees were tested. The coefficient of variability was relatively high for diameter (22%) in compare with wood density which fluctuated at very low level between 9% and 11% (Tab. 1).

Tab. 1: Measured features for the whole population of clones grown on the plantation. Basic statistics.

	d1.3 (cm)	CS0% (MPa)	CS>30% (MPa)	DD (kg·m⁻³)	BD (kg·m⁻³)
Min	15.2	32.83	11.26	376.90	345.32
Max	38.5	94.49	24.85	746.44	598.01
Mean	25.78	65.39	16.60	537.89	446.50
Sd	5.65	10.02	2.54	60.52	41.75
Cv	22	15	15	11	9
N	28	248	264	278	277

The two types of wood density showed different distribution of population which is clearly visible in the violin plots (Fig. 2).
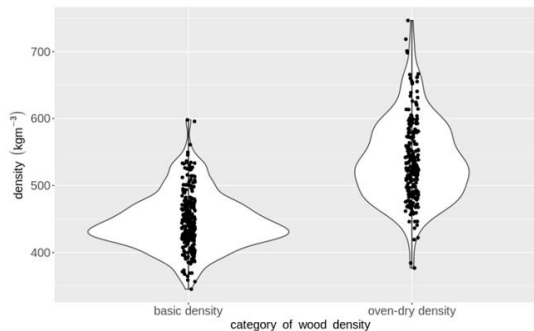

Fig. 2: Distribution of basic wood density and dry wood density in birch samples.

In the case of basic density there were more samples around the median (the center of the violin appears much wider) than in the case of oven-dry density. The distance between maximum and minimum is also shorter for basic density (252.78 kg·m^{-3}) than for dry density (369.54 kg·m^{-3}) which points to more stable distribution in BD. Standard deviation also indicate greater fluctuation in the case of oven-dry density (Tab. 1).

The mean density of oven-dry wood is 537.89 kg·m^{-3} which is 91 kg·m^{-3} higher than basic density, indicating that the basic density is lower by 16%. Difference were confirmed statistically using Mann-Whitney test at the level $\alpha = 0{,}05$. Density in oven-dry samples varies much more than density in green samples. We can see that distance between first and third quartiles are longer for oven-dry samples (Fig. 3).
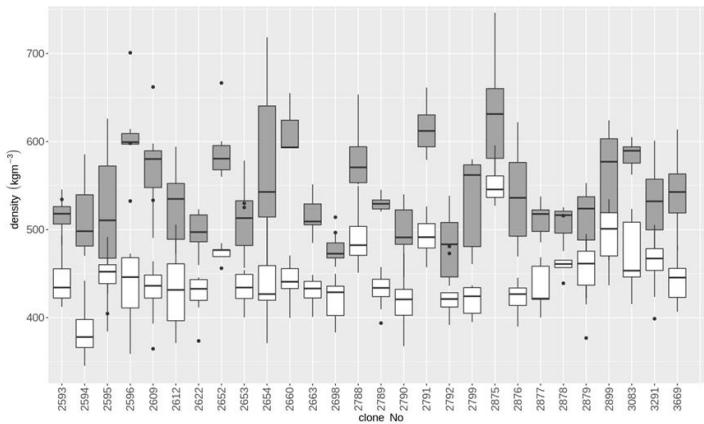
Fig. 3: Standard boxplot of oven-dry density (grey) and basic density (white) of 28 birch clones. Horizontal line – median, box – 1st and 3rd quartile, vertical lines – whiskers, dots- outliers.

Radial distribution of the analyzed properties is rather typical for tree trunks, with all value increasing from pith to bark. We observed that value of samples connected with water (CS$_{>30\%}$ and BD) showed a relatively mild and stable increase (Figs. 4, 5). There is complete different situation in case of oven-dry samples (Figs. 6, 7) were the increase was not distinct in all cases. Confidence level also takes high values.
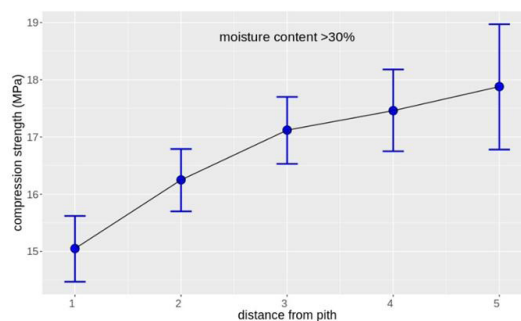
Fig. 4: Average compression strength with confidence level (+0.95) for birch samples over fiber saturation point.

Generally in all cases we observe that green wood shows gentle variation but for oven-dry samples the behaviour is extreme. This currently leads to difficulties in planning the use of wood as a material.
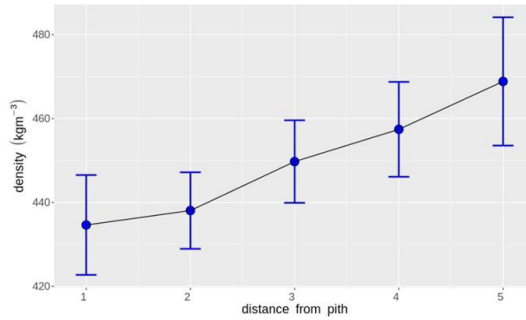
Fig. 5: Average basic density (kg·m⁻³) with confidence level (+0.95) in birch samples.

We observed a very large difference in the strength of tested samples with two levels of moisture content. The mean compression strength of oven-dry samples ($CS_{0\%}$) was close to four times higher (65.39 MPa) than that of the green ($CS_{>30\%}$) samples (16.6 MPa).
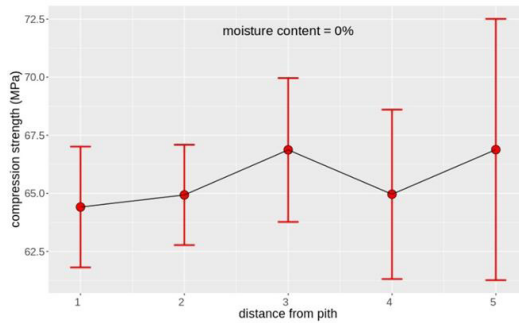
Fig. 6: Average compression strength with confidence level (+0.95) for tested birch samples at moisture content of 0%.
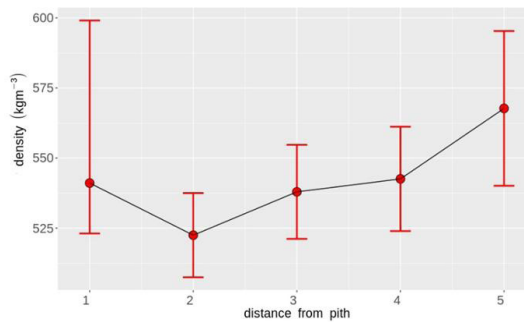
Fig. 7: Average oven–dry density (kg·m⁻³) with confidence level (+0.95) in birch samples.

An examination of the entire clone population showed that the compression strength of samples tested in dry conditions fluctuates much more than that of the green samples (Figs. 8, 9). The mean difference between the first and third quartile (Q1-Q3) in clones tested at 0% moisture content was 13 MPa. Green samples (moisture content of wood > 30%) produced a relatively narrow range of compression strength values and the mean difference (Q1-Q3) was only 4 MPa. These differences are based on absolute values, if we compare relative values, fluctuations of compression strength in both cases ($CS_{0\%}$ and $CS_{>30\%}$) are identical and equaled 15% (Tab. 1). Median in most of clones appears in to the center of the frame or near to center (Fig. 8), hence that population shows rather symmetrical value distribution. In a few clones we observed asymmetrical distribution.
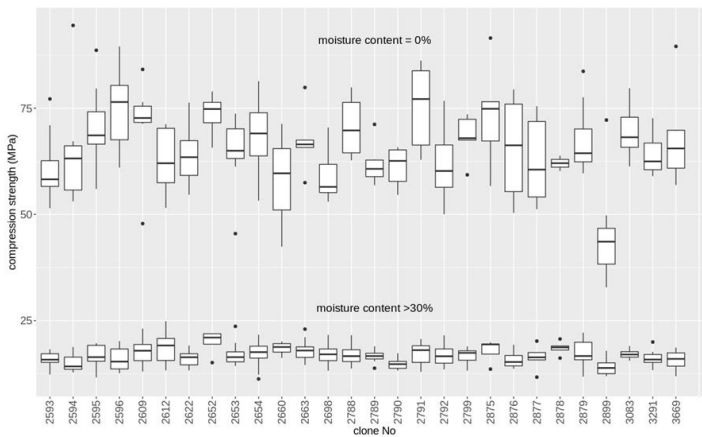
Fig. 8: Standard boxplot of compression strength of 28 birch clones with different moisture content. Horizontal line – median, box – 1st and 3rd quartile, vertical lines – whiskers, dots- outliers.
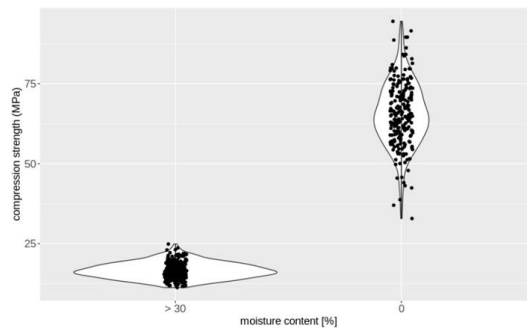
Fig. 9: Distribution of compression strength in different levels of moisture content.

The mean strength of most clones fluctuates within similar values. It is difficult to indicate especially strong specimens. Among the samples tested at higher moisture content a high mean was recorded for clones 2612 and 2652, while for oven-dry samples high means were obtained for clones 2596, 2652 and 2791. There was no real statistical difference between the tested clones and the entire population. However, it was relatively easy to identify the specimen with the lowest

strength values, clone 2899, which gave the worst results in both tests. Low strength properties were also recorded for samples from clone 2790. In the case of these weak clones, the differences from the rest of the population were confirmed as statistically significant.

Differences between the wood properties tested in most clones were observable, although they were not statistically significant in most cases. We found significant differences (LSD test) for clones 2596, 2652, 2660, 2698, 2791, 2875 and 2899. A more restrictive test (the Tuckey test) confirmed significant differences only for clone 2899. This may be result of the high variation in properties within a tree and the limited number of samples. No dependence was found between the properties tested and stem diameter in the analyzed trees. The plantation from which the wood was harvested was only 23 years old at the time of felling, greater differences appear to be observed in older trees.

DISCUSSION

The biometric features of trees are generally similar on most plantations oriented for wood production. In this case, we observed very large differences in diameter at breast height which ranged between 15 and 37 cm for various clones. Because the age (23 years) and conditions are the same, the difference probably results only from genetic variations between clones. The variations in diameters are related to the number of samples that was possible to obtain for testing purposes. We are aware that one sample tree for each clone represents low value, but at this time it is not possible to obtain more trees. This is a pilot study, and we expect that information obtained from single trees will be verified in subsequent research at the next stages of the plantation.

The average basic density obtained in this study (446.5 kg·m^{-3}) is a much lower than that reported by Lachowicz et al. (2019) who obtained higher values for various Polish provenances (mean = 528 kg·m^{-3}). However, because the populations investigated were much older, results may not be directly comparable. Only one of the populations tested by Lachowicz et al. (2019) gave a similar result (447 kg·m^{-3}) and this was found in Łobez District and consisted of relatively young trees (30-years). Other authors have reported lower mean values for birch in Poland, Helińska-Raczkowska and Fabisiak (1995) gave 480 kg·m^{-3}. Basic density in birch varies within a wide range: between 375 and 590 kg·m^{-3} (Helińska-Raczkowska 1996), or between 400 and 652 kg·m^{-3} (Lachowicz et al. 2019). Values depend on various factors, including age, habitat, geographic location and others (Lachowicz et al. 2019, Repola 2006).

In this study only a small change in wood density was observed between pith and bark. Basic density increased from 435 to 470 kg·m^{-3}, dry density from 525 to 557 kg·m^{-3}. Birch has a diffuse porous wood, and so the structure of the wood tissue is quite similar across the whole cross-sectional area. The increasing tendency is probably a mechanical response of the stem to the load of the crown mass. The crown undergoes extensive growth in the early phase of a young plantation. It should be emphasized that we studied a young plantation with trees growing in loose conditions. In older trees major changes have been observed (Heräjärvi 2004). A relatively large increase in basic density was reported by that author for mature trees of *Betula pendula*, with values increasing from 480 near the pith to 520 kg·m^{-3} (or even 550 kg·m^{-3}) near the bark (Heräjärvi 2004). The same author reported a lower radial increase of basic density for *Betula pubescens*.

The strengthening of wood is accompanied by a reduction in its moisture content, as has been described in other works (Kollman and Côté 1967), and this features has also been as a helpful factor for wood quality estimation (Szymański et al. 2013). Generally the relationship between

wood strength and moisture content has been subject of several studies (Gerhards 1982, Silva et al. 2012, Jakubowski et al. 2011). Changes in compression strength in our research were observed only in extreme conditions (0% moisture content), but this conditions reflect the behavior of samples after drying. We observed that the variation in strenght in most of the population is similar and not statistically differ, although some samples gave extreme values, which are probably symptoms of disturbances in the wood structure. For this reason, observations of strength under extreme moisture content conditions may be more helpful than the standard level of 12% used for crash tests.

Wood properties considered in relation to distance from pith show the generally typical increasing trend also reported by other authors (Heräjärvi 2004). Variation in compression strength was greater for oven-dry samples (Fig. 4, 6), and appears to be less predictable because of the more extreme values. Problems of testing birch samples during a drying process were studied by Zongying et al. (2016). Authors pointed that radial drying stress in birch disks may be the result of combination of several factors connected to shrinkage anisotropy.

CONCLUSIONS

1. Trees from a seed plantation having the same age and environmental conditions show large variation in the diameter at breast height, but relatively low variability in wood density. Coefficient of variability was 22% for diameter of breast height, 11% for oven-dry density and 9% for basic density.
2. The tests revealed large differences in compression strength for different moisture contents. The compression strength at 0% moisture content was four times higher (65 MPa) than the strength at humidity above the fiber saturation point (16.6 MPa). The results of tests carried out at 0% moisture content were also characterized by highly extreme values.
3. Most of clones had similar properties within the limits of statistical errors, but a few clones produced statistically significantly lower values. It appears to be too early for final clone selection at this stage of research, but the current results may be helpful for later tests.
4. In view of the rapid growth of plantations and the fact of preservation of the genotype through vegetative propagation, such experimental results should be verified for the purpose of developing a potential method to produce high-quality timber in short periods.

REFERENCES

1. Baliuckienė, A., Baliuckas, V., 2006: Genetic variability of Silver birch (*Betula pendula* L.) wood hardness in progeny testing at juvenile age. Baltic Forestry 12(2): 134-140.
2. Bijak, S., Zasada, M., Bronisz, A., Bronisz, K., Czajkowski, M., Ludwisiak, Ł., Wojtan, R., 2013: Estimating coarse roots biomass in young silver birch stands on post-agricultural lands in central Poland. Silva Fennica 47(2): 1-14.
3. Bronisz, K., Strub, M., Cieszewski, C., Bijak, S., Bronisz, A., Tomusiak, R., Zasada, M., 2016: Empirical equations for estimating aboveground biomass of *Betula pendula* growing on former farmland in central Poland. Silva Fennica 50(4): 1-17, id 1559.
4. Cameron, A.D., 1996: Managing birch woodlands for the production of quality timber. Forestry 69(4): 357-371.
5. Gartner, B. L., 2005: Assessing wood characteristics and wood quality in intensively managed plantations. Journal of Forestry 103: 75-77.

6. Gerhards, C. C., 1982: Effect of moisture content and temperature on the mechanical properties of wood: an analysis of immediate effects. Wood and Fiber V 14(1): 4-36.

7. Haapala, A., Kontunen-Soppela, S., Oksanen, E., Rousi, M., MolaYudego, B., 2017: Tree provenance affects the growth and bioenergy potential of juvenile Silver birch. In 6th. International Scientific Conference on Hardwood Processing: Proceedings. Natural Resources Institute Finland, pp. 310-318.

8. Helińska-Raczkowska, L., Fabisiak E., 1995: Zależność między długością elementów anatomicznych i gęstością drewna brzozy (*Betula pendula* Roth). (Relation between the length of anatomical elements and the density of birch wood (*Betula pendula* Roth)). Prace Komisji Technologii Drewna PTPN 14, Pp 43-48.

9. Helińska-Raczkowska, L., 1996: Zmienność wilgotności i gęstości drewna w świeżo ściętych pniach brzozy (*Betula pendula* Roth). (Wood moisture content and density variation in the freshly cut birch (*Betula pendula* Roth) stem). Folia Forestalia Polonica. Seria B. Zeszyt 27: 23–30.

10. Heräjärvi, H., 2004: Variation of basic density and Brinell hardness within mature Finnish *Betula pendula* and *B. pubescens* stems. Wood and Fiber Science 36(2): 216-227.

11. Hynynen, J., Niemistö, P., Viherä-Aarnio, A., Brunner, A., Hein, S., Velling, P., 2010: Silviculture of birch (*Betula pendula* Roth and *Betula pubescens* Ehrh.) in northern Europe. Forestry 83: 103-119.

12. Jakubowski, M., Gonet, A., Kałuziński, D., 2013: Gęstość umowna drewna świerka pospolitego (*Picea abies* L. Karst) pozyskanego z plantacji nasiennej (Wood density of Norway spruce (*Pice aabies* L. Karst) harvested from seed orchard). Forestry Letters 106: 9-13.

13. Jakubowski, M., Tomczak, A., Jelonek, T. 2001: Compression strength along the grain in twin samples (wet and absolutely dry) coming from wood of wind- broken trees of Scots pine (*Pinus sylvestris* L.). Annals of Warsaw University of Life Sciences – SGGW. Forest and Wood Technology 74: 104-109.

14. Kelty, M. J., 2006: The role of species mixtures in plantation forestry. Forest Ecology Management 233(2-3): 195-204.

15. Klašnja, B.; Orlović, S., Galić, Z., Drekić, M., Vasić, V., Pilipović, A., 2008: Poplar biomass of high density short rotation plantations as raw material for energy production. Wood Research 53(2): 27-38.

16. Kollmann, F.F.P., Côté, W.A., 1968: Principles of wood science and technology I Solid wood. Springer-Verlag, Berlin, Heidelberg, New York. 592 pp.

17. Lachowicz, H., Paschalis-Jakubowicz, P., Wojtan, R., 2018: Multivariate analysis of the variability in the density of oven-dry wood of silver birch (*Betula pendula* Roth) in Poland. Drewno 61(201): 39-56.

18. Lee, S. J., Connolly, T., Wilson, S. McG., Malcolm, D. C., Fonweban, J., Worrell, R., Hubert, J., Sykes R. J., 2015: Early height growth of silver birch (*Betul apendula* Roth) provenances and implications for choice of planting stock in Britain. Forestry: An International Journal of Forest Research 88 (4): 484-499.

19. Maja, M. M., Kasurinen, A., Holopainen, T., Kontunen-Soppela, S., Oksanen, E., Holopainen, J. K., 2015: Volatile organic compounds emitted from Silver birch of different provenances across a latitudinal gradient in Finland. Tree Physiology 35(9): 975-986.

20. Margono, B. A., Potapov, P. V., Turubanova, S., Stolle, F., Hansen, M. C., 2014: Primary forest cover loss in Indonesia over 2000–2012. Nature Climate Change (4): 730–735.

21. Mola-Yudego, B., Arevalo, J., Díaz-Yáñez, O., Dimitriou, I., Haapala, A., Filho, A. Selkimäki, M., Valbuena, R., 2017: Wood biomass potentials for energy in northern Europe: Forest or plantations? Biomass and Bioenergy 106: 95-103.

22. Przybylski, P., 2015: Are we narrowing genetic variability in seed orchards? An attempt to answer, based on the analysis of microsatellite DNA of grafts growing in Scots pine (*Pinus sylvestris* L.) seed orchard in the Forest District Susz. Leśne Prace Badawcze / Forest Research Papers 76(3): 240–249.

23. Repola, J., 2006: Models for vertical wood density of Scots pine, Norway spruce and birch stems, and their application to determine average wood density. Silva Fenika 40(4): 673-685.

25. Riege, D. A., Sigurgeirsson, A., 2018: Provenance variability in establishment of native downy birch in a 14-year trial in southwest Iceland. Icelandic Agricultural Sciences 31: 3-9.

26. Šefc, B., Trajković, J., Slavko, G., Radovan, D., Hasan, M., 2009: Selected tree characteristics and wood properties of two poplar clones. Wood Research 54(1): 15- 22.

27. Stibig, C.F., Achard, H.J., Carboni, F., S., Raši, R., Miettinen, J., 2014: Change in tropical forest cover of Southeast Asia from 1990 to 2010. Biogeosciences 11: 247–258.

28. Szaban, J., Kowalkowski, W., Karaszewski, Z., Jakubowski, M., 2014: Effect of tree provenance on basic wood density of Norway spruce (*Picea abies* [L.] Karst.) grown on an experimental plot at Siemianice Forest Experimental Station. Drewno 57(191): 135-143.

29. Szczukowski, S., Stolarski, M., 2013: Plantacje drzewi krzewów szybko rosnących jako alternatywa biomasy z lasu – stan obecny, szansei zagrożenia rozwoju (Plantations of fast growing trees and bushes as an alternative to biomass from the forest - current status, opportunities and threats to development). In: Gołos P., Kaliszewski A., 2013: Biomasa leśna na cele energetyczne . Instytut Badawczy Leśnictwa (ResearchForest Institute), Sękocin Stary. Pp 32-46.

30. Szymański, M., Pazdrowski, W., Szykowny, T., Nawrot, M., 2013: Wzmocnienie desorpcyjne jako podstawa oceny jakości drewna dębu szypułkowego (*Quercus robur* L.) i dębu burgundzkiego (*Quercus cerris* L.). (Desorption strengthening as a basis for the assessment of wood quality of pedunculate oak (*Quercus robur* L.) and Turkey oak (*Quercus cerris* L.)) Sylwan 157(11): 811–816.

31. Wang, X. W., Weng, Y. H., Liu, G. F., Krasowski, M., J., Yang, C. P. 2015: Variations in carbon concentration, sequestration and partitioning among *Betula platyphylla* provenances. Forest Ecology and Management 358: 344-352.

32. Wang, X., Zhao, D., Liu, G., Yang, C., Teskey, R., O., 2018: Additive tree biomass equations for *Betula platyphylla* Suk. plantations in Northeast China. Annals of Forest Science 75(2): 60.

33. West, P.W., 2006: Growing plantation forests. Springer-Verlag Berlin Heidelberg, 233 pp.

34. Zasada, M., Bijak, S., Bronisz, K., Bronisz, A., Gawęda, T. 2014: Biomass dynamics in young silver birch stands on post-agricultural lands in central Poland. Drewno 57(192): 29-39.

35. Zongying, F., Zhao, J., Lv, Y., Huan, S., Cai, Y.. 2016: Stress characteristics and stress reversal mechanism of white birch (*Betula platyphylla*) disks under different drying conditions. Maderas. Ciencia y tecnología 18(2): 361-372.

36. Zwoliński J., 2008: Rola leśnictwa plantacyjnego w warunkach kryzysu środowiskowego i surowcowego świata. (The role of plantation forestry in the conditions of environmental and raw material crisis in the world) Leśne Prace Badawcze/Forest Research Papers 69(4): 371-379.

Marcin Jakubowski*, Arkadiusz Tomczak, Tomasz Jelonek
Witold Grzywiński
Poznan University of Life Sciences
Faculty of Forestry
Department of Forest Utilisation
Wojska Polskiego 71A
60-625 Poznań
Poland
*Corresponding author: marcin.jakubowski@up.poznan.pl

EFFECTS OF NATURAL WEATHERING ON SURFACE CHARACTERISTICS OF SCOTS PINE IMPREGNATED WITH WOLMANIT CX-8 AND VARNISHED

Caglar Altay[1], Ergun Baysal[2], Hilmi Toker[2], Turkay Turkoglu[2]
Mustafa Kucuktuvek[3], Ahmet Gunduz[2], Huseyin Peker[4]

[1]Adnan Menderes University
Aydin, Turkey
[2]Mugla Sitki Kocman University
Mugla, Turkey
[3]Antalya Bilim University
Antalya, Turkey
[4]Artvin Coruh University
Artvin, Turkey

ABSTRACT

In this study, it was aimed to investigate the effects of weathering on some surface characteristics such as color and surface roughness changes of Scots pine impregnated with copper-containing chemical such as Wolmanit CX-8 (WCX-8) and varnished with synthetic varnish (SV), cellulosic varnish (CV), and polyurethane varnish (PV) were investigated. Results showed that while the WCX-8 impregnated and PV coated Scots pine specimens showed better color stability than other treatment groups after weathering, only CV coated Scots pine gave the most negative effect on color stability. While, the untreated (control) wood surface turned from red to green and yellow to blue respectively, after weathering, other all treatment groups gave reddish and yellowish tone after weathering. Weathering conditions increased the surface roughness of control (untreated) and other all treatment groups. The control group gave a rougher surface than other treatment groups after weathering. Surface roughness increases were the lower for CV coated Scots pine wood than other treatment groups. The results showed that while WCX-8 impregnation before varnishing gave better color characteristics, generally it caused to increase the surface roughness of Scots pine after weathering.

KEYWORDS: Varnish, impregnation, color, surface roughness, natural weathering.

INTRODUCTION

The wood material is a versatile natural resource in aesthetic, engineering, and structural applications. Because of its superior properties, wood material maintains its importance. Wood is used as a raw material in many areas (Ors and Keskin 2001, Bhat et al. 2010). Besides the positive properties of the wood material, there are also negative features. The wood is destructed by fungi and insects due to its natural structure and it is deformed due to the hygroscopic feature and changing its dimensions depending on the humidity and temperature of the atmosphere due to its hygroscopic feature. Therefore, the natural stability of wood materials cannot be long enough due to weaknesses such as resistance against different environmental factors during its service life (Usta 1993, Uysal 2005).

The wood material cannot withstand the effects of heat, light (UV, IR), humidity (rain, snow, humidity, and dew), mechanical effects (wind, sand, dirt) and biological pests (Budakci and Atar 2001, Kilic and Hafizoglu 2007, Williams 2005). Wood materials are usually exposed to solar radiation, water, wind, and dust during their useful life when used outdoor (Feist 1989). In outdoor climatic conditions, the effect of sun rays on the surface of the wood material changes the wood color very rapidly, and it causes a decrease in hardness, brightness, and mechanical properties. This is reported to be caused by wood extractives and chemical degradation of lignin (Feist 1989, Budakci 2006, Kilic and Hafizoglu 2007, Anderson et al. 1991, Sivrikaya et al. 2011). When exposed to outdoor conditions, smooth surface of wood material increases surface roughness due to lignin degradation and creates thin or deep cracks on the surface, washing with rainwater and color change by photodegradation (Feist 1989). Color is a basic visual feature for wood and wood-based products (Aydin and Colakoglu 2005). The color change is caused by the fact that the wood material absorbs all wavelengths of the electromagnetic radiation that initiates the photochemical reactions (Hon 1981).

There are many ways to protect wood products from outdoor degradation. One of these methods is to impregnate wood with various chemicals (Ozgenc et al. 2013). Photodegradation of wood can be limited by using some copper-containing chemicals (Jin et al. 1991, Cornfield et al. 1994, Zhang et al. 2009, Temiz et al. 2005, Ozgenc et al. 2012, Baysal et al. 2016, Ustun et al. 2016) treatment with inorganic salts particularly hexavalent chromium compounds (Feist 1979, Feist and Williams 1991, Evans et al. 1992, Yalinkilic et al. 1999, Baysal 2012). The most effective method of preventing the photodegradation of wood involves treating inorganic salts with dilute aqueous solutions, particularly hexavalent chromium compounds (Evans et al. 1992). Evans et al. (1992) and Kiguchi and Evans (1998) reported that the application of chromium trioxide to wood surfaces prevents lignin degradation during natural weathering. Williams et al. (1996) determined that the chromium oxides in copper-chromate-arsenic (CCA) which bond to the wood after treatment, decrease photodegradation of the wood surface. Sell and Feist (1985) reported that CCB-impregnated wood has high resistance and a protective effect against weathering. Feist and Ross (1995) and Jirouš-Rajković et al. (2004) determined that CCA provided long-term protection against weathering and erosion. However, it is no longer being produced for use in most residential settings, because it contains chromium and arsenic. Nowadays, some copper-containing wood preservatives such as Tanalith® E (TN-E) and Adolit-KD5 (AD-KD5) are being used in the forest products industry instead of CCA (Turkoglu et al. 2015a, Turkoglu et al. 2015b). The focus on copper-based preservatives has increased following concerns about the environmental effects of chromium and arsenic (Freeman et al. 2008). Therefore, the weathering aspects of treated wood with new preservatives become of practical importance (Temiz et al. 2007). Copper forms certain complexes with wood

components, such as copper-cellulose complexes, copper-lignin complexes, and crystalline or amorphous inorganic/organic copper compounds, and reduces the degradation of the wood surface from weathering factors (Grelier et al. 2000, Temiz et al. 2005). The mechanism of action of copper-containing preservatives has been explained well in a study by Schmid et al. (2000).

Another method used to protect the wood surface against the UV effect is to cut the UV light and water contact with the wood surface by surface treatments (paints, varnishes, water repellent substances, etc.) (Ozgenc et al. 2013). Varnishes can provide wooden materials with the desired aesthetical properties like color and gloss (Meijer 2001). But, varnishing alone imparts to wood only superficial protection against some deteriorating agents for a limited time, often less than two years (Williams et al. 1996). Therefore, impregnation of wood with an appropriate water repellent or applying a varnish compatible preservative chemical prior to hazardous service conditions has been undertaken to make wood more stable against photochemical degradation, dimensional changes, biological decomposition, and fire (Wilkinson 1979, Williams et al. 1996, Yalinkilic et al. 1999). Moreover, the surface properties of wood materials can be improved easily by impregnating and finishing with various preservatives to provide different performance characteristics for individual applications, such as high hardness, impact resistance, suitable gloss, and chemical resistance (Chang and Lu 2012). Baysal et al. (2014) studied the effect of accelerated weathering on surface properties of Scots pine impregnated with Wolmanit-CB, TN-E, and AD-KD5 and coated with synthetic varnish (SV) and polyurethane varnish (PV). According to the findings of their study, while weathering caused an increase in the hardness of impregnated and varnished specimens, the gloss of specimens decreased after weathering. Nzokou et al. (2011) determined that when the polyurethane varnish, which is water-repellent to the wood surface, is applied to the wood surface during impregnation operations, the color darkening caused by open weather is delayed and the increasing roughness on the wood surface is prevented. Yalinkilic et al. (1999) investigated the weathering performance of Scots pine and chestnut wood impregnated with chromium-copper-boron (CCB) and applied with polyurethane varnish or alkyd-based synthetic varnish. They found that CCB impregnation greatly stabilized the surface color and reduced the mass loss of wood. It was also claimed that preservative treatment followed by a surface varnishing system protected the wood in long-term weathering conditions. Turkoglu et al. (2015a) investigated the color stability of the impregnated and varnished wood. They determined that the color stability of impregnated and varnished wood specimens gave better results than solely varnished wood specimens after natural weathering. In another study, Turkoglu et al. (2015b) studied some surface properties of wood impregnated with CCA, TN-E, AD-KD 5 and coated with polyurethane and synthetic varnishes after natural weathering. They found that after 6 months of natural weathering, the surface hardness and gloss loss of Scots pine and Oriental beech was the lowest in the TN-E impregnated and PV coated wood specimens.

In this study, some surface characteristics such as color and surface roughness changes of Scots pine impregnated with copper-containing chemical such as wolmanit CX-8 (WCX-8) and varnished Scots pine after 6 months of weathering were studied. Cellulosic, synthetic, and polyurethane varnishes were used as a coating material. Weathering was performed in Mugla, which is in the Southern Aegean Region of Turkey.

MATERIALS AND METHODS

Preparation of wood specimens

Scots pine wood specimens measuring 10 x 100 x 150 mm (radial by tangential by longitudinal) were prepared from air-dried sapwood of Scots pine (*Pinus sylvestris* L.) lumber.

Wood surfaces were lightly sanded with 120 grit sandpaper, and then specimens were divided into three groups. The first group comprised non-impregnated and non-varnished (control) specimens. The second group comprised only varnished specimens. Finally, the third group consists of both impregnated and varnished samples. All specimens were conditioned at 20°C and 65% moisture content for three weeks before the impregnation procedure. According to technical data sheets of products, WCX-8 contains 2.8% bis-(n-cyclohexyldiazeniumdioxy)-copper (II) (copper (II)-HDO), 13.04% basic copper (II) carbonate, 4% boric acid and 2-amino ethanol (Wolmanit 2018).

Impregnation process

The Scots pine wood specimens were impregnated with the 5% aqueous solution of Wolmanit CX-8 (WCX-8), according to the ASTM D1413-07 (2007). All specimens were conditioned at 20°C and 65% moisture content for three weeks before tests. Ten replications were made for each treatment group. Retention values of chemicals were calculated using the following Eq. 1:

$$\text{Retention (kg·m}^{-3}) = [(G \times C)/V] \times 10 \tag{1}$$

where: $G = (T_2 - T_1)$ - treatment solution absorbed by the wood specimens (g),
   T_1 - the weight of the wood specimens before impregnation (g),
   T_2 - the weight of the wood specimens after impregnation (g),
   C - concentration (%),
   V - the volume of the wood specimen (cm^3).

Varnishing process

In this study, synthetic, polyurethane, and cellulosic varnishes were used to cover the wood material. The varnishes were applied to all surfaces and sides of the Scots pine specimens with a spray gun according to the ASTM D3023-98 standard (2003). Filler was used as the first varnishing applied to the wood surface was for filling the voids, and the second and third varnishing were applied for top varnishing. Sufficient time for layer settling was allowed between successive applications until the target retention of 100 g·m^{-2} for the primer and 100 g·m^{-2} for the top varnishing were reached, controlled by consecutive weighting. Specimens were left in ambient conditions for 24 h according to the manufacturer's recommendations after the first varnishing, and then surfaces were gently sanded using fine-grit sandpaper (220 grit) to obtain a smooth surface before the top varnishing. After the top varnishing of varnishes to the wood surfaces, test specimens were conditioned for three weeks.

Color test

The color parameters L^*, a^*, and b^* were determined by the CIEL*a*b* method. The L^* axis represents the lightness, whereas a^* and b^* are the chromaticity coordinates. The $+a^*$ and $-a^*$ parameters represent the colors red and green, respectively. The $+b^*$ parameter represents yellow, whereas $-b^*$ represents blue. The L^* value can vary from 100 (white) to zero (black) (Schmid et al. 2000). The colors of the specimens were measured by a colorimeter (X-Rite SP Series Spectrophotometer, X-ride Pantone, MI, USA) before and after weathering. The color difference, (ΔE^*) was determined for Scots pine wood according to ASTM–D 2244–14 (2016). The measured values are called the CIELab value. The color changes were determined using Eqs. 2 to 5:

$$\Delta a^* = a_f{}^* - a_i{}^* \qquad (2)$$
$$\Delta b^* = b_f{}^* - b_i{}^* \qquad (3)$$
$$\Delta L^* = L_f{}^* - L_i{}^* \qquad (4)$$
$$(\Delta E^*) = [(\Delta a^*)^2 + (\Delta b^*)^2 + (\Delta L^*)^2]^{1/2} \qquad (5)$$

where: Δa^*, Δb^*, and ΔL^* represent the changes between the initial and final interval values.

Surface roughness test

In the study, Mitutoyo Surftest SJ-301 model surface roughness tester was used to measure surface roughness. This instrument was used for the surface roughness measurements according to DIN 4768 (1990). Three surface roughness parameters were studied for surface roughness measurement of Scots pine such as mean arithmetic deviation of the profile (Ra), mean peak-to-valley height (Rz), and root mean square (Rq) (Hiziroglu 1996, Hiziroglu and Graham 1998). The Ra is the average distance from the profile to the mean line over the length of assessment. The parameter Rz can be calculated from the peakto-valley values of five equal lengths within the profile, and Rq is the square root of the arithmetic mean of the squares of profile deviations from the mean line (Mummery 1993).

Weathering test

Each group consisted of 10 individual wood specimens. In total, 7 groups of wood specimens for each species were exposed to natural weathering in April to October for 6 months in the Mugla region in 2017. Wood panels were prepared for weathering exposure according to ASTM D 358–55 (2017).

Tab. 1: The details of the climate condition of Mugla city for 6 months.

Months (2017)	April	May	June	July	August	September	October
Average temperature (ºC)	13.0	17.6	23.9	28.6	26.1	23.0	15.8
Highest temperature (˚C)	28.0	33.3	40.5	41.7	38.1	37.5	27.7
Lowest temperature (ºC)	2.2	6.5	12.6	16.8	17.0	11.6	4.7
Humidity (%)	63.5	61.0	49.3	36.6	51.4	45.2	59.7
Average wind speed (m/sn)	1.6	1.5	1.7	1.8	1.6	1.5	14
Total rainfall per month (mm=kg·m⁻²)	62.9	42.3	8.8	0.4	112.1	1.6	103.2
Number of rainy days	10	13	4	1	9	1	9

A test site was established close to the Regional Meteorological Observation Station of Mugla which is in the Southern Aegean Region of Turkey to enable practical assessments. The details of the climate condition of Mugla city in this period are given in Tab. 1.

RESULT AND DISCUSSION

Color Changes

Tab. 2 shows L^*, a^*, and b^* values of untreated (control), solely varnished, and impregnated and varnished Scots pine specimens before and after weathering and also illustrates the values of change for all three color parameters (ΔL^*, Δa^*, and Δb^*), as well as the total color changes (ΔE^*) of the wood specimens after 6 months of weathering. The retention value of the Scots pine

wood specimens was found to be 35.91 kg·m⁻³ for impregnated with WCX-8. Before natural weathering, all of the treatment groups were showed a decrease in L* values compared to the untreated (control) group. While the L* value of the control group was 75.16, it was changed from 61.92 to 67.18 for the only varnished Scots pine. L^* values of impregnated and varnished Scots pine wood specimens were changed from 36.38 to 41.21. Moreover, L* values of the only varnished Scots pine was higher than WCX-8 impregnated and varnished Scots pine before weathering.

Tab. 2: The color changes of Scots pine specimens before and after natural weathering.

	Retention (kg·m⁻³)	Before natural weathering						After natural weathering						After natural weathering			
		L_i^*		a_i^*		b_i^*		L_f^*		a_f^*		b_f^*		ΔL^*	Δa^*	Δb^*	ΔE^*
		Mean	SD	Mean	SD	Mean	SD	Mean	SD	Mean	SD	Mean	SD				
Control	-	75.16	2.46	6.32	1.09	32.76	2.65	55.81	2.34	3.14	0.64	17.45	3.90	-19.35	-3.18	-15.31	24.87
SV	-	64.55	3.67	8.74	1.49	45.72	0.69	51.99	4.60	11.59	0.39	49.65	4.79	-12.56	2.85	3.93	13.46
PV	-	61.92	3.94	7.96	1.06	41.58	0.82	53.98	3.95	8.93	0.57	44.18	2.98	-7.94	0.97	2.60	8.41
CV	-	67.18	4.93	8.85	1.65	36.01	2.19	50.85	5.15	11.98	0.35	46.67	4.45	-16.33	3.13	10.66	19.75
WCX-8+ SV	35.91	38.05	4.86	3.46	1.00	37.35	5.93	36.84	4.02	9.10	0.51	39.05	5.36	-1.21	5.64	1.70	6.01
WCX-8+ PV	35.91	36.38	2.60	1.22	0.76	29.86	2.82	36.21	2.24	6.40	0.61	30.86	2.41	-0.17	5.18	1.00	5.27
WCX-8+ CV	35.91	41.21	2.12	0.93	0.49	29.05	2.32	38.24	2.65	8.93	0.29	38.50	2.05	-2.97	8.00	9.45	12.73

Note: Ten replicates were made for each treatment group. **SD**: Standard deviation.

The decrease in the L* value of Scots pine wood specimens showed that the specimens became darker after the WCX-8 treatment. These results are in good agreement with that of Baysal (2012), Ustun et al. (2016), and Simsek and Baysal (2012) which studied the effects of some impregnation chemicals on color changes of wood. According to our results, a* and b* values of untreated (control) were 6.32 and 32.76 before weathering. While a^* values changed from 7.96 to 8.85, b^* values changed from 36.01 to 45.72 for the only varnished Scots pine before weathering. Our results showed that a* and b* values of the only varnished Scots pine was higher than the untreated (control) group before weathering. Impregnation with WCX-8 before varnishing caused to decrease a* and b* values of Scots pine. Baysal et al. (2014) studied color changes of Scots pine specimens impregnated with copper-chromate-boron, Tanalith® E, and Adolit KD-5 and coated with cellulosic and polyurethane varnishes. They reported that a* and b* values of the only varnished Scots pine was higher than impregnated and varnished Scots pine. Our results are compatible with data Baysal et al. (2014).

After 6 months of weathering, the negative lightness stability (ΔL*) values for untreated (control) and other all treated Scots pine specimens were occurred after weathering. Therefore, the wood surface became rougher and darker after weathering. The darkening of Scots pine might be have been due to the degradation of lignin and other non-cellulosic polysaccharides (Hon and Chang 1985, Grelier et al. 2000, Petric et al. 2004). WCX-8-impregnated and varnished Scots pine caused less change in the lightness than the only varnished Scots pine specimens in this study. It may be due to the fact that the WCX-8 impregnation developed the stabilization of wood color in the visible region through a reduction in the lignin degradation that resulted from UV light (Grelier et al. 2000). After 6 months of weathering, Δa^* and Δb^* values of control were found to be as -3.18 and -15.31, respectively. The negative Δa^* and Δb^* values showed that the wood surface turned from red to green and yellow to blue respectively, after weathering. Varnished and impregnated and the only varnished Scots pine wood surfaces gave positive Δa^* and Δb^* values after weathering. Positive Δa^* and Δb^* values show that wood specimen surface maintained reddish and yellowish tone after weathering. It was determined that except for untreated (control group), the Δa^* and Δb^* values of other all treatment groups showed positive values after weathering. As a result, except

for untreated (control), all of the treatment groups tended to reddish and yellowish respectively, after weathering. While total color change (ΔE^*) was 24.87 for untreated (control), it was changed from 5.27 to 19.75 for all treatment groups after weathering. Color change values showed that the best color stability was observed with WCX-8 impregnated and PV coated Scots pine after weathering. The reduction in ΔE^* of pre-impregnated and PV-coated Scots pine suggested a positive contribution to color stability in previous studies (Yalinkilic et al. 1999, Baysal 2008). The marked improvement in the performance of polyurethane varnishes on copper-chromate-treated surfaces was reported in a previous study (Black and Mraz 1974). Specimens impregnated with CCB+PV showed remarkable changes in lignin after weathering, but changes were distinctly different from those in untreated specimens (Yalinkilic et al. 1999). WCX-8 impregnation before varnishing reduced total color changes after weathering. It might be due to the photostabilization of wood via copper treatments that might be explained by retardation of the carbonyl group formation and reduced delignification after weathering (Temiz et al. 2005). These findings are compatible with the literature reporting that copper-containing treatments provided better protection for color changes than untreated wood specimens (Ozgenc and Yildiz 2014, Grelier et al. 2000, Temiz et al. 2005). Baysal et al. (2016) studied the color stability of bamboo wood impregnated with some copper-containing chemicals after accelerated weathering. They found that the best preservative for bamboo found to be CCB against color changes after accelerated weathering. The chromium and copper in the CCB formulation might create a synergistic effect to retard the surface degradation during weathering. Temiz et al. (2005), Ozgenc and Yildiz (2014) found that the best color stability was Tanalith® E with polyurethane varnishing for both Oriental beech and Scots pine wood specimens. Tanalith® E treatment both slowed down photodegradation by retarding the formation of carbonyl groups. The light resistance of Tanalith® E treated wood likely results from Cu (II) chelating with functional groups in wood. These chelates can photostabilize wood and retard the formation of carbonyl groups. Our results are in good agreement with these researchers' findings.

Surface roughness changes

The importance of surface roughness, as a significant parameter for determination of the surface quality of wood products, is well recognized, and the surface quality of wood is affected by many factors (Yildiz et al. 2013). Surface roughness parameters, such as Ra, Rz, and Rq values of Scots pine wood before and after weathering are given in Tab.3.

Tab. 3: The surface roughness values of Scot spine specimens before and after natural weathering.

	Before natural weathering						After natural weathering						Differences (%)		
	Ra		Rz		Rq		Ra		Rz		Rq		Ra	Rz	Rq
	Mean	SD	Mean	SD	Mean	SD	Mean	SD	Mean	SD	Mean	SD			
Control	1.28	0.76	7.08	2.23	1.41	0.44	3.00	1.23	17.27	4.88	3.68	1.50	135	144	161
SV	0.27	0.14	1.22	0.58	0.32	0.10	0.47	0.21	2.20	1.21	0.68	0.31	77	81	113
PV	0.07	0.03	0.69	0.15	0.12	0.06	0.12	0.04	1.46	0.38	0.24	0.04	85	112	104
CV	0.32	0.11	3.13	0.49	0.51	0.13	0.42	0.11	4.00	0.85	0.67	0.37	34	28	33
WCX-8+ SV	0.16	0.08	1.27	0.23	0.21	0.11	0.35	0.08	2.30	0.66	0.49	0.09	121	76	135
WCX-8+ PV	0.04	0.01	0.52	0.21	0.06	0.02	0.08	0.04	1.16	0.37	0.14	0.06	107	124	148
WCX-8+ CV	0.32	0.11	3.11	0.72	0.52	0.14	0.57	0.15	3.60	0.92	0.81	0.31	81	16	57

Note: Ten replicates were made for each treatment group. SD: Standard deviation.

The untreated (control) specimen had an average Ra, Rz, and Rq values of 1.28, 7.08, and 1.41, respectively, before weathering. Results showed that the surface roughness values of the untreated (control) group were higher than the other all treatment groups before the weathering. The wooden materials with rough surface require much more sanding process compared to one with a smooth surface, which leads to decrease in thickness of the material and, therefore, increases the losses due to the sanding process (Dundar et al. 2008). However, the roughness of wood is a complex phenomenon. Several factors such as the anatomical structure of wood, growing characteristics, machining properties and pre-treatments of wood before machining should be considered for the evaluation of the surface roughness of wood (Aydin and Colakoglu 2003, Aydin and Colakoglu 2005, Temiz et al. 2005).

Weathering caused to increase the surface roughness of un-treated (control) and other all treatment groups. Except for the untreated (control) group, surface roughness increases were the highest WCX-8 impregnated and PV coated Scots pine wood after weathering. Our results showed that surface roughness increases were the lowest for only CV coated Scots pine after weathering. The increase of Ra, Rz, and Rq were 34%, 28%, and 33% respectively, for CV coated Scots pine after weathering. This increase in smoothness is very important for many applications of solid wood. In addition, losses occurring in the planning machine are reduced and high-quality surfaces are attained (Unsal and Ayrilmis 2005). Kerberet et al. (2016) determined that in addition to the leaching of lignin degraded by natural weathering reactions, the increase in the roughness of the wood is also related to sudden changes of humidity (absorption and desorption of the humidity) causing the presence of superficial cracks. Turkulin (2017) reported that light irradiation mostly degraded the middle lamella, which is between two cell walls and holds the cells together. This degradation increases the surface roughness of the wood (Tolvaj et al. 2014). The increase in Ra, Rz, and Rq values were 135%, 144%, and 161%, respectively for the control group after natural weathering. The surface roughness of the untreated (control) group was higher than the only varnished Scots pine after weathering. In varnishes, cellulosic varnish gave the best results in terms of surface roughness of Scots pine after weathering. Except for Rz values of WCX-8 impregnated and then CV and SV coated Scots pine, WCX-8 impregnation before varnishing caused to increase the surface roughness of Scots pine after weathering compared to the only varnished Scots pine after weathering. Ozgenc and Yildiz (2014) investigated the surface roughness of some wood species impregnated with some copper-containing chemicals. They found that surface roughness values of impregnated wood species were lower than un-impregnated wood species during the weathering time. In impregnation chemicals, except for didecyldimethylammonium chloride (DDAC), other treatment groups decreased surface roughness of wood specimens after artificial weathering. Temiz et al. (2005) found that the surface roughness values of CCA-impregnated Scots pine were lower than that of un-treated Scots pine after accelerated weathering. Our results are compatible with these researchers' findings.

CONCLUCIONS

This study was performed to determine some physical characteristics such as color and surface roughness changes of Scots pine WCX-8 impregnated and varnished Scots pine after weathering. The lightness value of untreated (control) group was higher than the other treatment groups before the weathering. WCX-8 treatment before varnishing caused lightness loss of Scots pine before weathering. The negative lightness stability (ΔL*) values for untreated (control) and other all treatments were occurred after weathering. Moreover, except for untreated (control) group, varnished and impregnated and varnished Scots pine wood surfaces gave positive

Δa^* and Δb^* values after weathering, So, Scots pine wood surfaces indicate to become reddish and yellowish. The total color change (ΔE^*) values of the only varnished and impregnated and varnished Scots pine wood specimens were less than that of an untreated (control) specimen. Our results showed that the best color stability was obtained with WCX-8 impregnated and PV coated Scots pine after weathering. Untreated (control) and impregnated and varnished Scots pine wood surfaces were softened after weathering. The surface roughness increases of the treated Scots pine were lower than that of un-treated (control) Scots pine after weathering. In general, WCX-8 treatment before varnishing increased the surface roughness of Scots pine after weathering. The surface roughness increases were the lowest with CV coated Scots pine after weathering.

In conclusion, WCX-8 impregnation before varnishing was more effective in stabilizing the wood color. However, generally, it gave rougher wood surfaces with varnish than the only varnished wood surfaces after weathering.

REFERENCES

1. Anderson, E.L., Pawlak, Z., Owen, N.L., Feist, W.C., 1991: Infrared studies of wood weathering. Society for Applied Spectroscopy 45 (4): 641- 647.
2. ASTM-D 358-55, 1970: Standard specification for wood to be used panels in weathering tests of paints and varnishes.
3. ASTM-D, 3023-98, 2003: Standard practice for determination of resistance of factory-applied coatings on wood products to stains and reagents.
4. ASTM-D, 1413-07, 2007: Standard test method for wood preservatives by laboratory soil-block cultures.
5. ASTM-D, 2244-16, 2016: Standard practice for calculation of color tolerances and color differences from instrumentally measured color coordinates.
6. Aydin, I., Colakoglu, G., 2003: Roughness on wood surfaces and roughness measurement methods. Artvin Coruh University Journal of Forestry Faculty 4(1-2): 92-102.
7. Aydin, I., Colakoglu, G., 2005: Effects of surface inactivation, high temperature drying and preservative treatment on surface roughness and colour of alder and beech wood. Applied Surface Science 252 (2): 430-440.
8. Baysal, E., 2008: Some physical properties of varnish coated wood preimpregnated with copper-chromated boron (CCB) after 3 months of weathering exposure in Southern Eagen Sea region. Wood Research 53(1): 43-54.
9. Baysal, E., 2012: Surface characteristics of CCA treated Scots pine after accelerated weathering. Wood Research 57(3): 375-382.
10. Baysal, E., Tomak, E.D., Ozbey, M., Altin, E., 2014: Surface properties of impregnated and varnished Scots pine wood after accelerated weathering. Coloration Technology 130(2): 140-146.
11. Baysal, E., Tomak, E. D., Topaloglu, E., Pesman, E., 2016: Surface properties of bamboo and Scots pine impregnated with boron and copper based wood preservatives after accelerated weathering. Maderas. Ciencia y Tecnología 18(2): 253-264.
12. Bhat, I.H., Khalil, H.P.S., Awang, K.B., Bakare, I.O., Issam, A.M., 2010: Effect of weathering on physical, mechanical and morphological properties of chemically modified wood materials. Materials and Design 31(9): 4363-4368.
13. Black, J.M., Mraz, E.A., 1974: Inorganic surface treatments for weather-resistant natural finishes. In: Forest Products Laboratory Lab Madison Wis, Forest Service, U.S. Department of Agriculture. Washington , Pp. 1-41.

14. Budakci M., Atar M., 2001: Effects of bleaching process on hardness and glossiness of pine wood (*Pinus sylvestris* L.) exposed to outdoor conditions. Turkish Journal of Agriculture and Forestry 25: 201-207.

15. Budakci, M., 2006: Effect of outdoor exposure and bleaching on surface color and chemical structure of scots pine. Progress in Organic Coatings 56 (1): 46-52.

16. Chang, C.W., Lu, K.T., 2012: Natural castor oil based 2-package waterborne polyurethane wood coatings. Progress in Organic Coatings 75(4): 435-443.

17. Cornfield, J.A., Hale, M., Fettis, G., 1994: A comparison of analytical and visual techniques used for assessment of weathering properties of chromium and copper azole treated timber. In: International Resarch Group on Wood Preservation, IRG/WP/20023.

18. DIN 4768, 1990: Determination of values of surface roughness parameters Ra, Rz, Rmax using electrical contact (stylus) instruments, concepts and measuring conditions.

19. Dundar T., As N., Korkut, S., Unsal, O., 2008: The effect of boiling time on the surface roughness of rotary-cut veneers from oriental beech (*Fagus orientalis* L.). Journal of Materials Processing Technology 199(1-3): 119-123.

20. Evans, P.D., Michell, A.J., Schmalzl, K.J., 1992: Studies of the degradation and protection of wood surfaces. Wood Science and Technology 26(2): 151-163.

21. Feist, W.C., 1979: Protection of wood surfaces with chromium trioxide. Research Paper. FPL 339, Forest Products Laboratory, Madison, WI, Pp. 1-11.

22. Feist, W.C., 1989: Outdoor wood weathering and protection, 225. Series, United States of America. American Chemical Society, Pp. 263-298.

23. Feist, W.C., Williams, R.S., 1991: Weathering durability of chromium-treated Southern pine. Forest Products Journal 41(1): 8-14.

24. Feist, W.C., Ross, A.S., 1995: Performance and durability of finishes on previously coated CCA-treated wood. Forest Products Journal 45(9): 29–36.

25. Freeman, M.H., Mcintyre, C.R., 2008: A comprehensive review of copper-based wood preservatives with a focus on new micronized or dispersed copper systems. Forest Products Journal 58(11): 6-27.

26. Grelier, S., Castellan, A., Kamdem, D.P., 2000: Photo-protection of copper amine treated wood. Wood and Fiber Science 32(2): 196-202.

27. Hiziroglu, S., 1996: Surface roughness analysis of wood composites: a stylus method. Forest Products Journal 46 (7/8): 67–72.

28. Hiziroglu, S., Graham, S., 1998: Effect of press closing time and target thickness on surface rougness of particle board. Forest Products Journal 48: 50-54.

29. Hon, D.N.S., 1981: Photochemical degradation of lignocellulosic material. In: Developments in polymer degradations, N. Grassie, ed., Appl. Sci. Publ., London. Pp. 229-281.

30. Hon, D.N.S., Chang, S.T., 1985: Photoprotection of wood surfaces by wood-ion complexes. Wood and Fiber Science 17(1): 92-100.

31. Jin, L., Archer, K., Preston, A., 1991: Surface characteristics of wood treated with various AACs, ACQ and CCA formulations after weathering. In: International Research Group on Wood Preservation Conference. Kyoto, Japan IRG/WP/2369. Pp. 229-281.

32. Jirous-Rajkovic, V., Bogner, A., Radovan, D., 2004: The efficiency of various treatments in protecting wood surfaces against weathering. Surface Coatings International Part B: Coatings Transactions 87(1): 15–19.

33. Kerber, P. R., Stangerlin, D. M., Pariz, E., Melo, R.R., Souza, A.P., Leandro, C., 2016: Colorimetry and surface roughness of three amazonian woods submitted to natural weathering. Nativa 4 (5): 303-307.

34. Kiguchi, M., Evans, P.D., 1998: Photostabilization of wood surface using a grafted benzophenone UV absorber. Polymer Degradation Stability 61(1): 33-45.

35. Kilic, A., Hafizoglu, H., 2007: Influences of weathering on chemical structure of wood and protection treatments. Süleyman Demirel University Journal of Forestry Faculty 2: 175-183.

36. Meijer, M.D., 2001: Review on the durability of exterior wood coatings with reduced VOC-content. Progress in Organic Coatings 43(4): 217-225.

37. Mummery, L., 1993: Surface texture analysis. The Handbook. Hommelwerke, Muhlhausen, Germany, 106 pp.

38. Nzokou, P, Kamdem, D. P., Temiz, A., 2011: Effect of accelerated weathering on discoloration and roughness of finished ash wood surfaces in comparison with red oak and hard maple. Progress in Organic Coatings 71(4): 350-354.

39. Ors, Y., Keskin, H., 2001: Ağaç Malzeme Bilgisi, 1. ed, Ankara, Turkey. Nobel Publisher, 183 pp.

40. Ozgenc, O., Hiziroglu, S., Yildiz, U.C. 2012: Weathering properties of wood species treated with different coating applications. BioResources 7(4): 4875-4888.

41. Ozgenc, O., Yildiz, U.C, Yildiz, S., 2013: The wood surface protection with some new generation wood preservatives and coating processings against weathering conditions. Artvin Coruh University. Journal of Forestry Faculty 14 (2): 203-215.

42. Ozgenc, O., Yildiz, U.C., 2014: Surface characteristics of wood treated with new generation preservatives after artificial weathering. Wood Research 59(4): 605–616.

43. Petric, M., Kricej, B., Humar, M., Pavlic, M., Tomazic, M., 2004: Patination of cherry wood and spruce wood with ethanolamine and surface finishes. Surface Coatings International Part B: Coatings Transactions 87(3): 195-201.

44. Schmid, S., Webster, R. D., Evans, P. D., 2000: The use of ESR spectroscopy to assess the photostabilising effects of wood preservatives. In: International Research Group on Wood Preservation Conference. Hawaii, USA IRG/WP 00-20186, 2000. Pp. 1-9.

45. Sell, J., Feist, W.C., 1985: Weathering behavior of chromium-copper-boron treated wood. Holzals Roh- und Wekstoff 43(12): 518-523.

46. Simsek, H., Baysal, E., 2012: An investigation on colour and gloss changes of wood impregnated with borates. Wood Research 57(2): 271-277.

47. Sivrikaya H., Hafizoglu H., Yasav A., Aydemir D., 2011: Natural weathering of oak (*Quercus petraea*) and chestnut (*Castanea sativa*) coated with various finishes. Color Research and Application 36 (1): 72-78.

48. Temiz, A., Yildiz, U.C., Aydin, I., Eikenes, M., Alfredsen, G., Colakoglu, G., 2005: Surface roughness and colour characteristics of wood treated with preservatives after accelerated weathering test. Applied Surface Science 250(1-4): 35-42.

49. Temiz, A., Terziev, N., Eikenes, M., Hafren, J., 2007: Effect of accelerated weathering on surface chemistry of modified wood. Applied Surface Science 253(12): 5355–5362.

50. Tolvaj, L., Molnar, Z., Magoss, E., 2014: Measurement of photodegradation-caused roughness of wood using a new optical method. Journal of Photochemistry and Photobiology B: Biology 134: 23-26.

51. Turkoglu, T., Baysal, E., Toker, H., 2015a: The effects of natural weathering on color stability of impregnated and varnished wood materials. Advances in Materials Science and Engineering 1-9.

52. Turkoglu, T., Baysal, E., Toker, H., Ergün, M.E., 2015b: The effects of natural weathering on hardness and gloss of impregnated and varnished Scots pine and oriental beech wood. Wood Research 60(5): 833-844.

53. Usta, I., 1993: The current situation and recommendations developing of impregnation wood industry in Turkey. M.Sc. Thesis. Hacettepe University, Ankara, Turkey. 135 pp.

54. Uysal, B., 2005: Wood material course notes. Karabük, Turkey. 65 pp.

55. Ustun, S., Baysal, E., Turkoglu, T., Toker, H., Sacli, C., Peker, H., 2016: Surface characteristics of Scots pine treated with chemicals containing some copper compounds after weathering. Wood Research 61(6): 903-914.

56. Unsal, O., Ayrilmis, N., 2005: Variations in compression strength and surface roughness of heat-treated Turkish riverredgum (*Eucalyptus camaldulensis*) wood. Journal of Wood Science 51(4): 405-409.

57. Wilkinson, J.G., 1979: Industrial Timber preservation. The Rentokil Library. Associated Business Press, London. 532 pp.

58. Williams, R.S., Knaebe, M.T., Feist, W.C., 1996: Finishes for exterior wood: Selection, application, and maintenance. Forest Products Society, USDA Forest Service, 127 pp.

59. Williams, R.S., 2005: Handbook of Wood Chemistry and Wood Composites. Weathering of wood. Forest Products Laboratory. Madison, USA. 733 pp.

60. Yalinkilic, M.K., Ilhan, R., Imamura, Y., Takahashi, M., Demirci, Z., Yalinkilic, A.C., 1999: Weathering durability of CCB-impregnated wood for clear varnish coatings. Journal of Wood Science 45(6): 502–514.

61. Yildiz, S., Tomak, E.D., Yildiz, U.C., Ustaomer, D., 2013: Effect of artificial weathering on the properties of heat treated wood. Polymer Degradation and Stability 98(8): 1419-1427.

62. Zhang, J., Kamdem, P.D., Temiz, A., 2009: Weathering of copper-amine treated wood, Applied Surface Science 256 (3): 842-846.

Caglar Altay
Adnan Menderes University
Aydin Vocational School
Department of Furniture and Decoration
09000 Aydin
Turkey

Ergun Baysal*, Hilmi Toker
Mugla Sitki Kocman University
Faculty of Technology
Department of Wood Science and Technology
48000 Mugla
Turkey
*Corresponding author: ergun69@yahoo.com

Turkay Turkoglu
Mugla Sitki Kocman University
Koycegiz Vocational School
Department of Forestry
48800 Mugla
Turkey

Mustafa Kucuktuvek
Antalya Bilim University
Faculty of Fine Arts and Architecture
Department of Interior Architecture and Environmental Design
07190 Antalya
Turkey

Ahmet Gunduz
Mugla Sitki Kocman University
Faculty of Technology
Department of Wood Science and Technology
48000 Mugla
Turkey

Huseyin Peker
Artvin Coruh University
Faculty of Forestry
Department of Forest Industry Engineerng
080000 Artvin
Turkey

ANALYSIS OF MODULUS OF ELASTICITY OF SPRUCE BEAMS UNDER BENDING WITH AND WITHOUT FIBRE REINFORCEMENT

Krisztián Andor, Bertalan Bellovics
University of Sopron
Sopron, Hungary

ABSTRACT

The modulus of elasticity has been assumed constant during the finite element (FE) analysis of CFRP reinforced real sized timbers analyzed in load test in laboratory. The latest investigations have shown that it varies significantly during the loading process. Analysis of the modulus of elasticity during the loading provides answers to several questions, by which the FE analysis can be profoundly optimized and yield more accurate estimates. Analysis has been extended to load-modulus functions of previous investigations. Specimens without reinforcement were also included in the investigations, in order to eliminate anomalies of previous measurements and to get easier comparison.

KEYWORDS: Carbon fibre reinforcement, beam, modulus of elasticity, load-bearing, four-point bending.

INTRODUCTION

The application of fibre reinforced plastics (FRP) for the enhancement of structural elements has a long history, including intense investigation of timber structures since the 1990s (Plevris et al. 1992). Early applications of glass fibres were later joined by carbon fibres and occasionally other materials (Theakston 1965). Since a comprehensive overview of the related literature is well beyond the scope of this study, here we only review the most relevant aspects.

Like for reinforced concrete, the application of FRP for timber have looked feasible and promising, mainly to enhance structural behaviour of sawn timber beams (Gentile et al. 2002, Fiorelli et al. 2003, Li et al. 2009) or glued laminated (glulam) beams (Gilfillan et al. 2003, Fiorelli et al. 2011, Kánnár 2014). Retrospect reinforcement of old bridges or other historic buildings is also an important field of application (Amy et al. 2004, Borri et al. 2005, Nowak et al. 2013). Reinforcement elements featuring FRP materials include mostly sheets, fabrics, rods,

but also pultruded elements or connectors. Most typically the reinforcement is fitted to or near the tension surface of the structure, glued or embedded in grooves, etc. (Borri et al. 2005, Nowak et al. 2013, Jankowski et al. 2010, Schober et al. 2006). We mention here that a branch of research focuses on bonding between wood and reinforcement; however, it is not a common failure mode for typical applications.

Various experimental studies show that the reinforcement of timber structures yields the improvement of load-bearing capacity, stiffness, and ductility, in a wide range, most likely owing to the organic nature of wood. Most studies report an increase of capacity 20% to 50% (Gentile et al. 2002, Triantafillou et al. 1992) or sometimes higher (Li et al. 2009, Borri et al. 2005, Nowak et al. 2013), a negligible increase of stiffness (Amy et al. 2004, Buell et al 2005) or occasionally much higher (Borri et al. 2005, Fiorelli et al. 2011), and a general improvement of ductility. Numerical simulations have also been carried out for several years (Gentile et al. 2002, Li et al. 2009, Gilfillan et al. 2003, Buell et al. 2005, Kim et al. 2010, Fiorelli et al. 2011, Nowak et al. 2013). Another important aspect of the investigation of modulus of elasticity is the effect of different treatments or the anatomical variations of the wood material, for example effect of impregnation methods or knots (Komán et al. 2013, Németh et al. 2015).

Andor et al. (2015) dealt with experimenting on various amount of CFRP reinforcement on spruce timbers. The aim of the research led by the second author of this paper was to determine the increase of load-bearing capacity and stiffness of composite beams due to carbon fibre reinforcement by means of real size experiments and therefore verify the effectiveness of reinforcement via statistical analysis that gave numerical support to the reliability of the tests.

In the case of real size specimens, it becomes possible to draw conclusions from the analysis of beams fraught with wood defects. Small test specimens with wood defects are usually omitted because their size is a risk to the continuity of specimens, which is ensured by the flawless parts in the case of larger specimens, embedding the defects evolved during growth of the wood (knots, damages).

The diversity of experimental results on fibre reinforcement of timber beams highlights the significance of several factors, e.g. species, amount and material of fibres, shape and arrangement of reinforcement, size of specimens, etc. The aim of the research was to conduct experiments on timber beams reinforced with CFRP in order to assess the potential of this technique particularly with respect to solid beams made of Norway spruce, a species native and widespread in Europe (Andor et al. 2015). The reinforcement was chosen so that it was easy to apply in three different amounts along the full length. The measurements showed an increase of 18-33% of load-bearing capacity, 9-16% of stiffness, as well as 8-29% of deflection. In a project run simultaneously, we obtained similar results for beams of the same species but larger cross- sections, which supports the validity of the tests.

The increases of reinforcement data are well within the range of most results obtained for various wood species by other researchers (Fiorelli et al. 2003), however, it is important to note that values significantly higher or lower are also reported (Li et al. 2009). Species covered include several European, American, Asian, or other species. An overview of related results clearly indicates that the effectiveness of reinforcement varies in such a wide range from species to species, that it is unsafe to draw any conclusion regarding a new one. Moreover, wood material of the same species may differ significantly with respect to geographical locations. However, results reported in Andor et al. (2015) clearly make ground for further research and development of reinforced spruce beams.

A detailed statistical analysis has also been conducted in Andor et al. (2015), that has shown that the behaviour of reinforced beams was significantly affected by the quality of the wood

material. A distinction can be made within the test specimens based on the obvious presence of knots and invisible defects, which most likely affects the potential in reinforcement. It can be observed that the strong specimens typically fail by tension of timber, while other modes like cross-graining, compression, shearing, etc. are more common in the case of weak specimens.

Analysis of modulus of elasticity

The analysis involved the bending of spruce beams with length 2000 mm (supported on 1800 mm) and cross-section 95 x 95 mm. Several problems arose during the modelling of spruce beams reinforced with carbon fibre materials because of difficulties in FE simulations. During the FE analysis the modulus of elasticity has been assumed constant while the latest investigations have shown that it varies significantly during the loading process. Analysis of the modulus of elasticity during the loading provides answers to several questions, by which the FE analysis can be profoundly optimized and yield more accurate estimates.

In laboratory measurements, moduli of elasticity of timber beams were determined by measurements based on dynamic principles using non-destructive and destructive procedures. The non-destructive procedure involved an instrument called Fakopp (Divós et al. 2005), which enables the calculation of the modulus of elasticity based on the propagation speed of sound. During the destructive procedure the moduli were determined by four-point bending of the beams till failure considering deflections (Dániel 2016, Kánnár 2014).

Since the modulus of elasticity of the wood material alone could be determined for specimens both reinforced and non-reinforced, we used modified values of moduli measured for the specimens to be equivalent to 12% moisture content.

We conducted experiments for the a priori estimation of the modulus of elasticity by means of bending loading up to 5% of the ultimate load and repeating it after applying reinforcement. The results showed a mixed picture disabling any clear conclusions.

At the measurement of the modulus of elasticity we only determined average values according to respective standards, hence recording during the loading procedure was missing. We noted that the modulus of elasticity was not constant during the loading, therefore in a related collaborative study several finite element types were applied to approximate laboratory data curves (Saad 2017). We also applied a method when the modulus of elasticity was computed based on the measured deflection data, which led to surprising results.

The behavior of the modulus of elasticity

It was difficult to analyse the modulus of elasticity primarily responsible for the stiffness of the beams, partly because there was little similarity between the individual specimens, that can be attributed to the anisotropy of wood and the presence of wood defects.

The original aim of this study was to develop a finite element model that can give good estimates greatly depends on our knowledge on the behaviour of wood properties under the loading process. Using the finite element models developed during our research and the stress-strain data in the specimens we made a well applicable computational procedure. We also aimed to compute the modulus of the composite reinforcement in fibre direction (Bellovics 2016, Saad 2017). Specimens used in laboratory testing formed the bases of reference in order to make the finite element model as realistic as possible.

Thus during the first phase of modelling, the internal properties (stresses and strains) were compared with the results of laboratory measurements. This comparison was necessary to assess whether stresses and strains obtained from the finite element modelling approximated those of laboratory measurements. The conclusions were determined by the analysis particularly made for

the laboratory measurements (Bellovics 2016) as well as the modelling procedure. The comparison has shown that the unreinforced timber could be modelled approximatively as the stress and strain data were not in full agreement (Fig. 3). In the case of reinforced specimens, the stress distribution could not be measured but only computed approximatively, though these computations did not provide the expected overall picture. Therefore, here there was no basis for comparison and we could rely only on the data obtained from the finite element computation (Fig. 1).
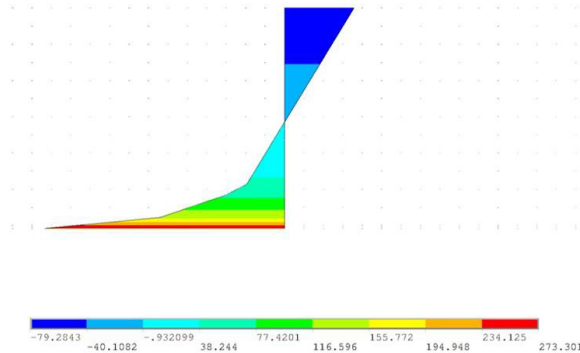

Fig. 1: Normal stress distribution along the cross section of a bended beam (95 x 95 x 2000 mm) reinforced with 1 layer of CFRP

There were also extreme differences regarding the strains. Measurement of strains in the laboratory was performed using strain gauges, which have the disadvantage of measuring plane strains only and thus the internal distribution could only be estimated. This approach was unable to determine whether the major problem is with the model or the measurements.

MATERIAL AND METHODS

Material

Timber for the beams with 2000 mm length was sawn of Norway spruce (*Picea abies*) in rectangular solid cross-sections of 95 x 95 mm with random orientation with respect to growth-rings (i.e. R and T directions were not aligned with the contour of the cross-section). All specimens were dried to moisture content of 12%. Via visual inspection and non-destructive tests it was ensured that the test specimens had no major visible defects or damage, such as drying splits, biological deterioration, etc. Presence of knots was allowed as a natural feature of the species.

Fibre reinforcements were prepared in situ using unidirectional (99% of fibres with respect to surface in warp, 1% in weft) carbon fibre fabric of 300 $g \cdot m^{-2}$ weight and a two-component epoxy resin of the company SIKA AG. applied manually in approximately 0.5 $kg \cdot m^{-2}$ amount. The epoxy resin was applied on the surface in the prescribed amount following manufacturer's instruction using rollers. The fabric was then placed and impregnated with resin completely manually such that the strengthening took place simultaneously with the bonding to the wood. The product application instructions required no clamps or any mechanical device to apply pressure because the system is designed for retrofitting for concrete or timber even in an overhead position.

Measurement set-up

Four-point bending tests of a series of specimens have been prepared with supports of 1800 mm span. The geometric parameters of the beams were set to comply with the European standards regarding testing. The experiments were conducted in a laboratory accredited for timber structural testing using a standard MTS testing device with two cylinders with capacity of 250 kN each. Load was applied by a single actuator and transmitted to the test specimens at two points via an intermediate beam of 600 mm span centrally aligned, see Figs. 2 and 3. Measurements of the loading and the deflection of the middle cross-section of the beam have been performed by the testing device and a video extensometer, respectively, and the data have been recorded digitally for analysis.

The investigation was supplemented with 8 beams without reinforcement in addition to the analysis in Andor et al. (2015) for the sake of easier comparison, therefore a total of sixteen non-reinforced beams were analysed. A total of fifty-two specimens were prepared, of which thirty-six with various amounts of CFRP fabric (Tab. 1).
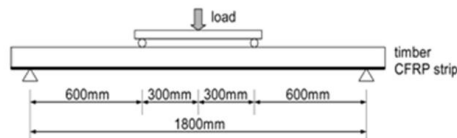
Fig. 2: Four–point bending test arrangement.

Fig. 3: Bending test arrangement and a specimen with the CFRP strip glued to the tensile face of the beam at full width.

Twenty specimens were fitted with a single and eight with a double layer of fabric on the entire width of cross-section, respectively, while the remaining eight specimens were reinforced with a narrower strip (50 mm) of single layer CFRP fabric centrally aligned with respect to the vertical symmetry plane (Fig. 4).

Fig. 4: Scheme of the various amount of CFRP fabric in each test group (S1, S2, SN).

In all cases the CFRP fabric was glued to the tensile face of the beam at full length and then were cut through just near the supports. The four types of test specimens are denoted by S0, S1, S2, and SN, respectively. The different number of specimens in each groups were managed with statistical analysis in Andor et al. (2015). Additional specimens were also investigated to increase the amount of samples. A summary of the data are shown in Tab. 1.

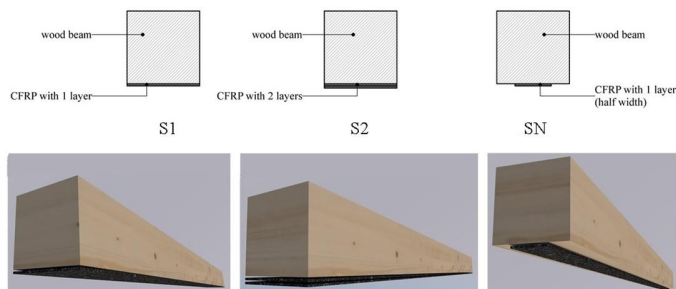The density of the wood of all specimens was measured with xilodyne device (penetration device) giving an average of 473 kg·m^{-3} with relative standard deviation of 8.5%. The data were grouped and analysed with respect to the division into groups S0, S1, S2, and SN, yielding averages and relative standard deviations as 456 kg·m^{-3} (5.4%), 495 kg·m^{-3} (9.2%), 465 kg·m^{-3} (7.5%), and 459 kg·m^{-3} (5.6%), respectively.

Tab. 1: Types of investigated timbers.

Test group	Reinforcement	Density (mean) kg·m^{-3}	Amount of CFRP	Number of specimens
S0	None	456	–	16
S1	CFRP fabric	495	1 layer, full width	20
S2	CFRP fabric	465	2 layers, full width	8
SN	CFRP fabric	459	1 layer, 50 mm width	8

They have obtained an average increase of 30% for load-bearing and 16% for stiffness in the case of a single layer of CFRP (amount of 300 g·m^{-2}) documented in Andor et al. 2015.

Analysis of the change of the modulus of elasticity during loading

During the laboratory testing, measurements were carried out in a way that both deflection and load values were digitally recorded every half second from the start of the loading process until failure. In order to keep track of the change of behaviour, the modulus of elasticity was computed as follows: five samples were picked out of the data series, considered five values of the load evenly spaced between zero and the ultimate load, recorded respective deflections, and finally the modulus of elasticity was computed. The deflections were also calculated using FE simulation to check accuracy.

The deflection (y) can be formulated based on the four-point bending layout as follows:

$$y = \frac{23 \cdot F \cdot l^3}{1296 \cdot E \cdot I} \qquad \text{(m)} \tag{1}$$

from which the modulus of elasticity is obtained:

$$E = \frac{23 \cdot F \cdot l^3}{1296 \cdot y \cdot I} \qquad \text{(N·m}^{-2}\text{)} \tag{2}$$

where: F - load (concentrated) (N),
l - span (m),
I - moment of inertia for bending axis (m^4).

This procedure was performed for several timber specimens, as well as reinforced specimens. The data have revealed that the modulus of elasticity varied during the loading process, therefore we examined the modulus of elasticity during the entire process for all the test specimens considered in (Andor et al. 2015), as well as they were supplemented with additional non-reinforced timber beams to enables a more indirect comparison.

RESULTS AND DISCUSIONS

Modulus of elasticity against load is plotted for non-reinforced beams, for reinforced beams with 1 layer, for reinforced beams with 2 layers, and for reinforced beams with half layer in Figs. 5 to 8, respectively.
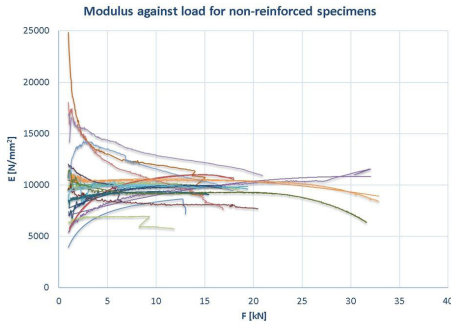
Fig. 5: Modulus of elasticity against load for non–reinforced beams.
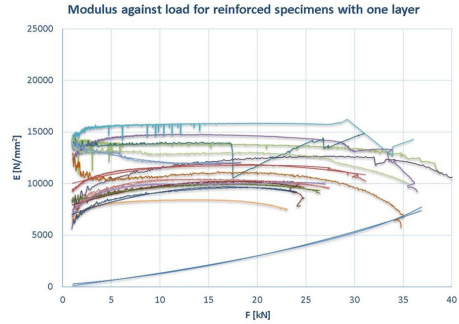
Fig. 6: Modulus of elasticity against load for reinforced beams with 1 layer.
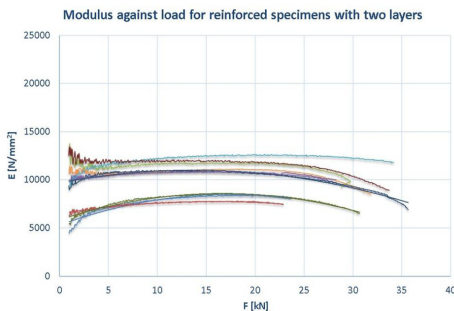
Fig. 7: Modulus of elasticity against load for reinforced beams with 2 layers.
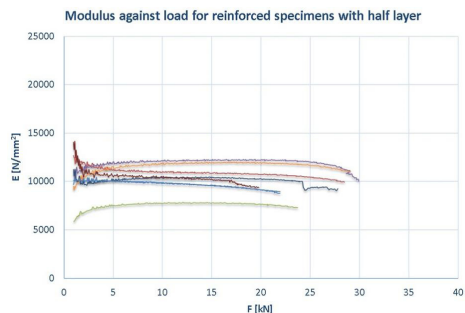
Fig. 8: Modulus of elasticity against load for reinforced beams with half layer.

Characteristic values of the modulus of elasticity were computed at abscissas where the settlement of the specimens under loading had already taken place. For reinforced specimens it was set to 20 kN, while for non-reinforced ones it was only 15 kN due to early failure.

Consequently, the characteristic average modulus of elasticity for each specimen group was obtained as 9622 MPa (S0), 11572 MPa (S1), 10366 MPa (S2), 10183 MPa (SN), respectively, which correlate with other studies analyzing modulus of elasticity of CRP reinforced wooden construction elements (Fiorelli et al. 2003, Fedyukov et al. 2017, Togay et al. 2017, Essert et al. 2018).

The diagrams show that the modulus of elasticity of wood within the effective load-bearing range varies significantly from specimen to specimen, all in positive, negative, and mixed directions. It can also be noted that the initial sections (up to approx. 7 kN) of the curves are variable because the specimens have not settled yet under the load. Incidental torsion or skewness resulting in non-ideal situation of the beam on the supports may have their influence in this

phase, but then beyond this the stretching of the beam leads to a relatively pure bending until failure.

It is quite apparent that the behavior of wood is characteristic to fibre bundle systems exhibiting imperfections (knots, loose end fibres). Failures of individual fibre bundles can be observed as well as activation of new bundles. Larger jumps are due to disturbances of video-extensometer used for measuring the deflections (e.g. sudden changes in lighting).

In the case of reinforced specimens, the settlement phase is shorter (5 kN), beyond that the modulus of the composite beam is more or less constants, and starts declining at the end.

CONCLUSIONS

1. Typical value of the modulus of elasticity for the non-reinforced timber beams is 19 244 MPa.
2. Carbon fibre reinforcement is active all the time of the loading, and there is no distinguishable finite phase that might mark the start of its contribution to load-bearing.
3. CFRP applied to timber beams continuously contributed to load-bearing.
4. The curve of the modulus of elasticity enables to predict failure.
5. The modulus of elasticity is constant within the effective load-bearing range of reinforced beams that have large load-bearing capacity.
6. Typical value of the modulus of elasticity for beams reinforced with a single layer is 23 144 MPa.
7. Typical value of the modulus of elasticity for beams reinforced with a double layer is 20 733 MPa.
8. Typical value of the modulus of elasticity for beams reinforced with a half layer is 20 365 MPa.

In terms of further potential research, it is necessary to do a full statistical and function analysis on the new load-modulus diagrams, which goes beyond the scope of this paper. It would be preferable to perform similar analysis also on the finite element models in the future. In addition it is recommended to make similar analysis with Glu-Lam beams (Kánnár 2014).

ACKNOWLEDGEMENTS

REFERENCES

1. Amy, K., Svecova, D., 2004: Strengthening of dapped timber beams using glass fibre reinforced polymer bars. Canadian Journal of Civil Engineering 31 (6): 943-955.

2. Andor, K., Lengyel, A., Polgár, R., Fodor, T., Karácsonyi, Z., 2015: Experimental and statistical analysis of spruce timber beams reinforced with CFRP fabric. Construction and Building Materials 99 (8): 200-207.

3. Bellovics, B., 2016: FEM Analysis of CFRP reinforced timber. MSc thesis. (In Hungarian) University of West Hungary, 50 p.

4. Borri, A., Corradi, M., Grazini, A., 2005: A method for flexural reinforcement of old wood beams with CFRP materials. Compos. Part B 36 (2): 143-153.

5. Buell, T.W., Saadatmanesh, H., 2005: Strengthening timber bridge beams using carbon fibre. Journal of Structural Engineering 131 (1): 173-187.

6. Dániel, B., 2016: Utilization of CFRP reinforced wood beam. BSc Thesis. University of Sopron, 46 pp.

7. Divós, F., Tanaka, T., 2005: Relation between static and dynamic modulus of elasticity of wood. Acta Silvatica et Lignaria Hungarica (1): 105-110.

8. Essert, S., Rede, V., Svagelj, Z., 2018: The bending modulus of elasticity of subfossil elm wood. Wood Research 63 (2): 239-248.

9. Fedyukov, V., Saldaeva, E, Chernova, M., 2017: Different ways of elastic modulus comaritive study to predict resonant properties of standing spruce wood. Wood Research 62 (4): 607-614.

10. Fiorelli, J., Dias, A.A., 2011: Glulam beams reinforced with FRP externally-bonded: theoretical and experimental evaluation. Materials and Structures 44 (8): 1431-1440.

11. Fiorelli, J., Dias, A.A., 2003: Analysis of the strength and stiffness of timber beams reinforced with carbon fiber and glass fiber. Materials Research 6 (2): 193-202.

12. Gentile, C., Svecova, D., Rizkalla, S.H., 2002: Timber beams strengthened with GFRP bars: development and applications. Journal of Composites for Construction 6 (1): 11-20.

13. Gilfillan, J.R., Gilbert, S.G., Patrick, G.R.H., 2003: The use of FRP composites in enhancing the structural behaviour of timber beams. Journal of Reinforced Plastics and Composites 22 (15): 1373–1388.

14. Kánnár, A., 2014: Evaluation of glulam beams' performance in special environmental conditions. Wood Research 59 (5): 803-812.

15. Kim, Y.J., Harries, K.A., 2010: Modeling of timber beams strengthened with various CFRP composites. Engineering Structures 32: 3225-3234.

16. Komán, Sz., Fehér, S., Ábrahám, J., Taschner, R., 2013: Effect of knots on the bending strength and the modulus of elasticity of wood. Wood Research 58 (4): 617-626.

17. Jankowski, L.J., Jasienko, J., Nowak, T.P., 2010: Experimental assessment of CFRP reinforced wooden beams by 4- point bending tests and photoelastic coating technique. Materials and Structures 43: 141-150.

18. Li, Y.F., Xie, Y.M., Tsai, M.J., 2009: Enhancement of the flexural performance of retrofitted wood beams using CFRP composite sheets. Construction and Building Materials 23 (1): 411–422.

19. Molnár, S., Varga, F., Fehér, S., Németh, R. 2000: Technical parameters of Norway spruce. Handbook of wood technology, Vol. I., Pp 34-88.

20. Németh, R., Tsalagkas, D., Bak, M., 2015: Effect of soil contact on the modulus of elasticity of beeswax-impregnated wood. BioResources 10 (1): 1574-1586.

21. Nowak, T.P., Jasienko J., Czepizak, D., 2013: Experimental tests and numerical analysis of historic bent timber elements reinforced with CFRP strips. Construction and Building Materials 40: 197–206.
22. Plevris, N., Triantafillou, T.C., 1992. FRP reinforced wood as structural material. Journals of Materials in Civil Engineering 4 (3) 300–317.
23. Saad, K., 2017: Finite element modeling of timber beams reinforced with CFRP. MSc Thesis. Budapest University of Technology, 119 pp.
24. Schober, K.U., Rautenstrauch, K., 2006: Post-strengthening of timber structures with CFRP's. Materials and Structures 40: 27–35.
25. Theakston, F.H.,1965. A feasibility study for strengthening timber beams with fiberglass. Canadian Agricultural Engineering, Pp 17–19.
26. Togay, A., Döngel, N. , Sögütlü, C., Ergin, E., Uzel, M., Günes, S., 2017: Determination of the modulus of elasticity of wooden construction elements reinforced with fiberglass wire mesh and aluminium wire mesh. BioResources 12 (2): 2466-2478.
27. Triantafillou ,T.C. , N. Deskovic, 1992: Prestressed FRP sheets as external reinforcement of wood members. Journal of Structural Engineering 118 (5): 1270–1284.

Krisztián Andor*, Bertalan Bellovics
University of Sopron
Faculty Simonyi Károly of Technics Wood Science and Art
Institute For Applied Mechanics and Structures
9400 Sopron
Bajcsy-Zs. E. U. 4.
Hungary
*Corresponding author: andor.krisztian@uni-sopron.hu

WATER RESISTANT PLYWOOD OF INCREASED ELASTICITY PRODUCED FROM EUROPEAN WOOD SPECIES

Tomasz Biadała, Rafał Czarnecki, Dorota Dukarska
Poznan University of Life Sciences
Poznan, Poland

ABSTRACT

The paper investigates the possibility of producing the water-resistant plywood of increased elasticity with use of veneers attained from European wood species, such as alder, birch, beech, pine as well as linden, poplar, willow and spruce. Plywood was produced in two variants. Variant I of plywood was made from various wood species, yet the veneers were of the same thickness. In variant II the centre layer in each case was made from 1 mm thick pine veneer and the face layers were made from 1.4 mm thick veneers of various wood species. The produced plywood was subjected to tests on modulus of rupture, modulus of elasticity and tensile strength, bond quality and compression ratio. Specific values of modulus of rupture and modulus of elasticity were also determined taking into consideration the differences in the thickness of applied veneers. Based on these investigations, the authors concluded that, regardless of the manufacturing method, the highest values of modulus of rupture as well as modulus of elasticity and bond quality are achieved for plywood made from linden, poplar, willow and spruce. The change in the plywood structure (variant II) resulted in a considerable decrease in the values of modulus of rupture and modulus of elasticity (and their specific values) both parallel and across the grain. The lowest values of these parameters were obtained for poplar, linden and willow plywood. What is more, as a result of the applied procedure the bond quality of the produced plywood increased and the compression ratio was reduced. Taking the above into account, we can assume that linden, poplar and willow wood is an optimum choice for the face veneers of plywood with increased elasticity. The centre layer of this kind of plywood can be made from pine veneer of lesser thickness.

KEYWORDS: Plywood, wood species, flexible plywood, water resistance.

INTRODUCTION

The current trends in the wood based materials industry are aimed at searching for new innovative technological solutions, such as using materials that have not been applied so far in the

process of producing or creating new hybrid materials. These activities are purposed to restrain the production costs, to obtain a new material of better or pre-designed properties or to widen the applicability of the traditional materials.

Due to high production volume as well as the characteristics of the manufacturing process, it is necessary to supply a large quantity of good quality timber. In the production of traditional plywood the most commonly used wood species are birch, alder, beech, pine and spruce. So far, the results of investigations have shown that both plywood and LVL can be manufactured with use of not only these wood species, but also plantation wood species. Investigations by Bal and Bektas (2012, 2014) and Bal (2016) prove that mechanical properties (bending strength and modulus of elasticity) of LVL and plywood manufactured from eucalyptus are comparable to those made from beech. Research works conducted by Iwakiri et al. (2006, 2013) also confirm that various types of eucalyptus wood can be successfully applied in the production of plywood. Satisfactory results have also been attained for three kinds of pine, i.e. *Pinus maximinoi, Pinus oocarpa* and *Pinus tecunumannii* which also grow in plantations (Iwakiri et al. 2012). Plywood produced with their use is characterized by bending strength and modulus of elasticity whose values are comparable to those obtained for commercial products made from *Pinus taeda*. Iwakiri et al. (2018) have also found out that another species of great potential is cypress *Cupressus torulosa*, which either alone or combined with pine veneer can be used in the production of plywood of good strength properties and high bond quality. An alternative to fast-growing species which can be used in the production of plywood is *Gmelina arborea*. Investigations by Shukla and Kamden (2008) prove that low-density wood such as silver maple, yellow poplar and aspen can also be effectively applied in the production of LVL. According to Knudson and Brunette (2015) yellow poplar (*Liriodendron tulipifera* L.) as well as red alder (*Alnus rubra* Bong.) which are used in the production of interior design elements can be substituted by hybrid Walker poplar (*P. deltoides P. petrowskyana*) which is characterized by low density, similar to that of aspen, i.e. 390 kg·m^{-3}. The use of veneers attained from this this kind of poplar, either alone or combined with other species such as aspen or spruce, makes it possible to produce high quality plywood. In case of LVL, it is advisable to use this kind of wood for centre layers as the strength parameters of the ready product are better then. According to Öncel et al. (2019) the combination of poplar and other wood species, such as alder, spruce of pine also favourably affects the bond quality in plywood as determined by their tensile-shear strength after preliminary procedures (soaking in water and boiling).

The final properties of plywood, such as bending strength and modulus of elasticity, are affected by not only the wood species veneers are made from but also by wood density, type of adhesive, thickness and number of veneers and the effect of their growth conditions, steaming and drying temperatures (Peker and Tan 2014). An alteration in mechanical properties can also be achieved by changing the position of veneer in the plywood structure (Kljak et al. 2006, 2007, Popovska et al. 2017). This principle is used e.g. in the production of flexible plywood.

In the process of manufacturing flexible plywood, apart from the type of wood, the diversification of veneer thickness in the particular layers is the key factor. The elasticity of the product grows as the face layer thickness/core layer thickness coefficient increases. In the production of flexible plywood manufacturers use wood of exotic species, e.g. okoume (gaboon), ceiba (fuma) and balau (meranti), which generates high costs for the European plywood industry in terms of both materials and transport. Ecological aspect is also significant. Owing to the decrease in the consumption of exotic wood species, the scale of illegal logging of rainforests may be reduced and the biodiversity and climatic conditions on Earth may improve. That is why, researchers have begun to investigate the possibility of substituting exotic timber with cheaper

domestic species in the production of flexible plywood and other wood based materials. The growing demand for this type of products indicates how significant and valid the subject is. As flexible plywood offers individual and innovative solutions, for a number of years it has been used in the furniture industry, boat building, interior design and décor but also in the production of toys made from natural materials and wooden accessories. The surface of flexible plywood, similarly to wood and traditional plywood, is easily processed and it can be waxed, painted, oiled and varnished. It can also be printed and, therefore, it can be used to produce invitations, business cards or labels. Flexible plywood can be processed with use of all the typical machines used for wood. Moreover, it can also be treated with a laser and a waterjet so that precise and complex elements, such as jewellery, toys or models can be manufactured. Last but not least, it can supplement other wood-based materials of high flexibility, e.g. MDF used for ski building. Manufacturing flexible plywood from domestic wood species would not only decrease the production and transport costs but it would also expand the resource base. Owing to the specific structure of flexible plywood, researchers look for such domestic wood species that can be used in the core layer and in the face layers. It is necessary to select material for the core layer from species of medium density and high bending strength, whereas the face layers must be made from wood species characterized by thin-walled cells, low density and high elasticity. Although none of the European species meets the first criterion, the literature on the subject as well the authors' investigations show that beech, pine, birch and alder attain the highest values of bending strength. The investigations conducted by both the authors and other researchers prove that it is possible to produce flexible plywood with use of veneers made from domestic species. The investigations by Borysiuk et al. (2003, 2007) made it possible to determine the effect of various wood species, i.e. pine, aspen, beech, on elastic properties of plywood made from them. The researchers found out that best results can be achieved when the centre layer is made from 0.8 mm thick pine veneer and the face layers are made from birch veneers. The previous studies conducted by the authors of the present paper also confirm that pine veneer is highly useful as the centre layer of flexible plywood. What is more, taking into account the fact that mechanical properties of plywood are strictly related with the strength properties of applied veneers, we determined bending strength and modulus of elasticity for veneers made form species such as alder, birch, beech, linden, poplar, willow, pine and spruce. Therefore, we have come to the conclusion that face layers of plywood with increased elasticity can be made from such wood species as poplar, linden, willow and spruce (Biadała et al. 2015).

The aim of the present work is to determine the possibility of applying domestic wood species to the production of both traditional and flexible plywood glued with PF resin. In the paper, we determine the effect of the wood species on the mechanical properties of the produced experimental plywood.

MATERIALS AND METHODS

Raw materials

In course of the research we used phenol-formaldehyde (PF) resin often applied as a bonding agent for OSB and water-resistant plywood. The characteristics of the resin was as follows: dry mass content - 49.5%, viscosity - 760 mPa·s, density - 1.208 g·cm^{-3}, pH - 12.5. The adhesive mixture was prepared according to industrial recipes, i.e. 13.6 parts by weight (PBW) of tannic filler/100 PBW of PF resin.

Three-layer experimental panels were produced with use of veneers made from the following wood species: alder (*Alnus glutinosa* Gaertn.), beech (*Betula pendula* Roth), birch (*Fagus sylvatica* L.), pine (*Pinus sylvestris* L.), linden (*Tilia cordata* Mill.), poplar (*Populus alba* L.), willlow (*Salix alba* L.), spruce (*Picea abies* L.). The methods of plywood manufacturing as well as preparation of the material for research were presented in the previous study published by Biadała et al. (2015).

Panels' production

Plywood was produced in two variants. In variant I plywood was made of veneers with thickness of 1.7 mm, obtained from various wood species. In variant II plywood was produced with use of long-grain wood of medium density and high bending strength in the core layer, and this veneer was thinner than the face layer veneers. In this variant, the core layer was made from pine veneer with thickness of 1.0 mm, and the face layers were 1.4 mm thick, made from veneers from the other wood species. Variant 2 was an attempt to produce experimental plywood that would be alike 3 mm-thick flexible plywood. Plywood was pressed with use of the following parameters: pressing time 5 minutes, pressing temperature 135ºC, unit pressure 1.4 N·mm^{-2}, resin load 140 g·m^{-2}.

Experimental methods

For the produced plywood we determined modulus of rupture (MOR) and modulus of elasticity at bending (MOE) both across (⊥) and parallel to (II) the grain in the face layers according to the standard EN 310. We also determined the tensile strength (TS) across (⊥) and parallel to (II) the grain and at the angle of 45º according to EN-789. Taking into consideration the fact that wood species used in the investigation vary in terms of density, we determined the specific values of modulus of rupture (SMOR) and modulus of elasticity (SMOE) according to the following Eqs:

$$SMOR = \frac{MOR}{D_i} \quad (km) \tag{1}$$

$$SMOE = \frac{MOE}{D_i} \quad (km) \tag{2}$$

where: MOR – modulus of rupture (N·mm^{-2})
MOE – modulus of elasticity (N·mm^{-2})
D_i – density of veneer (kg·m^{-3}).

Calculations of this type, applied also by other researchers, make it possible to compare modulus of rupture and elasticity of veneer or LVL made from wood species of various densities (Lee et al. 1999, Bao et al. 2001, Bal and Bektas 2012, 2014).

For the produced plywood, we also evaluated the bond quality by shear testing after soaking and boil test according to EN 314-1; the applied tests are required for class 3 quality of bond.

In order to determine the compression ratio Sn in the process of producing plywood from the investigated wood species we determined the nominal compression ratio according to the Eq. 3:

$$S_n = \frac{h_n - h_t}{h_n} \times 100 \quad (\%) \tag{3}$$

where: h_n - nominal height of a set calculated as the sum of nominal thickness of veneer sheets (mm),
h_t - plywood thickness after conditioning (mm).

Statistical analysis

The results of studies on the physical and mechanical properties of the experimental boards were compiled and analysed statistically with use of STATISTICA software, version 13.1. To compare average values of physical and mechanical properties of investigated boards we carried out a one-way ANOVA (analysis of variance) and post hoc Tukey's test, and based on them homogenous groups of average values were determined for each investigated property, assuming that the statistical significance level p equals 0.05.

RESULTS AND DISCUSSION

Tab. 1 shows the elasticity of plywood produced according to variant I, determined based on modulus of rupture (MOR) and modulus of elasticity (MOE) depending on the kind of applied wood. The results of investigations on the typical plywood materials, such as beech, birch, alder, are characteristic of plywood made from the investigated wood species. For these species the obtained values of MOR and MOE, both parallel to grain and across the grain, were the highest. Moreover, Tukey's test for homogenous groups shows that alder and birch plywood belong to virtually the same homogenous groups, which means that as for MOR and MOE (regardless of the test direction) there are no statistically significant differences between the two types of plywood. It is important due to the fact that alder is one of the most promising and yet still underused wood species in Europe (Bekhta and Sedliacik 2019). Moreover, Toksyn et al. (2006) found out that alder plywood shows lower strength properties than beech plywood. However, when the annual increments of beech and alder trees in 1 ha and the time they need to reach suitable diameters for the manufacturing rotary cut veneers were taken into consideration, it was calculated that alder trees allow 3.82 times additional physical harvesting than beech trees.

As expected, beech plywood was characterized by the highest values of bending strength and modulus of elasticity, especially parallel to the grain. It results from the fact that beech wood has higher density than other investigated wood species. These findings are confirmed by studies of other authors, who investigated wood of the following density: beech 0.69 $g \cdot cm^{-3}$, birch 0.61 $g \cdot cm^{-3}$, alder 0.59 $g \cdot cm^{-3}$, pine 0.49-0.53 $g \cdot cm^{-3}$ and poplar 0.39-0.46 $g \cdot cm^{-3}$ (Wilczyński and Wambier 2012, Bal and Bektas 2014, Ozturk et al. 2019). In these studies plywood produced from beech wood showed much higher values of bending strength and modulus of elasticity than those made from other kinds of wood. The results obtained from investigations conducted by Bal and Bektas (2014) may serve as an example: values of MOR and MOE for beech plywood parallel to the grain were 80.2 and 8258 $N \cdot mm^{-2}$, and for poplar plywood they were 56.6 and 67747 $N \cdot mm^{-2}$ (the tendency for the properties across the grain was similar). On the other hand, Cakiroglu et al. (2019) claim that beech plywood is more expensive than that made form birch, which is cheaper and at the same time it has good strength properties and a similar colour.

In case of other types of wood, i.e. linden, poplar, willow and spruce, values of these properties were considerably lower.

Based on the analysis of data included in Tab. 1, we found out that plywood produced from linden, poplar and willow wood, which attained the lowest values of MOE across the grain, according to EN 636 can be classified as E5 modulus of elasticity class and as F10 modulus of rupture class. Whereas, beech plywood produced in the same conditions can be classified as E15 and F20 respectively.

These properties are quite different if we take into the account the density of plywood (Tab. 1). The lowest specific modulus of rupture (SMOR) and elasticity (SMOE) parallel to the grain is observed for the willow plywood.

Tab. 1: Bending strength and modulus of elasticity in bending of plywood produced according to variant I.

Type of plywood	Density of plywood	MOR	MOE	MOR	MOE	SMOR	SMOE	SMOR	SMOE
		II		⊥		II		⊥	
	(kg·m⁻³)	(N·mm⁻²)				(km)			
Alder	600	125.3	11 940	24.1	1 180	21.3	2030	4.1	201
		(3.7 c)*	(290 a)	(0.8 ab)	(40 bc)	(0.6 bd)	(50 a)	(0.1 a)	(6.7 b)
Birch	650	137.6	11 910	24.0	1 200	21.6	1 870	3.8	187
		(9.2 c)	(1030 a)	(1.0 ab)	(40 c)	(1.4 b)	(160 ab)	(0.2 ab)	(12.8 bc)
Beech	680	158.4	13 720	26.8	1 110	23.8	2 060	4.02	167
		(7.2 d)	(680 d)	(2.2 b)	(110 bc)	(1.1 b)	(100 a)	(0.34 a)	(16.3 ac)
Linden	610	91.9	11 890	22.0	940	15.4	1 990	3.7	154
		(4.1 ab)	(1030 a)	(3.2 a)	(50 ae)	(0.7 a)	(170 a)	(0.5 a)	(8.2 a)
Poplar	570	105.5	10 500	20.6	820	18.8	1 880	3.7	147
		(12.9 b)	(1200 ab)	(2.1 a)	(70 de)	(18.9 cd)	(200 ab)	(0.34 ab)	(12.6 a)
Willow	670	79.9	8 600	21.7	970	12.2	1 310	3.3	148
		(7.4 a)	(420 c)	(2.0 a)	(100 a)	(1.1 e)	(60 c)	(0.3 b)	(15.5 a)
Pine	630	105.9	10 610	15.6	750	17.1	1 720	2.5	120
		(5.62 b)	(850 ab)	(2.2 c)	(40 d)	(0.9 ac)	(140 b)	(0.4 c)	(6.6 d)
Spruce	520	78.9	9 550	21.7	1 040	15.5	1 870	4.3	204
		(8.4 a)	(580 bc)	(3.1 a)	(90 ab)	(1.7 a)	(110 ab)	(0.6 a)	(1.5 b)

*standard deviation; a, b, c … - homogenous groups according to Tukey's test (α = 0.05).

The lowest values of MOR and MOE parallel to the grain were obtained for willow and spruce plywood; and the values attained for poplar plywood were similar to those of pine plywood (homogenous groups, b and ab respectively). The investigations on MOR and MOE across the grain do not show such significant differences between the particular wood species. Only for pine plywood we noted that the value of MOR was 42% lower than the highest value, which was obtained for beech plywood. Fig. 1 illustrates the percentage differences in the values of MOR and MOE for the all the other types of experimental plywood in relation to beech plywood, for which the best strength properties were obtained.

The post hoc analysis for this type of plywood generated homogenous groups (*e* and *c* respectively) for which the statistical significance level p took values much lower than the assumed value of 0.05. Linden and spruce plywood showed values of SMOR and SMOE at a comparable level (SMOR – homogeneous group *a*, SMOE – *a* or *ab*), which was only a little lower than that for willow plywood. On the other hand, plywood made from beech, birch and alder wood were characterized by much higher values of SMOR and SMOE than willow plywood: the growth in these values reached, respectively, approx. 48% and 36%. For the investigations performed across the grain in the face layers, the lowest values of SMOR and SMOE were obtained for pine plywood while the highest were for alder and spruce. As for the latter types, the values of the parameters are at a similar level, which is proven by the post hoc analysis – homogenous groups, *a* and *b*, respectively.
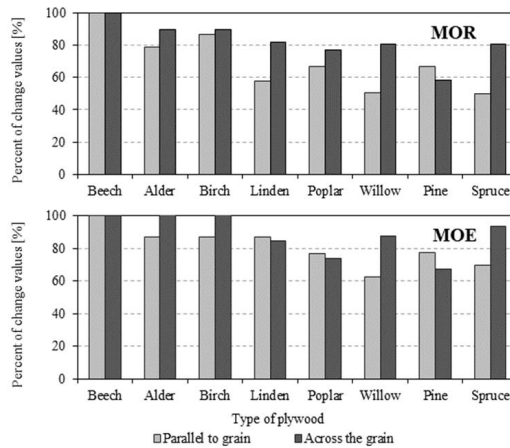
Fig. 1: Percentage changes in modulus of rupture (MOR) and modulus of elasticity (MOE) of investigated plywood in comparison with beech plywood.

The other types of plywood showed slightly lower values of SMOR and SMOE. Yet, for linden, poplar and willow plywood there were no statistically significant differences (homogenous groups *a* and *ab*). The analysis of these results leads to the conclusion that properties of plywood made from linden, poplar and willow are most similar to that of flexible plywood.

Tab. 2 shows the properties of water-resistant plywood with increased elasticity made from veneer of various wood types according to variant II. Results of our investigations as well as works by other authors show that elastic properties of plywood depend on the wood species that the veneers are made from and their thickness and position in the structure of plywood (Kljak and Brezovic 2007, Biadała et al. 2015, Muhammad-Fitri et al. 2018). Therefore, at this stage of studies plywood was produced with use of 1.0 mm thick pine veneer in the centre layer and 1.4 mm thick face veneers made from various wood species.

The change in the structure of plywood and substituting centre veneer of a given wood type with pine veneer significantly affected the values of modulus of rupture and the modulus of elasticity of the produced experimental plywood.

As for linden, willow and spruce plywood, when compared with plywood produced according to variant I, there is an increase in the values of MOR and MOE determined parallel the grain in the face layers of the plywood. These parameters, especially MOR, differ considerably which was confirmed by post hoc analysis in which three homogenous groups were determined (a, c and d). It is accompanied by analogous changes in the values of SMOR and SMOE taking into consideration the density of the particular types of plywood. On the other hand, plywood made from birch and beech wood was characterised by values of MOR parallel to grain comparable to those for plywood produced from the same wood types according to variant I. The highest values of MOR and MOE parallel to grain were obtained for beech and linden veneer and the lowest were for poplar plywood. However, considering the values of modulus of rupture and modulus of elasticity across the grain in the face layer of the plywood, we observe that plywood manufactured according to variant II shows significant decrease in these parameters regardless of the applied material.

Tab. 2: Bending strength and modulus of elasticity in bending of plywood produced according to variant II.

Type of plywood	Density of plywood	MOR	MOE	MOR	MOE	SMOR	SMOE	SMOR	SMOE
		II		⊥		II		⊥	
	(kg·m⁻³)	(N·mm⁻²)				(km)			
Alder	520	95.6	10 400	16.6	800	18.7	2 040	3.25	157
		(3.6 ab)*	(1 030 a)	(0.9 ab)	(40 b)	(0.7 a)	(200 a)	(0.2 c)	(7.3 d)
Birch	640	130.0	14 390	17.3	850	20.7	2 730	3.40	167
		(10.7 cd)	(1 590 b)	(2.1 b)	(110 b)	(1.6 bc)	(350 c)	(0.4 c)	(22.4 d)
Beech	760	156.4	16 690	16.1	870	21.0	2 240	2.2	116
		(7.2 e)	(940 c)	(0.8 ab)	(110 b)	(1.0 bc)	(130 a)	(0.1 a)	(14.3 a)
Linden	740	139.9	16 230	10.9	500	19.3	2 260	1.5	69
		(6.1 d)	(730 bc)	(1.3 c)	(50 a)	(0.9 ab)	(100 a)	(0.2 b)	(6.8 bc)
Poplar	640	85.1	9 940	8.0	290	13.6	1 580	1.3	46
		(5.7 a)	(1 090 a)	(0.3 e)	(30 c)	(0.9 d)	(170 b)	(0.1 b)	(4.8 b)
Willow	560	97.7	10 430	12.5	510	17.8	1 900	2.3	93
		(5.7 b)	(1 450 a)	(0.7 cd)	(80 a)	(1.0 a)	(260 ab)	(0.1 a)	(14.4 a)
Spruce	590	125.0	16 290	14.5	560	21.6	2 810	2.5	96
		(6.3 c)	(1 050 bc)	(1.7 ad)	(80 a)	(1.1 c)	(180 c)	(0.3 a)	(13.4 a)

*Standard deviation; a, b, c … - homogenus groups according to Tukey's test (α = 0.05).

The most substantial changes in values of MOR and MOE and, in consequence, SMOR and SMOE were observed in case of linden and poplar plywood. For linden plywood the value of bending strength is 10.9 N·mm⁻² and the values of modulus of elasticity is 500 N·mm⁻². In case of poplar plywood these parameters are lower, i.e. 8.0 and 290 N·mm⁻², respectively. The other types of plywood were characterized by much higher bend strength and stiffness, especially alder, birch and beech plywood, whose strength properties were at a similar level (the post hoc analysis did not indicate statistically significant differences). For these types of plywood values of MOR varied from 16.1 to 17.3 N·mm⁻² and of MOE from 800 to 870 N·mm⁻². The recorded values of SMOR and SOME were also high and ranged from 2.2 to 3.4 and from 116 to 167 km.

It is also noteworthy that the lowest values of strength parameters, i.e. MOR and MOE as well as SMOR and SMOE, regardless of the test direction, were obtained mainly by poplar plywood, and next by linden. Low values of these parameters, especially across the grain, were attained for willow plywood: MOE and MOR amounted to 12.5 and 510 N·mm⁻². Similar results were obtained by Bal and Bektas (2014), who compared properties of plywood made from poplar, eucalyptus and beech. Therefore, it is reasonable to conclude that the change in the structure of plywood has enhanced its elasticity and the optimum types of wood to apply as face veneers are linden, poplar and willow. All these findings correspond with results of earlier research works done by the authors of the present paper (Biadała et al. 2015).

Tab. 3 shows results of investigations on tensile strength of the produced plywood depending on the structure (variant I and II) and the wood species used for the veneers.

The obtained values are very high, however, the values attained for plywood according to variant II are noticeably lower, especially those determined in the across-the-grain direction. It is because the core layer is made from pine wood, which as other coniferous species attains low values of tensile strength across the grain. It also explains low values of TS for pine plywood, regardless of the test direction. The fact that veneer position in the structure of plywood affects the tensile strength is confirmed by investigations by Popovska et al. (2017).

Tab. 3: Tensile strength of experimental plywood.

Type of plywood	TS (N·mm^{-2})					
	Variant I			Variant II		
	At the angle of 45°	Parallel to grain	Across the grain	At the angle of 45°	Parallel to grain	Across the grain
Alder	22.11 (3.14 abc)*	69.33 (8.18 a)	41.19 (3.51 a)	16.60 (2.34 ab)	57.52 (5.97 a)	26.76 (2.89 a)
Birch	25.61 (2.46 cd)	78.84 (7.94 ab)	41.83 (3.26 a)	23.45 (1.72 d)	96.01 (7.14 c)	25.21 (1.74 a)
Beech	19.32 (3.37 ab)	81.66 (5. 18 bd)	45.82 (3.24 ab)	16.75 (1.00 ab)	115.72 (8.77 d)	35.18 (4.23)
Linden	22.81 (2.87 abc)	100.02 (2.79 d)	45.71 (2.48 ab)	19.80 (1.37 bc)	69.01 (3.60 a)	27.60 (2.50 a)
Poplar	30.42 (2.80 d)	75.47 (6.92 ab)	51.91 (3.07 ab)	15.05 (1.49 a)	61.07 (2.86 a)	18.80 (1.90 b)
Willow	25.68 (3.97 abcd)	72.32 (0.53 ab)	53.72 (9.36 b)	22.96 (1.53 cd)	37.38 (0.85 b)	16.97 (1.35 b)
Pine	18.92 (2.20 a)	52.17 (9.03 c)	26.21 (5.80 c)	-	-	-
Spruce	26.66 (2.49 bcd)	62.87 (4.80 ac)	25.60 (3. 92 c)	17.67 (1.00 ab)	55.73 (1.15 a)	29.25 (0.95 a)

*Standard deviation; a, b, c … - homogenus groups according to Tukey's test (α = 0.05).

The bond quality of veneers is a significant factor that affects the physical and mechanical properties of plywood. It depends on the characteristics of veneer surface, their moisture content, thickness, species and structure of wood, type and amount of adhesive and pressing conditions (Aydin et al. 2006, Bekhta et al. 2009, Šrajer et al. 2013). Thicker veneers and those of lower density tend to absorb more resin and, as a result, the curing process occurs in the veneer rather than in the glue line (Muniz et al. 2013, Muhammad-Fitri et al. 2018). Taking into account the fact that the investigated veneers were made from various wood species of various density and thickness, the produced plywood was subjected to investigations on bond quality by determining their shear strength after boiling and soaking tests. Results of these investigations are presented in Tab. 4.

Tab. 4: Bond quality of experimental plywood.

Type of plywood	fv (N·mm^{-2})			
	Variant I		Variant II	
	Soaking	Boiling test	Soaking	Boiling test
Alder	2.36 (0.30 b)*	2.04 (0.66 abc)	2.04 (0.22 a)	1.90 (0.33 ab)
Birch	3.27 (0.43 d)	2.47 (0.17 d)	2.69 (0.56 b)	2.66 (0.37 d)
Beech	2.99 (0.45 cd)	2.44 (0.7 cd)	2.30 (0.45 ab)	2.16 (0.35 ac)
Linden	2.57 (0.36 bc)	2.15 (0.23 bcd)	2.62 (0.29 b)	2.50 (0.43 cd)
Poplar	2.40 (0.30 b)	1.86 (0.22 ab)	2.24 (0.31 ab)	1.91 (0.27 ab)
Willow	1.81 (0.14 a)	1.67 (0.23 ab)	1.87 (0.25 a)	1.67 (0.23 b)
Pine	1.71 (0.19 a)	1.63 (0.16 a)	-	-
Spruce	1.89 (0.21 a)	1.70 (0.22 ab)	2.32 (0.36 ab)	2.25 (0.28 acd)

*Standard deviation; a, b, c … - homogenus groups according to Tukey's test (α = 0.05).

All the presented values significantly exceed 1 N·mm^{-2}; that is why, we decided not to analyse the image of bend shearing. However, the investigation shows that plywood produced

according to variant I from poplar, willow pine and spruce is characterised by the lowest bond quality, significantly lower than other investigated species; the latter three show similar level of bond quality (homogeneous group a after soak test and a or ab after double boil test). This phenomenon can be explained by the fact that owing to lower density of these species the resin can more easily penetrate into wood tissue (Mansouri et al. 2006, Cakiroglu et al. 2019). The shear strength determined after soaking and boiling test (fv) for these three types of plywood (willow, pine and spruce) varied from 1.71 to 1.89 N·mm^{-2} after soaking and from 1.63 to 1.70 N·mm^{-2} after double boiling test. As expected, the best gluability was observed for beech and birch plywood – the value of fv reached 2.99 and 3.27 N·mm^{-2} after soaking and 2.44 and 2.27 N·mm^{-2} after double boiling test. Such results correspond with works by other authors. For example, Bal and Bektas (2014) after boing test attained the values of shear strength of 2.44 N·mm^{-2} for beech plywood and 1.37 N·mm^{-2} for poplar plywood. The bond quality for polar plywood attained by Öncel et al. (2019) was at the similar level. Cakiroglu et al. (2019) with use of MUPF resin produced beech and birch plywood whose shear strength was 3.87 N·mm^{-2} and 3.06 N·mm^{-2} respectively. Investigations by Toksoy et al. (2006) showed that shear strength after 24 hour soaking for alder plywood was 2.54 N·mm^{-2} and for beech plywood it was 2.75 N·mm^{-2}.

The manufacturing of plywood according to of variant II, with use of pine veneer in the core layer, leads to the decrease in the average value of shear strength in case of plywood whose face layers were made from alder, birch and beech veneer. The most significant decrease in the bond quality was observed for beech plywood: the average values of fv after soaking fell by 23% and after boiling by 11%. As for linden, poplar and spruce plywood, the bond quality has considerably improved. The greatest improvement of gluability was observed for spruce plywood, whose fv values, deepening on the conducted test, increased by approx. 20% and 25%. The quality of willow plywood remained practically the same. Investigations by Muzin et al. (2013) prove that using wood of higher density in the core layer favourably affects the bond quality. It results from the obvious fact that wood of higher density is characterized by better shear strength (Bal 2016). That is why, in comparison to variant I, plywood produced according to variant 2, with face layers made from low density wood, such as linden, willow and spruce, shows better bond quality if the core layer is substituted with higher density pine veneer. Similar observations were made by Bal and Bektas (2014), Muhammad-Fitri et al. (2018) and Cakiroglu et a. (2019).

In the course of investigations, we applied the same value of pressure, i.e. 1.4 N·mm^{-2}, regardless of the type of wood and variant of manufacturing. When selecting the value of pressure it is crucial to make sure it allows both veneers to adhere evenly and therefore attain required bond quality. On the other hand, the pressing pressure should be quite low so that the thickness of the produced material is not decreased. It may result in an adverse growth of the specific weight of plywood and decrease in the material yield of the whole production process. The compression ratio is a resultant value depending on several technological factors: not only on the pressing pressure, but also moisture content and density of the material (Bal 2016). That is why, to provide a better characteristic of the produced experimental plywood, we determined their compression ratio, which is a crucial parameter from the technological point of view, especially when alternative materials are used. The results of tests on the compression ratio (Sn) of the investigated experimental boards are shown in Fig. 2. They prove that for plywood produced according to variant I the highest compression ratio is attained by willow, poplar, pine and spruce plywood.

It results from the fact that they are made from wood of lower density than that commonly used in industry, such as birch, alder and beech, which are species of higher density. In case of willow plywood, the recorded Sn value is twice as high as that for birch or beech plywood. Similar observation were made by Bal (2016) who produced LVL with use of two veneers of two wood

species (poplar and eucalyptus) of different density. The author concluded that when using the same pressure, the compression ratio for wood of lower density is higher than in case of wood characterized by higher density.
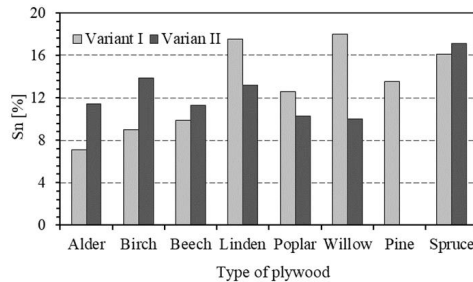

Fig.2: Compression ratio of experimental plywood depending on its structure and applied type of wood.

In the variant 2 of investigations, the change in the structure of plywood as well as the substitution of veneers in the core layer led to a significant increase in the compression ratio of alder, beech and birch plywood. This phenomenon results from the fact that the core layer is made from pine, which also leads to the decrease in Sn¬ value for linden, poplar and willow plywood.

CONCLUSIONS

1. Taking into consideration the density and modulus of elasticity, European species such as poplar, linden and willow are the most suitable types of wood to be used as face layers of plywood. In comparison with beech, birch and alder, plywood made from these species shows lower values of modulus of rupture, tensile strength and bond quality. Yet, values of these properties are still at an acceptable level.
2. It is possible to use these species in manufacturing plywood of increased elasticity purposed for use in humid conditions. Although the plywood shows a decrease in shear strength after boiling and double boiling test, the bond quality meets requirements of the EN 314-2 standard for plywood purposed for use in humid conditions ($fv > 1$ N·mm^{-2}).
3. Plywood produced from linden, poplar and willow veneers was characterized by higher compression ratio than that made from beech, birch and alder, which is quite an unfavourable feature as far as material efficiency is concerned.
4. The analysis of the attained results leads to the conclusion that the values of specific modulus of rupture and modulus of elasticity (SMOR and SMOE) may be an important index, which can be used to compare the elastic properties of plywood produced from wood of various density.

REFERENCES

1. Aydin, I., Colakoglu, G., Colak, S., Demirkir, C., 2006. Effects of moisture content on formaldehyde emission and mechanical properties of plywood. Building and Environment 41: 1311–1316.

2. Bal, B.C., Bektas, I., 2012: The effects of wood species, load direction, and adhesives on bending properties of laminated veneer lumber. BioResources 7(3): 3104-3112.

3. Bal, B.C., Bektas, I., 2014: Some mechanical properties of plywood produced from eucalyptus, beech, and poplar veneer. Maderas: Ciencia y Tecnologia 16(1): 99-108.

4. Bal, B.C., 2016: Some mechanical properties of laminated veneer lumber produced with fast-growing Poplar and Eucalyptus. Maderas: Ciencia y Tecnologia 18(3): 413-424.

5. Bao, F., Fu, F., Choong, E.T., Hse, C., 2001: Contribution factor of wood properties of three poplar clones to strength of laminated veneer lumber. Wood and Fiber Science 33(3): 345–352.

6. Bekhta, P., Hiziroglu, S., Potapova, O., Sedliacik, J., 2009: Shear strength of exterior plywood panels pressed at low temperature. Materials 2: 876–882.

7. Bekhta, P., Sedliacik, J., 2019: Environmentally-friendly high-density polyethylene-bonded plywood panels. Polymer 11(7): 1166.

8. Biadała, T., Czarnecki, R., Dukarska, D., 2015: Attempt to produce flexible plywood with use of European wood species. Wood Research 60(2): 317–328.

9. Borysiuk, P., Zado, A., Sosińska, K., Gowin, Ł., Mrozik, M., Nowakowski, M., 2003: Flexible plywood made of Polish timber. Annals of Warsaw Agricultural University. Forestry and Wood Technology 53: 23-27.

10. Borysiuk, P., Dziurka, D., Jabłoński, M., Sosińska, K., 2007: Selected properties of flexible plywood made of domestic wood species. Annals of Warsaw University of Life Sciences - SGGW. Forestry and Wood Technology 61: 71-74.

11. Cakiroglu, E.O, Demir A., Aydin, I., 2019: Comparison of birch and beech wood in terms of economic and technological properties for plywood manufacturing. Drvna Industrija 70(2): 169-174.

12. EN 310, 1993 Wood-based panels. Determination of modulus of elasticity in bending and of bending strength.

13. EN 314-1, 2004 Plywood. Bond Quality. Test methods.

14. EN 314-2, 2008 Plywood. Bond Quality. Requirements.

15. EN 636, 2012 Plywood. Specification.

16. Iwakiri, S., de Matos, J.L.M., Prata, J.G., Trianoski, R., da Silva, L.S., 2013: Evaluation of the use potential of nine species of genus eucalyptus for production of veneers and plywood panels. Cerne 19(2): 263-269.

17. Iwakiri, S., Neto, A.R., de Almeida, C.A., Biasi, C.P., Chies, D., Guisantes, F.P., Franzoni, J.A., Rigatto, P.A., Bettega, W.P., 2006: Evaluation of quality of phenolic plywood manufactured from Eucalyptus grandis. Ciencia Florestal 16(3-4): 437-443.

18. Iwakiri, S., Trianoski, R., Vieira, H.C., Andrade, R., Rocha, T.M.S., Ferreira, V.R.S., 2018: Viability of the use of wood of *Cupressus torulosa* for plywood production. Scientia Forestalis 46(120): 638-645.

19. Kljak, J., Brezovic, M., Jambrekovic, V., 2006: Plywood stress optimisation using the finite element method. Wood Research 51(1): 1-10.

20. Kljak, J., Brezovic, M., 2007: Influence of plywood structure on sandwich panel properties: Variability of veneer thickness ratio. Wood Research 52 (2): 77-88.

21. Knudson, R., Brunette, G., 2015: Evaluation of Canadian Prairie-Grown hybrid poplar for high value solid wood products. Forestry Chronicle 91(2):141-149.

22. Lee, J.N., Tang, R.C., Kaiserlik, J.H., 1999: Edge static bending properties of yellow-poplar laminated veneer lumber: effect of veneer-joint designs. Forest Product Journal 49(7-8): 64-70.

23. Mansouri, H.M., Pizzi, A., Leban, J.M., 2006: Improved water resistance of UF adhesives for plywood by small pMDI additions. Holz als Roh- und Werkstoff 64: 218-220.

24. Muhammad-Fitri, S., Suffian, M., Wan-Mohd-Nazri, W. A. R., Nor-Yuziah, Y., 2018: Mechanical properties of plywood from batai (*Paraserianthes falcataria*), eucalyptus (*Eucalyptus pellita*) and kelempayan (*Neolamarckia cadamba*) with different layer and species arrangement. Journal of Tropical Forest Science 30(1): 58-66.

25. Muniz, G.I.B., Iwakiri, S., Viana, L.C., Andrade, M., Weber, C., Almeida, V.C., 2013: Production of plywood panels from *Pinus taeda* using veneers of differing densities and phenol-formaldehyde resin with high and low molecular weights. Cerne 19(2): 315-321.

26. Öncel, M., Vurdu, H., Aydoğan, H., 2019: The tensile shear strength of outdoor type plywood produced from fir, alnus, pine and poplar wood. Wood Research 64(5): 913-920.

27. Ozturk, H., Demir, A., Demirkir, C., Colakoglu, G., 2019: Effect of veneer drying process on some technological properties of polystyrene composite plywood panels. Drvna Industrija 70 (4): 369-376.

28. Peker, H., Tan, H., 2014. The effect of growth conditions, steaming, drying temperature, number of layers and type of adhesives on the some mechanical properties of plywoods produced from Spruce. Journal of Forestry Research 1(1A): 50-59.

29. Popovska, V.J., Iliev, B., Zlateski, G., 2017: Impact of veneer layouts on plywood tensile strength. Drvna Industrija 68(2): 153-161.

30. Shukla, S.R., Kamdem, D.P., 2008: Properties of laminated veneer lumber (LVL) made with low density hardwood species: effect of the pressure duration. Holz als Roh- und Werkstoff 66: 119-127.

31. Šrajer, J., Král, P., Čermák M., Mazal P., 2013: Structure evaluation of compressing of spruce and beech plywoods. Part 1: Microscopic structure. Wood Research 58(1): 101-112.

32. Toksoy, D., Colakoglu, G., Aydin, I., Colak, S., Demirkir, C., 2006: Technological and economic comparison of the usage of beech and alder wood in plywood and laminated veneer lumber manufacturing. Building and Environment 41(7): 872-876.

33. Wilczyński, M., Warmbier, K., 2012: Elastic moduli of veneers in pine and beech plywood. Drewno 55(188): 47-58.

Tomasz Biadała, Rafał Czarnecki*, Dorota Dukarska*
Department of Wood Based Materials
Faculty of Wood Technology
Poznan University of Life Sciences
Wojska Polskiego Street 38/42
60–637 Poznań
Poland.
*Corresponding authors: rczarnec@up.poznan.pl and ddukar@up.poznan.pl

EFFECT OF FACE LAYER MANIPULATION ON THE DENSITY PROFILE AND PROPERTIES OF LOW DENSITY PARTICLEBOARD

Shupin Luo, Li Gao, Wenjing Guo
Chinese Academy of Forestry
Beijing, China

ABSTRACT

Density reduction has gradually become a trend for the particleboard and furniture industries due to increased price and insufficient supply of wood. However, reduced density of the panels by the simple reduction of the wood material comes along with deterioration of the properties. In this study, to achieve sufficient properties (bending properties in particular), the particle moisture content (MC) and geometry in face layers were manipulated to manufacture low density particleboards (500 kg·m^{-3}), with the core layer composed of a mixture of wood particles (92.5 wt %) and expanded polystyrene (7.5 wt %). This strategy was assumed to increase face layer density and generate a more pronounced vertical density profile, which is expected to improve panel properties. The density profile, mechanical properties and dimensional stability of the particleboards were investigated. Results showed that increasing the moisture content of face layer particles from 8% to 16% or using small-sized particle in face layer resulted in a more pronounced density profile, as well as using fiber in face layer. However, the higher density in the face layer was not necessarily related with better mechanical performance. The optimum physic-mechanical properties were obtained with the board of face layer made of 16% MC fiber, which met the requirements for P2 boards used in dry conditions (EN 312).

KEYWORDS: Low density particleboard, face layer, moisture content, particle geometry, density profile, panel properties.

INTRODUCTION

Nowadays, density reduction of wood-based panels has attracted interest at both academic and industrial levels, because of shortage and increasing price for wood resources (Gao et al. 2018, Parlin et al. 2014, Shalbafan et al. 2015). Prevalence of ready-to-assemble and flat pack furniture is driving the development of low density panels as well. Lightweight wood-based panels bring

many advantages such as more rational utilization of wood, easier transportation and handling, lower transportation cost due to mass reduction (Barbu 2016, Monteiro et al. 2018).

With an estimated production capacity of about 110.2 million m^3 worldwide in 2016, particleboard is one important type of wood-based panels, commonly used in the furniture. Currently, the average density of particleboard in the market is about 620~720 kg·m^{-3} (Report of Chinese Particleboard Industry 2016). According to ASTM D1554-10, particleboard with a density of less than 640 kg·m^{-3} is classified as low density particleboard (Monteiro et al. 2019). One interesting approach to achieve the density reduction of particleboards is partly substituting wood particles with non-wood light fillers. Materials like foamed starch (Monteiro et al. 2016), dried distillers grains with solubles (Sundquist and Bajwa 2016), expanded polystyrene (PS) (Bajzová et al. 2018) and expandable microspheres (Shalbafan et al. 2012b) have been reported to be applied in the core layer of particleboard. BASF company developed a technology for producing lightweight particleboards called Kaurit® Light, with the core layer comprised of the mixture of wood particles and foamed PS beads, achieving 20~30% lower density than the conventional particleboard (Monteiro et al. 2018). Shalbafan et al. (2012a; 2013) produced ultra-lightweight sandwich particleboards with a density around 300 kg·m^{-3} using only thermo-sensitive expandable PS as core layer material, but the bending strength did not meet the requirement of P2 boards according to EN 312. Dziurka et al. (2015) manufactured particleboards (density reduced to 500 kg·m^{-3}) using rape straw (or wood chips) and expanded polystyrene (7 wt %) in the core layer. It was found that the requirement of mechanical strength for particleboards intended for interior application (EN 312/ P2 boards) was not fulfilled. One of the reasons for the reduced properties of density-decreased particleboards is considered as the increased proportion of cavities and fewer adhesive bonding between particles (Bajzová et al. 2018, Benthien and Ohlmeyer 2017). Introduction of PS beads or other light fillers can fill up the cavities between wood particles, making the internal structure more uniform (Dziurka et al. 2015). However, the positive effect of light fillers cannot completely compensate for the decreased board properties.

One strategy to solve this problem is optimizing the panel's density profile via re-engineering the mat structure (Benthien et al. 2017). Vertical density profile in the thickness direction is considered as a crucial characteristic that correlates with performance of wood-based panels (Schulte and Frühwald 1996, Wang and Winistorfer 2000, Lee et al. 2017). The formation of density profile is influenced mainly by furnish moisture condition, mat structure, and pressing environment (Wong et al. 1999, Hunt et al. 2017). Literature reported that the difference between face layer and core layer density in the three-layer particleboard became smaller with reducing density (Benthien and Ohlmeyer 2016, Wong et al. 1999). To achieve a distinct density profile in low density particleboards, the wood particles in the core layer need to have a high compression resistance (Schneider et al. 2018). Benthien and Ohlmeyer investigated the effect of mat structure on the properties of lightweight particleboards (Benthien and Ohlmeyer 2016, 2017). Results revealed that the internal bond strength and dimensional stability were improved by changing face-to-core layer ratio, core layer resin content and core layer particle orientation, but the bending properties was not affected. To achieve sufficient mechanical properties, bending in particular, a pronounced density profile with higher density face layer is supposed to be an important factor, since the face layers of the panel bear most of the load during bending (Wong et al. 1998). Further research on face layer optimization is required to achieve higher density face layer in lightweight particleboards.

This study aims to produce low density particleboards (500 kg·m^{-3}) using wood particles and expanded PS foam as raw materials, which meet the required property requirements of EN 312/ P2 boards. Towards this goal, the particle size and MC in face layers was manipulated

to achieve a pronounced vertical density profile. The change in the density profile and its influence on the mechanical and physical properties of particleboards were investigated.

MATERIALS AND METHODS

Raw materials

Poplar (*Populus* spp.) particles (air-dried moisture content of about 8%) were provided by Ningfeng Wood-based Panels Corporation, China. The particles were sieved and divided into three fractions: fine (less than 0.5 mm), medium (0.5 - 1 mm) and coarse (1 - 4 mm) for use (Fig. 1).

Fig. 1: Wood particle and fiber used for manufacturing of low density particleboard.

Poplar wood fibers were bought from the Chinese Academy of Forestry (Beijing, China). An optical impression of the four types of wood raw material can be obtained in Fig. 1. Expanded polystyrene foams (4 - 6 mm in diameter) with a density of 50 - 60 $kg·m^{-3}$ was used as non-wood light fillers. A polymeric diphenylmethane di-isocyanate (PMDI) resin, WANNATE® PM-200 (viscosity: 150-200 mPa·s at 25°C, NCO content: 30.5 - 32.0 wt %, density: 1.22 - 1.25 $g·cm^{-3}$ at 25°C), was obtained from the Wanhua Corporation, Beijing, China. Acetone was used as a resin diluent for better adhesive distribution.

Particle size distribution analysis

Particle size distribution of the fine, medium and coarse particle sample was measured using the image analysis-based particle size measurement equipment (SCREENCAM 100 Optical Lab Screen for Wood Chips, IMAL-PAL GROUP, Italy). The wood particles were separated by the system without altering their dimensional characteristics, imaged by a digital camera, and analyzed by the software. The distribution of wood particles was given as a percentage over the total volume based on their dimensions. Approximately 100,000 particles were evaluated for each sample.

Particleboards manufacturing

Three layered particleboards with a target density of 500 $kg·m^{-3}$ were manufactured. The thickness was set for 15 mm in all panel variations. The core layer was composed of expanded PS foams and air-dried coarse wood particles at the weight ratio of 3:37. In the case of face layer, a type of material, MC and layer thickness were manipulated, as summarized in Tab. 1.

Tab. 1: Formulation of the face layer for the 15 mm low density particleboards and their actual mean densities.

Code	Face layer			Mean density (kg·m^{-3})
	Material type	Moisture content (%)	Thickness (mm)	
Fine particle-8MC-1.5	fine particle	8	1.5	489
Fine particle-16MC-1.5	fine particle	16	1.5	499
Med particle-8MC-1.5	medium particle	8	1.5	488
Med particle-16MC-1.5	medium particle	16	1.5	504
Med particle-16MC-2.5	medium particle	16	2.5	507
Fiber-8MC-1.5	fiber	8	1.5	463
Fiber-16MC-1.5	fiber	16	1.5	482

To obtain 16% MC, the wood particles were sprayed with required amount of deionized water and stored in zip lock bags. Resin content was 7% for core layer and 10% for face layer (based on the dry mass). The three-layered mat (340 x 360 mm) was made manually, and pressed at 120°C for 20 min using thickness gauges. Then the boards were cooled down at ambient conditions and conditioned prior to sample cutting. The boards were produced in two replications.

Evaluation of particleboards

Cross-sectional density profile was measured on a DENSE-LAB X densitometry (EWS, Germany), using X ray transmitted across the thickness of sample at a scanning speed of 0.5 mm·s^{-1}. Mechanical properties were analysed by determining internal bond strength (IB) according to EN 319, modulus of rupture (MOR) and modulus of elasticity (MOE) according to EN 310, using an Instron 5582 universal testing machine. Physical properties were characterized by measuring thickness swelling (TS) (EN 317) after 2 h of water immersion at 20°C. Eight replicates were tested for MOR and MOE, and twelve replicates were tested for IB and TS, respectively.

Statistical analysis

Data analysis was performed using the Statistical Package for the Social Science (SPSS software, IBM). Comparison of mean values was conducted to evaluate whether the differences between the properties of the particleboards manufactured at different conditions are significant or not. ANOVA test was performed by using Tukey-test method, at a significance level of $\alpha = 0.05$.

RESULTS AND DISCUSSION

Particle size characterization

The particle size distributions (length, width and slenderness) are shown in Fig. 2. It can be seen that the coarse particle sample has the largest dimensions with peaks in the distribution at longer lengths and widths than medium and fine particle. The fine particle sample has the smallest average length and width. The slenderness is the ratio between the length and width, displayed as a box plot graph that has three marks (25th, 50th and 75th percentile). This is useful for seeing how a sample which has passed through the same shifter is formed. The slenderness of coarse particle sample and medium particle sample exhibited a quite similar trend.
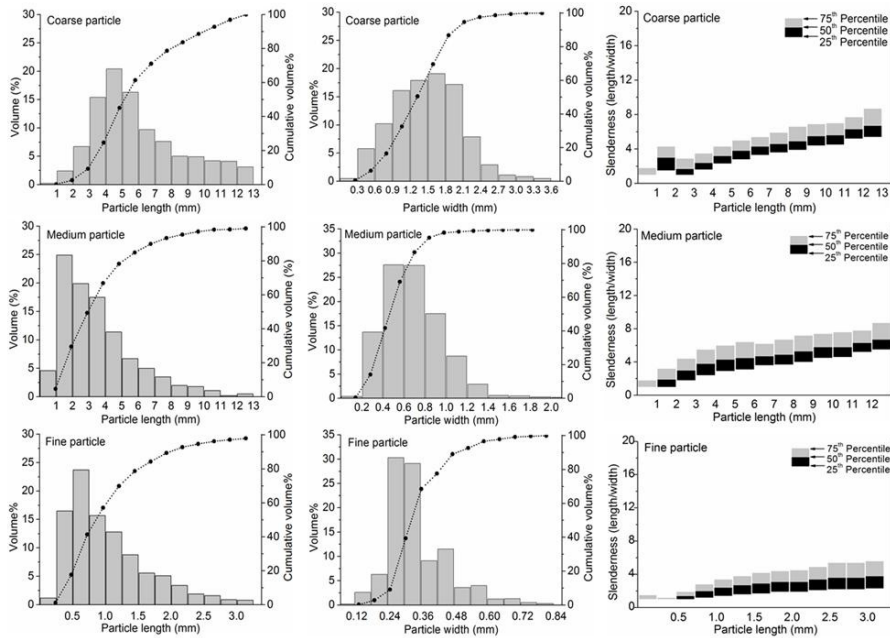
Fig. 2: Histogram of the distribution and cumulative distribution of the particle length and width, and Box plot of particle slenderness.

Density profile

In the current study, the coarse particle was applied in the core layer, due to the large particles are expected to give better mechanical strength, while the small ones was good for surface quality (Monteiro et al. 2018). The internal structure of the particleboards is shown in Fig. 3. The density profile of the particleboards generally resembles a U-shape, as shown in Fig. 4. The mean density of all these particleboards is similar (Tab. 1). For panels with different material type and MC in face layers, the density profiles varied. The increase in the face MC led to slimmer and higher peaks near to the surface (dotted lines). This is probably because the face layers were more compacted due to the increased plasticity of the moist particles, resulting in a larger difference between face and core densities (Wong et al. 1998).
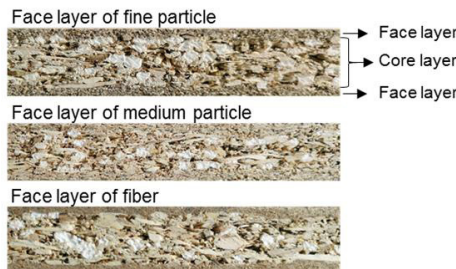

Fig. 3: Internal structure of 15 mm three-layer particleboards with 1.5 mm face layer made from fine particle, medium particle and fiber, respectively.

In order to clarify the effect of face layer thickness, the particleboards with 2 mm face layer made of medium particle was investigated as well. When the thickness of face layers was increased from 1.5 mm to 2 mm, the core layer particles were less compacted. In the density profile, this is expressed by a lower core region and less steep decrease of density from surface to core layer.
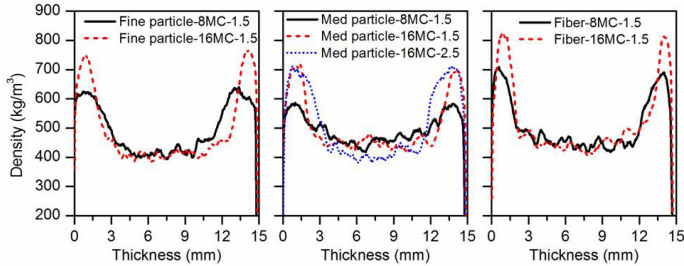

Fig. 4: Vertical density profiles of particleboards with different formulations. The sample code refers to Tab. 1.

When the face layer was altered from medium particle to fine particle, the contrast between face and core layer density became higher. This is probably due to that the compression resistance of small particles is lower than that of large particles (Benthien et al. 2017). To achieve highly compressed face layers, wood fiber was chosen as another face material. When the wood particle was replaced with fibre, a significantly more slender peak in the surface density was observed. Results indicated that at a similar mean density level, increasing the MC of face layer particles or using small-sized particle in face layer resulted in a more pronounced density profile, as well as using fiber in face layer.

Bending properties

As expected, the increase of face MC has a positive effect on the bending properties (Fig. 5). By increasing the face MC from 8% to 16%, the MOR raised by 5%, 22% and 11% for the panels with face of fine particle, medium particle and fibre, respectively, but the increased could not be detected as significant. The general effect of MC on MOE was similar with that on MOR.
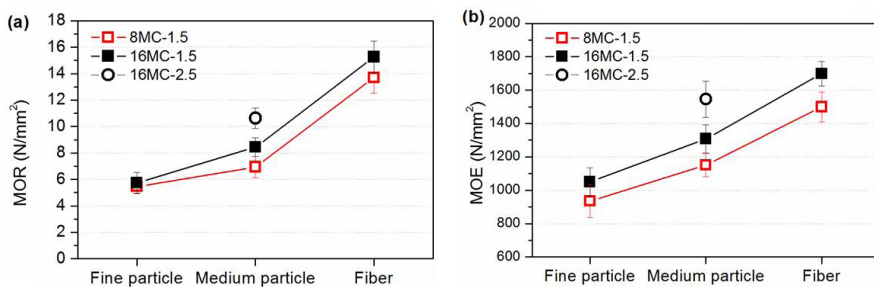
Fig. 5: MOR (a) and MOE (b) values of 15 mm particleboard. Note: the sample code refers to Tab. 1.

Comparing bending properties of particleboards with three types of face layer revealed the following trend: fine particle < medium particle < fibre. Despite the higher peak density of fine particle than medium particle, the sample with medium particle face layer showed higher MOR and MOE. Therefore, the presence of higher density in the face layer does not

necessarily result in better bending performance. The panel with face layers of 16% MC fiber met the minimum requirements of MOR and MOE for a conventional particleboard (EN312/P2: 13 N·mm^{-2} for MOR and 1600 N·mm^{-2} for MOE). Whereas, Dziurka et al. (2015) produced low density particleboards using mixture of wood chips and expanded PS beads (7 wt%) as core layer material, but the boards with density of 500 kg·m^{-3} cannot meet the requirement of MOR according to EN312/ P2. This is probably due to that the larger aspect ratio of fiber promoted their entanglement, which could strengthen the face layer.

In the case of 16% MC medium particle, by raising the face thickness from 1.5 mm to 2 mm, the MOR significantly increased from 8.4 N·mm^{-2} to 10.6 N·mm^{-2} and MOE from 1312 N·mm^{-2} to 1546 N·mm^{-2}, which was very close to the requirements of EN312. Boards with thicker face layers will be further investigated in our next study.

Internal bond (IB) strength

The IB values of the particleboards are shown in Fig. 6. Increasing face layer MC to 16% resulted in a slight higher IB, which was consistent with increased face density. This was probably because higher MC caused more effective internal cohesion. It is noted that in the case of fine particle, the destruction of the samples during IB test occurred within the face layer occasionally. This might be attributed to the weak adhesion between powder-like fine particles despite higher glue content of the face layer.
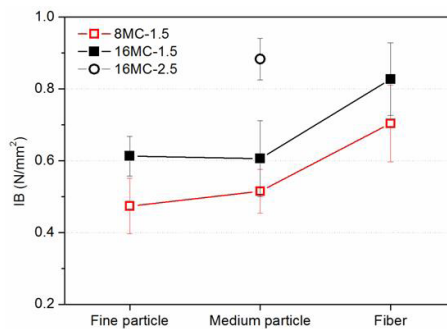
Fig. 6: Internal bond strength of 15 mm low density particleboard with different face layer material and MC. Note: the sample code refers to Tab. 1.

The difference between the IB values of particleboards with fine particle and medium particle in face layers was statistically insignificant, whereas using fiber in face layer significantly raised the IB. According to EN 312, IB values of all the boards outperformed the minimum requirements for P2 boards (0.35 N·mm^{-2}). Compared with the conventional particleboard of similar mean density, the IB values in this study were higher than that in previous study by Boruszewski et al. (2016) (less than 0.25 N·mm^{-2}).

The maximum value of IB (0.88 N·mm^{-2}) was obtained in the panel with 2.5 mm face layer (medium particle with 16% MC). The significantly raised IB value in the Med particle-16MC-2.5 sample is probably due to that its density profile presented a narrower zone of low density region in core layer (Fig. 4), therefore a lower possibility for failure occurred in the weak point within the core layer (Wong et al. 1999).

Thickness swelling (TS)

TS were determined after immersion in water for 2 h (Fig. 7). The 2 h TS of panels in the present study was lower than that of particleboards made of wooden particles with similar density, because PS is an inherent hydrophobic polymer (Shalbafan et al. 2015). Since the formulation of core layer kept unchanged, the TS of these samples was depended largely on the surface layer. The 16% MC face layer boards had lower TS than that of 8% MC boards manufactured under same processing conditions. The difference is probably due to that higher MC in face layer caused higher compressibility of the particles (or fiber) and hence less cavities for water absorption (Maraghi et al. 2018). In general, the TS showed negative correlations with the face layer density.
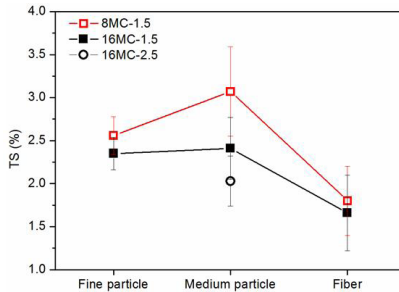

Fig. 7: Thickness swelling (TS) of particleboards after 2 h water soaking.

At the same MC level, TS did not change significantly as face layer changed from fine particle to medium particle, which is consistent with their similar density profile. But the TS of board with fiber as face layer material shows a significant lower TS than that of the other two materials. This is the consequence of a more compacted surface layer that caused less accessibility to the hydroxyl groups. The TS decreased with the increase of face layer thickness from 1.5 mm to 2.5 mm in 16MC boards, partially due to a higher proportion of more compressed face layer that is tight and hard.

CONCLUSIONS

This study showed that increasing the MC from 8% to 16% or substituting particle with fibre in face layer resulted in a more pronounced density profile, which had a positive influence on the MOR, MOE, IB and dimensional stability of the resulting particleboards. But the improvement of properties caused by increased MC cannot be detected as significant. The bending properties of panels were significantly enhanced when the face layer changed from fine particle to medium particle; whereas the internal bond strength and thickness swelling was not found to be affected. Compared to wood particle, using fibers as face layer material led to remarkable panel property improvements, probably due to its low compression resistance that resulted in the highly compacted face. Additionally, the entanglement between fibers could strengthen the face layer. The requirement of physic-mechanical properties for boards intended for interior design used in dry conditions (EN 312/ P2) was fulfilled by panels with 16% MC fiber as face layer. Further research is needed to produce low density particleboards using particle as face layer that meet required properties of a conventional particleboard.

ACKNOWLEDGEMENTS

REFERENCES

1. Bajzová, L., Bekhta, P., Iždinský, J., Sedliačik, J., 2018: The effect of veneering on the properties of lightweight particleboard with expanded polystyrene. Acta Facultatis Xylologiae Zvolen 60 (1): 93-100.
2. Barbu, M.C., 2016: Evolution of lightweight wood composites. Pro Ligno 11: 21-26.
3. Benthien, J.T., Ohlmeyer, M., 2016: Influence of face-to-core layer ratio and core layer resin content on the properties of density-decreased particleboards. European Journal of Wood and Wood Products 75 (1): 55-62.
4. Benthien, J.T., Ohlmeyer, M., 2017: Enhancement of low-density particleboard properties by core layer particle orientation. European Journal of Wood and Wood Products 76(3): 1087-1091.
5. Benthien, J.T., Ohlmeyer, M., Schneider, M., Stehle, T., 2017: Experimental determination of the compression resistance of differently shaped wood particles as influencing parameter on wood-reduced particleboard manufacturing. European Journal of Wood and Wood Products 76 (3): 937-945.
6. Boruszewski, P., Borysiuk, P., Mamiński, M., Czechowska, J., 2016: Mat compression measurements during low-density particleboard manufacturing. BioResources 11(3): 6009-6919.
7. Dziurka, D., Mirski, R., Dukarska, D., Derkowski, A., 2015: Possibility of using the expanded polystyrene and rape straw to the manufacture of lightweight particleboards. Maderas. Ciencia y tecnología 17 (3): 647-656.
8. Gao, L., Tang, Q., Chen, Y., Wang, Z., Guo, W., 2018: Investigation of novel lightweight phenolic foam-based composites reinforced with flax fiber mats. Polymer Composites 39 (6): 1809-1817.
9. Hunt, J. F., Leng, W., Tajvidi, M., 2017: Vertical density profile and internal bond strength of wet-formed particleboard bonded with cellulose nanofibrils. Wood and Fiber Science 49 (4): 1-11.
10. Lee, S.H., Lum, W.C., Zaidon, A., Fatin-Ruzanna, J., Tan, L.P., Mariusz, M., Chin, K.L., 2017: Effect of post-thermal treatment on the density profile of rubberwood particleboard and its relation to mechanical properties. Journal of Tropical Forest Science 29 (1): 93-104.
11. Maraghi, M.M.R., Tabei, A., Madanipoor, M., 2018: Effect of board density, resin percentage and pressing temperature on particleboard properties made from mixing of poplar wood slab, citrus branches and twigs of beech. Wood Research 63 (4): 669-681.
12. Monteiro, S., Martins, J., Magalhães, F., Carvalho, L., 2016: Low density wood-based particleboards bonded with foamable sour cassava starch: Preliminary Studies. Polymers 8 (10): 354.
13. Monteiro, S., Martins, J., Magalhães, F.D., Carvalho, L., 2018: Lightweight composites: Challenges, production and performance. In: Lignocellulosic Composite Materials (ed. Kalia, S.). Springer. Cham., Pp 293-322.

14. Monteiro, S., Martins, J., Magalhães, F.D., Carvalho, L., 2019: Low density wood particleboards bonded with starch foam-study of production process conditions. Materials 12 (12): 1975.

15. Parlin, N.J., Davids, W.G., Nagy, E., Cummins, T., 2014: Dynamic response of lightweight wood-based flexible wall panels to blast and impulse loading. Construction and Building Materials 50: 237-245.

16. Schneider, M., Stehle, T., Benthien, J.T., Ohlmeyer, M., 2018: Stiffness modelling particles in the core layer for the manufacturing of wood-reduced particleboard. European Journal of Wood and Wood Products 76 (3): 947-952.

17. Schulte, M., Frühwald, A., 1996: Some investigations concerning density profile internal bond and relating failure position of particleboard. Holz als Roh- und Werkstoff 54 (5): 289-294.

18. Shalbafan, A., Dietenberger, M.A., Welling, J., 2012a: Fire performances of particleboards continuously produced in a one-step process. European Journal of Wood and Wood Products 71 (1): 49-59.

19. Shalbafan, A., Luedtke, J., Welling, J., Fruehwald, A., 2013 properties of ultra-lightweight foam core particleboard: different core densities. Holzforschung 67 (2): 169-175.

20. Shalbafan, A., Luedtke, J., Welling, J., Thoemen, H., 2012 b: Comparison of core materials in innovative lightweight wood-based panels. European Journal of Wood and Wood Products 70 (1-3): 287-292.

21. Shalbafan, A., Tackmann, O., Welling, J., 2015: Using of expandable produce density particleboard. European Journal of Wood and Wood Products 74 (1): 15-22.

22. Sundquist, D.J., Bajwa, D.S., 2016: Dried distillers grains with solubles as multifunctional filler in low density wood particleboards. Industrial Crops and Products 89: 21-28.

23. Wang, S., Winistorfer, P.M., 2000: Fundamentals of vertical density profile in wood composites. Part II. Methodology of vertical density formation under dynamic conditions. Wood and Fiber Science 32 (2): 220-238.

24. Wong, E.D., Zhang, M., Wang, Q., Kawai, S., 1998: Effects of mat moisture and press closing speed on the formation of density profile and properties of particleboard. Journal of Wood Science 44 (4): 287-295.

25. Wong, E.D., Zhang, M., Wang, Q., Kawai, S., 1999: Formation of the density and its effects on the properties of particleboard. Wood Science and Technology 33 (4): 327-340.

Shupin Luo, Li Gao*, Wenjing Guo
Chinese Academy of Forestry
Research Institute of Wood Industry
No.1 Dongxiaofu, Haidian District
Beijing 100091
China
*Corresponding author: wojiushigl@126.com.

CONSIDERATION OF FOREST ECOSYSTEM SERVICES IN ENVIRONMENTAL MANAGEMENT ACCOUNTING

Miroslav Hájek, Pavla Vrabcová
Czech University of Life Sciences Prague
Czech Republic

ABSTRACT

The environmental management accounting aims at capturing economic and environmental benefits and it should include externalities too. The aim of the paper is to propose a methodological approach for how to include non-market forest ecosystem services in the environmental management accounting so that the information could be used in economic analyzes. For this purpose, it is necessary to identify information relevant to related costs, sales revenues and the value of non-production ecosystem services. It is possible to perform the financial analysis needed for decision making in forest management. In the University Forest Establishment, the rated value of non-market ecosystem services was 3.2 million EUR, and this value was estimated to be twice as much as the value of market ecosystem services. In the Forest Plant Židlochovice, the value of non-market ecosystem services was 0.4 million EUR. Profitability increased from 1.346 to 4.093 and from 1.181 to 3.492.

KEYWORDS: Ecosystem services, externalities, forestry enterprises, forest services, management accounting, valuation.

INTRODUCTION

In connection with the strategic international forestry documents, it is clear that increasing attention is being paid to forest ecosystem services and their development in response to the growing demand from the society (Costanza et al. 1997). In this context, consideration should be given to integrating ecosystem services into the decision-making process (Fisher et al. 2009, Kumar 2010, Filyushkina et al. 2016, Phan et al. 2017). There are pressures to provide timely information on the different aspects of their operations beyond those reflected in traditional financial and cost accounting methods (Burritt 2005, Schaltegger and Burritt 2010, Phan et al. 2017). One way to do this is to use environmental management accounting (EMA), which is a voluntary approach focused on economic and environmental benefits (Jasch 2003, Burritt 2004, Burritt and Saka 2006, Gale 2006). The concept of EMA was developed during the 1990s (Phan et al. 2017) as an emphasis on sustainable development accounting. Critics of this theory state

that organizations use environmental accounting only if they want to improve their financial performance or have the ambition to increase the sustainability of their business (Larrinaga-Gonzalez and Bebbington 2001, Springett 2003). However, the valuation of ecosystem services (Burritt 2004, Ninan and Inoue 2013, Sarkki and Karjalainen 2015) and their charging still remain a problem. Nevertheless, there are already some case studies on charging the forest ecosystem services (Jim and Chen 2009, Felardo and Lippitt 2016, Górriz-Mifsud et al. 2016).

Forestry has a long history of the environmental aspect (Smith and Heath 2004, Gustafsson et al. 2012). This is due to both a long and regular cycle of management (Elbakidze et al. 2013), and a number of environmental ecosystem services that are predominantly in the form of positive externalities in forestry (Myšáková et al. 2016). Unlike the market ecosystem services, most of non-market ecosystem services are often neglected and are normally not included in the environmental management accounting because they do not generate any sales (Jasch 2003).

As far as the non-market ecosystem services are concerned, from a private-ownership aspect, the wake theory is advocated in forestry (Glück 1982), i.e. that these ecosystem services are created in parallel with the wood-producing ecosystem services and therefore need not be supported. On the other hand, it is known that the demand for ecosystem services outweighs the supply (Robert and Stenger 2013).

Research in support of forest ecosystem services is primarily oriented on the public sector because if the forest owner is a state, a municipality, or another public entity interested in supporting these functions, one can refer to managerial accounting including positive externalities too (Papaspyropoulos et al. 2012). In such a case, the environmental management accounting may be an important tool to support all forest ecosystem services. In the case of private forest owners or private forest enterprises, it represents a voluntary tool or a data source for environmental reporting or for sustainable development reporting (Papaspyropoulos et al. 2012).

However, this may also be an area for changing the forestry policy towards charging the non-reproductive forest ecosystem services (Bartczak and Metelska-Szaniawska 2015, Roesch-McNally and Rabotyagov 2016), because the financial accounting system only reflects internalized positive and negative externalities which are subject to market or government regulation (Jasch 2003) according to the national and international accounting standards and frameworks (USGAAP, IAS/IFRS). These are issues of paying for ecosystem services. According to Knoot et al. (2015), paying for ecosystem services offers a potential financial benefit to landowners in exchange for active forest management. Given their non-timber focus, such payments might be particularly attractive to those landowners who do not participate in typical forestry programs (Knoot et al. 2015).

The aforementioned forestry research has not been completed yet, not only because the methods for valuating all non-market ecosystem services are still developing, but also because they have to be incorporated into the management accounting and used in the financial analyzes. It is important to discuss a solution, which comprehends all of the forestry ecosystem services and incorporate them in a system of environmental management accounting, so that forest-based ecosystem services can be included and managers have correct data for their decision-making.

The aim of the paper is to propose a methodological approach for how to include the non-market forest ecosystem services into the environmental management accounting so that the data could be used in the economic analyzes. The partial aim is to apply the proposed method to a selected practical example in forestry.

MATERIAL AND METHODS

In order to solve the objectives of the paper, a research was conducted, focusing on the application of environmental management accounting in forestry. So far, this issue has not been addressed in the scientific literature, as it cannot be easily applied in forestry in comparison to industrial enterprises. The presented methodology is based on research that addressed the use of environmental management accounting in view of the long production time in forestry and a number of ecosystem services that are not charged. The subject of the research was not the methodology of valuation of these services.

First, it is necessary to answer the question of whether environmental management accounting is the most appropriate basis for decision making in forestry. Forestry is closely linked to environment protection. It is an industry that uses the forest as a means of production, outputs from forestry are used by the whole society and their importance is growing. Therefore, it is advisable to focus on environmental management accounting tailored to monitor the environmental aspects of production.

Environmental management accounting is closely related to environmental management systems and tools for which many governments provide land managers with the targeted support. In using the environmental management accounting, it is assumed that all linkages between forestry and the environment will be considered. These are not only inputs and outputs, including waste and negative externalities, but also negative effects reflecting in higher costs, both of compensation and income (Rikhardsson et al. 2005). At the same time, the general benefits should be met, i.e. increased efficiency of materials and energy use, mitigation of the impact of corporate activities, products and services on the environment, reduced environmental risks and improved business performance (Jasch 2003).

Forest ecosystem services

It is clear that there are many of them in the context of forest and forestry (Filyushkina et al. 2016). The major focus is on timber that is linked most closely to forest ecosystems and forest-related communities and industries, but it extends to fuel and pulpwood as well. According to CICES (Common International Classification of Ecosystem Services) classification, ecosystem services are divided as outlined in Tab. 1. For the final ecosystem services, CICES describes them using a five-level hierarchical structure: section (e.g. provisioning), division (e.g. nutrition), group (e.g. terrestrial plants and animals for food), class (e.g. crops), and class type (e.g. wheat).

Another important issue in the classification of services is the distinction between private and public ecosystem services. Public services are characterized by non-rivalry and non-excludability. Non-rivalry implies that the use/consumption of a service by one individual does not reduce the availability thereof for another individual, for example, climate regulation. This view is based on the definition of externalities, i.e. costs that do not pass through the market and are not reflected in corporate financial indicators (Mäler 1991).

Tab. 1: Systematization of forest production and non-production functions in the concept of forest ecosystem services.

Production (goods and services)		
Production functions	Non-production functions, forest ecosystem services	
	Ecological functions	Social functions
Services	Basic services	Cultural services
Source of food, drinking water, building material, energy, genetic material	Soil, oxygen, carbon bonding, climate regulation, nutrient cycle, pollination	Recreation, aesthetic and spiritual experiences, spirituality, social functions, knowledge and learning, artistic inspiration, health-hygienic functions
Goods	Regulatory services	
Wood, game, non-timber functions	Water treatment, soil erosion prevention, air purification, waste assimilation, conservation of biological conditions	

Source: Ninan and Inoue (2013), Wallace (2007), own elaboration.

Forest management acts as a regulator or producer of ecosystem services, and is based on forest functions as a source of these services. Although there is a general theory by Glück (1982) that forest management is a wood-producing ecosystem service and other ecosystem services are created in parallel, in view of the development of forestry policy and the demand from the society, it is clear that this wood-producing ecosystem service may not be the key goal of forest management (Hájek and Lípa 2015). By incurring the costs of other than wood-producing ecosystem services in forestry, these environmental management costs can be assigned to different domains according to the environmental management accounting structure (Hájek 2013), such as carbon sequestration in air and climate protection.

For the choice of ecosystem services, we shall further deal with, a regional aspect that is important because ecosystem services, i.e. forest services used and supported, depend on habits and laws in individual countries or regions (Šišák 2013). At the same time, however, some ecosystem services are clearly of global character such as carbon sequestration.

The paper deals with the following ecosystem services: soil-protective, hydrological, carbon sequestration, health-hygienic, cultural-educational. This selection of ecosystem services needs to be done in specific cases in order to choose the most important ecosystem services provided or preferred in the given region at the time. In this particular case, the choice corresponds to the conditions of the Czech Republic.

Accounting in physical units

The commonly known accounting scheme in physical units can be supplemented by ecosystem services (see Tab. 3). However, this is not just about the positive externalities, as mentioned in Papaspyropoulos et al. (2012), but also about ecosystem services provided by forestry, which are linked to set objectives (priorities). This is why the main product/output in urban forests can be health-hygienic and cultural-educational ecosystem services (Hájek et al. 2012, Hájek and Lípa 2015).

It is also essential to distinguish between the low use of ecosystem services or the higher use where the non-rival becomes the rival (Merlo et al. 2000, Fisher et al. 2009) and whether it is the main product or side product according to EMA's classification. Next here comes a question whether certain ecosystem services should be considered as positive externalities.

In the EMA methodology guidance, it is further stated that the terms of Inputs and Outputs do not include capital items such as land. In forestry, however, land and particularly soil quality is a key input from which the quantity and quality of outputs are derived. On the other hand,

the quality of forest soil is a constant quantity. Therefore, it is important to mention this in the section of accounting in physical units, but it will not be included in the input / output analysis itself (Tab. 3).

Tab. 3: Inputs and Outputs.

Input in kg, GJ, l / period	Output in kg (or other / period)
Raw materials – tree seeds	Main product – wood-producing ecosystem function – raw wood, chips, timber, wood products and/or other ecosystem services if prioritized in forestry (e.g. health-hygienic, cultural-educational in urban forests)
Excipients – chemicals used in forest nurseries and in protecting young cultures against biotic agents	By-product – other ecosystem services if actively supported by forestry but not the main purpose of forest management
Operating substances – substances used to ensure the operation of administrative and production activities	Positive externalities – ecosystem services that arise spontaneously and are not associated with costs or sales
Energy	Waste
Fuel (forestry machines, harvesters, forwarders, timber transport units, timber loaders, passenger transport)	Common waste from administrative buildings
Electricity (administrative work, forest nurseries, sawmill)	Seedlings that failed
Biomass (logging residues, sawdust, bark)	Small wood (logging residues)
Water (municipal water, groundwater, surface water)	Waste water – in administrative buildings (amount of waste water, heavy metals, COD, BOD5)
	Emissions to air – from cultivation and logging machinery and from vehicles (CO_2, CO, NO_x, SO_2, dust, NH_4, volatile org. substances)
	Others – e.g. negative externalities – impact of logging machines on soil and vegetation, noise

Source: own

If we neglect the land as a specific capital, tree seeds and chemicals for the protection of young trees against biotic factors are the inputs. Fuel is also important because forestry operates on large sites. Specific is the view of water, which is mainly used for irrigation in forest nurseries (except in administrative buildings) throughout the forest growing period; however, water is taken from the air (precipitation, humidity) similarly to agriculture, unless irrigation is used. Essential for the ecosystem services are outputs. These are divided into:

i) The main product resulting from the objective or from the management priorities, as a rule the wood-production ecosystem service;

ii) By-products are other ecosystem services that are supported by forestry but are not of a priority character;

iii) Positive externalities are ecosystem functions that are not target-supported and emerge spontaneously with the wood-producing or other ecosystem services.

Monetary valuation

Forest management is similar to public enterprises, because public enterprises are established not only to generate a surplus, but also or mainly to meet social requirements. As a rule, public

enterprises produce worse operating results as compared with the private ones because they often set out to provide also services (positive externalities) for which they do not get paid directly or have to cover the costs of ecosystem services from their own, i.e. public, resources. The outcome is that public enterprises tend to have higher environmental costs, but revenues from the timber-production ecosystem services are no higher, and may be lower, compared with the private enterprises (Hájek and Lípa 2015). It can be stated that the public enterprises internalize the externalities (positive externalities) to a higher extent than the private ones, but at the expense of their profits (Zhang 2005). In spite of the fact that the environmental accounting methodology is well established and applied in different sectors, it is appropriate to consider the specific criteria relevant to forestry. When monitoring, in the context of environmental management accounting, the forest ecosystem services can be broken down into individual pillars, which are economic services, environmental services and social services (Ševčík et al. 2014). The economic part includes forest ecosystem services such as timber-production, game management, or other services passing through the market and these data are reported routinely. Other ecosystem services are non-market ecosystem services and it is necessary to use an appropriate method for their valuation (Vincent and Binkley 1993, Šišák 2013) if we want to include them in decision-making tools. In the context of environmental management accounting, corresponding costs and sales (subsidies) in the environmental areas are monitored (Jasch and Lavicka 2006). In connection with the forest ecosystem services, following data can be monitored.

Costs and sales that are allocated to ecosystem services are identified on the basis of annual income statements (Krieger 2001). It is important to assign costs to individual ecosystem services. These costs are related to the targeted support of these services (intensification) (see accounting in physical units). They are included in the main products or by-products. For private forest enterprises, these costs are generally zero or negligible because the ecosystem functions are supported in parallel with the production ecosystem functions in the sense of wake theory (Glück 1982). Another approach would be to budget the total costs of all ecosystem services. In that case, the ratio between them would have to be established, probably using an expert method, or a proportion corresponding to the priorities of individual ecosystem services. Furthermore, this ratio should correspond to the forest category in the sense of what is the main output, whether the wood-producing ecosystem service or another service, e.g. recreational (in the case of urban forests). This approach was not used for a large proportion of subjective assessments. Where no costs or revenues can be assigned, externalities in question are positive. For CBA (Cost Benefit Analysis) purposes, all ecosystem services are valued in the last row. This value is not reflected in the accounting and is calculated based on the methodology chosen.

There are a number of methodologies for valuing forest ecosystem services, which are based on different approaches. For the purposes of this article, methodological approaches of the Czech University of Life Sciences Prague were used for the valuation of forest-based ecosystem services dwelling on the society demand for forest functions. This methodology was selected for practical verification of the proposed methodological approach. The ambition of this paper is not to compare individual ecosystem valuation methodologies, but rather to suggest ways for how to include major non-wood ecosystem services in the decision-making process and how to use this information in the financial analysis. The system for evaluating the socio-economic importance of forest services for the society was derived for the conditions of the Czech Republic and the methodology was approved by the Ministry of Agriculture (Šišák 2013).

The socio-economic value of the forest services related to soil erosion control in stony and steep localities (intro-skeleton erosion) was derived on the basis of extra costs required for reforestation of the land including importing new soil and stabilizing the soil in the given plots. The socio-economic value of protection against eroded soil deposits in water streams and reservoirs was calculated using the costs of removing the soil deposits from watercourses and reservoirs.

The socio-economic valuation of the hydrological forest services was based on the "costs-of-prevention approach". The costs were calculated for technical measurements such as retention reservoirs, other constructions and equipment, which could be substituted in place of the hydrological forest services, which reduce and attenuate maximum runoff to watercourses, enhancing low-flows in watercourses and reducing the concentration of nitrogen oxides in watercourses and reservoirs.

According to (Myšáková et al. 2016) forests reduce greenhouse gas emissions and the level of pollution, increase security of supplies, and strengthen economic growth, competitiveness and regional development. The air protection forest services, especially CO_2 sequestration, have similar socio-economic characteristics as the hydrological and soil protection forest services. They influence market relations as the trade with CO_2 permits development of market.

The mean socio-economic value of non-market forest production services for the society was experimentally derived from the shadow market values (current prices) of main non-wood forest products collected by forest visitors.

An expert method was based on the comparison of the mean general socio-economic importance of health-hygienic forest services with the mean general socio-economic importance of timber production forest services. Thirty-nine Czech experts in forest services from all important research institutions in the Czech Republic were questioned about their preferences regarding the relative socio-economic importance of the respective services and timber production service. The resulting expert ratio was 0.33 (Šišák 2013). The mean general value of health-hygienic forest services was derived from the timber production forest service value by this rate.

For the expression of the socio-economic value of cultural-educational environmental forest services, the expert approach was employed using a comparative method, i.e. comparing their general mean socio-economic importance to the general mean socio-economic importance of timber production service. It was the same procedure as used in the case of health-hygienic forest services. The resulting ratio was 0.28 (Šišák 2013) for the Czech Republic and it was used for expressing the mean general socio-economic value of the cultural-educational forest services in the Czech Republic. Local differentiation was based on landscape zoning that represents different qualities and grades of nature conservation.

Profitability

The assessment is based on a table of environmental management accounting data. It is necessary to consider that costs and revenues related to the non-production ecosystem services are normally included in the financial statements, but the value of these services is usually not reflected there (Hájek 2013). If the value of these services is used in the analyses on the part of benefits (revenues), then it is necessary to have a corresponding reduction of this value in the revenues reported to avoid duplicate inclusion of some items.

The purpose of profitability indicators is to evaluate the success of achieving the organization's goals, considering the resources invested. Profitability is assessed in relation to costs and expenses and is analyzed against assets to determine how effective the company is in the deployment of assets for generating sales and/or profit.

In the financial analysis, as an example, profitability (P_C) is shown and calculated using conventional accounting (Kocmanová et al. 2013, Kojola et al. 2012):

$$P_c = \frac{revenues}{costs} \tag{1}$$

And corrected profitability (P_{CC}) is calculated using environmental management accounting which includes the value of non-production ecosystem services (V_{ES}) reduced by the revenues

attributable to these services (R_{ES}) (see monetary expression of EMA). Costs also include costs associated with non-productive ecosystem services (C_{ES}):

$$P_{cc} = \frac{revenues + V_{ES} - R_{ES}}{costs + C_{ES}} \qquad (2)$$

Reporting

Thanks to the process approach, environmental management accounting provides primarily the information on cost items related to environmental issues, but also a set of material and other system flows. In the form of environmental reporting, EMA-related reports are provided to relevant bodies. Environmental reporting is further specified in ISO 14063 – Environmental Management – Environmental Communication and EMAS (Eco-Management and Audit Scheme). Environmental reporting has evolved over time into sustainability reporting (Hahn and Kühnen 2013). In the growing scientific debate on sustainable forest management, the development of appropriate assessment tools plays a key role (Goio et al. 2008). The process of environmental reporting enables businesses to communicate better with the stakeholders. The most famous international activity is in the area of environmental reporting, The Global Reporting Initiative (GRI), which focuses on the standardization of Sustainable Development Reports (Papaspyropoulos et al. 2012).

Verification of practical use

The data is applied in two forest enterprises. Enterprises were chosen, in which the wood-producing ecosystem function is not a primary goal and a targeted support of some other functions is expected. The first of them was the University Forest Establishment in Kostelec nad Černými Lesy (UFE) and the second one was the Forest Plant Židlochovice (FPZ).

UFE was established under Act No. 111/1998 Coll., on Czech universities, as a special-purpose facility within the organizational structure of the Czech University of Life Sciences in Prague (CULS) in accordance with the position and program specified by the CULS Statute. Its main activity focuses on the material and human resources for learning and practical training, students' exercises, excursions, operation of practical demonstrations based within the premises of the facility and the provision of boarding and lodging services for CULS students and teachers.

The Forest Plant Židlochovice (FPZ) manages a total of 22,500 hectares of state-owned forests. The average percentage of forest land in the area covered by FPZ is only 15% due to the intensively farmed agricultural land. As regards the whole forest area, timber production is the most important output for the Forest Plant Židlochovice, but there is also the production of cultural-educational services (nature conservation forest service) and health-hygienic services (recreational service) although the benefits in conventional accounting only include timber production and hunting and game management (Lien et al. 2007).

RESULTS AND DISCUSSIONS

The results of research at the University Forest Establishment in Kostelec nad Černými Lesy (UFE) and the Forest Plant Židlochovice (FPZ) are found below. The results are based on available data available in selected forestry companies. These are data that are tracked outside the normal accounting system. It is therefore not possible to obtain these data for all businesses.

University Forest Establishment in Kostelec nad Černými Lesy

Item costs and prevention are based on actual (additional) costs of support to the ecosystem services concerned (see Tab. 4).

Tab. 4: Non-market ecosystem functions of UFE in thousands of EUR per year.

Categories of environmental costs and revenues	Ecosystem services				
	Soil-protective	Hydrological	Carbon sequestration	Health-hygienic	Cultural-educational
Environmental costs	0	0	0	144.5	31.0
Environmental revenues	0	0	0	0	65.6
Valuation of ecosystem services	1.0	432.0	241.6	691.8	1,673.0

Source: own

In the case of cultural and educational services, the costs in question are costs associated with the provision of teaching students. As to the health-hygienic services, the costs in question are primarily those associated with the maintenance of roads that serve recreation and forestry production. It is therefore necessary to avoid double accounting. In the statement of assets and liabilities, we can include an increase in the economic value of forest assets by the capitalized value of ecosystem services, which is 170 thousand EUR.

In the "Income Statement", all costs and revenues are reflected. However, the value of ecosystem services is not stated and amounts to 3.4 thousand EUR, which requires a corresponding reduction in revenues of 65.6 thousand EUR. After this adjustment of financial statements, we can proceed to the financial analysis itself. The selected indicator of cost profitability in this case – formula (1) will increase from 1.346 (classic profitability) to 4.093 (corrected profitability, formula 2), i.e. an increase of 304%.

Forest Plant Židlochovice

In FPZ, the costs and sales related to each of ecosystem services were not measured, but the ones related to multifunctional management were measured instead (see Tab. 5). Since the revenues related to the individual specified ecosystem services were not demonstrable, the values given correspond to the loss of income related to timber-production and only one value for all ecosystem services is provided.

In the statement of assets and liabilities, we can include an increase in the economic value of forest assets by the capitalized value of ecosystem services, which represents the amount of 587 thousand EUR.

In the "Income Statement", all costs and sales are reflected; however, the value of ecosystem services is not given and it amounts to 11,709 thousand EUR, which the authors have to reduce by the corresponding revenues, i.e. by – 34 thousand EUR.

Tab. 5: Non-market ecosystem functions of the Forest Plant Židlochovice in thousands of CZK per year.

Categories of environmental costs and revenues	Ecosystem services				
	Soil-protective	Hydrological	Carbon sequestration	Health-hygienic	Cultural-educational
Environmental costs	152.0				
Environmental revenues	−34.0				
Valuation of ecosystem services	12.0	2,381.0	950.0	3,289.0	4,727.0

Source: own

After the adjustment of financial statements, to take account of the ecosystem services, the authors can proceed to the financial analysis itself. The selected indicator of profitability in this case increased from 1.181 to 3.492, i.e. an increase of 195%. It is an example of multifunctional economy and that is why the costs and the revenues for all ecosystem services are combined (Kovalčík et al. 2012).

Traditional forest management and its related market opportunities often yield additional public benefits; for example, timber harvesting can improve forest health and yield financial returns that incentivize maintaining forest cover (Knoot et al. 2015). The proposed approach and practical results confirm that it is possible to integrate the forest ecosystem services into environmental management accounting (Maroto et al. 2013). The general methodology of this approach can be used in the case of monitoring the costs and benefits of environmental services (Prabhu et al. 1998). It is suggested that the use of such approaches to multifunctional forest management, or fostering non-traditional ecosystem services, should be applied and supported mainly by public forest owners (Maroto et al. 2013).

When analyzing the costs and revenues related to ecosystem services, the fundamental issue is that a substantial part of accounting for ecosystem services has been created on the basis of wake theory, which was originally based on the priority of the timber-producing ecosystem function (Dietrich 1941). Multi-functionality and the recognition of trade-offs have promoted silvicultural practices based on the continuous tree canopy coverage, uneven aged and mixed species forests which are considered to be more suitable in achieving soil conservation together with wood production (Papenfuß 2014). Other ecosystem functions like sports, leisure, ecology, landscape, habitats have been rather easily accepted because, at least some of them have followed in the "wake" of the soil conservation measures (Vincent and Binkley 1993, Bernatzki 2012). However, the most recent developments in accounting for ecosystem services show an increasing conflict amongst several emerging functions (e.g. sports versus conservation) (Merlo and Briales 2000). Another view is that forests are considered to be adequately managed for recreation if they are managed by following the principles of close-to-nature forest management (Jay and Schraml 2013).

Nowadays the importance of forests for the environment is estimated more highly than their economic value for timber production (Bernatzki 2012, Hájek and Lípa 2015). The specific share depends on all ecosystem services, which the forest in question performs. Forest services are differentiated by their diverse socio-economic essence and impact on the society, how they are used in the society and by the availability of input data.

It is important to include data obtained through using environmental management accounting in completing financial statements and when making operational and strategic decisions. Problems may occur in the annual calculation of the value of non-market ecosystem services, but it can be assumed that this value does not show significant annual variation and it is therefore possible to monitor any annual increase or decrease based on the factor that will be chosen. For example, cultural and hygienic services may vary mainly depending on the flow of visitors to the forests (Hillman and Keim 2001). Therefore, it would be appropriate to monitor the trend of the flow of visitors annually and to use the data to correct the value of this service.

Taking the ecosystem services on the balance sheet into account, we should reflect an increase in their value in the valuation of assets. Subsequently, the value of ecosystem services in the financial analysis should be considered (Roman et al. 1999). Current developments imply that the importance of non-production ecosystem services will continue to grow and hence the benefits expressed by the value of these functions will grow too (Schmithüsen 2007).

CONCLUSIONS

For enterprises in forestry, the environmental management accounting includes forest ecosystem services. The valuation of market and non-market ecosystem services can be included in costs and revenues. Based on the information obtained by this approach, it is possible to prepare a financial analysis that also takes environmental and social benefits of ecosystem services into account.

The example of two enterprises (UFE and FPZ) clearly shows how important it is to consider the value of all forest ecosystem services. In UFE, the profitability will increase from 1.346 to 4.093 and in FPZ, it will increase from 1.181 to 3.492.

Ecosystem and services of the forest have a higher value than the market ecosystem services and it is, therefore, important to consider their value and to make decisions based on economic analyses including the valuation of all ecosystem services of the forest. It can be expected that the importance of ecosystem services of the forest will grow in the future, particularly in the non-productive services, based on the increasing social demand. In this context, it can be also expected that economic calculations considering all ecosystem services will become increasingly important.

ACKNOWLEDGMENTS

REFERENCES

1. Bartczak, A., Metelska-Szaniawska, K., 2015: Should we pay, and to whom, for biodiversity enhancement in private forests? An empirical study of attitudes towards payments for forest ecosystem services in Poland. Land Use Policy 48: 261-269.
2. Bernatzky, A., 2012: Tree ecology and preservation (Vol. 2). Elsevier, 366 pp.
3. Burritt, R.L., 2004: Environmental management accounting: roadblocks on the way to the green and pleasant land. Business Strategy and the Environment 13(1): 13-32.
4. Burritt, R.L., 2005: Challenges for environmental management accounting. In: Implementing environmental management accounting: status and challenges. Eco-efficiency in industry and science (eds. Rikhardsson, P.M., Bennett, M., Bouma, J.J., Schaltegger, S.). Pp 19-44, Vol 18. Springer, Dordrecht.
5. Burritt, R.L., Saka, C., 2006: Environmental management accounting applications and eco-efficiency: case studies from Japan. Journal of Cleaner Production 14(14): 1262-1275.
6. Costanza, R., d'Arge, R., De Groot, R., Farber, S., Grasso, M., Hannon, B., Raskin, R.G., 1997: The value of the world's ecosystem services and natural capital. Nature 387(6630): 253-260.
7. Dietrich, V., 1941: Forestry Business Administration, Vol. III. Income statement, Berlin, 266 pp.
8. Elbakidze, M., Andersson, K., Angelstam, P., Armstrong, G.W., Axelsson, R., Doyon, F., Pautov, Y., 2013: Sustained yield forestry in Sweden and Russia: how does it correspond to sustainable forest management policy. Ambio 42(2): 160-173.

9. Felardo, J., Lippitt, C.D., 2016: Spatial forest valuation: The role of location in determining attitudes toward payment for ecosystem services policies. Forest Policy and Economics 62: 158-167.
10. Filyushkina, A., Strange, N., Löf, M., Ezebilo, E.E., Boman, M., 2016: Non-market forest ecosystem services and decision support in Nordic countries. Scandinavian journal of forest research 31(1): 99-110.
11. Fisher, B., Turner, R.K., Morling, P., 2009: Defining and classifying ecosystem services for decision making. Ecological Economics 68(3): 643-653.
12. Gale, R., 2006: Environmental management accounting as a reflexive modernization strategy in cleaner production. Journal of Cleaner Production 14(14): 1228-1236.
13. Glück, P., 1982: The misery of the wake theory. Internationaler Holzmarkt 73: 15-18.
14. Goio, I., Gios, G., Pollini, C., 2008: The development of forest accounting in the province of Trento (Italy). Journal of Forest Economics 14(3): 177-196.
15. Górriz-Mifsud, E., Varela, E., Piqué, M., Prokofieva, I., 2016: Demand and supply of ecosystem services in a Mediterranean forest: computing payment boundaries. Ecosystem Services 17: 53-63.
16. Gustafsson, L., Baker, S.C., Bauhus, J., Beese, W.J., Brodie, A., Kouki, J., Neyland, M., 2012: Retention forestry to maintain multifunctional forests: a world perspective. BioScience 62(7): 633-645.
17. Hahn, R., Kühnen, M., 2013: Determinants of sustainability reporting: a review of results, trends, theory, and opportunities in an expanding field of research. Journal of Cleaner Production 59: 5-21.
18. Hájek, M., Pulkrab, K., Hyršlová, J., 2012: Forestry externalities in the environmental management accounting system. Problems of Management in the 21st Century, 5 pp.
19. Hájek, M., 2013: Problematika externalit při využití environmentálního manažerského účetnictví v lesním hospodářství. (The issue of externalities and the use of environmental management accounting in forestry). Zprávy lesnického výzkumu 58(3): 280-2085 (in Czech).
20. Hájek, M., Lípa, J., 2015: Evaluation of ecosystem services from urban forests in the city of Prague. Forestry Journal 61(1): 52-57.
21. Hillman, A.J., Keim, G.D., 2001: Shareholder value, stakeholder management, and social issues: What's the bottom line? Strategic Management Journal 22(2): 125-139.
22. ISO 14063, 2006: Environmental management – Environmental communication – Guidelines and examples.
27. Jasch, C., 2003: The use of environmental management accounting (EMA) for identifying environmental costs. Journal of Cleaner Production: 11(6): 667-676.
28. Jasch, C., Lavicka, A., 2006: Pilot project on sustainability management accounting with the Styrian automobile cluster. Journal of Cleaner Production 14(14): 1214-1227.
29. Jay, M., Schraml, U., 2013: Managing city forests for or in spite of recreation? Perspectives of forest managers. European Journal of Forest Research 132(1): 93-105.
30. Jim, C.Y., Chen, W.Y., 2009: Ecosystem services and valuation of urban forests in China. Cities 26(4): 187-194.
31. Knoot, T.G., Rickenbach, M., Silbernagel, K., 2015: Payments for ecosystem services: Will a new hook net more active family forest owners? Journal of Forestry 113(2): 210-218.
33. Kocmanová, A., Hřebíček, J., Dočekalová, M., Hodinka, M., Hornungová, J., Chvátalová, Z., Trenz, O., 2013: Měření podnikové výkonnosti [Measuring of corporate performance]. Littera, Brno (in Czech), 252 pp.

34. Kojola, S., Ahtikoski, A., Hökkä, H., Penttilä, T., 2012: Profitability of alternative management regimes in Scots pine stands on drained peatlands. European Journal of Forest Research 131(2): 413-426.

35. Kovalčík, M., Sarvašová, Z., Schwarz, M., Moravčík, Z., Oravec, M., Lásková, J., Tutka, J., 2012: Financial and socio-economic impacts of nature conservation on forestry in Slovakia. Journal of Forest Science 58(10): 425-435.

36. Krieger, D.J., 2001: Economic value of forest ecosystem services: a review. The Wilderness Society, Washington, 40 pp.

37. Kumar, P., 2010: The economics of ecosystems and biodiversity: ecological and economic foundations (ed. Pushpam Kumar). Earthscan. London & Washington, 456 pp.

39. Larrinaga-Gonzalez, C., Bebbington, J., 2001: Accounting change or institutional appropriation? A case study of the implementation of environmental accounting. Critical Perspectives on Accounting 12(3): 269-292.

40. Lien, G., Størdal, Z., Baardsen, S., 2007: Technical efficiency in timber production and effects of other income sources. Small-Scale Forestry 6(1): 65-78.

41. Mäler, K.G., 1991: National accounts and environmental resources. Environmental and Resource Economics 1(1): 1-15.

42. Maroto, C., Segura, M., Ginestar, C., Uriol, J., Segura, B., 2013: Sustainable forest management in a Mediterranean region: social preferences. Forest Systems 22(3): 546-558.

43. Merlo, M., Briales, E.R., 2000: Public goods and externalities linked to Mediterranean forests: economic nature and policy. Land Use Policy 17(3): 197-208.

44. Merlo, M., Milocco, E., Panting, R., Virgilietti, P., 2000: Transformation of environmental recreational goods and services provided by forestry into recreational environmental products. Forest Policy and Economics 1(2): 127-138.

46. Myšáková, D., Jáč, I., Petrů, M., 2016: Investment opportunities for family businesses in the field of use of biogas plants. E&M Economics and Management, Business Administration and Management 19(4): 19-32.

47. Ninan, K.N., Inoue, M., 2013: Valuing forest ecosystem services: what we know and what we don't. Ecological Economics 93: 137-149.

48. Papaspyropoulos, K.G., Blioumis, V., Christodoulou, A.S., Birtsas, P.K., Skordas, K.E., 2012: Challenges in implementing environmental management accounting tools: the case of a nonprofit forestry organization. Journal of Cleaner Production 29-30: 132-143.

49. Papenfuß, U., 2014: How (should) public authorities report on state-owned enterprises for financial sustainability and cutback management - a new quality model. Public Money and Management 34(2): 115-122.

50. Phan, T.N., Baird, K., Su, S., 2017: The use and effectiveness of environmental management accounting. Australasian Journal of Environmental Management 24(4): 355-374.

51. Prabhu, R., Colfer, C., Shepherd, G., 1998: Criteria and indicators for sustainable forest management: new findings from CIFOR's forest management unit level research (Rural Development Forestry Network Paper (ODI) No. 23a, 20 pp), Rural Development Forestry Network, UK.

52. Rikhardsson, P.M., Bennett, M., Bouma, J.J., Schaltegger, S. (Eds.), 2005: Implementing environmental management accounting: Status and challenges (Vol. 18). Springer, Science and Business Media, Pp 19-44.

53. Robert, N., Stenger, A., 2013: Can payments solve the problem of undersupply of ecosystem services? Forest Policy and Economics 35: 83-91.

54. Roesch-McNally, G.E., Rabotyagov, S.S., 2016: Paying for forest ecosystem services: voluntary versus mandatory payments. Environmental Management 57(3): 585-600.

55. Roman, R.M., Hayibor, S., Agle, B.R., 1999: The relationship between social and financial performance: Repainting a portrait. Business and Society 38(1): 109-125.
56. Sarkki, S., Karjalainen, T.P., 2015: Ecosystem service valuation in a governance debate: Practitioners' strategic argumentation on forestry in northern Finland. Ecosystem Services 16: 13-22.
57. Schaltegger, S., Burritt, R.L., 2010: Sustainability accounting for companies: Catchphrase or decision support for business leaders? Journal of World Business 45(4): 375-384.
58. Schmithüsen, F., 2007: Multifunctional forestry practices as a land use strategy to meet increasing private and public demands in modern societies. Journal of Forest Science 53(6): 290-298.
59. Smith, J.E., Heath, L.S., 2004: Carbon stocks and projections on public forestlands in the United States. Environmental Management 33(4): 433-442.
60. Springett, D., 2003: Business conceptions of sustainable development: A perspective from critical theory. Business Strategy and the Environment 12(2): 71-86.
61. Ševčík, M., Hájek, M., Mikulková, A., 2014: Specifics in the introduction of sustainability reporting by companies in the forestry sector. Journal of Forest Science 60: 226-235.
62. Šišák, L., 2013: Differentiated valuation of forest services by their relationships to the market and its implementation in the Czech Republic. Socio-economic Analysis of Sustainable Forest Management. Czech University of Life Sciences, Faculty of Forestry and Wood Sciences, Prague, Pp 116-122.
63. Vincent, J.R., Binkley, C.S., 1993: Efficient multiple-use forestry may require land-use specialization. Land Economics 69(4): 370-376.
64. Wallace, K.J., 2007: Classification of ecosystem services: problems and solutions. Biological conservation 139(3-4): 235-246.
65. Zhang, Y., 2005: Multiple-use forestry vs. forestland-use specialization revisited. Forest Policy and Economics 7(2): 143-156.

MIROSLAV HÁJEK
CZECH UNIVERSITY OF LIFE SCIENCES
DEPARTMENT OF FOREST TECHNOLOGIES AND CONSTRUCTION
PRAGUE
CZECH REPUBLIC

PAVLA VRABCOVÁ*
CZECH UNIVERSITY OF LIFE SCIENCES
FACULTY OF FORESTRY AND WOOD SCIENCES
DEPARTMENT OF WOOD PROCESSING AND BIOMATERIALS
KAMÝCKÁ 1176, PRAGUE 6 – SUCHDOL
165 21, PRAGUE
CZECH REPUBLIC
*Corresponding author: vrabcovap@fld.czu.cz

ALTERNATIVE WOOD SPECIES FOR PLAYGROUNDS

WOOD FROM FRUIT TREES

Candan Kus Sahin, Busra Onay
Suleyman Demirel University
Isparta, Turkey

ABSTRACT

A number of orchard woods have been investigated for suitability in the playgrounds, in the view of responders. In this sense, photos were taken of the specially prepared samples as stimuli, and there were three different groups of respondents. It was observed that the participants were effective in terms of age grouping and material preferences. For group A and C, majority of the participants preferred wooden elements for playground material. However, the majority of participants in group B (50.5%) preferred plastic elements, followed by wooden (31.5%), and then metal (18.0%). Moreover, it was seen that the most significant factors for selection of material for a playground should be safety for both Group A (79%), and C (76.5%), whereas it was aesthetic appearance, for group B (71%). Similar results were found for color properties of wood — the majority of participants of all three groups preferred light colored wooden elements in playgrounds. The results for the aesthetic preferences of wood species judged one-by-one and judged together received similar results. The preference scores for fig wood (*Figus canica*) is significantly higher than for other wood species, while "wood color" and "aesthetic appearance" are reliable positive predictors to aesthetic preferences.

KEYWORDS: Children playground, wood, hardness, fruit-trees, fig, mulberry, apple, apricot, plum.

INTRODUCTION

The playground design and equipment are important to keep children happy while still developing their learning abilities. These should be developed in order to suit different age groups of children at different stages of learning. The health benefits of physical activity in children are predominantly noted in the amelioration of risk factors for disease, avoidance of weight gain, achieving a peak bone mass and mental well-being. However, it was concluded that for children ages 0–4, climbers (40%) had the highest accident incidence rates, followed by slides (33%). Moreover, for children ages 5–14, climbing equipment (56%) had the highest incidence

rates, followed by swings (24%), respectively (Tinsworth and McDonald 2001). Furthermore, it was concluded that most injuries on public playground equipment were associated with climbing equipment (53%), swings (19%), and slides (17%) but falls to the ground surface was a contributing factor in 79% of all injuries (Tinsworth and McDonald 2001).

As a result, they tend to seek out alternative play areas, which may be very unsafe. At the present time, wood has been considered as environmentally friendly material that can be used safely in many specific areas including children's playgrounds. Wood species typically show many advantages over other materials. The wood is a natural material that has an aesthetic appearance and the natural color properties are specific to its own characteristics. Moreover, wood can offer a great range of forms from curved glue-laminated structured members to carved relief pieces. This is due to easy cut and join, and it contrasts with almost any other construction materials that would be difficult to use (i.e., steel, block, concrete). Hence, many kinds of wood-based elements can be manufactured and utilized in city neighborhoods, gardens, parks and playgrounds.

Forests no doubt serve as a source of life for the forest-based industries worldwide. However, due to the shrinking forest areas those industries are facing a wood-shortage problem. There is a need for research into improve durability and use of alternative raw materials for the production of wood-based elements due to the anticipated shortages in the supply of raw materials for the wood-based material industry. There is increasing interest in using wood species from alternative sources, especially fruit-tree woods for many purposes.

Sahin and Mantanis (2011) reported that nanoparticulate based treatment effective for protecting natural colour of some wood species. However, it was proposed that the addition of chips from fruit tree branches to particleboards up to 50% can be considered successful-since no appreciable effects on the properties of particleboards were observed (Grigoriou and Passialis 1999). In one research, it was found that olive tree pruning's (OTP) were an interesting raw material for paper production because its properties are comparable to those of the other agricultural residues, currently used in the paper industry (Requejo et al. 2012). Kiaei et al. (2014) studied plum (*Prunus domestica*) tree to examine its biometrical and chemical properties. Results indicated that there were no significant differences in the chemical properties and fiber length, cell wall thickness and morphological properties when different types of wood (branch and stem) were used. Garcia-Maraver and his group (2015) suggested the best pelleting conditions for the residual biomass from olive trees. Passialis and Grigoriou (1999) again studied the technical properties of branch-wood produced by pruning of fruit-tree plantations (i.e. apple, pear and apricot). From the species that were studied, the branch-wood of apple and pear trees belongs to the diffuse porous group and is characterized by homocellular rays, whilst that of apricot belongs to the ring porous group with heterocellular rays. They found that apple had the larger cell dimensions and apricot trees the shorter/smaller cells. In recent study, Sahin (2010) determined anisotropic swelling and water sorption properties of chesntnut wood which grown in Turkey.

In the Mediterranean areas of southwest Europe, orchard tree pruning generates substantial amounts of residual wood biomass. However, large quantities of branch wood remain in the fields after pruning during the winter period and they are not utilized properly. So far this biomass has not been turned into a useful wood resource. Kiaei et al. (2014) suggested that fruit trees can help solve the problem of the lack of raw materials for the forest products industry. As mention above playgrounds should be act as a more natural environment for the children to play and environmentally friendly wooden material is suitable for such places. However, a present there is no information on utilizing wood from fruit trees in landscape applications.

The objective of this study is to discuss the suitability of some wood species from fruit-trees as the wooden element for certain landscape applications (e.g. playgrounds). Hence we investigated and discuss the aesthetic appearance (color), hardness properties and general specifications of

selected orchard species. The developments in the use of alternative wood-based material in landscape applications (playgrounds) that use fruit tree wood material for general properties and natural appearance are described in this study. The use of fruit-tree species for playgrounds may create alternative utilization and serve as basis for future studies about those species.

MATERIALS AND METHODS

The wood-based materials since they are safe and highly suitable for use in children's playgrounds. However, changes over time in some wood species impact if they can meet /satisfy the aesthetic preferences of a landscape practices. Finding out these influences for playgrounds, eight fruit tree wood species that found cultivated/grown in orchards were selected for this study. These are: apple (*Malus domestica* L.), apricot (*Prunus armeniaca*), fig (*Ficus canica*), mulberry (*Morus Alba*), olive (*Olea europaea*), pear (*Pyrus anatolica*), plum (*Prunus domestica*) and rowanberry (*Sorbus aucuparia* L.); they were selected for experiments. The selected fruit-tree woods were acquired from the Isparta region in Turkey. Samples of 60 x 60 x 20 mm were prepared and sub-divided into two groups: heartwood and sapwood. The special surface preparation includes sanding to achieve the best appearance.

Progress in the appearance description by means of color and pattern characteristics would be suitable to classify the woods. It would also help to match pieces to study the wood color variability. The quantitative color measurements were carried out with an X-Rite SP 968 spectrophotometer and using CIE L*a*b*c*, h* color scale 1976. The radial and tangential surfaces were measured. The surface whiteness and yellowness color properties were also determined according to standard ASTM E-313, and ASTM D-1925, respectively.

A shore hardness (Scale D) instrument was utilized to measure the hardness properties of the wood samples. The tests were conducted according to the ASTM D-2240 standard. It measures the depth of an indentation in the material created by a given force on a standardized presser foot. This depth is dependent on the hardness of the material and its viscoelastic properties. The measurements were made of five samples in each direction. The average values were then presented as shore hardness of wood samples (Scale D).

Photos of wood species were taken to display to subjects asked for aesthetic assessment and judgment of the suitability of the material for playgrounds during a face-to-face (questionnaire) survey. The photos of eight wood species were taken and stuck to one slide. All of the respondents completed judging natural appearances and their aesthetic preferences based on a slide (Fig. 2).

The face-to-face questionnaire survey method has been intensively used for many kinds of research to collect reliable data. For determining opinion on playgrounds, standard survey questions prepared in advance, were asked to individuals and their answers were recorded. Each survey took about 5.0 minutes to complete. Hence, all respondents were chosen as volunteers and divided into three groups. These are: public people (Group A), children (age level of 5-12 years) (Group B), and university students (undergraduate and graduate) (Group C). Members of the three groups were invited to state their aesthetic preferences for those wood species and to give opinions on playgrounds.

Hands and Brown (2002) suggested that the aesthetic assessment could be divided into 7 ranks (scores). However, there were eight wood species in this study to determine responder's aesthetic preferences. Hence, following scores were chosen to be best applicable in our study. These ranks are; 1: Extremely beautiful; 2: Very beautiful; 3: Beautiful; 4: Moderate; 5: Unbeautiful; 6: Very unbeautiful; 7: Extremely unbeautiful; 8: Unsuitable (awful). The SPSS 13.0 (Statistical

Program for the Social Sciences) was used to analyze results and these are given in Tabs. and Figs. ANOVA analysis was used to check the differences between the groups. Correlation analysis and stepwise multiple linear regression analysis were conducted to explore the relationships between wood species and aesthetic preferences as well as opinions on playgrounds.

RESULTS AND DISCUSSIONS

Tab. 1 shows the comparative summary of selected fruit tree wood species including scientific names, densities, hardness (according to Janka) and crushing strength properties. It appears that wood density has a clear effect on the strength properties. The highest crushing strength (77.1 MPa), and hardness (12.1 kN) were reported for the olive tree that has the density value of 0.73 g·cm^{-3} in comparison to the other samples. However, apricot and mulberry woods have considerably higher crushing strength of 46.0 MPa and 48.2 MPa, respectively. It has already been predicted by a number of researchers that wood having different density properties could influence their strength and hardness properties (Barnett and Jeronimidis 2003, Chowdhury et al. 2012, Kollmann and Côté 1968). Hence, it is assumed that the botanical variations might influence the wood strength properties to some degree in addition to affecting the physical characteristics (density) of woods.

Tab. 1: The properties of some fruit trees.

Common name	Scientific name	Density (g·cm^{-3})	Hardness (Janka) (kN)	Crushing strength (MPa)	Reference
Apple	Malus domestica	0.62	7.7	41.6	Meier (2015)
Apricot	Prunus armeniaca	0.75	6.9	46.0	Meier (2015)
Fig	Ficus canica	0.39	-	-	Brown (1997)
Mulberry	Morus alba	0.69	7.5	48.2	Meier (2015)
Olive	Olea europaea	0.76	12.1	77.1	Meier (2015)
Pear	Pyrus anatolica	0.69	7.4	44.1	Meier (2015)
Plum	Prunus domestica	0.62	6.2	29.3	Govarcin et al. (2012), Meier (2015)
Rowanberry	Sorbus aucuparia	0.57	6.8	22.2	Korkut and Guller (2008)

Numerous literature on determining biological durability of forest based some wood species (hardwoods and softwoods) has already been reviewed and pointed by a number of researchers. Some excellent bibliographies provide a thorough index to the literature on those sources (EN 350 2016, Golpayegani et al. 2010, Hassan et al. 2018, Mantanis 2017, Meier 2015, Scheffer and Morrell 1998). However, the orchard trees are different trees in a different manner than the traditional forest, and the wood properties can be different as well. Tab. 2 summarizes the biological durability of wood of some fruit trees that has already reported in literature (EN 350 2016, Golpayegani et al. 2010, Hassan et al. 2018, Meier 2015, Scheffer and Morrell 1998). It appears that there some variance in respect to the biological resistance of these woods against fungi, insects (*Anobium*) and termites. The most resistant against fungi from these fruit species, are actually: Olive wood followed by Mulberry wood. It was reported that Mulberry wood has very high durable properties against insects due to its toxic wood constituents (Hassan et al. 2018).

Tab. 2: Biological durability of wood from some fruit trees.

Common name	Scientific name	Against fungi	Against insects	Against termites	Reference
Apple	*Malus domestica*	4	n/a	n/a	EN 350 (2016)
Apricot	*Prunus armeniaca*	3-5	S	D	EN 350 (2016)
Fig	*Ficus canica*	Non-durable	Non-durable	n/a	De Guzman and Siemonsma (1999), Scheffer and Morrell (1998)
Mulberry	*Morus alba*	Durable	Very durable	Moderately durable	Cassens and Makra (2014) Golpayegani et al. (2010) Hassan et al. (2018)
Olive	*Olea europaea*	Very durable	Non-durable	n/a	Meier (2015)
Pear	*Pyrus anatolica*	Non-durable	n/a	n/a	Meier (2015)
Plum	*Prunus domestica*	3-4	S	D	EN 350 (2016)
Rowanberry	*Sorbus aucuparia*	Non-durable	n/a	n/a	Palm et al. (2005)

The graphical plots of wood density versus hardness (Shore D) (Fig. 1) show a basic trend similar to that in Tab. 1. It is known that increasing density usually affects hardness positively on all woods. However, the highest hardness was measured for olive wood (74), followed by apricot (70), pear (64) and mulberry (63). Wiemann and Green (2007) suggested that the hardness and specific gravity relationship is a phenomenological parameter which is determined by both its density and botanical origin. They suggested that wood-density and hardness display an approximately similar trend for tropical and temperate hardwoods, but that the relationship for softwoods is different from that for hardwoods. Moreover, the wood hardness properties are not well understood for most wood species. To determine the hardness, one has to understand factors such as: wood anatomical structure, chemical content and growing conditions.
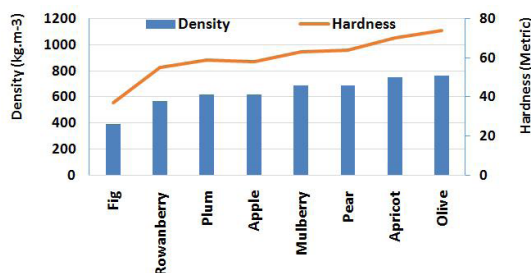
Fig. 1: Wood density and hardness properties of fruit tree wood species.

Tab. 3 summarizes the color values of wood species. It appears that there are clear variations in color properties of selected wood species. The highest lightness values of (L*) 87.25 were observed for fig followed by mulberry (74.47) and pear (73.35), respectively. In contrast, the lowest lightness values of 51.57 were observed for apricot samples. Moreover, the green-red (a*) and yellow-blue (b*) color coordinates were also considerable variations among species.

For a* properties, except fig which shows only negative values of (-3.67) which means green is dominant in its natural color, all other wood species show positive values (+a) and that means red is dominant in their natural color. However, as mentioned above, the color properties of wood are not well understood for most wood species. Hence, variations among color patterns of wood specimens are very complicated and it is not intended (possible) to explain all color characteristics. It should be emphasized that the determination of a* and b* must be considered as being only suggestive intimating / hinting / alluding.

The C* represents Chroma or 'saturation' properties of a given color. The Chroma is the strength of an object color and describes the vividness or dullness of a color. However, the high Chroma (saturation) represents 'color purity' and both hue angle and chroma both relate to human color perception. As seen in Tab. 3 the highest chroma value was observed for apricot (66.59), followed by fig (26.06), plum (22.6), olive (20.53), pear (18.82), rowanberry (17.38), apple (15.89) and mulberry (14.7), respectively.

The **H*** (°) represents the angle of the line starting from the point to the zero origin in CIE L*, a*, b* color space. It is basically the degree to which a stimulus can be described as similar to or different from stimuli that are described as: red, yellow, green and blue or a combination of two of them. Hence, hue is the attribute of color that is related to the perceived colors. The units are in the form of degrees° (or angles), ranging from 0° (red) through 90° (yellow), 180° (green), 270° (blue) and back to 0°. The highest hue value (degree) was observed for fig (98.1°), followed by mulberry (80.28°), pear (80.17°), rowanberry (76.92°), olive (71.15°), apple (68.89°), and apricot (21.35°), respectively.

Tab. 3: Colour properties of fruit tree wood samples (CIE L*a*b*, 1976).

Wood species	L*	a*	b*	C*	H (°)	Whiteness (ASTM-E313)	Yellowness (ASTM-D1925)
Apple	54.27	5.72	14.82	15.89	68.89	6.5	47.68
Apricot	51.57	9.54	22.04	66.59	21.35	17.06	71.05
Fig	87.25	-3.67	25.83	26.06	98.1	35.07	43.79
Mulberry	74.47	2.48	14.49	14.7	80.28	0.61	34.07
Olive	57.65	6.63	19.43	20.53	71.15	14.46	57.02
Pear	73.35	3.21	18.54	18.82	80.17	12.53	43.02
Plum	54.9	9.24	20.63	22.6	65.87	15.95	64.87
Rowanberry	58.88	3.93	16.93	17.38	76.92	10.02	47.61

Whiteness is defined as a measure of how closely a surface matches the properties of a perfect reflecting diffuser, the highest whiteness indices was found for fig (35.07) whereas the lowest whiteness was found for mulberry (0.62). However, yellowness is defined as a measure of the degree to which the color of a surface is shifted from preferred white towards yellow. It can be seen in Tab. 3 that apricot has a very high yellowness value of 71.05, compared to other wood species.

Fig. 2 shows the natural appearance of fruit tree species. However, colors with the same hue are usually distinguished with adjectives referring to their lightness and/or colorfulness, such as with "light color", "pastel color", "vivid color". Interestingly, apple and plum; mulberry and pear; olive and rowanberry are more or less similar (approx. ± 0.11 to 7.0 differences) L*, a*, b*, chroma and hue values. Hence these wood species could be described as having similar color properties. However, it should be noticed that the determination of exact color properties of a given wood is very complicated and it is not intended to determine exact color properties of the wood samples. It should be emphasized that the given color parameters could be considered as being only suggestive.

It has already been thoroughly emphasized that wood's natural appearance could have an important role in many applications (i.e. architecture practices) and supports the selection of wooden elements. Therefore, the scientific appreciation and evaluation of the aesthetic characters can help to better understand the reasons for the wood species preferences and why people prefer a certain piece of wooden decoration for the playgrounds. This assessment process contained two steps. The first step was general material selection preferences assessment for playground use. The second step was judging the natural appearance of wood as shown in Fig. 2.

Fig. 2: The natural appearance of fruit tree wood samples (Meier, 2015).

Survey data of participant's demographic characteristics obtained as a result of face-to-face survey application are shown in Tab. 4. A total of 600 individuals (200 from each group) participated in the survey. It was observed that the participants were effective in terms of age group and material preferences. For group A, majority of the participants (45%) preferred wooden elements for playground material, followed by plastic (42.0%), metal (13.0%), in order of importance. For group C, the recorded order of importance materials preferences were similar. However, for group B, some differences were found in material selection. The majority of participants in group B (50.5%) preferred plastic elements, followed by wooden (31.5%), metal (18.0%), and other material (0.02%), for playgrounds.

However, it was seen that the most effective factors for selection of material for playground should be security for both Group A (79%), and C (76.5%), whereas aesthetic appearance was selected by group B (71%). Similar results were also found for color properties of woods a majority of participants of both group A and C preferred light-colored wooden elements in playgrounds. The group B participants almost equally (46% vs. 42.5%) preferred light and dark colored wooden elements in playgrounds.

Stamps (1999) proposed that students can substitute for the public in landscape assessment. However, Yao et al. (2012) also suggested that there was no significant difference between undergraduate students and the public for aesthetic assessment. The results found in this study clearly support this information.

Tab. 4: The demographic properties of respondents.

	Group A (Public people)	Group B (Children)	Group C (University students)
Gender			
Male	82 (41%)	96 (48%)	98 (49%)
Female	118 (59%)	104 (52%)	102 (51%)
Age groups			
Years old	20-29: 69 30-39: 45 40-49: 43 50-59: 28 > 60: 14	< 5: 15 6-8: 69 9-12: 101 > 12: 15	17-21: 114 22-26: 74 27-31: 5 > 32: 7
Material preferences for playgrounds			
a: Plastic	84 (42.0%)	101 (50.5%)	79 (39.5%)
b: Wood	90 (45.0%)	63 (31.5%)	115 (57.5%)
c: Metal	26 (13.0%)	36 (18.0%)	6 (3.0%)
Reason for selecting that material for playgrounds			
a: Should be secure for children b: Should be longer service time c: Should be aesthetic appearance d: Should be cheap	158 (79.0%) 26 (13.0%) 14 (7.0%) 2 (1.0%)	32 (16.0%) 18 (9.0%) 142 (71.0%) 8 (4.0%)	153 (76.5%) 10 (5.0%) 33 (16.5%) 4 (2.0%)
What colour properties of woods should have			
a: Light colored	127 (63.5%)	92 (46.0%)	140 (70.0%)
b: Dark coloured	61 (30.5%)	85 (42.5%)	51 (25.5%)
c: No preferences	12 (6.0%)	23 (11.5%)	9 (4.5%)

However, in order to assess the aesthetic appearance of woods in playgrounds, the participants were asked questions regarding wood's scoring (rank) according to their natural appearance. Tab. 5 shows the scores of woods according to natural appearance. It must be understood that the scoring of wood appearance is very complicated and it is not intended to explain/ take into account all the variances.

Only the fig wood was scored to have the extremely beautiful natural appearance, which is very attractive to use in playground applications by wood of all these three groups. This is not surprising considering the color properties of fig wood that are grouped as having a light colored (Fig. 2) appearance. This result also supports the finding for the preferences of color properties of woods. Hence the majority of participants in these three groups preferred light colored wooden elements in playgrounds. According to results presented in Tab. 5, it is not easy to measure aesthetic appearance of wood samples. However, the results indicate that wood with good/attractive appearance were mostly found among light colored wood species.

Tab. 4: The scores of woods according to natural appearance (1: Extremely beautiful, 2: Very beautiful, 3: Beautiful, 4: Moderate, 5: Unbeautiful, 6: Very unbeautiful, 7: Extremely unbeautiful, 8: Unsuitable (awful).

Woods	Group A (Public people)	Group B (Children)	Group C (University students)
	Valid questionnaires (persons)		
	189	154	193
Apple (*Malus domestica* L.)	1: 33 (17.5%) 2: 15 (7.9%) 3: 9 (4.8%) 4: 13 (6.9%) 5: 15 (7.9%) 6: 21 (11.1%) 7: 41 (21.7%) 8: 42 (22.2%) **C**	1: 2 (1.3%) 2: 12 (7.9%) 3: 9 (5.8%) 4: 10 (6.5%) 5: 19 (12.3%) 6: 20 (13.0%) 7: 36 (23.4%) 8: 32 (20.8%) **AB**	1: 31 (16.1%) 2: 14 (7.3%) 3: 15 (7.8%) 4: 26 (13.5%) 5: 28 (14.5%) 6: 24 (12.4%) 7: 30 (15.5%) 8: 26 (13.5%) **BCD**
Apricot (*Prunus armeniaca*)	1: 10 (11.2%) 2: 5 (2.6%) 3: 35 (18.5%) 4: 28 (14.8%) 5: 33 (17.5%) 6: 35 (18.5%) 7: 7 (3.7%) 8: 8 (4.2%) **BC**	1: 18 (11.7%) 2: 10 (6.5%) 3: 22 (14.3%) 4: 17 (11.0%) 5: 19 (12.3%) 6: 41 (26.6%) 7: 12 (7.8%) 8: 12 (7.8%) **CD**	1: 12 (6.2%) 2: 23 (11.9%) 3: 37 (19.2%) 4: 33 (17.1%) 5: 31 (16.1%) 6: 24 (12.4%) 7: 19 (9.8%) 8: 11 (5.7%) **BC**
Fig (*Ficus canica*)	1: 69 (36.5%) 2: 23 (12.2%) 3: 11 (5.8%) 4: 8 (4.2%) 5: 9 (4.8%) 6: 13 (6.9%) 7: 19 (10.1%) 8: 37 (19.6%) **AB**	1: 57 (37.0%) 2: 19 (12.3%) 3: 17 (11.0%) 4: 7 (4.5%) 5: 11 (7.1%) 6: 7 (4.6%) 7: 12 (7.8%) 8: 24 (15.6%) **A**	1: 48 (24.9%) 2: 17 (8.8%) 3: 8 (4.1%) 4: 18 (9.3%) 5: 15 (7.8%) 6: 26 (13.5%) 7: 29 (15.0%) 8: 32 (16.6%) **BCD**
Mulberry (*Morus alba*)	1: 9 (4.8%) 2: 54 (28.6%) 3: 13 (6.9%) 4: 22 (11.6%) 5: 13 (6.9%) 6: 24 (12.7%) 7: 32 (16.9%) 8: 22 (11.6%) **BC**	1: 24 (15.6%) 2: 36 (23.4%) 3: 24 (15.6%) 4: 14 (9.1%) 5: 10 (6.5%) 6: 21 (13.6%) 7: 23 (14.9%) 8: 12 (7.8%) **ABC**	1: 10 (5.2%) 2: 29 (15.0%) 3: 17 (8.8%) 4: 17 (8.8%) 5: 24 (12.4%) 6: 32 (16.6%) 7: 37 (19.2%) 8: 27 (14.0%) **CD**

Olive (*Olea europaea*)	1: 11 (5.8%) 2: 19 (10.1%) 3: 28 (14.8%) 4: 36 (11.6%) 5: 43 (22.8%) 6: 29 (15.3%) 7: 11 (5.8%) 8: 12 (6.3%) **BC**	1: 7 (4.5%) 2: 11 (7.1%) 3: 21 (13.6%) 4: 40 (26.0%) 5: 31 (20.1%) 6: 17 (11.0%) 7: 14 (9.1%) 8: 12 (7.8%) **ABCD**	1: 30 (15.5%) 2: 13 (6.7%) 3: 23 (11.9%) 4: 21 (10.9%) 5: 34 (17.6%) 6: 23 (11.9%) 7: 21 (10.9%) 8: 23 (11.9%) **BCD**
Pear (*Pyrus anatolica*)	1: 7 (3.7%) 2: 17 (8.9%) 3: 33 (17.5%) 4: 26 (13.8%) 5: 29 (15.3%) 6: 36 (19.1%) 7: 21 (11.1%) 8: 20 (10.6%) **C**	1: 11 (7.1%) 2: 30 (19.5%) 3: 23 (14.9%) 4: 17 (11.0%) 5: 14 (9.1%) 6: 21 (13.6%) 7: 27 (17.5%) 8: 11 (7.1%) **ABCD**	1: 13 (6.7%) 2: 12 (6.2%) 3: 21 (10.9%) 4: 22 (11.4%) 5: 24 (12.4%) 6: 34 (17.6%) 7: 28 (14.5%) 8: 39 (20.2%) **D**
Plum (*Prunus domestica*)	1: 35 (39.3%) 2: 28 (14.8%) 3: 40 (21.2%) 4: 31 (16.4%) 5: 34 (17.9%) 6: 12 (6.3%) 7: 5 (2.6%) 8: 8 (4.2%) **A**	1: 26 (16.9%) 2: 14 (9.1%) 3: 20 (12.3%) 4: 31 (20.1%) 5: 34 (22.1%) 6: 10 (6.5%) 7: 9 (5.8%) 8: 10 (6.5%) **AB**	1: 24 (12.4%) 2: 38 (19.7%) 3: 41 (19.2%) 4: 37 (19.3%) 5: 28 (14.5%) 6: 11 (5.7%) 7: 8 (4.1%) 8: 6 (3.1%) **A**
Rowanberry (*Sorbus aucuparia L.*)	1: 13 (6.9%) 2: 27 (14.3%) 3: 20 (10.6%) 4: 25 (13.2%) 5: 12 (6.3%) 6: 24 (12.7%) 7: 27 (14.3%) 8: 41 (21.7%) **C**	1: 13 (8.4%) 2: 21 (13.6%) 3: 18 (11.7%) 4: 19 (12.3%) 5: 19 (12.3%) 6: 14 (9.1%) 7: 20 (13.0%) 8: 30 (19.5%) **BCD**	1: 22 (11.4%) 2: 35 (18.5%) 3: 27 (14.0%) 4: 26 (13.5%) 5: 17 (8.8%) 6: 26 (13.5%) 7: 19 (9.8%) 8: 22 (11.4%) **AB**

CONCLUSIONS

It is important to select suitable materials for children's playgrounds. However, it was realized that the factors for selection of material for a playground were security and aesthetic appearance. For wood materials; color and natural appearance are found to be important predictors to aesthetic preferences. It appears that there are clear variations on color properties of selected fruit-tree wood species. It was understood that wood appearance or preferences was associated with responders of different age groups and who belong to different professions. It is important to note that the majority of participants preferred light colored wooden elements in playgrounds.

The use of fruit tree woods has not yet been considered to be used for the manufacture of wood-based elements in playgrounds. This study may provide preliminary data for landscaping improvement of playgrounds using fruit tree woods.

ACKNOWLEDGEMENTS

REFERENCES

1. Barnett, J.R., Jeronimidis, G., 2003: Wood quality and its biological basis. Blackwell Scientific Publisher, 226p. Oxfordshire, UK, 226 pp.
2. Brown, S., 1997: Estimating biomass and biomass change of tropical forests: a primer. FAO Forestry Paper 134, Rome, 55 pp.
3. Cassens, D., Makra, E., 2014. Urban wood and traditional wood: a comparison of properties and uses. FNR-490-W, Purdue University Extention, IL. 13 pp.
4. Chowdhury, M.Q., Ishiguri, F., Hiraiwa, T., Matsumoto, K., Takashima, Y., 2012: Variation in anatomical properties and correlations with wood density and compressive strength in *Casuarina equisetifolia* growing in Bangladesh. Australian Forestry 75(2): 95-99.
5. Deborah, K.T., McDonald, J.E., 2001. Special study: injuries and deaths associated with children's playground equipment. Directorate for Epidemiology, U.S. Consumer Product Safety Commission, Washington, 37 pp.
6. De Guzman, C. C., Siemonsma, J. S.(Eds). 1999.Species Prosea. Plant resources of South-East Asia 13: Backhuys Publishers, Leiden, Netherlands, 400 pp.
7. EN 350, 2016: Durability of wood and wood-based products. Testing and classification of the durability to biological agents of wood and wood-based products.
8. Garcia-Maraver, A., Rodriguez, M.L., Serrano-Bernardo, F., Diaz, L.F., Zamorano, M., 2015: Factors affecting the quality of pellets made from residual biomass of olive trees. Fuel Processing Technology 129: 1-7.
9. Golpayegani, A.S., Thevenon, M.F., Gril, J., Pourtahmasi, K., 2010: Natural durability of Mulberry wood from Iran. In 41st Annual Meeting of the International Research Group on Wood Protection. Biarritz, France, 9-13 May 2010. IRG Secretariat.
10. Govorcin, S., Sinkovic, T., Sedlar, T., Istok, I., Vukadin, M., 2012: Some physical and mechanical properties of plum tree (Prunus Domestica L.). Drvna Industrija 63 (4): 291-295.
11. Grigoriou, A., Passialis, C., 1999: Utilization of branch-wood from fruit-tree plantations for particleboard production. Holz als Roh-und Werkstoff 52 (2): 126-130.
12. Hassan, B., Mankowski, M.E., Kirker, G.T., Clausen, C.A., Ahmed, S., 2018: Effects of white mulberry (*Morus alba)* heartwood extract against *Reticulitermes flavipes* (Blattodea: Rhinotermitidae). Journal of Economic Entomology 111(3): 1337-1345.
13. Janin, G., Goncalez, J., Ananias, R., Charrier, B., da Silva, G.F., Dilem, A., 2001: Aesthetics appreciation of wood colour and patterns by colorimetry. Part 1. Colorimetry theory for the CIELab system. Maderas: Ciencia y Technologia 3(1/2): 3-11.
14. Kiaei, M., Tajik, M., Vaysi, R., 2014: Chemical and biometrical properties of plum woods and its application in pulp and paper production Maderas. Ciencia y Tecnología 16 (3): 312-332.

15. Kollmann, F.R., Côté, W.A., 1968: Principles of Wood Science and Technology. Springer-Verlag, Berlin, Germany, 592 pp.
16. Korkut, S., Guller, B., 2008: Physical and mechanical properties of European hophornbeam (*Ostrya carpinifolia* Scop.) wood. Bioresorce Technology 99: 4780-4785.
17. Mantanis, G.I. 2017: Chemical modification of wood by acetylation or furfurylation: A review of the present scaled-up technologies. BioResources 12(2): 4478-4489.
18. Meier, E., 2015: Wood! Identifying and using hundreds of woods worldwide. The Wood Database, USA, 31 pp.
19. Scheffer, T.C., Morrell, J.J. 1998: Natural durability of wood: a worldwide checklist of species. Oregon State Univesity, Forest Research Laboratory., Research Contribution, Corvallis, 62 pp.
20. Palm, J., Åhström, A., Wijk, G., Johansson, S., 2005: Hardwoods-The facts, Träcentrum Nässjö (Wood Centre Nässjö) Sweden, 43 pp.
21. Passialis, C.N, Grigoriou, A.H., 1999: Technical properties of branch-wood of apple, peach, pear, apricot and cherry fruit trees. Holz als Roh-und Werkstoff 57(1): 41-44.
22. Requejo, A., Rodriguez, A., Colodette, J.L., Gomide, J.L., Jimenez, L., 2012: TCF bleaching sequence in kraft pulping of olive tree pruning residues. Bioresource Technology 117: 117-123.
23. Sahin, H. T., Mantanis, G. I. 2011. Colour changes in wood surfaces modified by a nanoparticulate based treatment. Wood Research, 56 (4): 525-532.
24. Sahin, H. T. 2010. Experimental determination of the anisotropic swelling and water sorption properties of chesntnut wood. Wood Research 55(1): 33-40.
25. Wiemann, M.C., Green, D.W., 2007: Estimating Janka hardness from specific gravity for tropical and temperate species. USDA Forest Service, FPL-RP-643. Madison, WI. 21 pp.

Candan Kus Sahin*, Busra Onay
Suleyman Demirel University
Faculty of Architecture
Department of Landscape Architecture
Doğu Kampusu, 32260 Isparta
Turkey
*Corresponding author: candansahin@sdu.edu.tr

TANG DYNASTY CHAIR FEATURE DESIGN BASED ON
KANSEI EVALUATION AND EYE TRACKING SYSTEM

Zhonghua Zhagn, Boming Xu
College of Furnishings and Industrial Design
Nanjing Forestry University
Nanjing, China

ABSTRACT

Tang dynasty (AD 618–907) chairs were manufactured during an important period of Chinese furniture development. This paper aims to identify design elements that impact on people's subjective impressions, so as to guide the design of Tang dynasty style chairs. The study combined eye tracking and Kansei evaluation methods to assess the semantic reception of Tang dynasty chairs. The results showed that the influential factors can be grouped into two main categories: decoration and shape. The decorative features of Tang dynasty chairs that have the most significant impact on visual attention were identified. The study determined that the backrests, armrests, and legs of Tang dynasty chairs design were the most important morphological features. Through these morphological features, we can define the Tang dynasty chair style, guide the design of modern Tang dynasty style chairs, and carry out targeted design of Tang dynasty chair style features.

KEYWORD: Kansei evaluation, eye tracking, Tang dynasty, chair.

INTRODUCTION

The Tang dynasty was a prosperous period of China's history during which it was predominantly a feudal society. The stylized form and elegant decoration of Tang dynasty furniture are material manifestations of the splendid culture (Zhu 2016, Lee et al. 2018) and aesthetics of the Tang dynasty, and pieces dating from the period which has significant research value when studying the developmental history of traditional Chinese furniture. During the Tang dynasty, high and low furniture coexisted and there was a considerable variety of forms produced. At present, research on Tang dynasty chairs is mainly conducted from the historical perspective (Zanous and Sangari 2018, Ying 2018) and using traditional craftwork analysis (Wang et al. 2015, Hu et al. 2019a). No in-depth study of the emotional impact of Tang dynasty chairs on people who view or use them has been carried out. With the development of modern society,

people have higher requirements regarding furniture styles and individual tastes (Wan et al. 2018). Tang dynasty chairs have unique styles and characteristics (Hu et al. 2019b, 2019c), but the style has not been widely developed. The reason is that Tang dynasty chair design features are not obvious, and at the same time, the subjective feelings of people regarding Tang dynasty chairs have been ignored. As a result, the general aim of this study is to identify design elements that impact on people's subjective impressions, so as to guide the design of Tang dynasty style chairs. In the majority of studies investigating the relationships between form and eye movement (Loyola et al. 2015, Zhou et al. 2014), Kansei evaluations and eye movement analyses have been carried out separately (Guo et al. 2016, Hsu et al. 2017, Vieira et al. 2017, Wang et al. 2016), so it is difficult to identify exactly which features of the samples affected people's Kansei evaluations. The present study used an eye tracking system to record the eye movements of subjects while they performed Kansei evaluations of Tang dynasty chairs. Eye tracking systems can accurately measure the eye fixation points during subjective evaluations (Khalighy et al. 2015), so as to determine which of the Tang dynasty chair features played the principal role influencing the subjective evaluations.

The Tang dynasty had a history lasting more than a thousand years (Wang et al. 2015). At that time, the materials used to make chairs were predominantly woods (Dong et al. 2017), which are not easy to store or preserve. There are, therefore, only a few examples of Tang dynasty chairs now in existence. Samples in this research are reconstructed based on the shape of the chairs depicted in paintings, the proportions of the chairs compared to people in the paintings, information regarding the size of the surviving Tang dynasty chairs, and those recorded in ancient literature. With these sources and the size of other cultural relics, the proportions and forms of Tang dynasty chairs were estimated. Finally, using the principle of two-point perspective, the Tang dynasty chairs were then depicted by line drawings. Through the above process, the style of Tang dynasty chairs was clearly represented, and this work, therefore, plays an important role in the restoration and cultural appreciation of Tang dynasty chairs.

MATERIALS AND METHODS

Stimuli

The first step in a Kansei evaluation is to gather as many relevant words and expressions as possible for the definition of the semantic scope of the study (Trujillo et al. 2016, Castilla et al. 2017). The majority of the words selected were adjectives used to describe Tang dynasty chairs and the Tang dynasty style. In the present research, the majority of the words were found in documents on the Internet, in newspapers, journals, scientific publications, and professional magazines. During this phase, a total of 140 expressions were collected. There were too many adjectives to be used in the Kansei questionnaire, and most of the words were repeated or similar, so further selection was required. A group including two professors, two design experts, and two students were organized to analyze and reduce the semantic adjectives down to an appropriate number. Finally, only 8 pairs of adjectives were preserved: (a) plain-luxury, (b) flowing-stable, (c) disordered-harmonious, (d) simple-intricate, (e) round-straight, (f) delicate- robust, (g) stocky-exquisite, and (h) slim-thick.

In this study, images of the chairs on objects, in paintings, and in murals were collected and classified. Incomplete, unclear, or ambiguous depictions were then excluded, leaving a total of 11 pieces in the study group (Fig. 1). In order to emphasize sample morphology, it was necessary to exclude variations in color, material, light, and shadow from the sample images to avoid visually misleading subjects. The samples were, therefore, all presented in the form of line drawings

and observed at a 45° angle. The present study concluded with using 11 chairs as stimuli and 8 pairs of Kansei words as measurement scales for the following semantic differential (SD) evaluation and eye tracking experiment.
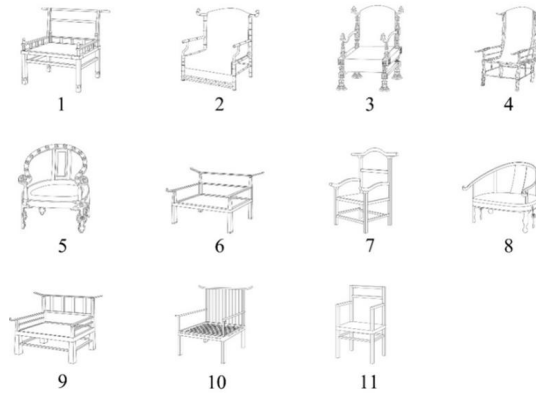

Fig. 1: Experimental stimuli.

Subjects

In the current study, subjects required a certain cognitive and sensory sensitivity to morphology. Many scholars have studied (Winston and Cupchik 1992, Nodine et al. 1993) that formal art training influences perception and reception. The responses of people trained in artistic methods or theory differ from controls in their perception of form. Most of the subjects chosen for the experiment were experienced practitioners in a relevant field. The average age of the subjects was 28 years (Tab. 1). All of the subjects had normal or corrected-to-normal vision. They all signed written consent before the experiment and received a gift as a reward afterwards.

Tab. 1: Subject structure.

Subject structure		N	%
Gender	Male	10	50
	Female	10	50
Age	Up to 30 years	12	60
	Above 30 years	8	40
Education	University education	11	55
	Non-university education	9	45
Working status	Furniture industry practitioners	18	90
	Non-furniture industry practitioners	2	10

Procedure

The experiment was carried out at Nanjing Forestry University in China. The environment of the laboratory was quiet in order to eliminate external interference, and the lighting conditions were stable. A TOBII eye tracker was used in the experiment (Fig. 2).
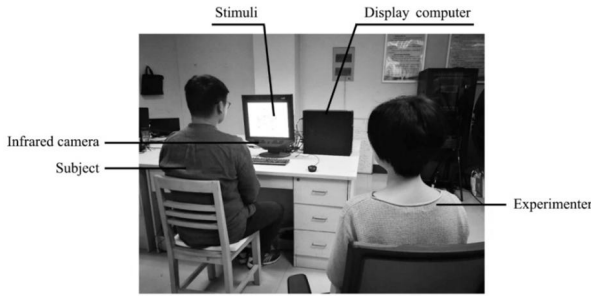
Fig. 2: Experimental environment and equipment.

Eye movement data was recorded using a Clearview 2.7.0 software system. In order to make the experimental results more accurate and meaningful, it was necessary to pre-define the areas of interest (AOIs) in the images. Each of the Kansei words was explained to allow the participants to fully understand intended meanings. In order to allow subjects to better understand the samples, each participant was required to experience a brief introduction to the style and characteristics of Tang dynasty chairs whose specific information or names were not introduced. Before the experiment, participants were also given instructions regarding the test procedures and underwent an experiment trial so that they would be familiar with the task requirements and methodology in advance.

During the experiment, subjects were asked to carry out a Kansei evaluation of each chair and evaluate their reception according to a 7-point-Likert scale, based on the stimuli that appeared on the screen. In order to avoid subjects' fixation points moving outside the screen, the results of perceptual evaluations were dictated by the subjects, and the experimenter recorded the scores for the subjects. In order to keep the subjects focused during the experiment and to avoid visual fatigue, computers or mobile phones could not be used for two hours before the experiment was carried out, and a rest was taken every ten minutes during the experiment. The experimental process is shown in Fig. 3.
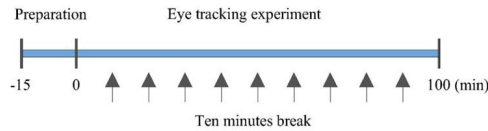

Fig. 3: Experimental flow chart.

When the experiment started, subjects observed the first pair of perceptual vocabulary scales (5s), the gaze concentration point (2s), then the chair stimuli (7s), and finally, the first pair of perceptual vocabulary scales again (5s). The subjects then dictated their scores. Then they observed the second of the semantic vocabulary pairs and repeated the process, until the last chair and the last vocabulary scale was dictated, and the experiment ended (Fig. 4). The research flowchart is shown in Fig. 5.
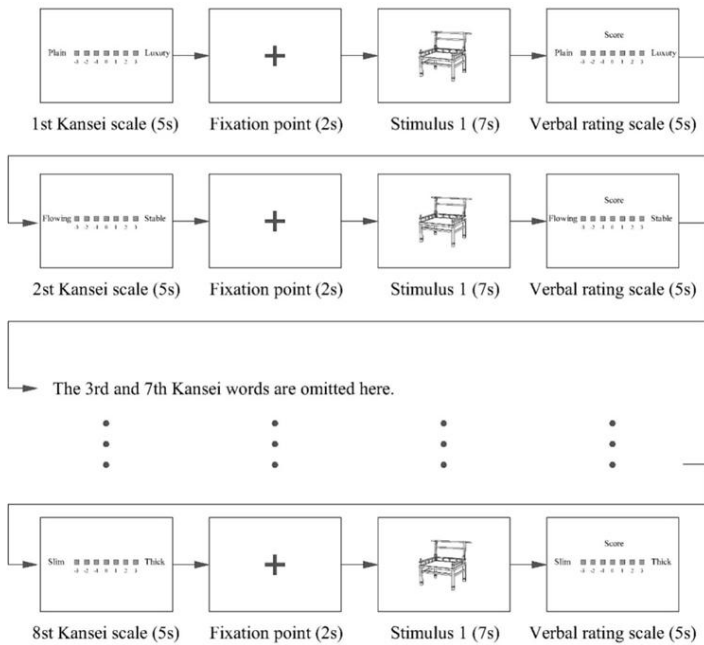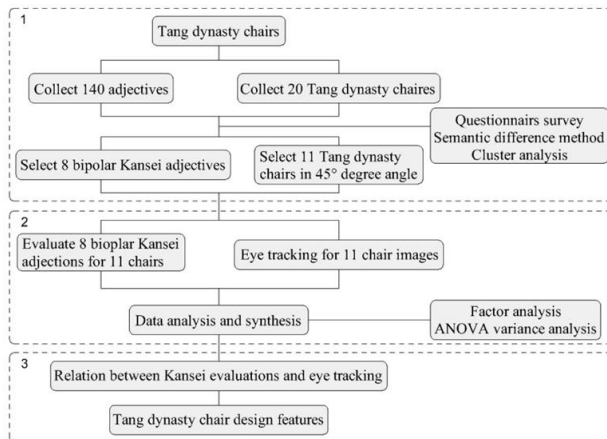
Fig. 4: Experimental procedure for stimulus 1.

Fig. 5: Flowchart.

Data processing

Data were processed statistically using Statistical Product and Service Solutions (SPSS22) software. First, factor analysis was used to obtain the information about the general impressions eople experienced in response to the Tang dynasty. The second stage of the analysis consisted of an ANOVA variance analysis to analyze the relationship between the Kansei evaluation and eye movements. The significance level was set at $p < 0.05$.

RESULTS

Factor analysis for the Kansei evaluation

The results the Tang dynasty evaluation are shown in Fig. 6. It can be seen from the subjective evaluations that the profiles produced vary in response to the different stimuli.
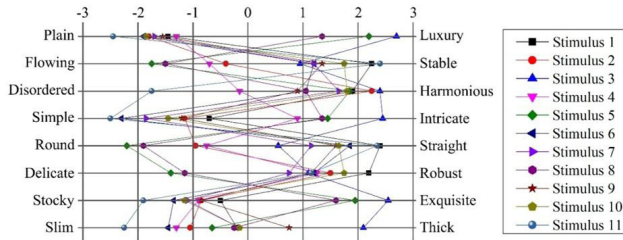

Fig. 6: Evaluation results Tang dynasty chairs.

Factor analysis was conducted to extract the factors from the SD evaluation data. According to factor extraction conventions, the eigen value must be larger than one. Two factors were generalized from the eight Kansei word pairs, and factor rotation was applied with the varimax method (Tab. 2).

Tab. 2: Factor analysis of Kansei evaluation.

Bipolar adjectives	Factor 1	Factor 2	Communality
Round-Straight	0.944	0.094	0.898
Delicate-Robust	0.890	0.025	0.593
Plain-Luxury	0.681	0.671	0.843
Simple-Intricate	−0.678	−0.619	0.900
Slim-Thick	0.077	−0.947	0.793
Disordered-Harmonious	0.035	0.769	0.942
Stocky-Exquisite	0.651	0.720	0.903
Variance (%)	49.191	35.639	
Cumulative variance (%)	49.191	84.830	

Factor 1 consisted of flowing-stable, round-straight, delicate-robust, plain-luxury, and simple-intricate. Factor 2 included slim-thick, disordered-harmonious, and stocky-exquisite. Factor 1 explained 49.2% of the variance and Factor 2 explained 35.6% (the cumulative explained variance equaled 84.8%). The adjectives in Factor 1 (e.g. round-straight, simple-intricate) represented aspects of shape, whereas those in Factor 2 (e.g. slim-thick, disordered-harmonious) represented decoration.

Spanning the Kansei space based on responses to the stimuli

The dimensions of the Kansei space were established based on subjects' responses to the stimuli through the factor analysis. Shape was assigned to the X-axis, with shape-flowing and shape-stable as the two extreme values. Decoration was assigned to the Y-axis, with decoration-disordered and decoration-harmonious as the two extreme values.

Tab. 3: The factor scores for the Tang dynasty backrest armchair stimuli.

Sample	Factor 1	Factor 2
1	1.14	0.57
2	−0.14	−0.31
3	0.06	2.29
4	−0.65	−0.86
5	−1.87	0.21
6	0.51	−0.67
7	0.48	−0.04
8	−1.65	0.07
9	0.68	0.28
10	0.91	0.21
11	0.52	−1.73

The sample factor score matrix was then extracted (Tab. 3), delineating the distribution of the stimuli in the Kansei space (Fig. 7).
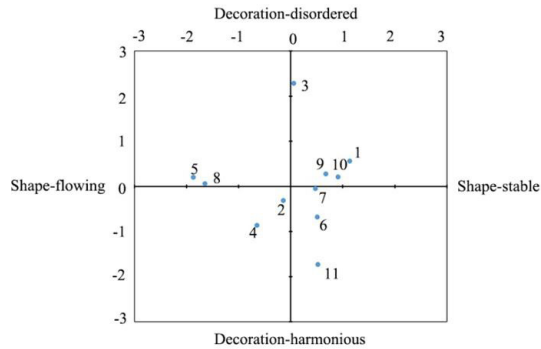

Fig. 7: Distribution of the stimuli in the Kansei space.

Analysis of eye-tracking outcomes

In order to understand whether there was a significant difference in the number of fixation points between the four quadrants and whether the two factors had an effect on the fixation points, a two-way ANOVA analysis was used for data analysis and processing. Tab. 4 shows the average fixation points and fixation time for the stimuli.

Tab. 4: The average fixation points and fixation time for the stimuli.

Stimuli	Fixation points (number)	Fixation time (s)
1	16.06	3.56
2	14.43	3.06
3	16.51	3.44
4	13.97	2.94
5	16.76	3.17
6	14.03	3.09

7	14.75	3.60
8	16.28	3.36
9	15.98	3.13
10	15.76	3.24
11	12.79	2.86

Tab. 5 shows the results for the two-way ANOVA analysis of fixation points. The effect of interaction between the two factors on the number of fixation points was insignificant (p > 0.05). In addition, there was no significant correlation between shape-stable and the number of fixation points (p > 0.05). There was, however, a significant correlation between decoration-disordered and the number of fixation points.

Tab. 5: 2-way ANOVA of fixation points.

Source	type III Sum of squares	df	Mean square	F	sig
Shape-stable	0.390	1	0.390	1.099	0.329
Decoration-disordered	13.023	1	13.023	36.690	0.001
Shape-stable * decoration-disordered	0.006	1	0.006	0.017	0.898
Error	2.485	7	0.355		
Total	2561.551	11			
Corrected total	16.462	10			

In order to determine if there was a significant difference in fixation time between the four quadrants, and if the two factors had a significant effect on the fixation time, further analysis was needed.

Tab. 6 shows the results of a two-way ANOVA analysis of fixation time. This showed that the effect of interaction between the two factors on the fixation time was insignificant (p > 0.05). In addition, there was no significant correlation between shape-stable and the fixation time. Similarly, there was no significant correlation between decoration-disordered and the fixation time.

Tab. 6: 2-way ANOVA of fixation time.

Source	type III Sum of squares	df	Mean square	F	sig
Shape-stable	0.043	1	0.043	0.708	0.428
Decoration-disordered	0.114	1	0.114	1.873	0.213
Shape-stable * decoration-disordered	0.007	1	0.007	0.117	0.743
Error	0.425	7	0.061		
Total	114.835	11			
Corrected total	0.589	10			

DISCUSSION

Relationship between the eye movements and Kansei evaluation of Tang dynasty chairs.

By using SD method and eye tracking system, the semantic space occupied by the Tang dynasty chairs could be divided into two main factors, which were shape and decoration. When the decoration of the chairs tended to be complicated, the number of fixation points increased, so the decoration had a significant correlation with the number of fixation points. Previous studies have indicated the relationship between people's attention and decoration (Zhang and Seo 2015). When the decoration is increased or complicated, people's attention and fixation points will focus on the decoration (Susac et al. 2019). This is because when people observe a product, if the decorative pattern is more complicated, people need to pay more attention to understand the relationship between the decorative pattern and other parts. When the decorative pattern of the chair is simple and harmonious, people's attention is mostly concentrated on the chair as a whole, and the fixation points are more concentrated (Hsu et al. 2017).

Stimuli in the four quadrants

Chairs in the shape-stable and decoration-disordered quadrant

The shape-stable and decoration-disordered quadrant included stimuli 1, 3, 9, and 10 (Fig. 8).
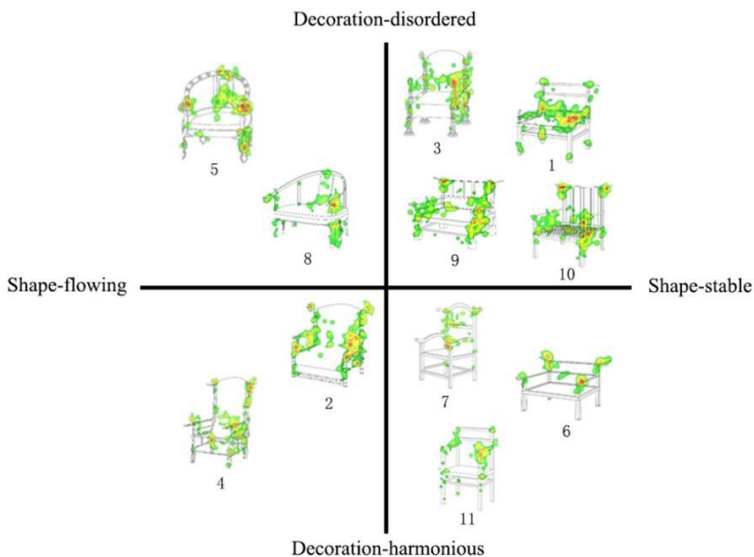

Fig. 8: Heat maps for stimuli in the quadrants of the Kansei space.

Stimulus 1 is the red-lacquered keyaki chair. This chair is a relic from the Imperial Household Agency. Stimulus 3 is the chair in Lu Luojia's painting "The Six Buddhas". Stimulus 9 is the chair in the "Zhen Yan Wu Zu" painting by Li Zhen from Tang dynasty. Stimulus 10 is the chair in the painting called "Eighteen Instruments of the Monk". Most of the chairs in this quadrant were evaluated as stable in shape and relatively complicated in decoration. Chairs in this quadrant were dominated by straight lines and stable forms. In previous studies, it has been

found that smooth and stable straight lines generate a steady feeling in observers (Mata et al. 2017). The quantity of chair decoration in this quadrant is relatively high. The overall shape is complex. According to previous research (Hsu et al. 2017), when the decoration of chairs is too complicated, it will stimulate a subjective feeling of noise and disorder in observers.

Chairs in the shape–stable and decoration–harmonious quadrant

The shape-stable and decoration-harmonious quadrant included stimuli 6, 7 and 11. Stimulus 6 has the same origin as sample 9, but sample 6 is simpler in shape and has no excessive decorative components. Stimulus 7 is a chair in the mural of cave 9 in the Dunhuang Mogao Grottoes. Stimulus 11 is a chair in the mural of cave 148 in the Mogao Grottoes in Dunhuang. In stimuli 6, 7, and 11, the main shapes are straight lines, and the decoration is concentrated on the top of the backrest. The decoration of stimuli 6 and 7 is restricted to an upturned line on the upper side of the backrest, and the curved form of the armrest. The other components are simpler structural elements. Previous research shows that less-decorated products with simple lines and shapes (Du and Macdonald 2018) will generate both monotonous and harmonious subjective feelings in observers.

Chairs in the shape–flowing and decoration–disordered quadrant

The shape-flowing and decoration-disordered quadrant included stimuli 5 and 8. Stimulus 5 is a chair in the painting called "Emperor Taizong's Portrait". Stimulus 8 is a chair from the painting "Fair Lady", with a streamlined curve on the back of the chair. The decoration of stimuli 5 and 8 is more complicated, mainly due to the processes used to decorate the parts, including engraving and inlaying. The shape is streamlined, in the armrests, seat surfaces, and legs. As the study of Kapkin and Joines (2018), these smooth lines are considered feminine.

Chairs in the shape–flowing and decoration–harmonious quadrant

The shape-flowing and decoration-harmonious quadrant included stimuli 2 and 4. Stimulus 2 is a chair in Lu Luojia's painting called "The Six Buddhas". Stimulus 4 is a chair in the painting called "Xiao Yi Cheated of the Orchid Pavilion". The shapes of stimuli 2 and 4 reflect the texture of the natural material. The top of the backrest, the armrest, and other parts have a curved shape. At the same time, the texture of the wood material itself reflects the fluidity. The decoration is reflected in the texture of the natural material. Research carried out by Song et al. (2016) shows that shapes based on natural materials give people a feeling of nature and harmony.

Effect of Tang dynasty chair features on eye movements in Kansei evaluations

Previous research (Nodine et al. 1993) has indicated that feature importance is correlated with a variety of gaze response data variables such as fixation time (Isham and Geng 2013), fixation points, and first-located time (Kubler et al. 2017). This gaze data provided insight into how people evaluate the features while making preference decisions (Du and Macdonald 2014, Ho and Lu 2014, Husic-Mehmedovic et al. 2017). In this study, the combination of subjective evaluation and eye-movement tracking meant that people's gazes could be more accurately and rapidly understood (Du and Macdonald 2015), so that responses to the morphological characteristics of Tang dynasty chairs could be assessed and understood. Hsu et al. (2017) concluded that the seats and backrests were the two most important features of chair design; however, the results of the current experiment are inconsistent with this conclusion. According to the heat maps produced in this experiment, backrest, armrests, and legs were all important features of the Tang dynasty chairs (Fig. 9).
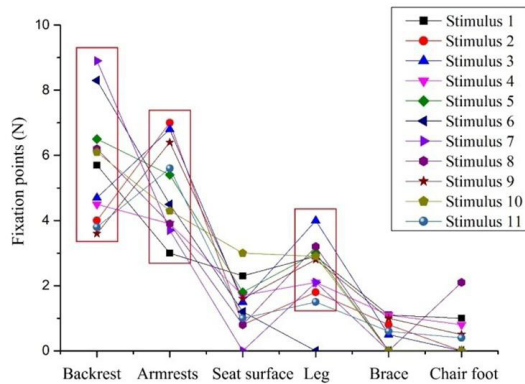
Fig. 9: Fixation points of stimuli's different parts.

This indicates that the subjects considered these all to be important features of the overall chair forms. These results can be used to guide modern designs based on these ancient precursors. As summarized by the study of Wan et al. (2018), subjects paid more attention to the decorative details on the chairs, implying that appropriate design and decoration may improve people's levels of interest in the chairs. When designing a Tang dynasty style chair, designers can, therefore, focus on the backrest, armrests, and legs of the chairs, in accordance with the observed cognitive responses to the Tang dynasty chairs. Through the careful design of the morphological characteristics of modern Tang dynasty style chairs, it will be possible to accurately recreate the style of the Tang dynasty chairs on the basis of the ancient designs characteristics.

The decoration of Tang dynasty chairs can be complicated, but it is mostly concentrated on the upper side of the backrest, on the armrests, and on the legs. In the future, designers attempting to create modern chairs based on Tang dynasty style chair designs should, therefore, focus on all three important areas of the Tang dynasty chairs.

CONCLUSIONS

The main conclusions of this study are as follows: (1) Through SD evaluation method, it was shown that the two factors that affected the Kansei evaluations were shape and decoration. The complex and harmonious levels of decoration had significant impact on participants' fixation points. (2) By combining Kansei evaluations and eye tracking, it was found that the main features that affect people's evaluation of the Tang dynasty chairs are backrests, armrests, and legs.

This finding demonstrated that designers need to consider these three main features when designing Tang dynasty style furniture. By combining Kansei evaluations with eye tracking, the eye movements associated with Tang dynasty chairs can be observed, so that the Tang dynasty furniture features hat affect people's perceptual cognition can be quickly and accurately analyzed. Significant features identified in the experiment can be researched in more detail, new chairs can be designed with an emphasis on these details, and the discovery in this experiment can also be used to predict people's perceptual evaluations of new designs. The methods used and the conclusions drawn in this study can be provided to designers, engineers, and related researchers to guide future designs of Tang dynasty style chairs.

ACKNOWLEDGMENT

REFERENCES

1. Castilla, N., Llinares, C., Bravo, J.M., Blanca, V., 2017: Subjective assessment of university classroom environment. Building and environment 122: 72-81.
2. Dong, M.Y., Zhou, H.B., Jiang, X.M., Lu, Y., Wang, W.B., Yin, Y.F., 2017: Wood used in ancient timber architecture in Shanxi Province, China. IAWA Journal 38(2): 182-200.
3. Du, P., Macdonald, E.F., 2014: Eye-tracking data predict importance of product features and saliency of size change. Journal of Mechanical Design 136(8): 081005.
4. Du, P., Macdonald, E.F., 2015: Products' shared visual features do not cancel in consumer decisions. Journal of Mechanical Design 137(7): 071409.
5. Du, P., Macdonald, E.F., 2018: A test of the rapid formation of design cues for product body shapes and features. Journal of Mechanical Design 140(7): 071102.
6. Guo, F., Ding, Y., Liu, W.L., Liu, C., Zhang, X.F., 2016: Can eye-tracking data be measured to assess product design? : Visual attention mechanism should be considered. International Journal of Industrial Ergonomics 53: 229-235.
7. Ho, C.H., Lu, Y.N., 2014: Can pupil size be measured to assess design products? International Journal of Industrial Ergonomics 44(3): 436-441.
8. Hsu, C.C., Fann, S.C., Chuang, M.C., 2017: Relationship between eye fixation patterns and Kansei evaluation of 3D chair forms. Displays 50: 21-34.
9. Hu, W.G., Liu, N., Guan, H.Y., 2019b: Experimental study of the contact forces and deformations of mortise-and-tenonjoints considering the fits and grain orientations of the tenon. Bioresources 14(4): 8728-8737.
10. Hu, W.G., Liu, N., Guan, H.Y.,2019c: Optimal design of a furniture frame by reducing the volume of wood. Drewno 62(204): 85-97.
11. Hu, W.G., Wan, H., Guan, H.Y.,2019a: Size effect on the elastic mechanical properties of beech and its application in finite element analysis of wood structures. Forests 10(9): 783.
12. Husic-Mehmedovic, M., Omeragic, I., Batagelj, Z., Kolar, T., 2017: Seeing is not necessarily liking: Advancing research on package design with eye-tracking. Journal of business research 80: 145-154.
13. Isham, E.A., Geng, J.J., 2013: Looking time predicts choice but not aesthetic value. Plos One 8(8): e71698.
14. Kapkin, E., Joines, S., 2018: An investigation into the relationship between product form and perceived meanings. International Journal of Industrial Ergonomics 67: 259-273.
15. Khalighy, S., Green, G., Scheepers, C., Whittet, C., 2015: Quantifying the qualities of aesthetics in product design using eye-tracking technology. International Journal of Industrial Ergonomics 49: 31-43.
16. Kubler, T.C., Rothe, C., Schiefer, U., Rosenstiel, W., Kasneci, E., 2017: SubsMatch 2.0: Scanpath comparison and classification based on subsequence frequencies. Behavior Research Methods 49(3): 1048-1064.

17. Lee, J., Kong, Y.H., Luo, M., 2018: Syntactic patterns in classical Chinese poems: A quantitative study. Digital Scholarship in the Humanities 33(1): 82-95.

18. Loyola, P., Martinez, G., Munoz, K., Velasquez, J.D., Maldonado, P., Couve, A., 2015: Combining eye tracking and pupillary dilation analysis to identify website key objects. Neurocomputing 168: 179-189.

19. Mata, P.M., Ahmed-Kristensen, S., Brockhoff, P.B., Yanagisawa, H., 2017: Investigating the influence of product perception and geometric features. Research in Engineering Design 28(3): 357-379.

20. Nodine, C.F., Locher, P.J., Krupinski, E.A., 1993: The role of formal art training on perception and aesthetic judgment of art compositions. Leonardo 26(3): 219-227.

21. Song, S.S., Wan, Q., Wang, G.G., 2016: Eye movement evaluation of different wood interior decoration space. Wood Research 61(5): 831-843.

22. Susac, A., Bubic, A., Planinic, M., Movre, M., Palmovic, M., 2019: Role of diagrams in problem solving: An evaluation of eye-tracking parameters as a measure of visual attention. Physical Review Physics Education Research 15(1): 013101.

23. Trujillo, J.L.H., Avino, A.M.I., Millan, C.L., 2016: User evaluation of neonatology ward design: An application of focus group and semantic differential. Herd-Health Environments Research & Design Journal 10(2): 23-48.

24. Vieira, J., Osorio, J.M.A, Mouta, S., Delgado, P., Portinha, A., Meireles, J.F., Santos, J.A., 2017: Kansei engineering as a tool for the design of in-vehicle rubber keypads. Applied Ergonomics. 61: 1-11.

25. Wan, Q., Song, S.S., Li, X.H., Zhang, Q., Yang, X., Zhang, Y.C., Fei, B.H., Yao, L.H., 2018: The visual perception of the cardboard product using eye-tracking technology. Wood Research 63(1): 165-178.

26. Wan, Q., Wang, G.G., Zhang, Y.C., Song, S.S., Fei, B.H., Li, X.H., 2018: Cognitive processing toward traditional and new Chinese style furniture: evidence from eye-tracking technology. Wood research 63(4): 727-739.

27. Wang, C.C., Yang, C.H., Wang, C.S., Chang, T.R., Yang, K.J., 2016: Feature recognition and shape design in sneakers. Computer & Industrial Engineering 102: 408-422.

28. Wang, Y.H., Zhang, H.H., Zhao, Y.N., Hao, W., Ning, X.J., Shi, Z.H., Zhao, M.H., 2015: Three-dimensional reconstruction method of Tang dynasty building based on point clouds. Optical Engineering 54(12): 123111.

29. Winston, A.S., Cupchik, G.C., 1992: The evaluation of high art and popular art by naive and experienced viewers. Visual Arts Research 18(1): 1-14.

30. Ying, W., 2018: A national flower's symbolic value during the Tang and Song dynasties in China. Space and Culture 21(1): 46-59.

31. Zanous, H.P., Sangari, E., 2018: The last sasanians in Chinese literary sources: recently identified statue head of a sasanian prince at the Qianling Mausoleum. Iranian Studies 51(4): 499-515.

32. Zhang, B.Y., Seo, H.S., 2015: Visual attention toward food-item images can vary as a function of background saliency and culture: An eye-tracking study. Food Quality and Preference 41: 172-179.

33. Zhou, J., Guo, G., Dong, F.Y., Li, H., Lin, L., Yang, F., 2014: Multi-dimensional method for evaluating a product's conceptual schemes. South African Journal of Industrial Engineering 25(3): 184-198.

34. Zhu, Y., 2016: Different cultures of computation in seventh century China from the viewpoint of square root extraction. Historia Mathematica 43(1): 3-25.

Zhonghua Zhagn, Boming Xu*
College of Furnishings and Industrial Design
Nanjing Forestry University
Nanjing 210037
China
*Corresponding author: xubomingnjfu@126.com
Phone: +8615568370432

SHORT NOTE

SHEAR STRENGTH ESTIMATION MODEL FOR TROPICAL WOOD SPECIES

Anderson Renato Vobornik Wolenski
Federal Institute of Santa Catarina
São Carlos, Brazil

Rodrigo Guerra Peixoto, Veronika Fedotova
Federal University of Minas Gerais
Belo Horizonte, Brazil

André Luís Christoforo
Federal University of São Carlos
São Carlos, Brazil

Francisco Antonio Rocco Lahr
University of São Paulo
São Carlos, Brazil

ABSTRACT

For safety reasons, wood strength values are calculated based on their characteristic values. Brazilian national standard (NBR, in Portuguese "Norma Brasileira Regulamentadora") 7190 (1997) establishes ratios for characteristic strength estimation and three forms of wood characterization, with an emphasis on the simplified procedure for common species, which allows obtaining the strength characteristic values through equations correlating different mechanical properties. The present work evaluates the accuracy of the relation proposed by NBR 7190 (1997) of shear strength along the grain ($f_{v0,k}$) to compression strength along the grain ($f_{c0,k}$) ($f_{v0,k}$=0.12$f_{c0,k}$). 960 experimental measurements of shear and compression strength values were performed for 40 hardwood species, and the precision of the relation proposed by the Brazilian standard was evaluated using the analysis of variance (ANOVA) method. Linear, exponential, logarithmic, and geometric regression models were used as an alternative to the NBR relation for shear strength estimation. The statistical analysis revealed that the geometric regression is the model of best fit.

KEYWORDS: Wood, strength properties, characteristic value, strength along the grain.

INTRODUCTION

Timber structures have an elevated applicability potential in Brazil due to a vast number of wood species existing in the Amazonian rainforest. According to Steege et al. (2016), by 2015 there were already discovered more than 10 000 wood species. This expressive number induces development of new research aiming at characterization of species that can potentially substitute those that already are commonly used in civil construction. Works of Mascia and Nicolas (2013), Silva et al. (2014), Segundinho et al. (2015), dos Reis et al. (2018) can be mentioned among other works that sought to investigate the species for structural purposes.

In Brazil, the standard NBR 7190 (1997) regulates the use of timber for structural needs, establishing the requirements for project development, construction and control of wooden structures, based on probabilistic methods, which assess fracture strength, instability, excessive deformation, and durability of the structure. The standard also specifies the complete, minimal and simplified characterization methods of wood physical and mechanical properties. According to Almeida et al. (2017), such characterization is justified by anatomic structure of wood, distinct for each species, and loading type, grain direction and moisture content shall be taken into account.

Hence, it is of great importance to examine the equations that estimate the mechanical properties of the species used in construction. Such equations are established in the standard NBR 7190 (1997, p. 15) defining the simplified characterization method, which allows obtaining different strength properties of common wood species when experimental data are not available.

However, Logsdon et al. (2010) stress that this simplified method should not be the only rule for determination of characteristic wood properties. These authors sought to benchmark a model for characteristic compression strength ($f_{c0,k}$) estimation, aiming to obtain a more appropriate statistical model for *Dinizia excelsa* Ducke species. They have concluded that NBR equation is more conservative as it provides slightly lower $f_{c0,k}$ values.

Similarly to the previous study, Matos and Molina (2016) investigated a correlation between compression and shear strength ($f_{v0,k}$ and $f_{c0,k}$) of *Pinus elliotti* and *Corymbia citriodora* species, comparing an experimental relation with the standardized relations of NBR 7190 (1997) and ISO 1391 (2005), and concluded that the values obtained from relations of the Brazilian standard were superior to those of the European standard for both species. Krajewski et al. (2016) compared shear strength along the grain of 16-18th century *Pinus sylvestris* L. heartwood from Central Poland and that of modern wood, and found that the aged wood had better technical quality.

Other authors also investigated some of the hardwood species that are studied in the present work, focusing on physical and mechanical properties for distinct sites: *Apuleia leiocarpa* (Soriano et al. 2015), *Goupia glabra* Aubl. (Silva et al. 2018), and *Cedrela odorata* (Tenorio et al. 2018).

Previous studies demonstrate the importance of assessing physical and mechanical properties of wood in order to obtain reliable and safe estimates for structural dimensioning. Therefore, there is a notable relevance of research seeking equations that estimate mechanical properties of different species for structural use. A need for such estimates motivated the present work, in which 40 species of dicot woods were assessed. NBR 7190 (1997, p. 90, Appendix E) presents average values of physical and mechanical properties of 43 species of native and afforestation woods, and this list of species is similar to the species evaluated in the present study, thus reinforcing the reliability of the statistical analyses carried out here exclusively for woods of native Brazilian forests.

MATERIALS AND METHODS

As required by NBR 7190 (1997), homogeneous batches were used in all the tests, with the batch volume not exceeding 12 m³, and specimens randomly extracted, limited to one sample per beam, as shown on Fig. 1. In order to carry out the tests, all wood species were stored at 12% moisture level, which corresponds to equilibrium moisture content as defined by this standard. All the tests were performed at the LaMEM (in Portuguese Laboratório de Madeiras e Estruturas de Madeira) of the University of São Paulo (USP), following the procedures described in Appendix B of NBR 7190 (1997). 12 samples of each species were tested, giving a total of 960 experimental values of shear (f_{V0}) and compressive (f_{c0}) strengths parallel to the grain (Fig. 1, Tab. 1).
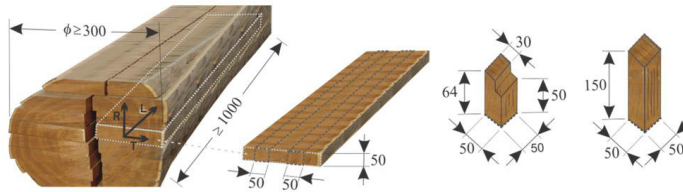

Fig. 1: Extraction scheme and dimensions (in mm) of the specimens for compressive and shear tests.

In order to validate the equation given in NBR 7190 (1997):

$$f_{v0,k} = 0.12 \cdot f_{c0,k} \qquad \text{(MPa)} \tag{1}$$

Thus, these properties ($f_{v0,k}$ / $f_{c0,k}$) were determined following the simplified procedure described in NBR 7190 (1997). It should be emphasized that Eq. 1 is only applicable for characterization of commonly used species in cases when experimental data from complete characterization are not available. The simplification found in Eq. 1 may or may not be consistent with actual results of experimental analyzes.

Alternatively, this research sought to evaluate an applicability of regression models for estimation of mechanical parameters ($f_{v0,k}$ from $f_{c0,k}$). Experimentally obtained strength values were fit into Eqs. 2 to 5 to verify if any of the regression models (linear, exponential, logarithmic or geometric) can be used for wood strength estimation.

$$Y = a + b \cdot X \qquad \text{(linear)} \tag{2}$$
$$Y = a \cdot e^{b \cdot X} \qquad \text{(exponential)} \tag{3}$$
$$Y = a + b \cdot ln\,(X) \qquad \text{(logarithmic)} \tag{4}$$
$$Y = a \cdot X^b \qquad \text{(geometric)} \tag{5}$$

where: Y (MPa) - a dependent variable,
X (MPa) - an independent variable,
a and b (dimensionless) - parameters of the model, obtained by the least squares method.

The analysis of variance (ANOVA) was used to determine the equivalence of strength values estimated by the models and those experimentally obtained (with the significance level set to 0.05). The coefficient of determination (R^2) was used to determine the regression model of best fit.

RESULTS AND DISCUSSION

Tab. 1 shows experimentally obtained compression and shear strength values for 40 species of hardwood. Comparison of the values presented in Tab. 1 with the values found in Appendix E of NBR 7190 (1997) demonstrates agreement of experimental results with those already registered.

Tab. 1: Strength values (MPa) for 40 species of hardwood.

Wood Species[1]	Experimental values		$f_{v0,k}$	Wood species[1]	Experimental values		$f_{v0,k}$
	$f_{c0,k}$	$f_{v0,k}$	(Eq. 1)		$f_{c0,k}$	$f_{v0,k}$	(Eq. 1)
Vatairea cf. guianensis	51.06	12.10	6.13	*Micropholis venulosa*	90.41	17.39	10.84
Dinizia excelsa	72.73	13.35	8.73	*Peltophorum dubium*	56.34	17.47	6.76
Parkia cf. pendula	41.87	12.72	5.02	*Mezilaurus itauba*	68.44	16.32	8.21
Anadenanthera colubrina	55.55	17.95	6.67	*Hymenaea courbaril*	89.96	23.08	10.80
Sebastiania commersoniana	45.58	13.75	5.47	*Ocotea neesiana*	50.60	10.40	6.07
Andira anthelmia	40.50	6.64	4.86	*Sextonia cf. rubra*	49.14	9.77	5.90
Erisma cf. fuscum	27.30	11.62	3.28	*Manilkara cf. inundata*	79.46	20.77	9.54
Cassia ferruginea	36.37	12.97	4.36	*Qualea paraensis*	61.53	14.34	7.38
Bertholletia excelsa	38.93	7.04	4.67	*Clarisia racemosa*	62.41	15.18	7.49
Calycophyllum multiflorum	54.54	15.55	6.54	*Pradosia sp.*	72.34	14.63	8.68
Calophyllum longifolium	50.91	12.30	6.11	*Parinari excelsa*	55.22	12.01	6.63
Cedrela odorata	33.18	8.56	3.98	*Copaifera langsdorffii*	45.06	10.62	5.41
Cedrela cf. fissilis	29.99	7.13	3.60	*Tapirira sp.*	43.74	12.39	5.25
Cedrelinga cateniformis	29.06	8.37	3.49	*Erisma uncinatum*	27.20	6.70	3.26
Dipteryx odorata	96.16	13.51	11.54	*Geissospermum sericeum*	61.60	11.37	7.39
Copaifera multijuga	44.13	10.25	5.30	*Vochysia haenkeana*	44.79	9.30	5.38
Goupia paraensis	55.28	12.63	6.63	*Diplotropis sp.*	93.02	17.42	11.16
Apuleia leiocarpa	65.36	16.28	7.84	*Tachigali glauca*	75.46	14.54	9.06
Planchonella pachycarpa	43.10	12.14	5.17	*Bagassa guianensis*	59.84	19.18	7.18
Luetzelburgia cf. guaissara	58.92	17.51	7.07	*Ruizterania retusa*	51.28	9.83	6.15

*Brazilian Flora 2020 in construction, Rio de Janeiro Botanical Garden, Brazil.

40 experimentally obtained results of $f_{v0,k}$ (Tab. 1, middle column) were compared to $f_{v0,k}$ (MPa) values calculated from experimental $f_{c0,k}$ (MPa) values (Tab. 1, left column) using Eq. 1 (Tab. 1, right column) and ANOVA. The Tab. 2 and Fig. 2 show the result of the analysis.

Tab. 2: Results of ANOVA for the sample sets: $f_{v0,k}$ (experimental values) and $f_{v0,k}$ (Eq. 1).

Source	DF	SS_{aj}	MS_{aj}	F-Value	P-Value
Condition ($f_{v0,k} = 0.12 \cdot f_{c0,k}$)	1	814.4	814.39	78.01	0.000
Error	78	814.0	10.44	--	--
Total	79	1628.6	--	--	--

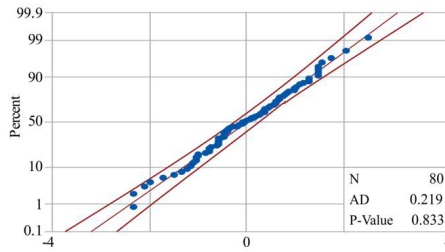* DF – Degrees of Freedom; SS_{aj} - sum of squares; MS_{aj} - mean squares.

Fig. 2: Probability plot for transformed data for condition: $f_{v0,k} = 0.12 \cdot f_{c0,k}$.

It can be seen that the compared groups of values are not equivalent (P-Value = 0.000, Tab. 2), indicating an inexactness of Eq. 1 proposed by NBR 7190 (1997). The Fig. 2 confirms the results of ANOVA, for a normal distribution of data and by P-Value = 0.833.

Alternatively, the Tab. 3 and Fig. 3 present regression models for estimation of $f_{v0,k}$ (MPa) values from $f_{c0,k}$ (MPa) values for 40 examined wood species. P-value allows evaluating the applicability (P<0.05) or non-applicability (P> 0.05) of the regression model.

Tab. 3: Regression models for estimation of $f_{v0,k}$ from $f_{c0,k}$.

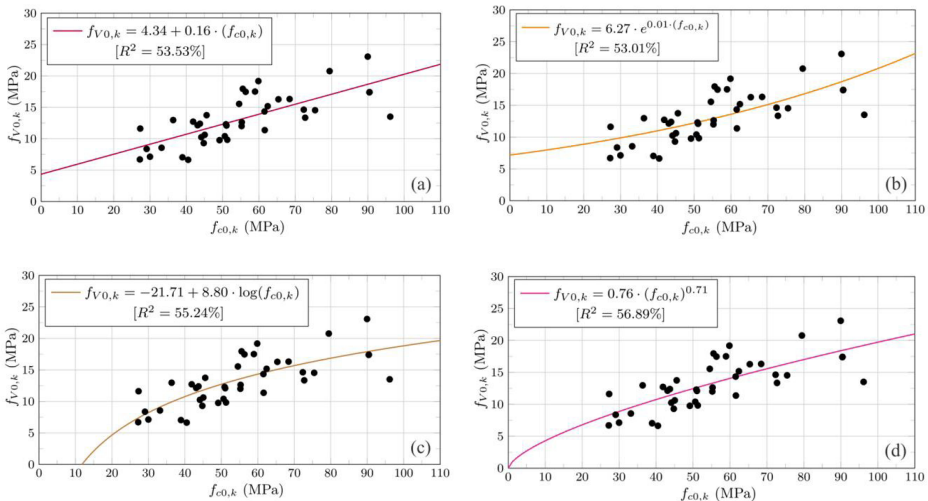| Model	Equation	a	b	P-value	R² (%)
Linear	$f_{v0,k} = a + b \cdot (f_{c0,k})$	4.34	0.16	0.000	53.53
Exponential	$f_{v0,k} = a \cdot e^{b \cdot (f_{c0,k})}$	6.27	0.01	0.000	53.01
Logarithmic	$f_{v0,k} = a + b \cdot \ln(f_{c0,k})$	-21.71	8.80	0.000	55.24
Geometric	$f_{v0,k} = a \cdot f_{c0,k}{}^{b}$	0.76	0.71	0.000	56.89

Fig. 3: Regression models for shear strength: Linear (a), Exponential (b), Logarithmic (c), and Geometric (d).

The present study expanding the number of studied species for the total of 40 hardwood species. This large sample supports a validity of the equation $f_{v0,k} = 0.76 \cdot (f_{c0,k})^{0.71}$ (MPa) (Fig. 3d) as the most adequate for estimation of shear strength from compression strength for native Brazilian species, which lack a complete physical and mechanical characterization.

CONCLUSIONS

Mechanical properties of 40 wood species were experimentally determined, and the obtained values were in accordance with those found in the literature (NBR 7190, 1997). Comparison of shear strength values obtained experimentally and calculated using the Eq. 1 ($f_{v0,k} = 0.12 \cdot f_{c0,k}$) demonstrated a significant difference between the compared groups, indicating weakness of the equation proposed by NBR 7190 (1997).

The regression models proposed in this work (Tab. 3 and Fig. 3) are an alternative to the equation of the standard. The higher coefficient of determination (R^2=52.89%) was found for the geometric model, suggesting that it is the model of best fit, $f_{v0,k} = 0.76 \cdot (f_{c0,k})^{0.71}$(MPa), and is the most appropriate for estimation of shear strength along the grain from compression strength values. The analyzed tropical wood species, classified as Brazilian hardwood, demonstrate a potential for structural use in civil engineering.

REFERENCES

1. Almeida, T.H., Almeida, D.H., Araújo, V.A., Silva, S.A.M., Christoforo, A.L., Lahr, F.A.R, 2017: Density as estimator of dimensional stability quantities of Brazilian tropical woods. BioResources 12 (3): 6579-6590.
2. Dos Reis, P.C.M., Souza, A.L., Reis, L.P., Carvalho, A.M.M.L., Mazzei, L., Rêgo, L.J.S., Leite, H.G., 2018: Artificial neural networks to estimate the physical-mechanical properties of Amazon second cutting cycle wood. Maderas. Ciencia y Tecnología 20 (1): 343-352.
3. ISO 13910, 2005: Structural timber – characteristic values of strength-graded timber – sampling, full-size testing and evaluation.
4. Krajewski, A., Kozakiewicz, P., Witomski, P., 2016: Shear strength of scots pine (*Pinus sylvestris* L.) from the historical buildings. Wood Research 61 (5): 845-850.
5. Logsdon, N.B., De Jesus, J.H., Penna, J.E., 2010: Evaluation of the estimators of the characteristic strength to compression parallel to the grain. Scientia Forestalis 38 (1): 579-587.
6. Mascia, N.T., Nicolas, E.A., 2013: Determination of Poisson's ratios in relation to fiber angle of a tropical wood species. Construction and Building Materials 41 (4): 691-696.
7. Matos, G.S., Molina, J.C., 2016: Shear strength of wood in direction parallel to the grain according to the standards ABNT NBR 7190: 1997 and ISO 13910: 2005. Revista Matéria 21 (4): 1069-1079.
8. NBR 7190, 1997: Design of wooden structures. Rio de Janeiro, Brazil, 107 pp.
9. Segundinho, P.G.A., Lahr, F.A.R., Regazzi, A.J., Carreira, M.R., 2015: Variation of modulus of elasticity obtained through the static bending method considering the S/h ratio. Wood Research 60 (2): 189-200.
10. Silva, F., Higuchi, N., Matos, J.M., Paula, E.M., Santos, J., 2014: Nondestructive evaluation of hardness in tropical wood. Journal of Tropical Forest Science 26 (1): 69-74.

11. Silva, C.E.G, Almeida, D.H., Almeida, T.H., Chahud, E., Branco, L.A.M.N., Campos, C.I., Lahr, F.A.R, Christoforo, A.L., 2018: Influence of the procurement site on physical and mechanical properties of Cupiúba wood species. BioResources 13 (2): 4118-4131.

12. Soriano, J., Veiga, N.S., Martins, I.Z., 2015: Wood density estimation using the sclerometric method. European Journal of Wood and Wood Products 73 (1): 753-758.

13. Steege, H., Vaessen, R.W., López, D.C., Sabatier, D., Antonelli, A., Oliveira, S.M.; Pitman, N.C.A., Jørgensen, P.M., Salomão, R.P., 2016: The discovery of the Amazonian tree flora with an update checklist of all known tree taxa. Scientific Reports 6 (1): 1-15.

14. Tenorio, C., Moya, R., 2018: Evaluation of wood properties of four ages of *Cedrela odorata* trees growing in agroforestry systems with *Theobroma cacao* in Costa Rica. Agroforestry Systems 1 (1): 1-16.

Anderson Renato Vobornik Wolenski*
Federal Institute of Santa Catarina
Department of Civil Engineering
Avenida Aloísio Stoffel, 1271, Cep 89885-000
São Carlos, Sc, Brazil
*Corresponding author: anderson.wolenski@ifsc.edu.br

Rodrigo Guerra Peixoto, Veronika Fedotova
Federal University of Minas Gerais
Department of Structural Engineering
Avenida Antonio Carlos, 6627, Cep 31270-901
Belo Horizonte, Mg, Brazil

André Luís Christoforo
Federal University of São Carlos
Department of Civil Engineering
Rodovia Washington Luís, Cep 13565-905
São Carlos, Sp, Brazil

Francisco Antonio Rocco Lahr
University of São Paulo
Department of Structural Engineering
Avenida Trabalhador São-Carlense, 400, Cep 13566-590
São Carlos, Sp, Brazil